
# DIAGNOSTIC UTILITY AND PREDICTIVE ABILITY OF ELECTROCARDIOGRAPHY IN DETECTING MYOCARDIAL ABNORMALITIES IN CARDIAC MAGNETIC RESONANCE IMAGING

**DR. AZLAN HELMY ABD SAMAT**
**MB BCh BAO (DUB) DrEmMed (UKM)**

**SUPERVISORS:**
**PROF MASLIZA MAHMOD**
**PROF BETTY RAMAN**
**PROF ADAM LEWANDOWSKI**

**ST. CATHERINE'S COLLEGE**
**RADCLIFFE DEPARTMENT OF CARDIOVASCULAR MEDICINE**
**UNIVERSITY OF OXFORD**

**THESIS SUBMITTED FOR THE DEGREE OF**
**DOCTOR OF PHILOSOPHY IN MEDICAL SCIENCES**
**HILARY TERM 2024**

## ACKNOWLEDGEMENTS

First, I thank God Almighty for this lifetime opportunity and all His blessings. I believe in His divine decree that every individual I encountered was meant to be. With His mercy, I pray for the blessings of every individual directly or indirectly involved throughout this noble pursuit of knowledge.

My most profound appreciation goes to all my supervisors, Prof. Masliza Mahmod, Prof. Betty Raman, and Prof. Adam Lewandowski, for their continuous support, guidance, and knowledge shared throughout my DPhil endeavour. I could not have undertaken this journey without their tremendous help. I am also extremely grateful to my head of department (Prof. Stefan Neubauer), professors and colleagues at Oxford Centre for Clinical Magnetic Resonance Research (OCMR) and Radcliffe Department of Medicine, John Radcliffe Hospital, University of Oxford (Dr Zakariye Ashkir, Dr Mark Cassar, Dr Abid Akhtar, Dr Lucy Finnigan, Claudia Nunes, Dr Ng May, Dr Hanan Lamlum, Celeste McCracken, Prof Ladislav Valkovic, Prof. Vanessa Ferreira, Prof. Stefan Piechnik, Catherine Krasopoulos, Liliana Rodriguez, Rebecca Mills, Joana Leal Pelado, Annabelle McCourt, In Jung, Polly Whitworth, Elena Lukaschuk, Mike MacDonald, Jacob Wooding, amongst others). Thank you for your friendship and support and for making my years in Oxford an unforgettable experience. My sincerest appreciation to all the investigators and co-authors of the CMORE and PHOSP-COVID collaborative group including Prof Christopher E Brightling and Prof Gerry P McCann, Rachael A Evans, Prof Charlotte Manisty, Prof Declan P O'Regan, Jonathan R Weir-McCall, Prof Richard P Steeds, Prof Dan J Cuthbertson, Prof Graham J Kemp, Prof Alexander Horsley, Prof Christopher A Miller, Caitlin O'Brien, Prof Amedeo Chiribiri, Prof Susan T Francis, Prof James D Chalmers, Prof Sven Plein, Prof James M

Wild, Thomas A Treibel, Michael Marks, Mark Toshner, and Prof Louise V Wain. My utmost appreciation to the the IMPROVE-HCM clinical trial team for the lifetime and transformative learning experience. It has been an absolute privilege to be part of these impactful multi-centre studies.

To my DPhil funder, the Ministry of Higher Education Malaysia and the National University of Malaysia (UKM), thank you for your generous support. Special appreciation to the head of the Department of Emergency Medicine UKM, Dr Faizal Amri Hamzah, my mentor, Prof. Ismail Mohd Saiboon, members and colleagues of the Emergency Department and the Faculty of Medicine UKM, whose support play a pivotal role throughout this DPhil journey.

My special gratitude goes to the main pillars: my family. To my dearest wife, Sr Dr Nurshuhada Zainon, her encouragement will always be my inspiration. I cannot express my gratitude enough for her love, sacrifices, honest criticism, and patience. To my beloved children (Batrisyia, Aqeel, Hamza and Ahmed), this journey would be impossible without their endless understanding. Thank you for making our journey as a family so colourful and exciting, and may the experience inspire them to continue to strive in the pursuit of knowledge. My deepest gratitude to my beloved parents (Dato' Haji Abd Samat Sabri, Datin Hjh Amimah Ahmad), parents-in-law (Tuan Haji Zainon Hamzah, Puan Hjh Nor Rashidah Abd Rahman), and all my siblings and family members for their continuous support and prayers from thousands of miles apart, and for this, I am deeply grateful.

Finally, to my grandmother, Su Atkah Meor Ahmad, who sadly passed away recently (November 2023), I am sorry for not being there in your final moments. I dedicate this thesis to you. Your loss is immeasurable, but so is your love, inspiration and prayers. May Allah rest her soul in eternal peace and grant her the highest place in heaven.

## DECLARATION

The work presented in this thesis is my own, and the research questions underpinning the work are authentically driven to provide a pragmatic solution for improvement in clinical management based on experience and challenges as a frontline clinical specialist in the emergency department. Excluding the references, front pages and abstracts, the word count of the thesis is 34 000 words. Dr. Mark Cassar recruited and scanned the post-hospitalised COVID-19 patients in this study, especially the Oxford cohort. Investigators from the CMORE/PHOSP-COVID collaborative group provided data on post-hospitalised COVID-19 patients from outside of Oxford, encompassing eleven sites across the United Kingdom, facilitated by data scientist Celeste McCracken. Dr Abid Akhtar contributed partly to ECG analysis. Prof. Betty Raman and Elena Lukaschuk helped with independent CMR image analysis. I recruited and scanned the control patients in the study and assisted with the CMR scans for post-hospitalised COVID-19 patients in Oxford alongside the staff and fellows of the OCMR. I analysed all the ECGs, curated the CMR and ECG data from all the sites, interpreted the data, conducted all the statistical analyses and wrote the manuscripts and thesis. Apart from being one of the CMORE/PHOSP-COVID study fellows, I also played an integral role as the Clinical Research Fellow and sub-investigator for a multicentre phase II clinical trial called the IMPROVE-HCM study. During this DPhil, I was funded by the National University of Malaysia (UKM) and the Ministry of Higher Education Malaysia.

# ABBREVIATIONS

| | |
|---|---|
| AUROC | Area under the receiver operating characteristic |
| CI | Confidence interval |
| CMR | Cardiac magnetic resonance imaging |
| COVID-19 | Coronavirus disease |
| cTPe | Corrected T peak-to-T-end interval |
| C-Statistics | Concordance Statistics |
| EAT | Epicardial adipose tissue |
| ECG | Electrocardiography |
| ECMO | Extracorporeal membrane oxygenation |
| ECV | Extra-cellular volume |
| EDV | End-diastolic volume |
| EF | Ejection fraction |
| ESV | End-systolic volume volumes were used to calculate |
| fQRS | Fragmented QRS |
| Hct | Hematocrit |
| HERG | Human ether-a-go-go-related gene |
| JTc | Corrected JT interval |
| JTPc | Corrected JT peak interval |
| LGE | Late gadolinium enhancement |
| LVEF | Left ventricular ejection fraction |
| MOLLI | Modified Look-Locker Inversion Recovery |
| MRI | Magnetic resonance imaging |
| NIV | Non-invasive ventilation |
| NPV | Negative predictive value |
| PAC | Premature atrial complexes |
| PPV | Positive predictive value |
| PSIR | Phase-sensitive inversion recovery |
| PVC | Premature ventricular complexes |
| QTc | Corrected QT interval |
| QTPc | Corrected QT peak interval |
| ROI | Region of interest |
| RT-PCR | Reverse transcription and polymerase chain reaction. |
| RVEF | Right ventricular ejection fraction |
| SARS-CoV-2 | Severe acute respiratory syndrome coronavirus-2 |
| ShMOLLI | Shortened Modified Look-Locker $T_1$ mapping |

| | |
|---|---|
| SN | Sensitivity |
| SP | Specificity |
| SSFP | Steady-state free precession |
| SV | Stroke volume |
| WHO | World Health Organisation |

# TABLE OF CONTENTS

## THESIS ABSTRACT

**Background**: The role of electrocardiography (ECG) to screen for cardiac sequelae on cardiac magnetic resonance imaging (CMR) in COVID-19 infection is unclear. This study examined the burden of CMR abnormalities (e.g. cardiac dysfunction, abnormal myocardial tissue characteristics such as high T1, high T2, high extracellular volume (ECV) and pathological late gadolinium enhancement (LGE)) and ECG abnormalities among post-hospitalised COVID-19 patients. The relationship of abnormal findings on both modalities and the diagnostic utility of a 12-lead ECG for CMR abnormalities were evaluated.

**Methods**: Moderate-to-severe post-hospitalised COVID-19 patients based on WHO Clinical Characterisations Score (n=212 for Chapter 3,4, n=50 for Chapter 5), age-and-comorbidities-matched uninfected controls (n=38 for Chapters 3,4, n=43 for chapter 5) underwent CMR and 12-lead ECG. Multi-faceted analysis of ECG, including repolarisation intervals i.e. corrected QT (QTc), QTc dispersion (QTc disp), corrected JT (JTc) and corrected T-peak-to-end (cTPe), and CMR parameters, (function, myocardial tissue characteristics (T1/T2/ ECV and LGE) were conducted in two phases. 1) A multicentre observational study to analyse the burden of cardiac abnormalities, the diagnostic utility of ECG for CMR abnormalities and the impact of clinical covariates (e.g. age, sex, body mass index and co-morbidities) on the ECG-CMR association. 2) A single-centre longitudinal follow-up study exploring the natural history of ECG-CMR association and the impact on the diagnostic ability of ECG over time.

**Results**: During post-hospitalisation, patients (Chapter 3, 4, n=212) had a higher burden of ECG abnormalities compared to controls (n=38) (72.2% vs 42.1%, p=0.001). CMR abnormalities among patients and controls were comparable. The diagnostic performance of routinely reported ECG features, not including the repolarisation intervals in detecting

abnormal CMR, was poor (area under the receiver operating characteristic (AUROC) of 0.56, p=0.185) with sex-dependent variabilities. Adding the repolarisation intervals particularly the QTc disp and JTc interval improved the AUROC to 0.64, p=0.002, and specifically, with QTc disp ≥ 55ms and JTc interval ≥ 340ms, the sensitivity increased from 67% in women and 90% in men to 99.9% in both sexes. The single-centre follow-up study (Chapter 5, n=50) revealed a greater burden of ECG abnormalities and longer repolarisation intervals among patients (n=50) than controls (n=43) at three-and-six months post-hospitalisation, with a decrease in ECG's diagnostic performance over time.

**Conclusions**: COVID-19 patients had a comparable burden of CMR abnormalities but a high burden of ECG abnormalities compared to age-sex-and-comorbidity-matched controls during post-hospitalisation. As the study was statistically underpowered, the outcomes were hypothesis-generating, which demonstrates significant associations of ECG and CMR parameters with sex-dependent diagnostic potential to exclude CMR abnormalities.

# CHAPTER 1: GENERAL INTRODUCTION

## 1.1 WHY INVESTIGATE ECG AND CMR?

Electrocardiography (ECG) is potentially a lifesaver for physicians working in the emergency departments or primary care settings. Essential decision-making sometimes involves potentially life and death matters and often relies on gut feelings and rapid bedside investigations such as an ECG. It is a convenient clinical tool which is inexpensive and widely accessible across many healthcare settings. From the clinical standpoint, in the absence of visual imaging tools such as bedside echocardiography, which is the case in many healthcare facilities in under-resource settings, ECG is the only tool that may 'communicate' effectively with the treating clinicians about the heart. Countless information can be deduced from just a 10-second strip of an ECG. Information on the electrophysiological function, including the conductive system, structural and mechanical function, can potentially be drawn from an ECG. ECG is an ideal tool that reflects electrical activities, namely depolarisation and repolarisation. For example, the P wave reflects atrial depolarisation, the QRS complex reflects ventricular depolarisation, whereas the QT interval including ST-T segment represents ventricular repolarisation[1]. In other words, different information is obtainable concerning the various segments of the ECG. Over the years, growing evidence has highlighted the ability of ECG to detect the 'red flag' features, potentially precursors to the development of malignant arrhythmias[2,3]. Many risk scores for cardiovascular outcomes still include ECG as one of the essential diagnostic criteria[4]. Therefore, ECG remains relevant clinically, although it is one of the oldest medical investigation tools, dating back to the period before Einthoven in the late 1800s[5].

The vast amount of information from an ECG also means that the findings can be non-specific. For example, the ST segment is reliable in detecting acute myocardial infarction but is poor in detecting acute myocarditis[6,7]. This drawback is quite fundamental as

clinically; patients have suffered complications due to unnecessary treatment decided solely based on ECG with false positive findings[8]. Moreover, tremendous financial burdens due to litigations have also been reported due to ECG misdiagnoses[9]. These disadvantages, compounded further by the need for diagnostic studies based on gold-standard tests such as cardiac magnetic resonance imaging (CMR), limit the utility of ECG as a diagnostic tool in the clinical setting. Therefore, ECG remains only a vital adjunct, complementing the roles of other investigation methods, the history and other clinical findings. Nonetheless, as the saying goes, "absence of evidence is not the evidence of absence." The lack of diagnostic studies exploring this aspect of ECG may have limited its true potential in clinical application; hence the question remains if we are using "the right tool for the right job" to unlock this potential and whether the diagnostic utility of an ECG can perhaps be further optimised.

## 1.2 CMR THE GOLD STANDARD TOOL TO DETECT MYOCARDIAL INJURY

With the advancement of science and technology in the last decade alone, we have seen rapid development in clinical medicine. Cardiac imaging, in particular, is potentially experiencing this advancement more than any other speciality in medicine. Cardiac magnetic resonance imaging (CMR) usage began in the 1970s as a medium for assessing high-energy phosphate myocardial metabolism with 31P spectroscopy in rat hearts[10]. In the following decade (1980s), the assessment of the cardiac function, morphology and characterisations of the myocardium by utilising the relaxation properties of the hydrogen (proton) called the T1 and T2 technique started[11]. In the 1990s, assessment of myocardial perfusion vasculature was made possible with the development of paramagnetic contrast agents, which was subsequently followed by viability assessment with the detection of myocardial scar in the early 2000s[11]. Ever since, MRI has undergone tremendous evolution, more than any other imaging technology, especially in the aspects of acquisition techniques[11].

The strength of the magnetic field has also increased from 0.1 to 0.2 T to 1.5 to 3T, and recently, magnetic field strength as high as 7.0T has also been used[12]. At present, acute and chronic myocardial injuries, fibrosis, regression or improvement of myocardial contractile or strain properties, coronary perfusion, and myocardial disarray, among others, are all now objectively quantifiable using the CMR[13-16]. CMR is coined a "one-stop-shop for cardiac imaging" as it is a single technology that can assess ventricular function, cardiac morphology, the vessels, perfusion, viability and metabolism all in one setting: the so-called comprehensive cardiac examination[11]. Additionally, the most recent advancement achieved with CMR has been diagnosing myocardial inflammation, such as myocarditis, with great precision that otherwise relies on the invasive method, such as the endomyocardial biopsy, as the gold standard[17]. Abnormal tissue characteristics of CMR, such as the late gadolinium

enhancement, are a reliable surrogate for fibrosis[18]. Other measures, such as T1 and T2 mapping, are highly sensitive markers of fibrosis and oedema, increasing the diagnostic confidence of CMR for inflammatory conditions[19]. Due to its versatility, CMR is the imaging gold standard modality for non-invasive assessment of myocardial injury following coronavirus disease 2019 (COVID-19) infection[20] and other viral infections[20-22]. CMR's main advantages as an investigation of choice in the future are its efficiency and safety profile. No ionisation is involved like computed tomography, yet CMR can solve many relevant clinical questions.

Despite all the advancements, we are still poor at predicting the likelihood of patients at risk of myocardial injuries, which was further compounded by limited CMR availability and accessibility evident during the COVID-19 pandemic[23]. Although previous studies have explored the association of myocardial injury with either ECG[24] or CMR individually[25,26], there needed to be more emphasis on exploring both tools together. Understanding the relationship between ECG and CMR parameters may serve as a foundation to establish ECG's diagnostic and predictive potential for myocardial injuries based on a highly accurate gold-standard tool such as CMR.

This thesis is one such effort framed around the question: What can an ECG tell us about CMR? What is the association of ECG and CMR parameters? What is the diagnostic ability of ECG in detecting myocardial abnormalities on CMR? Do different ECG parameters (e.g., routinely reported ECG features with and without the repolarisation intervals) yield various diagnostic and predictive performances for CMR abnormalities? How do clinical covariates such as sex and age, affect ECG's diagnostic and predictive performance in detecting myocardial abnormalities based on CMR?

Developing good answers to the questions of why some ECG parameters perform differently in different clinical conditions or different CMR parameters may allow us to understand the mechanistic link between cardiac electrophysiological function on ECG and biological abnormalities detected on CMR, especially in diseases with a substantial public health burden, such as COVID-19 infection (**Figure 1.1**).

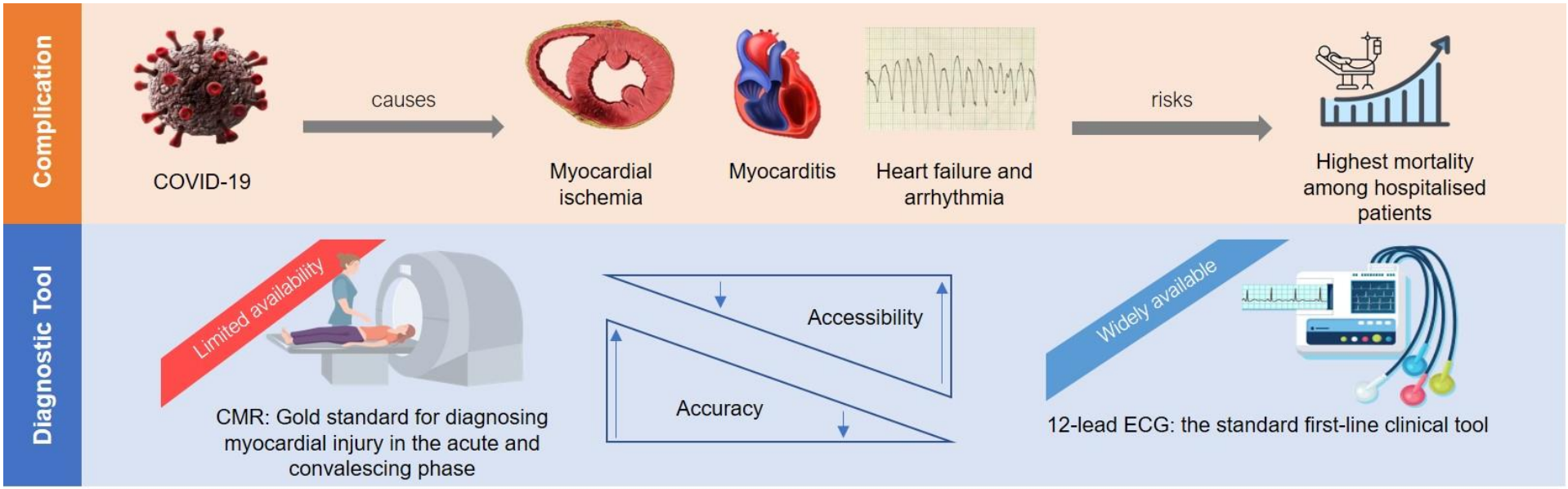


**Figure 1.1** Evaluating the diagnostic performance of 12-lead ECG to rule out myocardial injury based on CMR in post-hospitalised COVID-19 patients.

## 1.3 COVID-19 PANDEMIC

The devastating COVID-19 pandemic began in Wuhan, China, in December 2019[27]. The outbreak spread rapidly due to the air-borne nature of the illness, with mortality growing exponentially, overwhelming the healthcare systems in every country in the world[28,29]. To date, by early 2024, more than seven hundred million people have been infected, and around 7 million death has been reported globally[30], making it one of the worst and the most disruptive disasters in the last century. Beyond respiratory decompensation, it is now well established that SARS-CoV-2 causes multiorgan dysfunction in acute and post-acute phases from its interaction with the widely abundant angiotensin-converting enzyme 2 (ACE2) receptors found in the vascular endothelium in all structures such as the pneumocytes, smooth muscles in the pulmonary vessels, bronchial epithelium, epithelial cells of the intestine, kidneys, testes, blood vessels and particularly the heart[31-34].

## 1.4 CARDIAC INJURY AND THE ROLE OF COVID-19

One of the earliest reports on viral infection-associated cardiac injury dates back to the 1918 influenza pandemic[35]. Subsequently, more infectious pathogens causing cardiac injury, including SARS and SARS-CoV-2[36,37], are observed. Now, it is established that cardiac injury is a complication of SARS-CoV-2 infection affecting about a third of patients and portends high mortality, particularly in moderate-to-severe infection[26]. Early studies in Wuhan showed that individuals with cardiac injury had a 51% increase in hospital mortality[38]. Cardiac damage associated with COVID-19 may manifest as myocarditis[26,39], myocardial infarction[40], left and right ventricular dysfunction[41,42], cardiogenic shock[43,44], thrombosis[45], and malignant ventricular arrhythmia[46] during the acute and post-acute phase of infection[47]. Clinical risk factors identified include male sex, advanced age, and presence of cardiac comorbidities such as hypertension, diabetes and high body mass index (BMI)[48].

Both direct (e.g. SARS-CoV-2 viral toxicity) and indirect mechanisms (e.g. cytokine storm or hypoxemia leading to ischaemic injury resulting from respiratory distress syndrome) have been implicated in cardiac injury[49] (**Figure 1.2**). The severity of the cardiac manifestation is mainly attributed to the interaction of the viral spike protein with the host cells[34]. Although the direct mechanism caused by SARS-CoV-2 viral toxicity is not fully understood, it has been postulated that SARS-CoV-2 invades cardiac myocytes through ACE2 receptors, leading to down-regulation of ACE2 activity which in turn leads to capillary endothelial cells' dysfunction, profibrotic and proinflammatory effects[50]. An indirect mechanism occurs following exposure to the SARS-CoV-2 antigen. The T cells release anti-inflammatory cytokines as part of the cascade of dysregulated immune response, subsequently leading to cytokine storm[34]. Likewise, proinflammatory cytokines such as the interleukin-6 (IL-6) and tumour necrosis factor alpha (TNFα) protein are also released, which have been shown to

promote the formation of free radicals and reactive oxygen species, leading to myocardial tissue damage mediated by inflammation[51].

Both direct and indirect mechanisms of cardiac injury were supported by histopathological evidence from autopsy of COVID-19-positive decedents in the USA[52]. The histological evidence demonstrated the presence of direct viral toxicity, thrombotic-mediated endothelial injury, and immune-mediated injury in varying degrees, along with indications of myofibrillar or sarcomeric damage to the cardiomyocytes[52], which corroborated with the proposed mechanisms of cardiac injury in COVID-19[50]. Additionally, only a sparse distribution of SARS-CoV-2 within the cardiomyocytes was observed, thus supporting the roles of additional mechanisms other than direct injury to the heart in COVID-19[52]. Importantly, the American study also showed the first evidence of SARS-CoV-2 infection of percolating adipocytes within the myocardium and mononuclear predominant inflammatory infiltrate within the visceral epicardium[52] (**Figure 1.3**), which are essential layers involved in electrical activities of the heart. This finding supports the hypothesis that SARC-CoV-2 infects adipocytes[53], which was found to express high levels of ACE2 receptors in animal study[54]. The finding may provide a mechanistic explanation between histopathological evidence and electrophysiological findings on ECG in high-risk individuals[53,55].

Regardless of the mechanisms, screening for at-risk individuals is imperative as cardiac injury carries poor outcomes in the acute[56] and long-term phase post-COVID-19 infection[57], with ongoing burden impacting the healthcare systems globally[58].

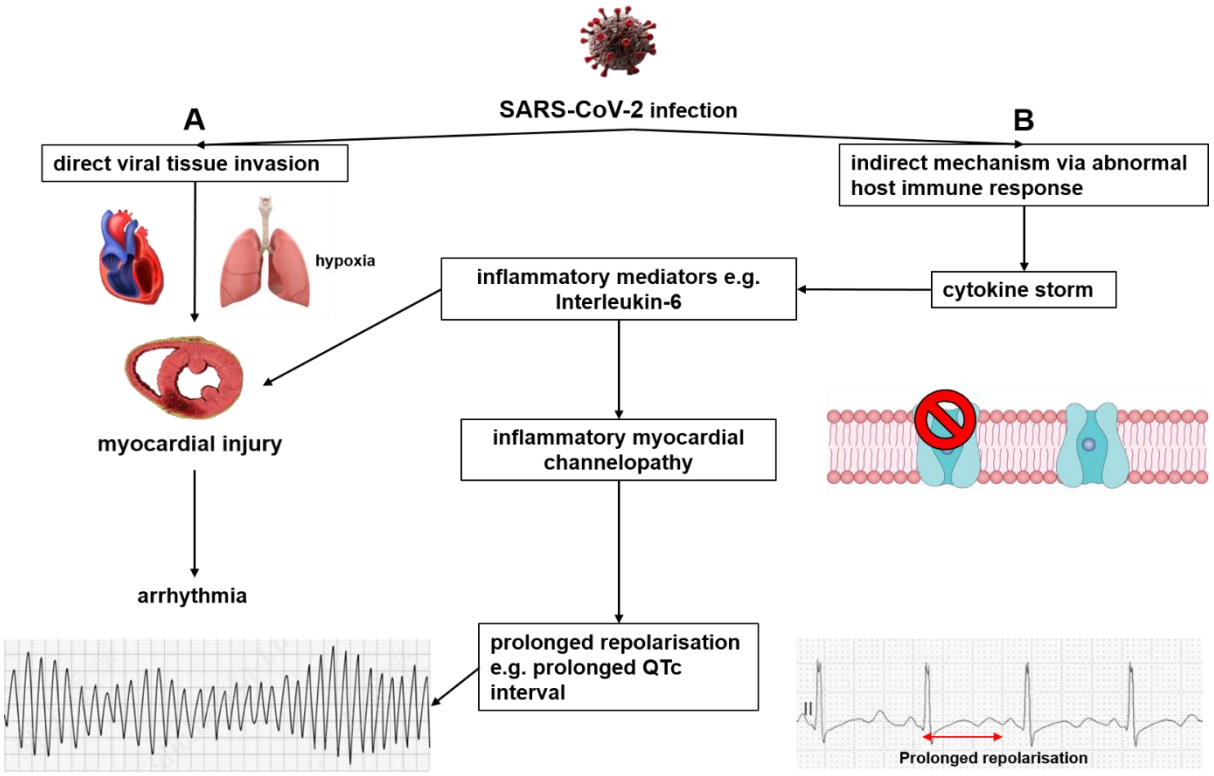


**Figure 1.2** Reputed potential mechanisms of arrhythmia in COVID-19.

**A**: SARS-CoV-2 infection may cause direct viral tissue invasion to the heart or due to lung involvement, leading to myocardial injury via hypoxia-mediated cardiomyocyte damage.
**B**: Myocardial injury can also be attributed to the abnormal systemic immune-inflammatory response triggered by the virus. This may lead to cytokine storms mediated by inflammatory mediators such as interleukin-6 (IL-6). IL-6, in particular, not only contributed to myocardial injury but also caused abnormal modulation of the ionic channels, leading to inflammatory channelopathies, which prolonged the repolarisation intervals. (Image modified from Lazzerini et al.)[59].

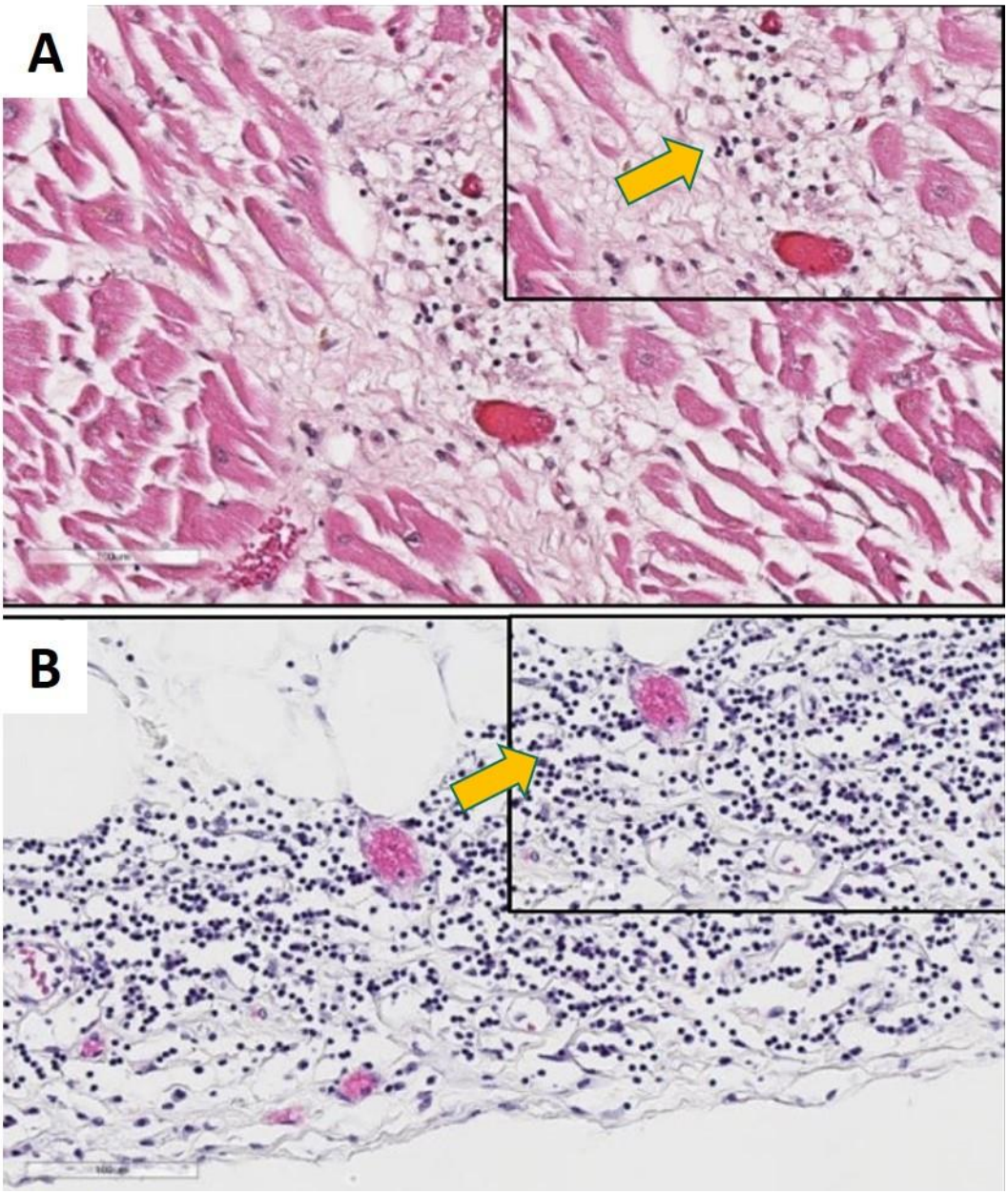


**Figure 1.3** Histopathology characteristics of cardiac injury in deceased COVID-19 patients

Haematoxylin and eosin staining of representative cardiac injury in COVID-19 patients. Patients exhibited features of direct and indirect viral injury to the heart.
**A**: Myocardial region with features of myocarditis.
**B**: Infiltration of predominantly mononuclear inflammatory cells within the visceral epicardium with surrounding adipocytes (yellow arrows pointing to inflammatory infiltrates). (Image modified from P.J Hanson et al.)[52].

## 1.5 ELECTROPHYSIOLOGICAL BASIS OF ECG

ECG is an ideal first-line screening tool for assessing patients with suspected cardiac injuries. The electrophysiological principle that underpins the 12-lead ECG is the movement of charged particles represented by intracellular and extracellular cations (Na+, K+, Ca2+), which flow across the cell membranes, generating electrical potential. As the electrical impulse spread between cells via the gap junctions[60], and travel across the heart, electrical potential difference is generated between two measurement points detectable by the ECG electrodes. The ECG machine compares, amplifies and filters the input recorded by the electrodes and generated a graphical output representation known as the ECG leads[1].

In the heart, electrical activities namely the depolarisation and repolarisation precede mechanical activities. Under normal conditions, the wave of depolarisation, which originates in the sino-atrial (SA) node, travels from the base to the apex via the electrical conduction system and from the endocardium to the epicardial layer[61]. It is essential to appreciate that repolarisation occurs in the opposite direction of depolarisation, from the epicardium to the endocardial layer. The cardiomyocytes at the epicardial layers will be the last to depolarise and the first to repolarise. Due to the inherent differences in the activities and distribution of ion channels between the epicardium, mid-myocardium (M-cells) and endocardium, the action potential duration across the thickness of the ventricular wall is not the same, giving rise to the phenomenon of inherent transmural dispersion of repolarisation (TDR)[62] (**Figure 1.4)**.

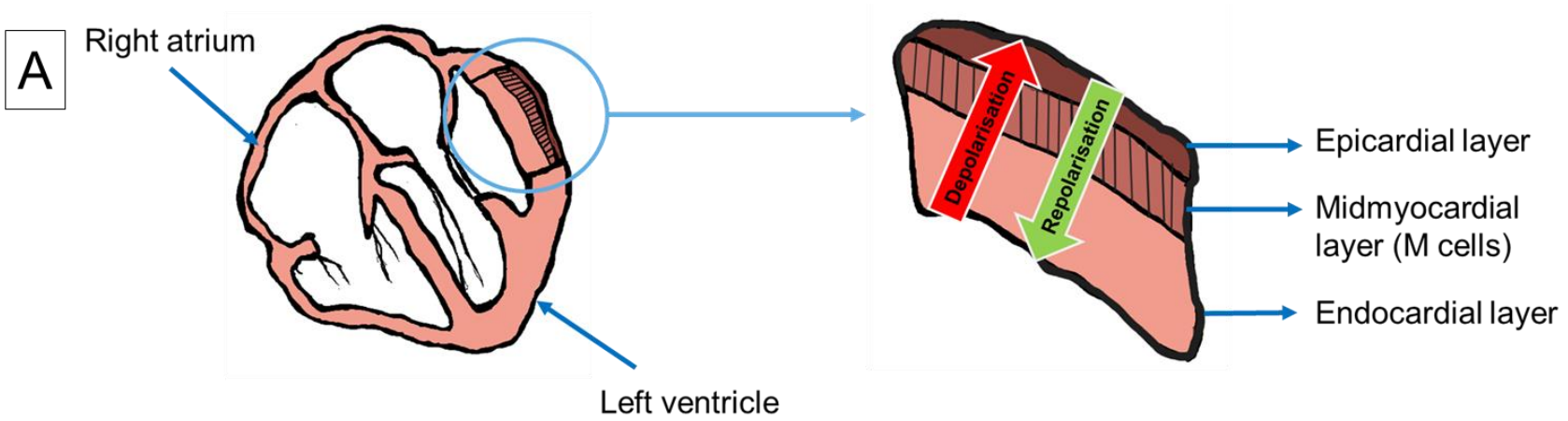
A
Right atrium
Left ventricle
Depolarisation
Repolarisation
Epicardial layer
Midmyocardial layer (M cells)
Endocardial layer

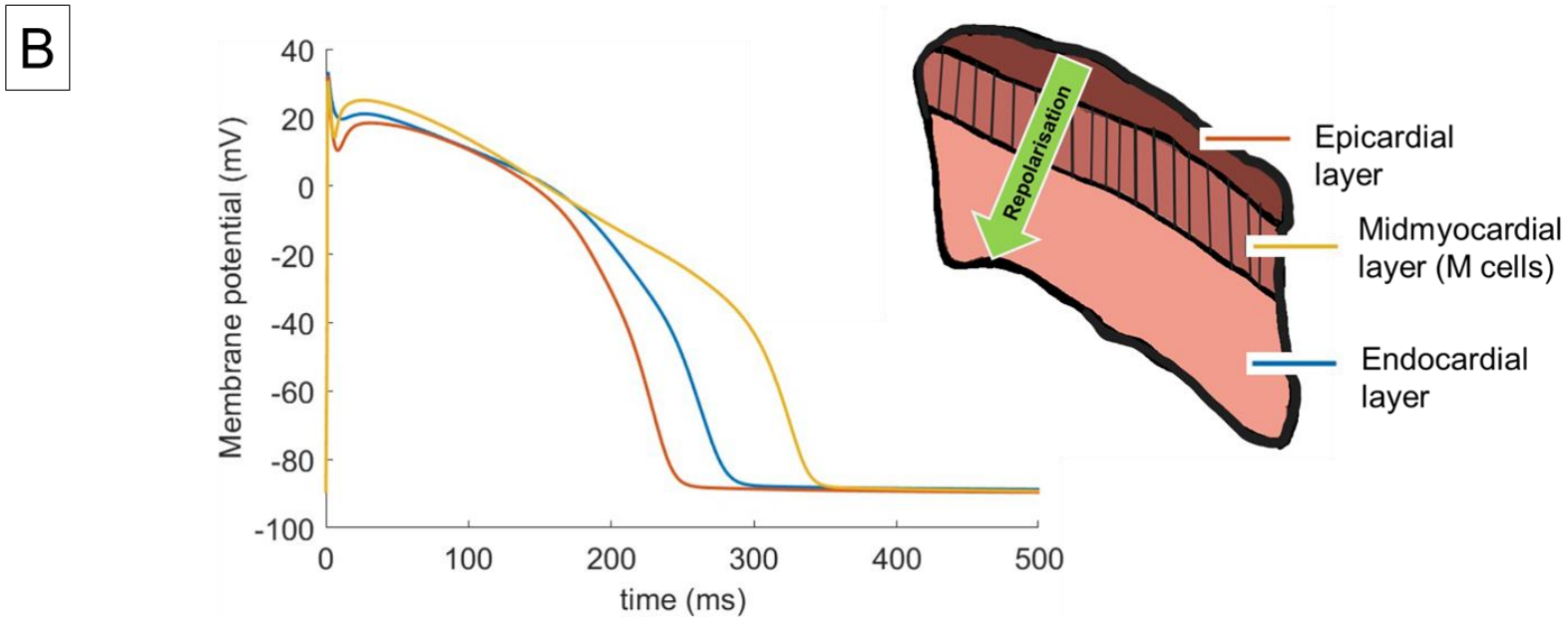
B
Membrane potential (mV)
40
20
0
-20
-40
-60
-80
-100
0
100
200
300
400
500
time (ms)
Repolarisation
Epicardial layer
Midmyocardial layer (M cells)
Endocardial layer

**Figure 1.4** Repolarisation duration varies between myocardial layers.

**A**: QT interval encompasses ventricular depolarisation (red arrow), followed by repolarisation (green).
**B**: The repolarisation duration of the myocardium varies between the layers. The outmost layer (epicardium) has the shortest duration, followed by the innermost layer (endocardium). The midmyocardial layer, also known as M cells, displays the most extended duration for repolarisation. The end of epicardial repolarisation corresponds with the peak of the T wave on the surface ECG. The end of endocardial/midmyocardial repolarisation corresponds to the end of the T wave. The longer the repolarisation period, the risk of developing arrhythmia is also increased. (Image illustrated by Aqeel Azlan, in reference to work by Drouin et al.)[63].

## M CELLS

There are three different cell types across the myocardial wall: epicardial, mid-myocardial (M cells) and endocardial cells, each with distinct action potential duration[64]. M cells are the predominant myocardial layer that contribute to the inherent heterogeneity in TDR across the ventricle[64]. M cells have been discovered in animal and human studies in the early 1990s[64-66], demonstrating similar histological features to cells in endocardial and epicardial layers but shared electrophysiological properties intermediate between those of ventricular and conducting (Purkinje) cells[66]. Similar to Purkinje fibres, M cells have distinctively longer APD than epicardium and endocardium[64], and are also more sensitive to produce early and delayed afterdepolarisations in response to pharmacologic agents[65]. The distinctive ability for APD prolongation in M cells is attributed to a smaller, slowly activating delayed rectifier current ($I_{Ks}$)[67] and a larger late sodium current (late $I_{Na}$)[68]. Drouin et al., who first reported the discovery of M cells in the human ventricle, suggested that M cells could be responsible for the repolarisation abnormalities such as the  T wave, QT syndrome, and the U waves frequently observed on the ECG[63].

## ECG CHANGES IN COVID-19

Deviations in electrical activation and conduction, including pathology-induced abnormalities, may be inferred from the 12-lead ECG through evaluation of various ECG intervals. Abnormalities and prolongation of repolarisation parameter,s including the ST-T changes[69], QT[70,71] and TPe interval prolongation[72], have been reported in COVID-19 and were associated with increased risk of arrhythmias and mortality[73-76]. Other ECG changes that have been reported in COVID-19 are summarised in **Table 1**. Essentially, the association of these ECG changes with myocardial injury is unclear, as CMR or histopathological-associated findings were rarely reported.

**Table 1** Previous studies* on COVID-19-related ECG reports

| ECG parameters | Reference |
|---|---|
| ST-T changes | Alsagaff et al.[69], Saririan et al.[77], Liu et al.[78], Romero et al.[79], Regan et al.[80], Nemati et al.[81], McCullogh et al.[82] |
| QT prolongation | Mehraeen et al.[66], Banai et al.[75], Schiavone M et al.[83], Nemati et al.[81] |
| TPe interval prolongation | Mahmoudi E et al.[72], Yenerçağ M et al.[84] |
| Left and right bundle branch block | Alsagaff et al.[69], Bertini et al.[41], McCullogh et al.[82] |
| Fragmented QRS | Yildirim et al.[73], Long B et al.[74] |
| Axis deviations | Loghin et al.[85], Yang D et al.[86] |
| PR abnormalities and heart block | Long B et al.[74], Pavri et al.[87], Liu et al.[78] |
| S1Q3T3 pattern | Bertini et al.[41], Jia He at al.[88] |
| Brugada features | Vidovich et al.[89] |
| Premature atrial and ventricular complex | McCullough et al.[82] |
| Atrial Fibrillation/Flutter | Reynbakh et al.[90],Xie et al.[57], Nemati et al.[81] |
| Supraventricular tachycardia | Reynbakh et al.[90] |
| Ventricular arrhythmia | Reynbakh et al.[90], Xie et al.[57], Liu Q et al.[91], Solaimanzadeh et al.[92] |

* The list is non-exhaustive.

## SYSTEMIC INFLAMMATION-RELATED MYOCARDIAL CHANNELOPATHY

It has been recently speculated that systemic inflammation-related myocardial channelopathies may contribute to ionic remodeling[93] and are one of the neglected risk factors of arrhythmias[94]. The infection triggers myriad immune responses, as mentioned earlier, which initially aimed to protect the host against the pathogenic effect of the antigen. For instance, inflammatory cytokines such as TNFα, IL-1 and IL-6 have been suggested to alter action potential durations by decreasing specific cardiac $K^+$ currents or/and increasing L-type $Ca^{2+}$ currents[93]. The reduction in transient outward $K^+$, resulting from the downregulation of channel expression (mediated by the inflammatory cytokines), prolongs the myocardial action potential duration, corresponding to the prolongation of repolarisation intervals on surface 12-lead ECG[62,95] (**Figure 1.5** and **Figure 1.6**).

Moreover, recent histopathological evidence has also raised the possibility of the link between epicardial fat, cardiac fibroblasts, myofibroblast and myocardial inflammation in COVID-19[96,97]. The link is demonstrated by the significant association of epicardial adipose tissue (EAT) with dense macrophage infiltrates, pro-inflammatory cytokines such as IL-6 and, more importantly, the ACE2 receptors[98,99]. EAT could be a functional reservoir for immune response amplification to pathogens such as SARS-CoV-2, with potential pathological perturbations to the ventricular repolarisation due to its direct anatomical and functional contiguity with the myocardium[96].

Although arrhythmia due to epicardial and pericardial fibrosis in the post-hospitalisation phase has been reported[92], the evidence is limited by retrospective acute cases of ECG reports in COVID-19 with no CMR or histological associations[69,82]. Therefore, whether the observed ECG correlates with myocardial injury on CMR and poor cardiovascular outcome

in the medium to longer term is subject to debate, and the mechanisms by which cardiac abnormalities contribute to ECG abnormalities following COVID-19 remain uncertain. Although the current guidelines[100,101] recommend the use of ECG in post-COVID management, the evidence, especially from prospective studies, in support of its use as a screening tool is lacking**.** Therefore, to use it effectively as a screening tool in the context of post-hospitalised COVID19, we need a much clearer understanding of what abnormalities it can detect, and its diagnostic and predictive ability in identifying them.

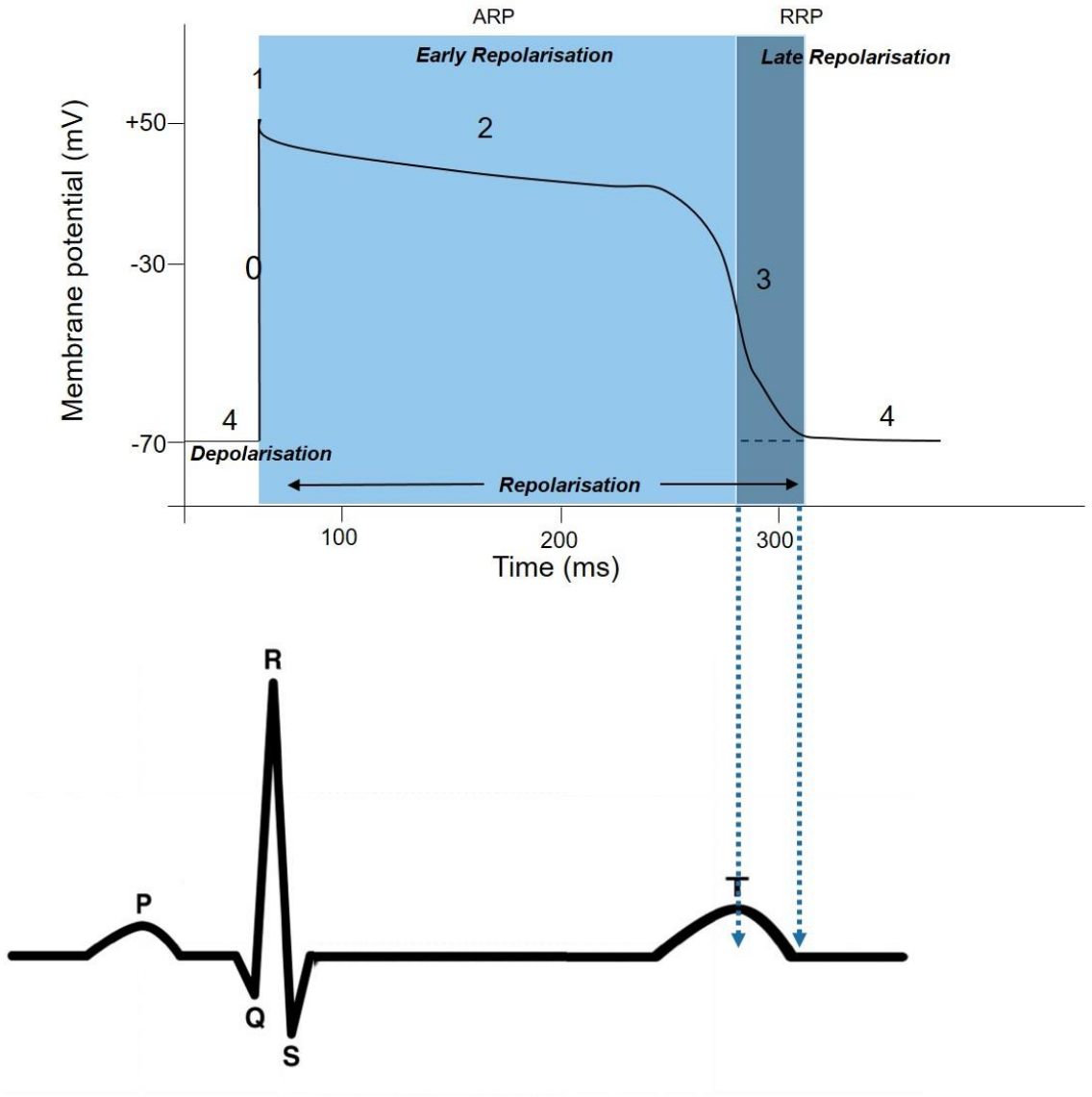


**Figure 1.5** Action potential of the myocardial cell.

The Action potential of the myocardial cells is divided into 4 phases. Phase 0 denotes the rapid depolarisation phase. Voltage-gated Na+ channels open, causing Na+ influx into the cardiomyocyte, changing membrane potential from -70mV to +50mV. Phase 1 represents Na+ channel inactivation and K+ channel activation. This results in a transient outward K+ current, denoting the onset of repolarisation. Phase 2 represents the plateau period. Voltage-gated L-type Ca2+ channels are activated, resulting in Ca2+ influx. The Ca2+ influx balances the K+ efflux, creating the plateau corresponding to the absolute refractory period (ARP). No stimulus can initiate any action potential during this phase. Phase 3 represents a rapid repolarisation period involving K+ efflux through activating the rapid delayed rectifier K+ channels, with concurrent inactivation of the voltage-gated Ca2+ channels. The midway of phase 3 till the end of phase 3 corresponds to the relative refractory period (RRP), where a strong enough stimulus may evoke an action potential. Phase 3 corresponds to the T wave on surface ECG (dark blue arrows). Phase 4 denotes the resting membrane potential of the cardiomyocytes, with the electrochemical gradient reverting to -70mV.

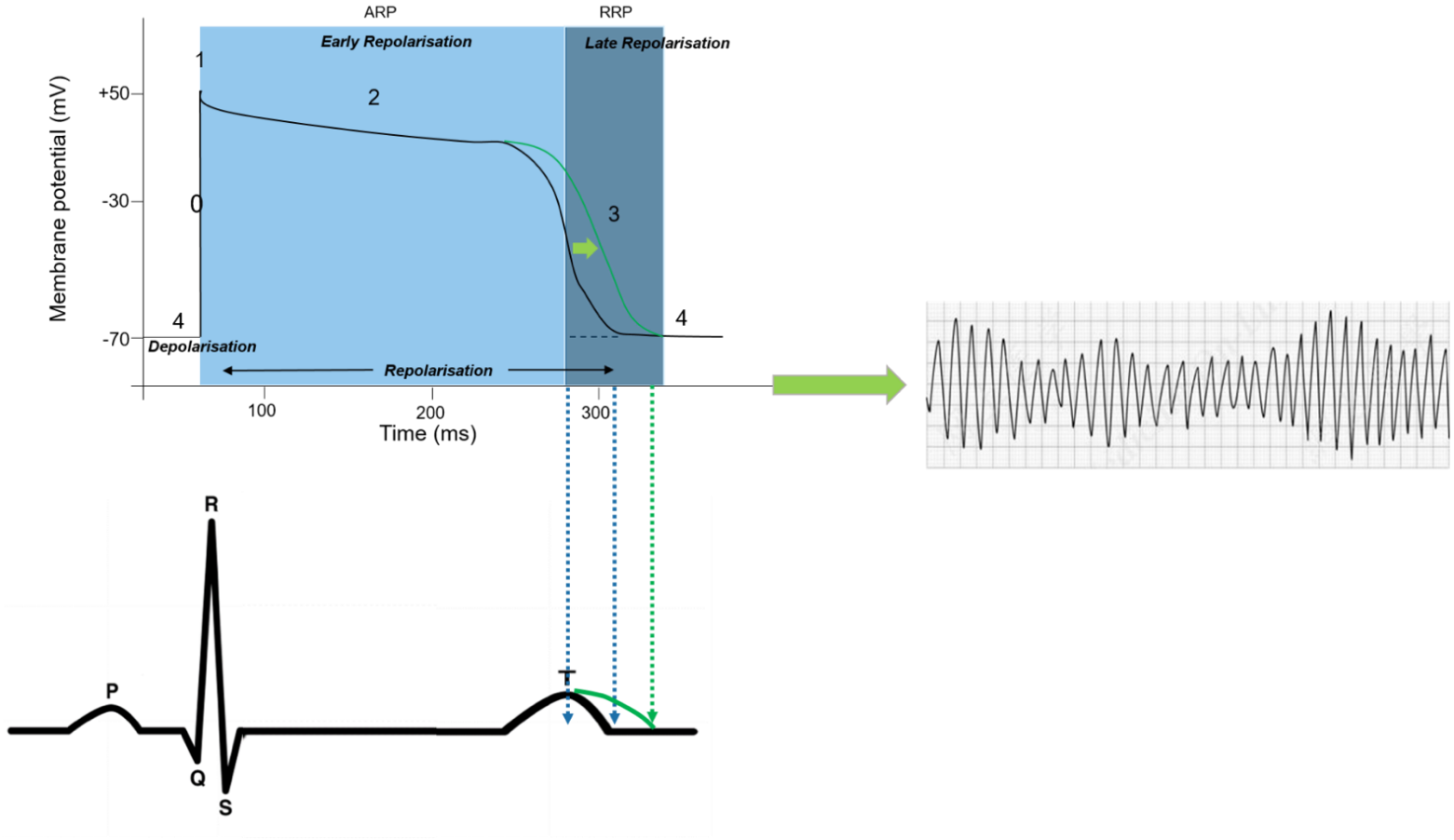


**Figure 1.6** Prolongation of repolarisation and risk of arrhythmia.

The action potential of the myocardium is divided into phases 0, 1, 2, 3 and 4. Phases 2 and 3 correspond to the repolarisation of the ventricle and ST-T segment on the surface ECG. Phase 3 in particular, corresponds with the late repolarisation phase or the relative refractory period (RRP) of the myocardium, which coincides specifically with the peak-to-end T wave (TPe). Prolongation of the relative refractory period (green line Phase 3) may correlate with a longer TPe interval (dotted green arrow), which renders the myocardial cells at a higher risk of ventricular arrhythmia.

## 1.6 ASSOCIATIONS OF ECG AND CMR PARAMETERS

As stated earlier, CMR imaging has several advantages over the 12-lead ECG, as it permits an accurate visual assessment of cardiac structure, function, and myocardial tissue characteristics. However, globally, its access and availability remain restricted due to high costs and limited domain expertise[23,102].

Studying the associations between ECG and specific CMR parameters may offer a pragmatic solution to improve disease detection, notably in under-resourced medical settings. Collectively, previous related studies have been limited to non-infective conditions, such as, ventricular hypertrophy with CMR-based myocardial mass[103], late gadolinium enhancement (LGE) based localisation of myocardial scarring[104-106] and myocardial infarction[107], QRS-based characterisations of hypertrophic cardiomyopathy (HCM)[108], conduction abnormalities with LGE-evident fibrosis[109,110], and more recently, the association of ECG parameters with diffuse myocardial fibrosis based on CMR tissue characteristics[111-113]. Although these studies emphasised the ongoing clinical significance of ECG-CMR-based associations, their clinical application in COVID-19 remains elusive.

## 1.7 HYPOTHESIS

i. Patients post-hospitalisation for moderate-severe COVID-19 infection will have a higher burden of cardiac abnormalities (ECG and/or CMR) compared to age, sex, and risk-factor matched controls.
ii. Those with CMR abnormalities like abnormal myocardial tissue characteristics will likely to have ECG abnormalities and prolonged ventricular repolarisation.
iii. 12-lead ECG will have a reliable diagnostic accuracy for screening post-hospitalised COVID-19 patients with CMR abnormalities.
iv. There are significant associations between covariates such as age and sex in the diagnostic and predictive performance of 12-lead ECG for CMR abnormalities in COVID-19.
v. Systemic inflammatory response is significantly associated with ventricular repolarisation on 12-lead ECG in the post-acute phase of COVID-19 infection.

## 1.8 RESEARCH AIM

To assess the burden of cardiac abnormalities on ECG and CMR, explore the association of ECG and CMR parameters and determine the diagnostic and predictive utility of ECG in detecting myocardial abnormalities on CMR among moderate-to-severe post-hospitalised COVID-19 patients.

## 1.9 THESIS OUTLINE

**Chapter 1** describes the general context, gaps in the literature, and the research questions. In **Chapter 2**, general methods are outlined to address the research questions. **Chapter 3** explores the burden of cardiac abnormalities and ECG associations with CMR abnormalities among post-hospitalised COVID-19 patients relative to controls. Relationship of ECG parameters with composite and individual markers of CMR abnormalities such as T1 (myocardial fibrosis), T2 (myocardial oedema), extracellular volume (ECV) (interstitial fibrosis), LGE (replacement fibrosis) and left ventricular ejection fraction (LVEF) are assessed. **Chapter 4** presents the diagnostic and predictive performance of the ECG for CMR abnormalities, adjusting for covariates such as sex, age, BMI and comorbidities. This chapter describes the contribution of sex-based differences in ECG parameters, the diagnostic and predictive performance and ECG association with myocardial abnormalities on CMR. **Chapter 5** explores the ECG-CMR association among post-hospitalised COVID-19 patients in a single-centre cohort at three- and six-month follow-up, to understand the natural history of the disease concerning the ECG-CMR associations, and the diagnostic performance of ECG over time. Finally, in **Chapter 6**, the key findings are summarised and the potential future research is discussed for the diagnostic and predictive role of ECG in detecting myocardial abnormalities on CMR.

# CHAPTER 2: GENERAL METHODS

## 2.1 OVERVIEW

The study was approved by the Yorkshire and The Humber-Leeds West Research Ethics Committee (reference 20/YH/0225) and registered on (ISRCTN10980107).

## 2.2 INCLUSION CRITERIA

Subjects were eligible for inclusion in the study if:

i) Aged between 18 and 80 years.

ii) Moderate to severe (WHO Score 4-9, **Figure 2.1**) acute respiratory distress syndrome Coronavirus-2 (SARS-CoV-2 infection) (see below for definition), confirmed by a reverse transcription and polymerase chain reaction (RT-PCR) nasopharyngeal swab test[1]. (*During the data collection period, alpha and delta were the predominant SARS-CoV-2 variants in the United Kingdom*[114]).

iii) Controls were non-hospitalised subjects without symptoms or signs of a respiratory tract infection of coronavirus disease, who were screened for SARS-CoV-2 antibodies and tested negative—matched with patients for age, risk factors and co-morbidities.

[1] RT-PCR Nasopharyngeal swab test showed high sensitivity (>95%) to detect all strains of SARS-CoV-2 virus especially the alpha and delta variants.

## 2.3 EXCLUSION CRITERIA

Subjects were excluded from the study if any of the following was present:

i) Contraindications to MRI (metal implant in body, known claustrophobia, pacemakers, contrast allergy).

ii) Severe comorbidities – end-stage renal, cardiac, liver, neurological disease, and

iii) Patients who did not complete cardiac MRI or had incomplete ECG, including having less than eight interpretable leads.

## 2.4 CLINICAL ASSESSMENT

### MODERATE-TO- SEVERE SARS-COV-2 INFECTION

The severity of acute illness on admission was defined by the World Health Organisation (WHO) progression scale[115] (**Figure 2.1**). All patients with clinical signs of pneumonia, such as respiratory rate > 30 breaths/min, severe respiratory distress, SpO2 < 90% (on room air) and were hospitalised for more than 48 hours, were considered to have moderate-to-severe COVID-19[116].

| Patient State | Descriptor | Score |
|---|---|---|
| Uninfected | Uninfected; no viral RNA detected | 0 |
| Ambulatory mild disease | Asymptomatic; viral RNA detected | 1 |
| | Symptomatic; independent | 2 |
| | Symptomatic; assistance needed | 3 |
| Hospitalised: moderate disease | Hospitalised; no oxygen therapy* | 4 |
| | Hospitalised; oxygen by mask or nasal prongs | 5 |
| Hospitalised: severe diseases | Hospitalised; oxygen by NIV or high flow | 6 |
| | Intubation and mechanical ventilation, $pO_2/FiO_2$ ≥150 or $SpO_2/FiO_2$ ≥200 | 7 |
| | Mechanical ventilation $pO_2/FIO_2$ <150 ($SpO_2/FiO_2$ <200) or vasopressors | 8 |
| | Mechanical ventilation $pO_2/FiO_2$ <150 and vasopressors, dialysis, or ECMO | 9 |
| **Dead** | Dead | 10 |

**Figure 2.1** WHO Clinical Characterisation of COVID-19.

It is adapted from the WHO Working Group on the Clinical Characterisation and Management of COVID-19. Lancet Infect Dis 20.8 (2020): e192-e197[115].

## 2.5 ELECTROCARDIOGRAPHIC MEASUREMENTS

### MANUAL VERSUS AUTOMATED QT MEASUREMENT

Automatic measurement of QT interval using commercial ECG machines offers considerable advantages in terms of its repeatability in measurement and rapid testing at lower cost[117]. However, significant errors in automatic measurement are not uncommon[118]. Errors in automatic measurement may occur due to recording factors or biological noise, and it has been previously reported before that automated ECG interval values can still be generated despite the leads being disconnected[119]. Such extreme incidents raise questions about whether the algorithm used in these commercial electrocardiography machines truly evaluates these ECG intervals. Furthermore, in a study measuring more than 8000 carefully selected ECGs with minimal biological noise, the difference between manual and automatic measurement was approximately ± 30 ms, larger than the required change precision of around 5 ms in QT studies[119]. The substantial errors contributed partly due to the challenge in the determination of terminal T waves[119]. Likewise, automatic reporting can also be misleading as the system may suppress the QT assessment statement if the heart rate is greater than 100 beats per minute[120].

Manual measurement has been advocated to overcome these biases. However, there needs to be a universal or standardised method of how this should be carried out. Some specialists recommend taking the average QT of three to five consecutive beats from a single lead at a paper speed of 50 mm per second[121]. Alternatively, the longer of one QT measurement between lead II and lead V5 using the universal paper speed (i.e. 25 mm per second) was also advocated[120]. Single lead II measurement is the most frequently advocated, although the practice is based mainly on custom and lacks evidence to substantiate its use[118]. Although

single lead II measurement may seem the most pragmatic from the electrophysiological standpoint, it overlooks a significant inherent variability due to the difference in projections of the three-dimensional T wave loop in different leads, which may result in substantial imprecision[118].

## AVERAGE VS MAXIMAL QT MEASUREMENT

Conventionally, interval such as the QT parameter, is taken from the average values from all the 12 leads[122], although there is no uniformity as to which lead or combination of leads is the recommended approach[122]. However, significant prolongation of repolarisation intervals has been demonstrated, localized to regions with high burden of subendocardial scarring[123]. In other words, an ECG taken in the same instance from an individual, may demonstrate an interval prolongation in one lead, but a normal value in another lead which analyses the heart from a different angle, leading to increased dispersion of the electrical conduction such as the repolarisation intervals[124]. Therefore, although considered a time-consuming method, some investigators considered taking the maximal QT interval in any lead of a standard 12-lead ECG to be the most accurate approach[124], and is more sensitive to detect myocardial injuries compared to the average QT. Henceforth, to avoid inaccuracies, especially in conducting research, the measurement of 12-lead ECG[118] and testing the lead with the maximal interval, formed the basis of the analysis in the present study.

## ECG ACQUISITION AND ANALYSIS

All patients underwent a 12-lead ECG on the same day as the CMR scan. Abnormal ECG parameters were interpreted in reference to the ECG features described in the Minnesota Code of Electrocardiographic Findings, a standardised ECG classification in epidemiology studies and clinical trials[125]. Standard ECG terms Group A and Group B ECG parameters are regularly used throughout this work and are defined in **Table 1**.

Depolarisation and repolarisation ECG measures are summarised in **Figure 2.2** and primarily focused on repolarisation intervals which included QT interval (denotes ventricular depolarisation and repolarisation), QT peak interval (denotes ventricular depolarisation and epicardial repolarisation), QT dispersion (represents myocardial repolarisation heterogeneity), JT (denotes only ventricular repolarisation) and T-peak-to-T-end or TPe interval (marker of transmural dispersion of repolarisation).

The ECG analysis for PR interval and QRS duration are automatic, but specific ECG intervals, particularly the repolarisation parameters, were manually analysed using Adobe Acrobat Pro DC (version 2022.001.20085) and Microsoft Excel Professional Plus 2019 (Product ID: 00414-50000-00000-AA821). Each digitised ECG was magnified to 400% for optimal resolution. Intervals were measured by selecting the 'snap to intersection' option for snap types and 'perimeter tool' for Adobe measurement types. The terminal end of the T-wave was initially identified using the tangent method (described below) in all the 12 leads. The intra and inter-observer variability were assessed with correlation coefficient (ICC) for repolarisation measures (e.g. QTc), which were 0.88 and 0.86, respectively.

**Table 1** ECG definitions.

| **ECG Parameter**s | **Definitions** |
|---|---|
| G**ROUP A:** | Composite of ECG features, which include: |
| ECG abnormalities or routinely reported ECG parameters (both are used interchangeably throughout) | Presence of any arrhythmia (i.e. atrial fibrillation, atrial flutter, premature ventricular complexes (PVC) and premature atrial complexes (PAC)) **or** abnormal axis or heart block or poor QRS progression **or** fragmented QRS (fQRS) **or** bundle branch block (including left bundle branch block, right bundle branch block, incomplete bundle branch block and non-specific intraventricular conduction delay) **or** ST-T changes[126]. |
| **GROUP B:** | Repolarisation related parameters |
| QT interval | The onset of the QRS complex to the end of the T wave. |
| QT Peak interval | The onset of the QRS complex to the peak of the T wave. |
| JT interval | Terminal end of the QRS (J point) to the end of the T wave. |
| JT Peak interval | The terminal end of QRS (J point) to the peak of the T wave. |
| T Peak-to-T-end interval | The peak of the T wave to the end of the T wave. |
| T Peak | The maximum positive or negative deflection of the T wave from the isoelectric line. |
| QT dispersion | The difference between the longest and the shortest QT interval. |

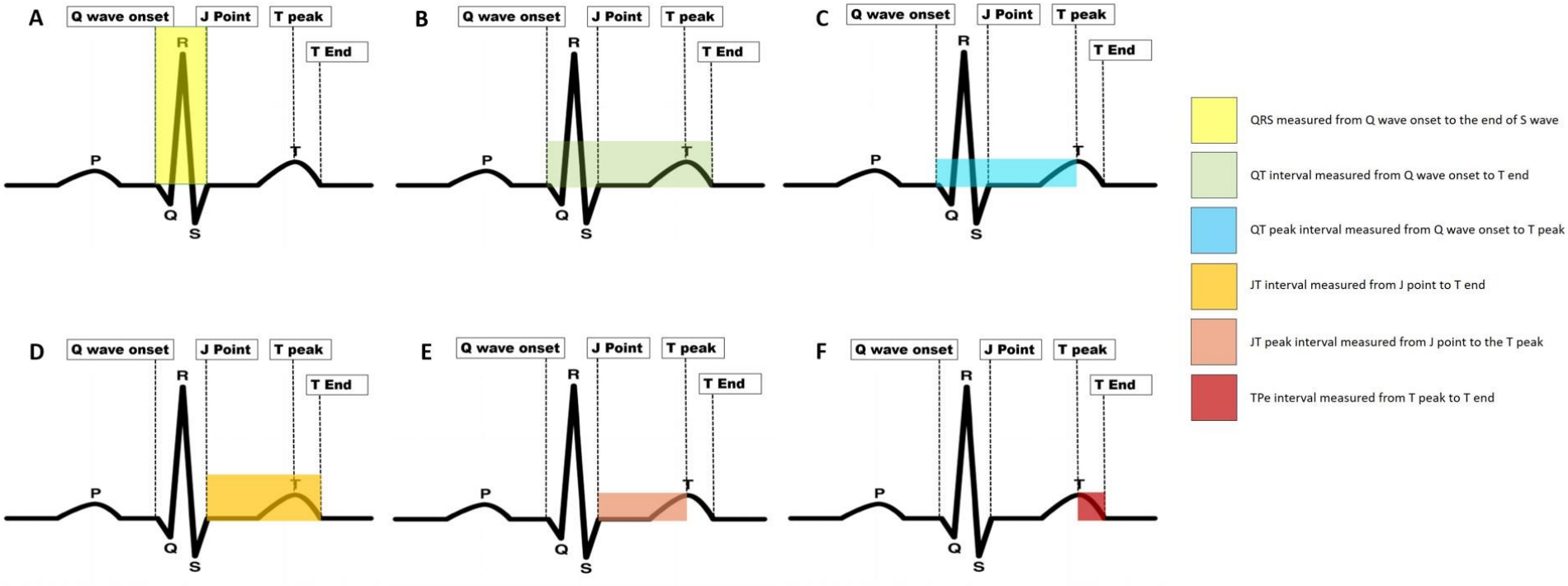


**Figure 2.2** Different components of ECG depolarisation and repolarisation.

### TANGENT METHOD

One of the most challenging parts of measuring the repolarisation parameters, such as the QT interval, is determining the end of the T wave[127]. The tangent method has been recommended as the standard manual method[128] to determine the end of the T wave in ECG with smaller inter-reader differences and better reproducibility[129,130]. In this method, a line is drawn down the steepest slope of the terminal limb of the T wave[128]. The terminal end of the T wave is identified by the intersection between the baseline and the tangent drawn along the steepest angle of the descending arm of the T-wave (**Figure 2.3**)[128]. The baseline is defined as the isoelectric line (TP interval or PR segment) on a standard ECG[131]. In instances where there is a bifid T wave, the second peak is included should it be at least half the amplitude of the first peak[132].

The longest QT interval among the 12 leads was recorded. The longest JT interval was determined by subtracting the mean QRS duration (autogenerated by the ECG machine) from the longest QT. QT peak interval was measured in all 12 leads by subtracting the TPe interval from the QT interval. The longest TPe interval was taken only from the representative lead II and all the 6 precordial leads (V1-V6)[130] (**Figure 2.3**).

For the measurement of the repolarisation intervals with bundle branch block (BBB), QT intervals were modified by subtracting 50% of the length of the BBB-QRS from the measured QT interval ($QT_m = QT_{BBB} - 50\%\ QRS_{BBB}$)[133]. On the other hand, to minimise the selection bias in the assessment of axis deviation[134], fragmented QRS [135] and ST-T changes[136], 21/212 (9.9%) of bundle branch block ECGs were excluded specific only for the analysis of these ECG features in **Chapter 3** and **4**.

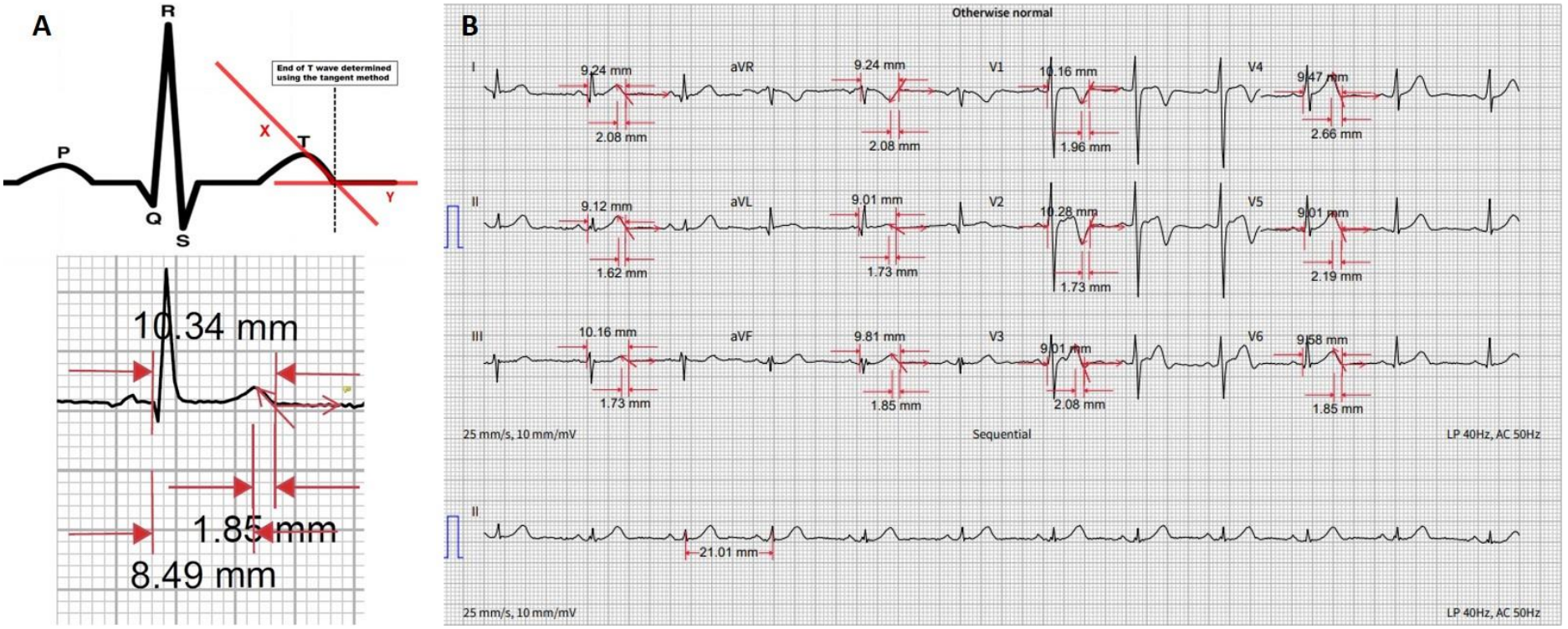


**Figure 2.3** Tangent method for objective determination of terminal T wave.

**A**: Tangent method displayed by the redlines on individual lead (isoelectric line (Y) intersecting with the tangent drawn along the steepest angle of the descending limb of the T wave) (X).

**B**: Representative case of tangent method analysis conducted on 12 leads ECG. The measurement from each lead in millimetres (mm) was subsequently converted to milliseconds (ms) using Excel (mm x 40 = ms).

## HEART RATE CORRECTION

Heart rate-corrected intervals were generated using Bazett's formula (e.g., Corrected QT interval [QTc] = QT/√R-R interval in second)[137]. The inter-rater correlation coefficients for QTc and corrected JT interval (JTc) between the two observers were 0.88 and 0.86 respectively.

## 2.6 CARDIOVASCULAR MAGNETIC RESONANCE IMAGING

The CMR protocol included standard and advanced parametric mapping sequences. The following CMR sequences were used to measure study endpoints:

i) Cine imaging is used to assess cardiac volume, function, and mass.
ii) Late gadolinium enhancement to assess for myocardial fibrosis.
iii) Native T1 mapping, native T2 mapping and ECV to assess for interstitial fibrosis or myocardial oedema.

All scans were undertaken at 3 Tesla (3T) (Siemens Healthineers, Erlangen, Germany or Philips Healthcare, The Netherlands) for **Chapter 3** and **4** (multi-centre), and 3 Tesla (3T) (Siemens Healthineers, Erlangen, Germany) for **Chapter 5** (single-centre).

## VENTRICULAR INDICES (VOLUMES, FUNCTION)

### ACQUISITION

Cine steady-state free precession (SSFP) imaging was used to acquire cardiac volumes as previously described[138]. Horizontal long axis (HLA), vertical long axis (VLA), left ventricular outflow tract (LVOT) and short axis (SA) stack cine images were acquired as shown in **Figure 2.4** at the end of the expiration to minimise the effects of respiratory motion. Scan parameters were typically: TR/TE = 3.16/1.38ms; R = 3; flip angle = 65°; field of view = 360 × 270 mm, matrix 208 × 139, slice thickness/spacing 7/3mm.

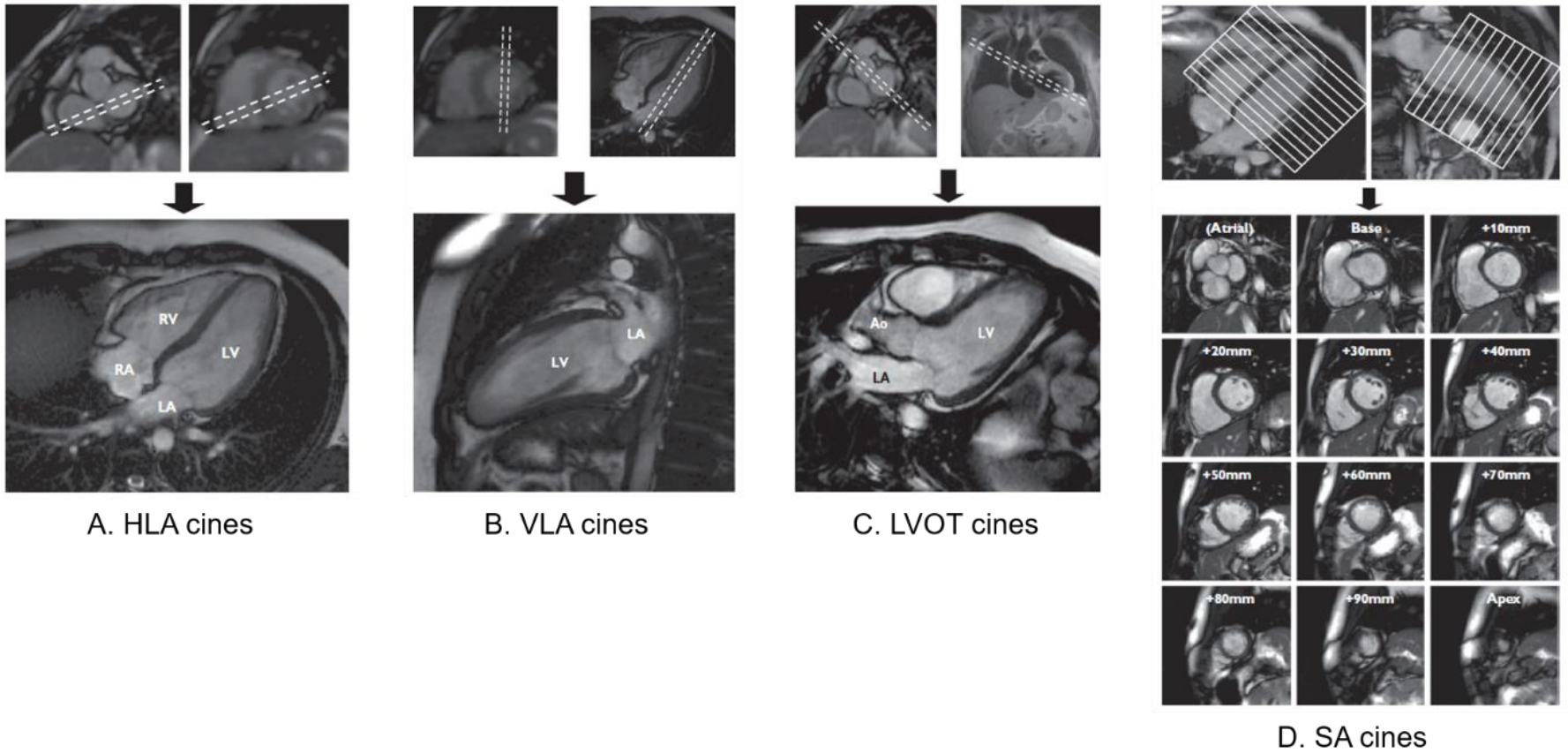


**Figure 2.4** Cine images on cardiac magnetic resonance. HLA, horizontal long axis; LVOT, left ventricular outflow tract; SA, short axis; VLA, vertical long axis.

## CMR ANALYSIS

Left ventricular (LV) short axis epicardial and endocardial borders were manually contoured at the end diastole and end systole as previously described[139] **(Figure 2.5)**. LV and RV end-systolic (ESV) and end-diastolic (EDV) volumes were used to calculate stroke volume (SV)[140]. Ejection fraction (EF) for both LV and RV were calculated as EF = SV/EDV. LV mass was calculated by subtracting the endocardial volume from the epicardial volume using the myocardial specific gravity as 1.05 g/cm[141]. LV papillary muscles were included as part of LV end-diastolic and end-systolic volumes, and excluded from LV mass.

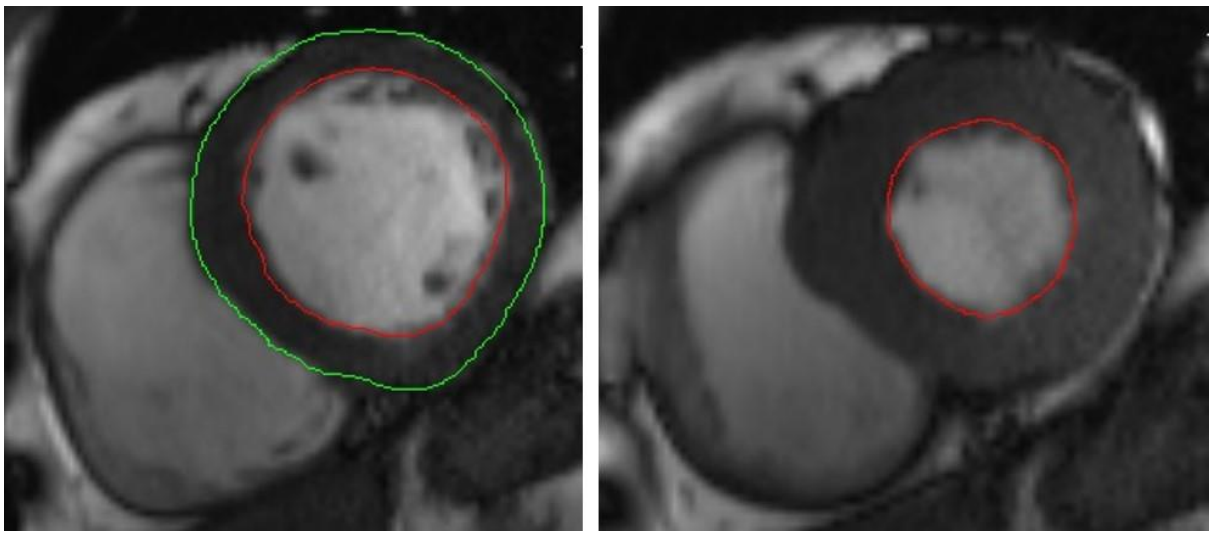

**Figure 2.5** Epicardial and endocardial contours drawn in diastole (*left*) and endocardial contour in systole (*right*). Myocardial mass is calculated by subtracting the endocardial volume from the epicardial volume during diastole (*left*).

## LATE GADOLINIUM ENHANCEMENT

### ACQUISITION

Late gadolinium imaging was acquired using a T1-weighted phase-sensitive inversion recovery sequence following a bolus injection of 0.15 mmol/kg of body weight of contrast agent (Dotarem) followed by a 10 ml saline flush. Typical scan parameters: [TR/TE/TI = 3.1/1.22 ms/subject-specific ms; R = 2; flip angle = 55°; matrix = 144×256, field of view 380×285 mm, slice thickness = 8 mm, spacing = 2mm.] as previously described[142].

### LGE ANALYSIS

LGE was quantified using cvi42 software (Circle Cardiovascular Imaging Inc., Server Version 5.13.7, Calgary, Canada). Endocardial and epicardial borders were drawn on the phase-sensitive inversion recovery (PSIR) images alone with a reference region of interest (ROI) with normal myocardial intensity as a 'remote' region (**Figure 2.6**). Care was taken to exclude artefacts, blood pool, fat and pericardium. The 5 standard deviations (SD) approach quantified hyper-enhanced pixels as a percentage of the enhanced myocardium and divided by the absolute left ventricular mass to determine LGE mass[142]. LGE was visually classified as follows:

*1) LGE absent,*

*2) possible/probable myocarditis pattern,*

*3) possible/probable myocardial infarction pattern,*

*4) LV/RV insertion point fibrosis,*

*5) mixed (infarction and myocarditis),*

*6) other (cardiomyopathy) (mid-wall/non-ischaemic or LGE in the presence of phenotypic cardiomyopathy, e.g. DCM, HCM). All cases were also assessed for the presence of significant pericardial effusion (>5mm).*

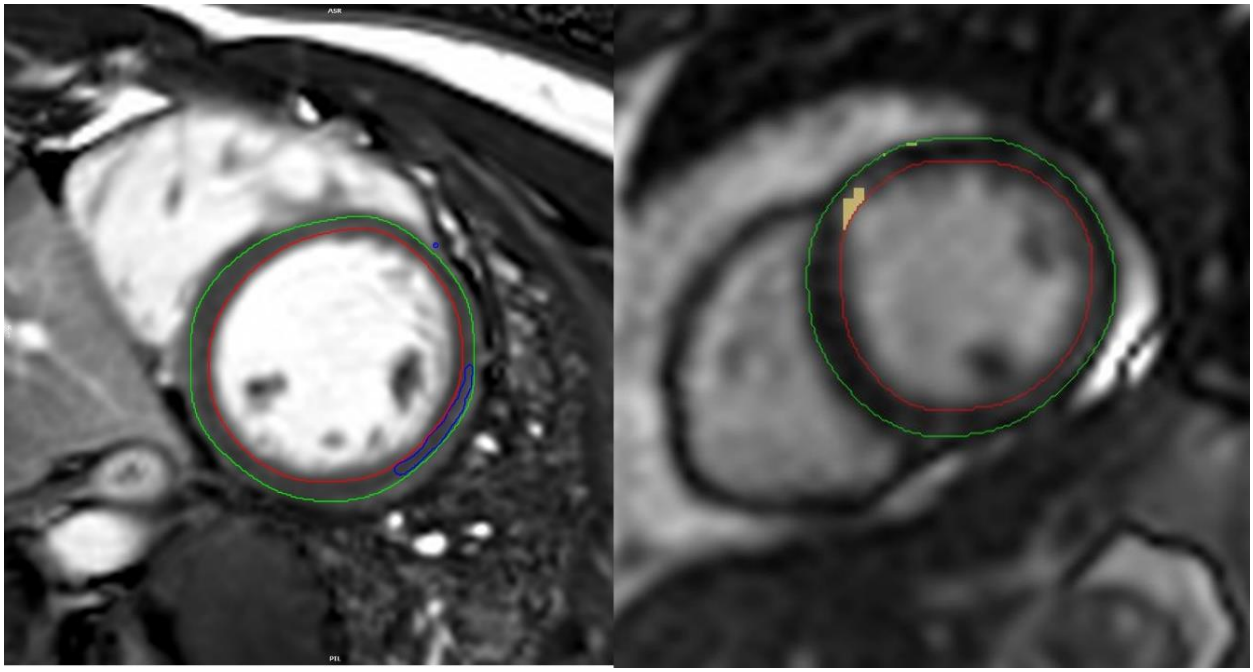

**Figure 2.6** Epicardial and endocardial borders are drawn, and a reference ROI with normal myocardial intensity is shown as a 'remote' region (blue contour) (*left*). Focal fibrosis was estimated from the extent of enhanced myocardial pixels (defined as signal intensity > 5 SD above ROI (*right*).

## T1 MAPPING, T2 MAPPING AND ECV

### ACQUISITION

Shortened Modified Look-Locker $T_1$ mapping (ShMOLLI, Siemens prototype sequence WIP1048B) [Base, mid, apex short axis slices] was used for native and post-contrast (15 minutes) acquisitions as previously described[143] (**Figure 2.7**). $T_2$ mapping was acquired using the Siemens Myomaps product sequence [Base, mid, apex short axis; SSFP readout; TR/TE = 3/1.3ms, R = 2, flip angle = 20°, Matrix = 192 x 42, field of view = 360 x 270 mm, slice thickness = 8 mm as previously described[142].

### MAP ANALYSIS

Epicardial and endocardial contours were manually drawn on the base, mid and apical slices of the myocardium and average slice $T_1$ and global $T_1$ were derived. Care was taken to avoid partial volume with the surrounding tissue, such as fat or blood pool. All $T_1$ and $T_2$ maps also underwent strict quality control. Manual epicardial and endocardial contours were drawn conservatively on base, mid and apical slices (acquired at identical slice positions to pre- and post-contrast $T_1$ maps). Average slice relaxation times were derived for each slice[144]. ECV for the three short slices required additional contouring of post-contrast $T_1$ maps and contouring of regions of interest in the blood pool of pre and post-contrast T1 maps. ECV was calculated from pre- and post-contrast $T_1$ maps and haematocrit (Hct) using the formula: $ECV = (\Delta[1/T_1 myocardium]/\Delta[1/T_1 blood]) * [1\text{-}Hct])$[145]. We defined high global T1 or T2 in **Chapters 3** and **4**, based on normalised Z scores (number of standard deviations from the mean of our normal range) of the patients, a method recently described by Artico et al.[146],(detailed description in **Appendix 2**).

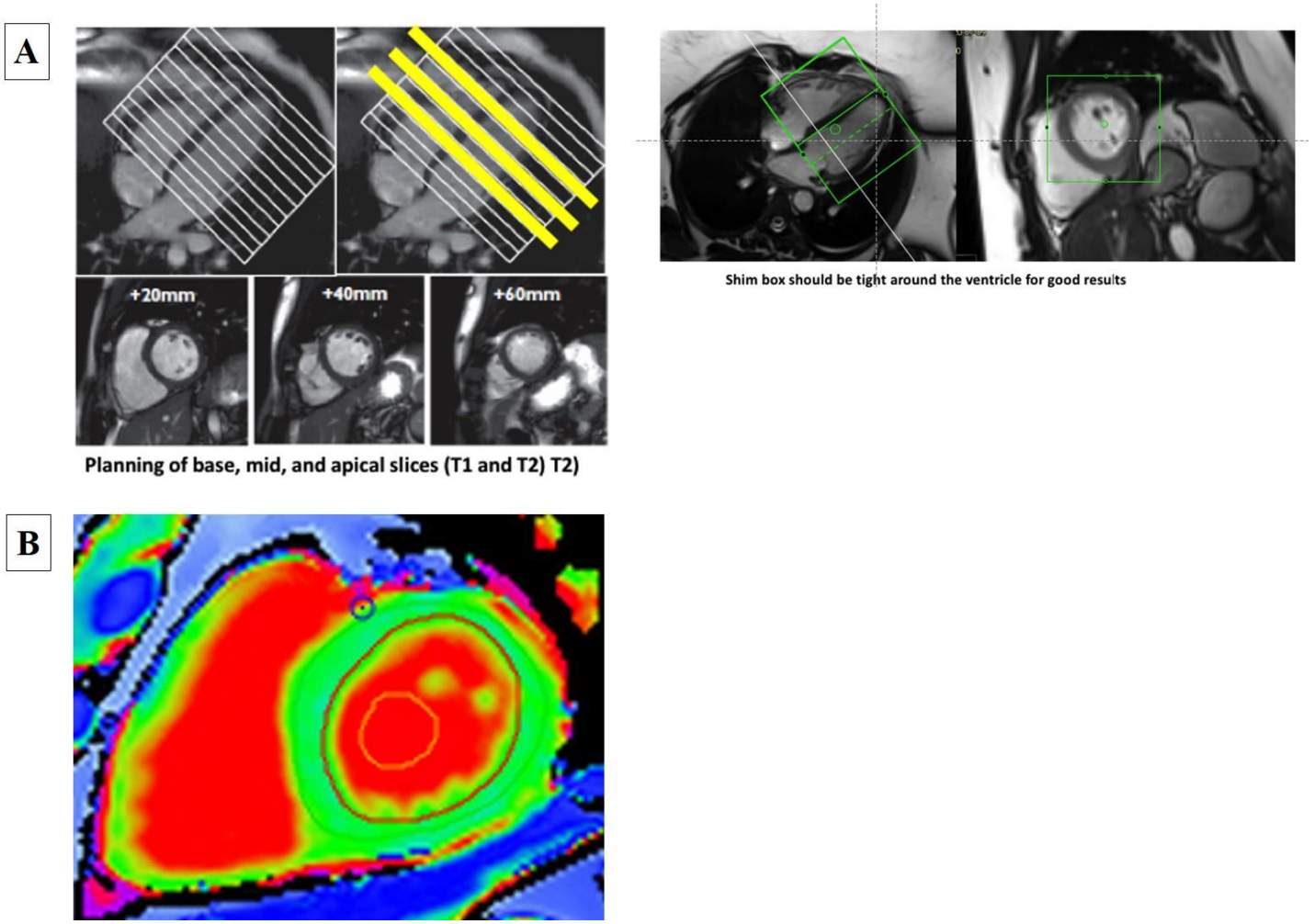


**Figure 2.7** Myocardial tissue characteristics assessment with CMR mapping technique.
**A**: Shortened Modified Look Locker $T_1$ mapping (ShMOLLI) image acquisitions.
**B**: Representative ShMOLLI image.

## 2.7 CARDIAC ABNORMALITIES BASED ON CMR

Cardiac abnormalities were defined in **Chapters 3** to **5** as the presence of:

i) Abnormal left ventricular ejection fraction (LVEF) < 52% and/or right ventricular ejection fraction (RVEF) < 48% and/or[147,148];

ii) pathological LGE pattern (ischemic, myocarditis, mixed pathology, cardiomyopathy (mid-wall/non-ischaemic or LGE in the presence of phenotypic cardiomyopathy, e.g. DCM, HCM)[149] and/or

iii) high T1 (T1 cluster normalised Z score above the 90$^{th}$ percentile of our study population[22], and high T2 (T2 cluster normalised Z score above the 90$^{th}$ percentile[22]; and/or

iv) abnormal ECV above the 90$^{th}$ percentile[148,150,151].

Representative examples in **Appendix 1, Figure 3**.

## 2.8 SAMPLE SIZE AND POWER CALCULATION

Based on the estimates of a previous study of abnormalities on CMR[47] (78% of post-hospitalised COVID-19 patients had CMR abnormalities), based on alpha (α) value of 0.05 and power (1-β) of 0.80, based on the formula $n = (Z^2 (P)(1-P))/d^2$, n = sample size, $Z^2$ = confidence interval (CI) (1.96), P = estimated prevalence, d = precision (α level) 0.05), a total sample size of 264 of post-hospitalised patients was estimated.

## 2.9 STATISTICAL ANALYSIS

Continuous variables were summarised as mean ± standard deviation (SD) or median (interquartile range/IQR), and categorical variables as frequencies and percentages. The distribution of data was visually assessed using the Shapiro-Wilk 2-tailed test for normality. Group differences were evaluated using Student's paired and unpaired t-tests, Mann Whitney U-tests, Wilcoxon-rank sign test, one-way analysis of variance (ANOVA) with post-hoc Tukey Honest Significant Difference (HSD) analysis or Kruskal-Wallis with pairwise comparisons adjusted by the Bonferroni correction as appropriate. The homogeneity of variances of mean difference in groups was determined based on Levene's test. It was used to check for the assumption that the variances of all three groups were equal for each of the dependent variable. If Levene's test was insignificant ($P>0.05$), post-hoc multiple comparisons were conducted with the Tukey HSD test. Otherwise, the Games-Howell test was used. The chi-square test, the Fisher-Freeman-Halton exact tests or McNemar's test (for paired data) were used for categorical variables. Pearson's test or Spearman's rank test was used to describe the correlation between two variables as appropriate. Univariable and multivariable binary logistic regression models were used to estimate variables associated with abnormal CMR/high T1/high T2/high ECV/pathological LGE/abnormal cardiac function (dependent variables). I conducted collinearity diagnostics to check for highly correlated variables (e.g. QTc and QTP) identified by a variance inflation factor (VIF) >2.5. Only one of the highly correlated variables was included in the final model. In the multivariable model, to predict CMR abnormalities, each ECG parameter was tested and adjusted for age, sex, BMI and comorbidities. Each ECG parameter was added singularly to the clinical model. The Hosmer-Lemeshow test was used to assess for calibration and the goodness-of-fit of the model. Nagelkerke $R^2$ was used to quantify the

total variation of the outcome explained by the predictors. I selected the optimal ECG variable in combination with the clinical data to formulate a final predictive model. Evaluation of model performance based on its calibrative and discriminative ability and diagnostic performance of ECG based on AUROC, SN, specificity (SP), predictive values (PV) and likelihood ratios are further described in **Appendix 1**. All p-values reported are from two-tailed tests. Data were presented with 95% Confidence Intervals (CI). All statistical analysis was performed with SPSS version 27.0 (IBM, Armonk, NY, USA).

# CHAPTER 3: DIAGNOSTIC UTILITY OF ECG IN SCREENING FOR MYOCARDIAL ABNORMALITIES IN COVID-19 PATIENTS

## 3.1 ABSTRACT

***Background***

The burden of cardiac abnormalities and ECG diagnostic utility for cardiac sequelae on CMR in COVID-19 infection is unclear. The study examined the burden of cardiac abnormalities and the diagnostic performance of ECG in detecting CMR abnormalities among post-hospitalised COVID-19 patients.

***Methods***

In this multicentre observational study, post-hospitalised COVID-19 patients (n=212) and matched controls (n=38) underwent CMR and 12-lead ECG. ECG parameters, including repolarisation intervals, were analysed. CMR abnormalities were defined as ventricular systolic dysfunction and/or high T1 and high T2 and/or high ECV and/or pathological LGE.

***Results***

At a median of 5.6 months post-discharge, patients had a higher burden of ECG abnormalities compared to controls (72.2% vs 42.1%, p=0.001), but the burden of CMR abnormalities was comparable, although left ventricular systolic function was lower in patients (p<0.001). The discriminative power of routinely reported ECG abnormalities not including the repolarisation intervals to detect abnormal CMR findings was low (AUROC of 0.56, p=0.185). Adding repolarisation intervals (e.g. JTc and QTc dispersion) to the criteria, improved the AUROC to 0.64, p=0.002. Including JTc (≥340ms) and QTc dispersion (≥55ms), improved the sensitivity and negative predictive value of ECG from 82% to 99.9%, and 85% to 99.9%, respectively.

***Conclusion***

Post-hospitalised COVID-19 patients had a high burden of ECG abnormalities with comparable CMR findings to controls. A normal 12-lead ECG with normal repolarisation

intervals reliably excludes significant cardiac abnormalities on CMR following COVID-19 infection.

## 3.2 INTRODUCTION

Cardiac injury is a known sequela of SARS-CoV-2 infection which is associated with high mortality, most notably among the hospitalised patients[56]. There is increasing evidence implicating myocardial abnormalities and poor cardiovascular outcomes in the medium-to-long term post-COVID-19 infection[57,78,152].

Prevalence of ECG abnormalities was common in post-acute phases of COVID-19 infection based on the early study in China[78]. However, the abnormalities reported were only confined to qualitative measures, such as the presence of arrhythmia and ST-T abnormalities, whilst the high-risk group B features, such as the QT interval[74], were not reported. The increased prevalence of cardiovascular injury at follow-up visits, evidenced by raised biomarkers and abnormal ECGs, may be indicative of persistent damage to the heart. To date, numerous other studies have evaluated the burden of cardiac injury after COVID-19 with the help of ECG[57,69,153] or CMR[47,154]. However, none have examined the association between ECG and CMR parameters of health and the diagnostic utility of an ECG as a screening tool for myocardial abnormalities detected in CMR.

The aim of the present study was first, to examine the burden of myocardial abnormalities among post-hospitalised COVID-19 patients. Second, to explore the association of ECG parameters with myocardial abnormalities and evaluate the association of specific ECG intervals (indicating depolarisation and repolarisation) with abnormal myocardial tissue characteristics on CMR. Third, to determine the diagnostic performance of ECG to screen for CMR abnormalities.

## 3.3 METHODS

### PARTICIPANTS

This was a multicentre observational cohort study (13 sites across UK, **Appendix 2 Figure 1**), of post-COVID-19 patients discharged from the hospital (confirmed by SARS-CoV-2 polymerase chain reaction positive), and individuals with no history of COVID-19 that had tested negative for SARS-CoV-2 nucleocapsid antibody negative on screening blood test (i.e., uninfected control participants), were prospectively recruited as part of a national UK-wide follow-up program called the Capturing Multiorgan Effects of COVID-19; The Post-hospitalisation COVID-19 study (C-MORE/PHOSP-COVID) (**Figure 3.1**). We included all consecutive patients with moderate-to-severe SARS-CoV-2 infection, confirmed by an RT-PCR nasopharyngeal swab test.

The study was approved in the United Kingdom by the Yorkshire and The Humber-Leeds West Research Ethics Committee (reference 20/YH/0225) and registered on ClinicalTrials.gov (ISRCTN10980107). All participants underwent a cardiac MRI, ECG and blood sampling between March 2020 and November 2021. Patients 3-7 months after discharge from hospital were enrolled. Uninfected controls[1] were prospectively recruited from the community and outpatient clinics and were matched for age, cardiac risk factors, cardiac comorbidities and BMI. Patients without paired CMR and electrocardiography were excluded, as were individuals with MRI contraindications. The eligibility criteria for all participants are detailed in the general method in **Chapter 2**.

---

[1] All controls were screened for SARS-CoV-2 nucleocapsid antibody as infected but asymptomatic patients have previously been reported.

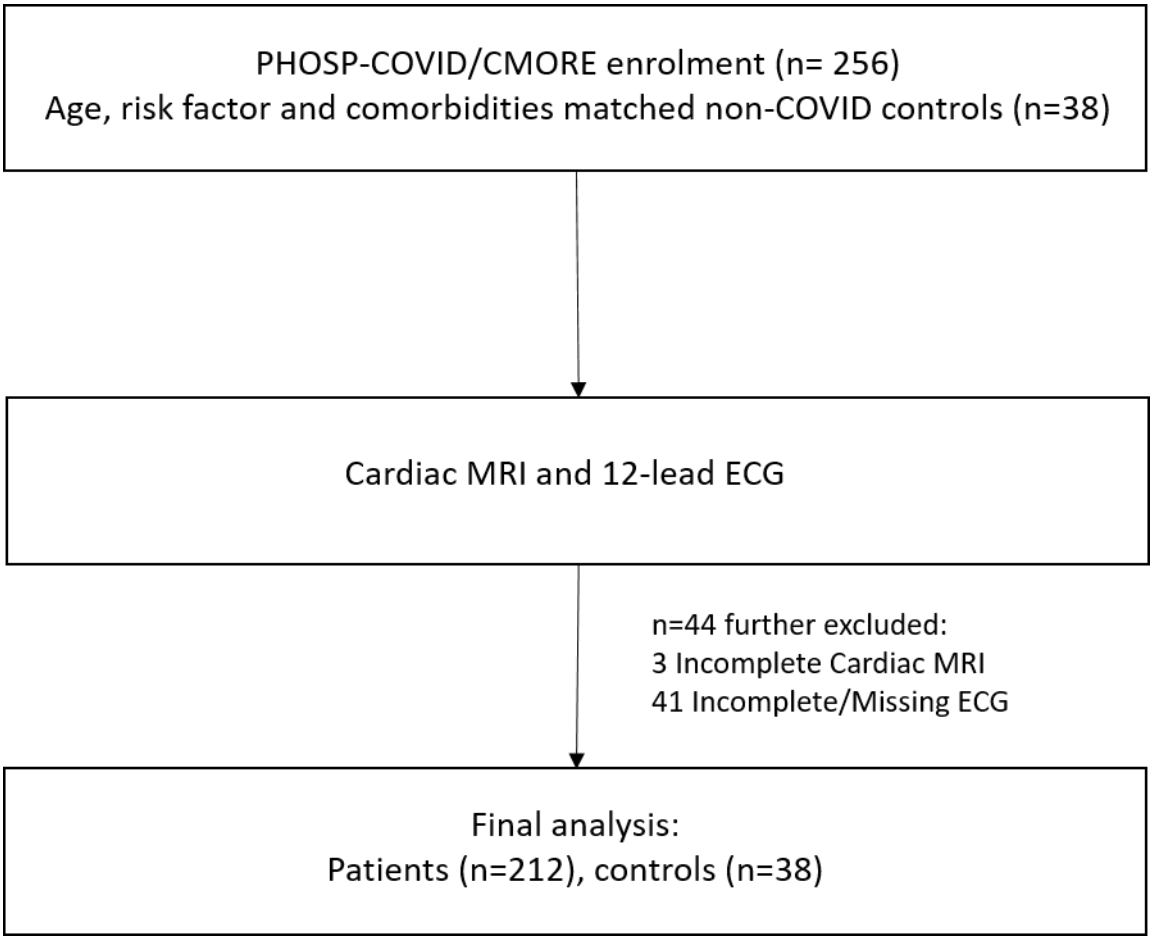


**Figure 3.1** STROBE diagram for progress through stages of analysis for this study (STROBE, strengthening the reporting of observational epidemiological studies).[1]

[1] Some cases were not included in individual analysis for myocardial tissue properties due to poor image quality or missing data, e.g. 3/212 (1.4%) for T1, 23/212 (10.8%) for T2 and 26/212 (12.3%) for ECV.

## STUDY PROTOCOL

All study subjects underwent 12-lead ECG, and CMR, carried out on a 3 Tesla scanner (Siemens Healthineers, Erlangen, Germany or Philips Healthcare, The Netherlands). Analysis was conducted according to the protocol described in **Chapter 2**.

## CMR AND IMAGE ANALYSIS

In this chapter, the specific method in data analysis of the CMR was conducted for harmonisation of T1 and T2 mapping to mitigate the variations in values between scanners, based on normalised Z scores as previously reported[146] (**Appendix 2)**. Abnormal normalised Z score was defined as being > 2 from a normal population, and above the 90$^{th}$ percentile of our entire population (cases and controls)[22]. Abnormal ECV was defined as the value above the 90$^{th}$ percentile of the entire population, i.e., ECV>0.32. A small number of cases were rejected in sub-analysis for tissue properties due to poor image quality or missing data, e.g. 3/212 (1.4%) for T1, 23/212 (10.8%) for T2 and 26/212 (12.3%) for ECV.

## 3.4 STATISTICAL ANALYSIS

All data are expressed as mean ± standard deviation (SD) or median (interquartile range /IQR), and categorical variables as frequencies and percentages. Normality of data, group differences were evaluated as described in the general method in **Chapter 2**. Pearson' and Spearman's tests were used to describe the correlation between CMR values and the ECG intervals. All p-values reported are from two-tailed tests. The discriminative ability of the repolarisation parameter model to differentiate between two outcome classes was evaluated using the AUROC curve and concordance statistics (C-index). Diagnostic performance and optimal cut-off point of ECG repolarisation intervals were also determined, and different intervals were compared by their sensitivities, specificities, and predictive values. Data are presented with 95% Confidence Intervals (CI). All statistical analysis was performed with SPSS version 27.0 (IBM, Armonk, NY, USA).

## 3.5 RESULTS

### STUDY POPULATION

The baseline characteristics and the clinical data of all the participants are summarised in

**Table 1**. Overall, 212 post-hospitalised moderate-to-severe COVID-19 patients [median age 57 years (IQR 49-65), 36% female)] and 38 risk factor-matched controls [(median age 52 years (IQR 44-62), 45% female)] were included in this study. 43% of the participants and 32% of controls were sixty years old and above (details of age distribution in **Appendix 2, Figure 2**). 30% had severe infection (WHO score 6-9), whilst 70% had moderate infection (WHO score 4-6) based on the WHO clinical characterisations of COVID-19 (**Figure 2.1**)[1]. During the initial hospital presentation, 6% had less than 90% oxygen saturation under room air. 78% of patients required oxygen supplementation during hospitalisation, with 19% requiring non-invasive mechanical ventilation and only a small proportion (9%) requiring escalation to invasive mechanical ventilation. 28% of patients had underlying hypertension, 12% had diabetes, and less than 5% had a history of ischemic heart disease or congestive heart failure. This was comparable to the burden of cardiac comorbidities among our controls.

[1]All the 212 post-hospitalised COVID-19 patients that have been recruited were diagnosed as moderate-to-severe infection, but the WHO Clinical Characterisation Score is only available in 189/212 (89.2%).

**Table 1** Clinical parameter of COVID-19 patients compared to controls.

| | **COVID-19 (n=212)** | **Control (n=38)** | **P values** |
|---|---|---|---|
| Age, years | 57.0 (49.0-65.0) | 52.0 (44.0-62.0) | 0.075[b] |
| Sex: female n (%) | 77 (36.3) | 17 (44.7) | 0.324[a] |
| Non-white ethnicity, n (%) | 59/196 (30.1) * | 5 (13.2) | 0.032[c] |
| BMI, $kg/m^2$ | 30.0 (26.7-34.5) | 28.0 (23.2-33.3) | 0.134[b] |
| Systolic pressure, mmHg | 130 (118-143) | 132 (120-153) | 0.146[b] |
| Diastolic pressure, mmHg | 78 (69 -87) | 75 (63-88) | 0.589[b] |
| Duration of admission, days | 6 (3-10) | NA | NA |
| WHO criteria (hospitalised severe score 6-9) | 56/189 (29.6) * | NA | NA |
| WHO criteria (hospitalised moderate score 3-5) | 133/189 (70.3) * | NA | NA |
| Smoker and ex-smoker n (%) | 57/194 (29.4) * | 7 (18.4) | 0.167[c] |
| Hypertension, n (%) | 50/176 (28.4) * | 14/38 (36.8) | 0.303[c] |
| Diabetes mellitus, n (%) | 22/179 (12.3) * | 7 (18.4) | 0.313[c] |
| History of IHD, n (%) | 6/178 (3.4) * | 1 (2.6) | 0.999[d] |
| Congestive heart failure, n (%) | 2/175 (1.1) * | 0 (0) | 0.999[d] |
| Oxygen supplementation, n (%) | 150/192 (78.1) * | NA | NA |
| Non-invasive mechanical ventilation, n (%) | 35/182 (19.2) * | NA | NA |
| Invasive mechanical ventilation, n (%) | 17/192 (8.9) * | NA | NA |
| ACE inhibitor, n (%) | 19/164 (11.6) * | NA | NA |
| Antibiotics, n (%) | 12/166 (7.2) * | NA | NA |
| NSAIDs, n (%) | 5/164 (3.0) * | NA | NA |
| **Laboratory Results** | | | |
| White cell count x $10^9$/L | 6.6 (5.6-8.4) | 6.2 (5.2-7.8) | 0.182[b] |
| NT Pro-BNP, pg/mL | 39.0 (32.0-76.0) | 52.4 (22.8-84.1) | 0.367[b] |
| Troponin, ng/L | 6.4 (4.8-16.2) | 2.0 (2.0-2.0) | **<0.001[b]** |
| C-Reactive Protein, mg/L | 2.3 (0.0-5.0) | 0.9 (0.6-2.3) | 0.274[b] |

[a]Independent T-Test, [b]Mann-Whitney Test, [c]Chi-Square Test, [d]Fisher-Freeman-Halton Exact Test.
Values are mean ± SD, median (IQR) or percentages. BMI, body mass index; IHD, ischaemic heart disease; NT Pro-BNP, N-terminal pro-B-type natriuretic peptide. *denominator n < 212.

## ECG FEATURES IN POST-COVID-19 PATIENTS AND CONTROLS

All the group A and group B ECG parameters were compared to explore how the burden of ECG abnormalities differs between post-hospitalised patients and controls. At a median of 5.6 [4.3-6.9] months post-hospitalisation, COVID-19 patients had a higher proportion of abnormal ECGs than comorbidity-matched non-COVID controls (72% vs 42%, p<0.001) (**Table 2**). Ventricular depolarisation represented by QRS duration was relatively longer among patients (p=0.05) (**Table 2**). The mean difference of QRS between patients and controls was more comparable after excluding 21 BBB cases (n=21), (p=0.198). Early ventricular repolarisation represented by corrected JT peak (JTPc) was shorter among patients than controls (p=0.066), whereas transmural dispersion of repolarisation represented by corrected T peak-to-T-end (cTPe) interval was longer among patients than controls (p=0.003). The proportion of patients with the longest QTc interval in each lead is summarised in **Appendix 2, Figure 3**. Precordial leads V2 and V3 had the highest proportion of patients with the longest QTc interval at 11% and 13%, respectively.

**Table 2** ECG characteristics of COVID-19 patients compared to controls.

| ECG | | | |
|---|---|---|---|
| **Group A ECG** | **COVID-19 (n=212)** | **Control (n=38)** | **P values** |
| Abnormal ECG (Composite Group A), n (%) | 153 (72.2) | 16 (42.1) | **<0.001[c]** |
| Atrial Fibrillation/Flutter, n (%) | 1 (0.5) | 0 (0) | 0.999[d] |
| Bundle Branch Block, n (%) | 21 (9.9) | 0 (0) | 0.051[d] |
| -LBBB, n (%) | 2 (1.9) | 0 (0) | 1.000[d] |
| -RBBB, n (%) | 8 (3.8) | 0 (0) | 0.615[d] |
| -ILBBB/IRBBB/IVCD, n (%) | 11 (5.2) | 0 (0) | 0.381[d] |
| Abnormal axis, n (%) * | 42/191 (22) | 8 (21.1) | 0.898[c] |
| ST-T changes, n (%) * | 79/191 (41.4) | 11 (28.9) | 0.152[c] |
| Abnormal R prog, n (%) | 37/210 (17.6) | 6 (15.8) | 0.750[c] |
| Fragmented QRS, n (%) * | 51/191 (26.7) | 5 (13.2) | 0.076[c] |
| Heart block, n (%) | 14 (6.8) | 0(0) | 0.135[d] |
| PVC/PAC, n (%) | 10/211 (4.2) | 0 (0) | 0.372[d] |
| **Group B ECG** | **COVID-19 (n=212)** | **Control (n=38)** | **P values** |
| Heart rate (bpm) | 72 (62-84) | 67 (60-77) | **0.040[b]** |
| PR interval, ms | 158.0 (142.8-174.0) | 152.5 (142.5-173.3) | 0.221[b] |
| QRS ms | 92.0 (85.3-98.0) | 87.5 (81.8-93.3) | 0.050[b] |
| QTc ms | 428.0 ± 34.6 | 422.2 ± 30.3 | 0.166[a] |
| QTc disp ms | 54.8 (41.5-69.0) | 50.3 (36.6-65.2) | 0.082[b] |
| QTPc ms | 347.4 ± 32.6 | 351.2 ± 27.8 | 0.506[a] |
| JTc ms | 331.7 ± 28.6 | 332.9 ± 22.4 | 0.820[a] |
| JTPc ms | 229.8 (210.1-248.5) | 237.2 (222.7-254.2) | 0.066[b] |
| cTPe ms | 99.1 (90.2-109.5) | 90.9 (84.2-99.2) | **0.003[b]** |

[a]Independent T-Test, [b]Mann-Whitney Test, [c]Chi-Square Test, [d]Fisher's Exact Test.

Values are mean ± SD, median (IQR) or percentages. Abnormal R prog, abnormal R wave progression; BBB, bundle branch block; BMI, body mass index; CMR, cardiac magnetic resonance; ECG, electrocardiography; Disp, dispersion; IVCD, intraventricular conduction delay; ILBBB, incomplete left bundle branch block; IRBBB, incomplete right bundle branch block; LBBB, left bundle branch block; PAC, premature atrial complex; PVC, premature ventricular complex; QTc, corrected QT; QTPc, corrected QT peak; RBBB, right bundle branch block; cTPe, corrected T-peak- to-T-end; *cases with BBB excluded.

## CMR FINDINGS BETWEEN PATIENTS AND CONTROLS

At 5.6 months after discharge, a quarter of patients had cardiac abnormalities on CMR. Post-COVID-19 patients had lower LV systolic function (60.3 ± 5.8% vs 63.0 ± 6.0%, p=0.007) and higher LGE mass (4.3 ±3.7gm vs 1.1 ±3.2 gm, p=0.008) compared to controls but myocardial T1, T2 and ECV were not significantly different between the two cohorts (**Table 3**).

**Table 3** CMR characteristics of COVID-19 patients compared to controls.

| **CMR – volumes and function** | | | |
|---|---|---|---|
| | **COVID-19 (n=212)** | **Control (n=38)** | **P values** |
| CMR abnormal, n (%) | 49 (23.1) | 7 (18.4) | 0.592[b] |
| LVEDV ml | 151 (127-170) | 147 (127-173) | 0.935[b] |
| LVESV ml | 59 (46-74) | 54 (48-66) | 0.213[b] |
| LVSV ml | 90 (77-100) | 91(78-107) | 0.424[b] |
| LV mass g | 111 ± 26 | 110 ± 28 | 0.948[a] |
| LV mass index g/m$^2$ | 52 (46-59) | 52 (48-61) | 0.601[b] |
| LVEF (%) | 60.3 ± 5.8 | 63.0 ± 6.0 | **0.007[a]** |
| LVEF < 52%, n (%) | 11 (5.2) | 1 (2.6) | 0.699[d] |
| RVEDV ml | 151 (126-171) | 160 (130-190) | 0.207[b] |
| RVESV ml | 60 (46-76) | 63 (48-85) | 0.300[b] |
| RVSV ml | 89 (75-99) | 87 (80-102) | 0.402[b] |
| RVEF (%) | 59.4 ± 6.6 | 59.5± 6.5 | 0.876[a] |
| RVEF < 48%, n (%) | 10 (4.7) | 1 (2.6) | 0.999[d] |
| **CMR - Myocardial Tissue Characterisations** | | | |
| T1 normalised Z score | 0.08 (-1.05 – 1.27) | 0.02 (-1.30 – 2.3) | 0.637[b] |
| T2 normalised Z score | 0.63 (-0.07-1.32) | 0.82 (0.17-1.61) | 0.219[b] |
| ECV (%) | 0.28 ± 0.03 | 0.29 ± 0.03 | 0.096[a] |
| High ECV (>0.32), n (%) | 15/186 (8.1) | 1 (14.8) | 0.274[d] |
| Pathological LGE, n (%) | 27/195 (13.8) | 4 (10.5) | 0.581[d] |
| LGE mass, g | 4.3 ± 3.7 | 1.1 ± 3.2 | **0.008[a]** |
| RV insertion LGE, n (%) | 5/195 (2.6) | 1 (2.6) | 0.999[d] |
| Ischemic LGE, n (%) | 12/195 (6.2) | 1 (2.6) | 0.699[d] |
| Myocarditis LGE, n (%) | 17/195 (8.7) | 4 (10.5) | 0.757[d] |
| Mixed LGE, n (%) | 2 /195 (1.0) | 0 (0) | 0.999[d] |
| Cardiomyopathy LGE, n (%) | 3/195 (1.5) | 0 (0) | 0.585[d] |

| | | | |
|---|---|---|---|
| Pleural effusion, n (%) | 2/195 (1.0) | 0 (0) | 0.999[d] |

[a]Independent T-Test [b]Mann-Whitney Test, [c]Chi-Square Test, [d]Fisher-Freeman-Halton Exact Test.
Values are mean ± SD, median (IQR) or percentages. CMR, cardiac magnetic resonance; ECV, Extracellular volume; LGE, late gadolinium enhancement; LV, left ventricular; LVEDV, left ventricular end-diastolic volume; LVESV, left ventricular end-systolic volume; LVSV, left ventricular systolic volume; LVEF, left ventricular ejection fraction; LVCO, left ventricular cardiac output; RVEDV, right ventricular end-diastolic volume; RVESV, right ventricular end-systolic volume; RVSV, right ventricular systolic volume; RVEF, right ventricular ejection fraction; RVCO, right ventricular cardiac output.

## ECG FEATURES IN PATIENTS WITH CMR ABNORMALITIES

**Figure 3.2** and **Table 4** summarise the ECG and CMR parameters findings among patients with and without CMR abnormalities relative to controls. The burden of ECG abnormalities defined by the composite group A ECG parameters was higher among patients with CMR abnormalities. The most commonly reported group A ECG features among patients with CMR abnormalities were ST-T changes. Patients with CMR abnormalities displayed longer group B repolarisation parameters, particularly the QTc disp, relative to patients without CMR abnormalities and controls. Likewise, JTPc interval was significantly greater among patients with than without CMR abnormalities, but was comparable to controls (**Table 4**).

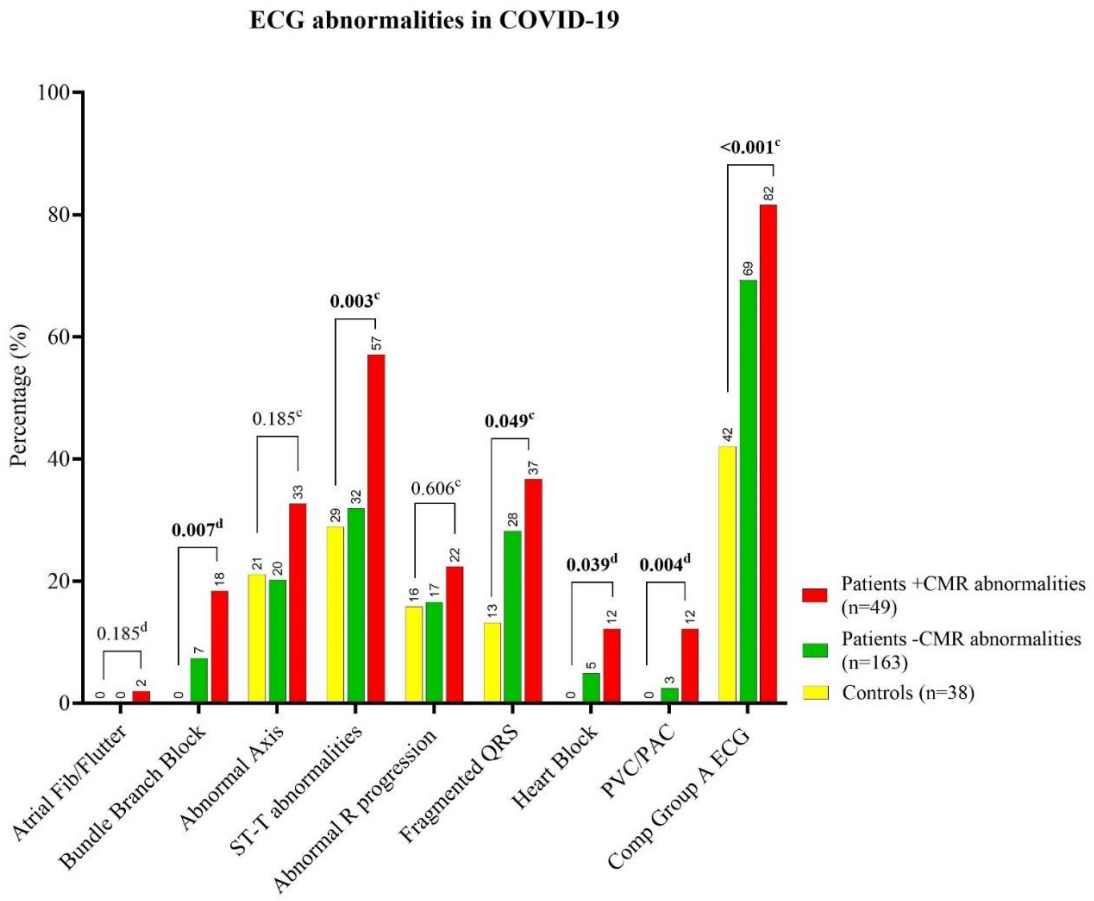


**Figure 3.2** ECG abnormalities in COVID-19 patients with CMR abnormalities (red bar), without CMR abnormalities (green bar) and control (yellow).

[c]Chi-square test, [d]Fisher's Exact test. COVID-19 with CMR abnormalities (red bar) demonstrate a higher frequency of ECG abnormalities relative to patients without CMR abnormalities and controls.

**Table 4** ECG of patients with and without CMR abnormalities and control.

| | **COVID-19 with CMR abnormalities (n=49)** | **COVID-19 without CMR abnormalities (n=163)** | **Control (n=38)** | **P values** |
|---|---|---|---|---|
| Age years | 62.0 (53.5-70.5) | 56.0 (47.0-63.3) ** | 52.0 (44.0-62.0) ** | **<0.001[b]** |
| Sex: female n (%) | 18 (36.7) | 59 (36.2) | 17 (44.7) | 0.536[c] |
| **Group A ECG** | | | | |
| Abnormal ECG (Composite Group A), n (%) | 40 (81.6) | 113 (69.3) | 16 (42.1) | **<0.001[c]** |
| Atrial fibrillation/flutter, n (%) | 1 (2.0) | 0 (0) | 0 (0) | 0.128[d] |
| Bundle branch block, n (%) | 9 (18.4) | 12 (7.4) | 0 (0) | **0.007[d]** |
| ST-T abnormalities, n (%) | 28 (57.1) | 52 (31.9) | 11 (28.9) | **0.003[c]** |
| Abnormal axis, n (%) | 16 (32.7) | 33 (20.2) | 8 (21.1) | 0.185[c] |
| Fragmented QRS, n (%) | 18 (36.7) | 46 (28.2) | 5 (13.2) | **0.049[c]** |
| Abnormal R prog, n (%) | 11 (22.4) | 27 (16.6) | 6 (15.8) | 0.606[c] |
| Heart block, n (%) | 6 (12.2) | 8 (4.9) | 0 (0) | **0.039[d]** |
| PAC/ PVC, n (%) | 6 (12.2) | 4 (2.5) | 0 (0) | **0.004[d]** |
| **Group B ECG** | | | | |
| PR interval ms | 164.0 (150.0-178.0) | 158.0 (142.0-173.0) | 152.5 (142.5-173.3) | 0.151[b] |
| QRS ms | 92.0 (85.0-103.0) | 91.0 (85.0-98.0) | 87.5 (81.8-93.3) | 0.098[b] |
| QTc ms | 434.3 ± 39.2 | 426.1 ± 33.0 | 422.2 ± 30.3 | 0.211[a] |
| QTc disp ms | 65.1 ± 27.0 | 54.0 ± 18.0 * | 51.6 ± 18.2 * | **0.001[a]** |
| QTPc ms | 355.1 ± 35.2 | 345.1 ± 31.5 | 351.2 ± 27.8 | 0.124[a] |
| JTc ms | 340.1 ± 33.5 | 329.2 ± 26.5 | 332.4 ± 22.4 | 0.052[a] |
| JTPc ms | 240.5 ± 32.9 | 228.2 ± 26.6 * | 239.5 ± 23.1 | **0.006[a]** |
| cTPe ms | 97.1 (86.9-113.2) | 99.6 (90.2-109.2) | 91.0 (84.2-99.2) *** | **0.013[b]** |

[a]ANOVA, [b]Kruskal-Wallis Test, [c]Chi-Square Test, [d]Fisher's Exact Test.

* P values ($p<0.05$) with post-hoc Tukey HSD test *vs* patients **with** CMR abnormalities.

** P values ($p<0.05$) with Bonferroni correction *vs* patients **with** CMR abnormalities.

*** P values ($p<0.05$) with Bonferroni correction *vs* patients **without** CMR abnormalities.
Values are mean ± SD, n (%) or, median (IQR) or percentages. Abnormal R prog, abnormal R wave progression; BBB, bundle branch block; CMR, cardiac magnetic resonance; ECG, electrocardiography; PAC, premature atrial complex; PVC, premature ventricular complex; QTc, corrected QT; QTPc, corrected QT peak; cTPe, corrected T-peak- to-T-end; disp, dispersion.

## ECG PARAMETERS IN PATIENTS WITH REDUCED LVEF AND HIGH MYOCARDIAL T1, T2, ECV, AND LGE.

To elucidate the relationship between electrical conduction and myocardial function or tissue abnormalities, I compared ECG parameters between patients with and without LV dysfunction or tissue abnormalities on CMR with non-COVID-19 controls. Patients with LV dysfunction (LVEF < 52%) had significantly longer QRS duration, QTc disp and cTPe intervals relative to controls (**Table 5**).

Patients with high myocardial T1 had significantly longer repolarisation intervals, including QTc, QTPc and JTc intervals, relative to those without high T1 and controls (**Table 5** and **Figure 3.3**). (*Important to note that female patients made up 75% of those with high T1*). By contrast, only QTc, JTc and cTPe intervals were significantly longer in patients with high myocardial T2 compared to those without high T2 or controls (**Table 5** and **Figure 3.4**). Patients with high ECV only demonstrated significant differences in QTPc and JTc intervals relative to patients without high ECV but not with controls (**Table 5** and **Figure 3.5**). In addition, I also observed a modest but significant positive correlation of global T1 values with repolarisation intervals, particularly with the QTc, QTPc and JTc intervals (**Figure 3.6).**

## ECG AND CMR PARAMETERS IN PATIENTS BASED ON WHO SEVERITY SCORE.

To understand the association of the severity of COVID-19 infection with ECG and CMR parameters, a comparison of clinical characteristics, ECG, and CMR parameters was stratified according to the WHO Clinical Characterisations of COVID-19 score (Moderate WHO score 3-5 vs Severe WHO score 6-9) and summarised in **Appendix 2, Table 1.**

Overall, the clinical characteristics were comparable. There was no significant difference in the Group A ECG abnormalities among moderate (WHO score 3-5) and severe (WHO score 6-9) infection. The Group B ECG features were also comparable between the groups except for QTc disp, which was significantly longer in severe infection 51 (IQR 40-66) ms vs 58 (IQR 46-74) ms, p=0.043. Likewise, the burden of composite or individual CMR abnormalities was also comparable between moderate and severe COVID-19 infection.

Correlation analysis between repolarisation interval (QTc) with native global T1 was generally moderate but relatively higher among those with severe infection ($R_s$ 0.204, p=0.040 vs $R_s$ 0.243, p=0.092) (**Figure 3.7**). Comparison of QTc interval between patients who required invasive mechanical ventilation (WHO score 7-9) versus patients who did not require invasive mechanical ventilation (WHO score 3-6) demonstrated a significantly longer interval among patients with WHO score 7-9 (446 ± 36 ms vs 426 ± 34 ms, p=0.025) **Appendix 2 Figure 4**.

**Table 5** ECG comparisons of patients with and without MRI abnormalities and control.

| | **COVID-19 with LVEF < 52% (n=11)** | **COVID-19 with LVEF ≥ 52% (n=201)** | **Control (n=38)** | **P values** |
|---|---|---|---|---|
| Age years | 64.0 (51.0-70.0) | 57.0 (49.0-65.0) | 52.0 (44.0-62.0) | 0.098[a] |
| Female, n (%) | 2 (18.2) | 75 (37.3) | 17 (44.7) | 0.239[c] |
| PR interval ms | 162.0 (134.0-188.0) | 158.0 (143.0-174.0) | 152.5 (142.5-173.3) | 0.567[a] |
| QRS ms | 98.0 (90.0-128.0) | 92.0 (85.0-98.0) | 87.5 (81.8-93.3) ** | **0.030[a]** |
| QTc ms | 426.4 ± 36.3 | 428.1 ± 34.6 | 422.2 ± 30.3 | 0.618[a] |
| QTc disp ms | 66.9 (52.2-102.2) | 53.8 (41.4-67.6) | 50.3 (36.6-65.2) ** | 0.050[a] |
| QTPc ms | 347.4 ± 40.8 | 347.4 ± 32.2 | 351.2 ± 27.8 | 0.802[a] |
| JTc ms | 334.9 ± 34.5 | 331.6 ± 28.3 | 332.9 ± 22.4 | 0.906[a] |
| JTPc ms | 237.5 + 35.6 | 230.7 ± 28.2 | 239.5 ± 23.1 | 0.166[a] |
| cTPe ms | 99.1 (86.2-104.0) | 98.8 (90.2-109.7) | 91.0 (84.2-99.2) *** | **0.011[b]** |
| | **COVID-19 with high T1 (n=16)** | **COVID-19 without high T1 (n=193)** | **Control (n=38)** | **P values** |
| Age years | 56.5 (43.5-62.8) | 57.0 (50.0-66.0) | 52.0 (44.0-62.0) | 0.123[b] |
| Female, n (%) | 12 (75.0) | 65 (33.7) | 17 (44.7) | **0.003[c]** |
| PR interval ms | 151 (138.3-169) | 161 (144.5-175.8) | 152.5 (142.5-173.3) | 0.215[b] |
| QRS ms | 88.0 (75.0-93.5) | 92.0 (86.0-98.0) ** | 87.5 (81.8-93.3) | **0.012[b]** |
| QTc ms | 466.1 ± 27.9 | 424.5 ± 33.2 * | 422.2 ± 30.3 * | **<0.001[a]** |
| QTc disp ms | 59.5 (53.5.0-81.8) | 52.4 (41.1-67.5) | 50.3 (36.6-65.2) | 0.058[a] |
| QTPc ms | 376.3 ± 26.3 | 348.4 ± 26.3 * | 351.2 ± 27.8 * | **<0.001[a]** |
| JTc ms | 364.4 ± 27.3 | 328.8 ± 26.9 * | 332.9 ± 22.4 * | **<0.001[a]** |
| JTPc ms | 258.1 ± 33.8 | 228.7 ± 26.7 * | 239.5 ± 23.1 | **<0.001[a]** |
| cTPe ms | 108.0 (92.6-121.1) | 98.8 (89.4-108.7) | 91.0 (84.2-99.2) **** | **0.005[b]** |
| | **COVID-19 with high T2 (n=17)** | **COVID-19 without high T2 (n=168)** | **Control (n=38)** | **P values** |

| | | | | |
|---|---|---|---|---|
| Age years | 59.5 ± 9.4 | 55.8 ± 12.5 | 53.2 ± 10.7 | 0.193[a] |
| Female, n (%) | 7 (41.2) | 63 (36.6) | 17 (44.7) | 0.628[c] |
| PR interval ms | 160.0 (150.0-176.0) | 158.0 (142.0-174.0) | 152.5 (142.5-173.3) | 0.518[b] |
| QRS ms | 86.0 (79.0-94.0) | 92.0 (85.3-94.0) | 87.5 (81.8-93.3) | **0.046**[b] |
| QTc ms | 446.7 ± 33.5 | 424.9 ± 32.9 * | 422.2 ± 30.3 * | **0.024**[a] |
| QTc disp ms | 59.4 (45.0-72.0) | 53.3 (40.9-67.2) | 50.3 (36.6-65.2) | 0.305[b] |
| QTPc ms | 362.3 (346.6-372.2) | 341.6 (323.2-370.0) | 348.5 (329.8-369.1) | 0.062[b] |
| JTc ms | 350.6 ± 27.6 | 329.3 ± 28.3 * | 332.9 ± 22.4 | **0.010**[a] |
| JTPc ms | 244.6 (230.8-253.5) | 228.6 (209.3-247.7) | 237.2 (222.7-254.2) | **0.023**[b] |
| cTPe ms | 107.7 (97.3-113.4) | 97.0 (89.7-109.2) | 91.0 (84.2-99.2) **** | **0.003**[a] |
| | **COVID-19 with high ECV (n=15)** | **COVID-19 without high ECV (n=171)** | **Control (n=27)** | **P values** |
| Age years | 63.0 (51.0-75.0) | 58.0 (50.0-65.0 | 56.0 (44.0-63.0) | 0.140[b] |
| Female, n (%) | 10 (66.7) | 52 (30.4) | 9 (33.3) | **0.017**[c] |
| PR interval ms | 152.0 (140.0-166.0) | 162.0 (144.0-176.0) | 151.0 (143.0-174.0) | 0.226[b] |
| QRS ms | 88.0 (74.0-94.0) | 92.0 (86.0-98.0) | 92.0 (81.0-94.0) | 0.074[b] |
| QTc ms | 443.8 ± 45.1 | 426.1 ± 33.9 | 423.9 ± 29.1 | 0.140[a] |
| QTc disp ms | 59.0 (39.2-78.4) | 55.2 (41.6-69.9) | 55.3 (37.4-70.7) | 0.666[b] |
| QTPc ms | 366.2 ± 38.8 | 345.3 ± 32.1 * | 353.3 ± 27.6 | **0.036**[a] |
| JTc ms | 352.0 ± 29.2 | 330.0 ± 28.2 * | 332.4 ± 22.3 | **0.013**[a] |
| JTPc ms | 256.1 (246.7-274.9) | 225.4 (209.3-246.4) ** | 240.5 (223.0-256.4) | **<0.001**[b] |
| cTPe ms | 92.7 ± 14.0 | 101.4 ± 15.2 | 92.8 ± 10.6 *** | **0.003**[a] |
| | **COVID-19 with pathological LGE (n=27)** | **COVID-19 without pathological LGE (n=185)** | **Control (n=38)** | **P values** |
| Age years | 67.0 (56.0-74.0) | 56.0 (47.0-63.5) ** | 52.0 (44.0-62.0) ** | **<0.001**[b] |
| Female, n (%) | 6 (22.2) | 71 (38.4) | 17 (44.7) | 0.166[c] |
| PR interval ms | 166.0 (154.0-185.8) | 158.0 (142.0-173.0) ** | 152.5 (142.5-173.3) ** | **0.018**[b] |
| QRS ms | 94.0 (90.0-108.0) | 91.0 (85.0-98.0) | 87.5 (81.8-93.3) | 0.062[b] |

| | | | | |
|---|---|---|---|---|
| QTc ms | 424.2 ± 35.9 | 428.5 ± 34.5 | 422.2 ± 30.3 | 0.515[a] |
| QTc disp ms | 59.6 (46.4-92.5) | 53.8 (41.4-67.5) | 50.3 (36.6-65.2) | 0.193[b] |
| QTPc ms | 348.9 ± 30.5 | 347.2 ± 33.0 | 351.2 ± 27.8 | 0.775[a] |
| JTc ms | 331.4 ± 30.0 | 331.8 ± 28.4 | 332.9 ± 22.4 | 0.971[a] |
| JTPc ms | 234.5 ± 32.2 | 230.5 ± 28.1 | 239.5 ± 23.1 | 0.179[a] |
| cTPe ms | 95.7 (85.5-106.5) | 99.7 (90.3-110.0) | 91.0 (84.2-99.2) *** | **0.006**[b] |

[a]ANOVA, [b]Kruskal-Wallis Test, [c]Chi-Square Test.

* P values (p<0.05) with post-hoc Tukey HSD test *vs* patients **with** (high T1/high T2/high ECV/LGE).

** P values (p<0.05) with Bonferroni correction *vs* patients **with** (high T1/high T2/high ECV/LGE).

*** P values (p<0.05) with Bonferroni correction *vs* patients **without** (high T1/high T2/high ECV/LGE).

**** P values (p<0.05) with Bonferroni correction *vs* both patients **with** and **without** (high T1/high T2/high ECV/LGE).

Values are mean ± SD, n (%) or, median (IQR) or percentages. BBB, bundle branch block; CMR, cardiac magnetic resonance; ECG, electrocardiography; ECV, Extracellular volume; LGE, late gadolinium enhancement; LVEF, left ventricular ejection fraction; QTc, corrected QT; QTPc, corrected QT peak; cTPe, corrected T-peak- to-T-end; disp, dispersion

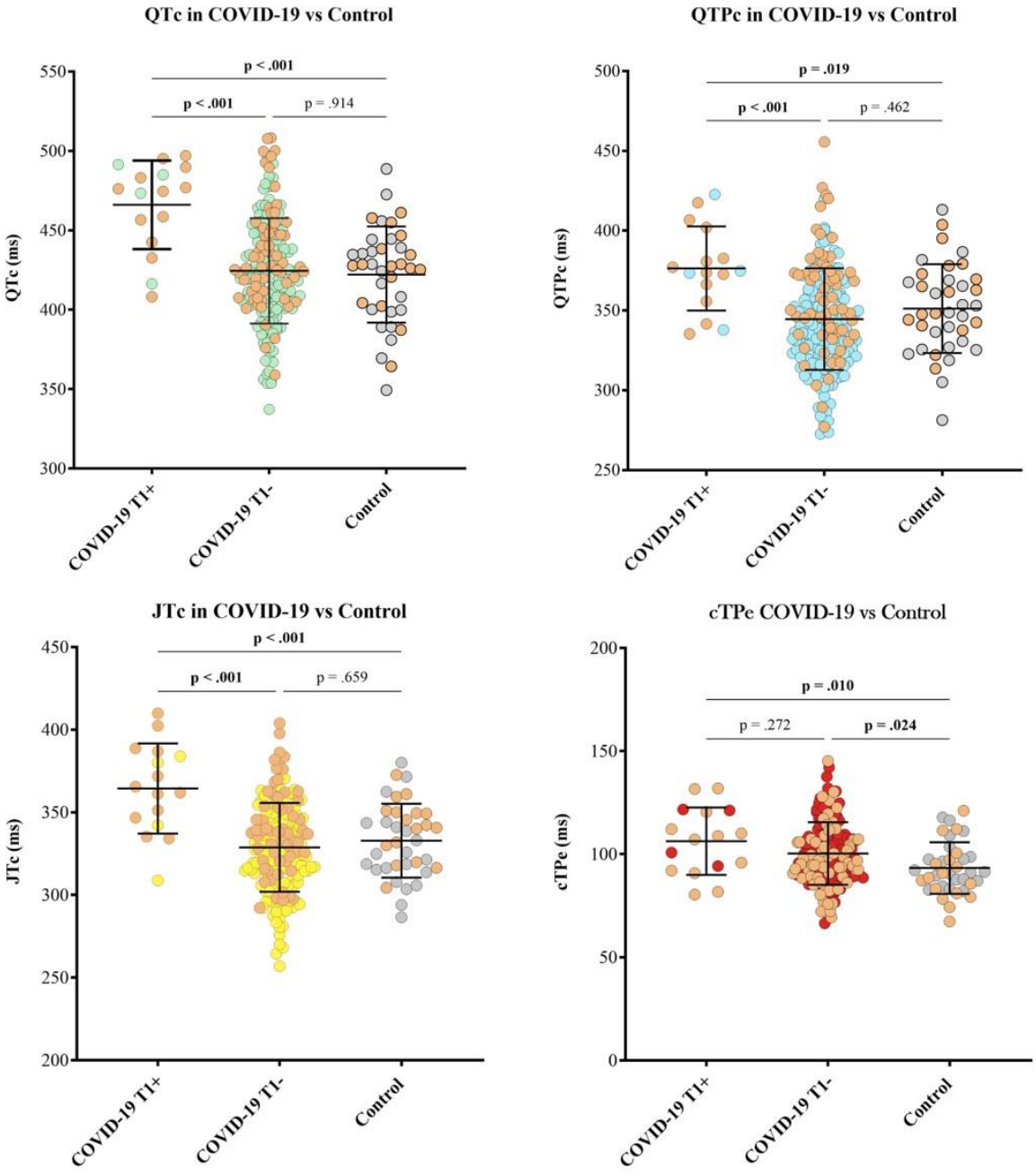


**Figure 3.3** Repolarisation parameters in COVID-19 patients with/out high T1 and controls.

Plots depicting mean values and variabilities for different repolarisation intervals between COVID-19 patients with high T1 (COVID-19 T1+), patients without high T1 (COVID-19 T1-) and control. P values based on Tukey's HSD post-hoc mean difference comparison or Bonferroni correction. Intervals are coded by colour ( green= QTc, blue = QTPc, yellow = JTc and red = cTPe). grey represents all controls and brown represents female participants in the respective group.

COVID-19 T1+ demonstrate significantly longer repolarisation intervals (QTc, QTPc, JTc and cTPe) than COVID-19 T1- and controls.

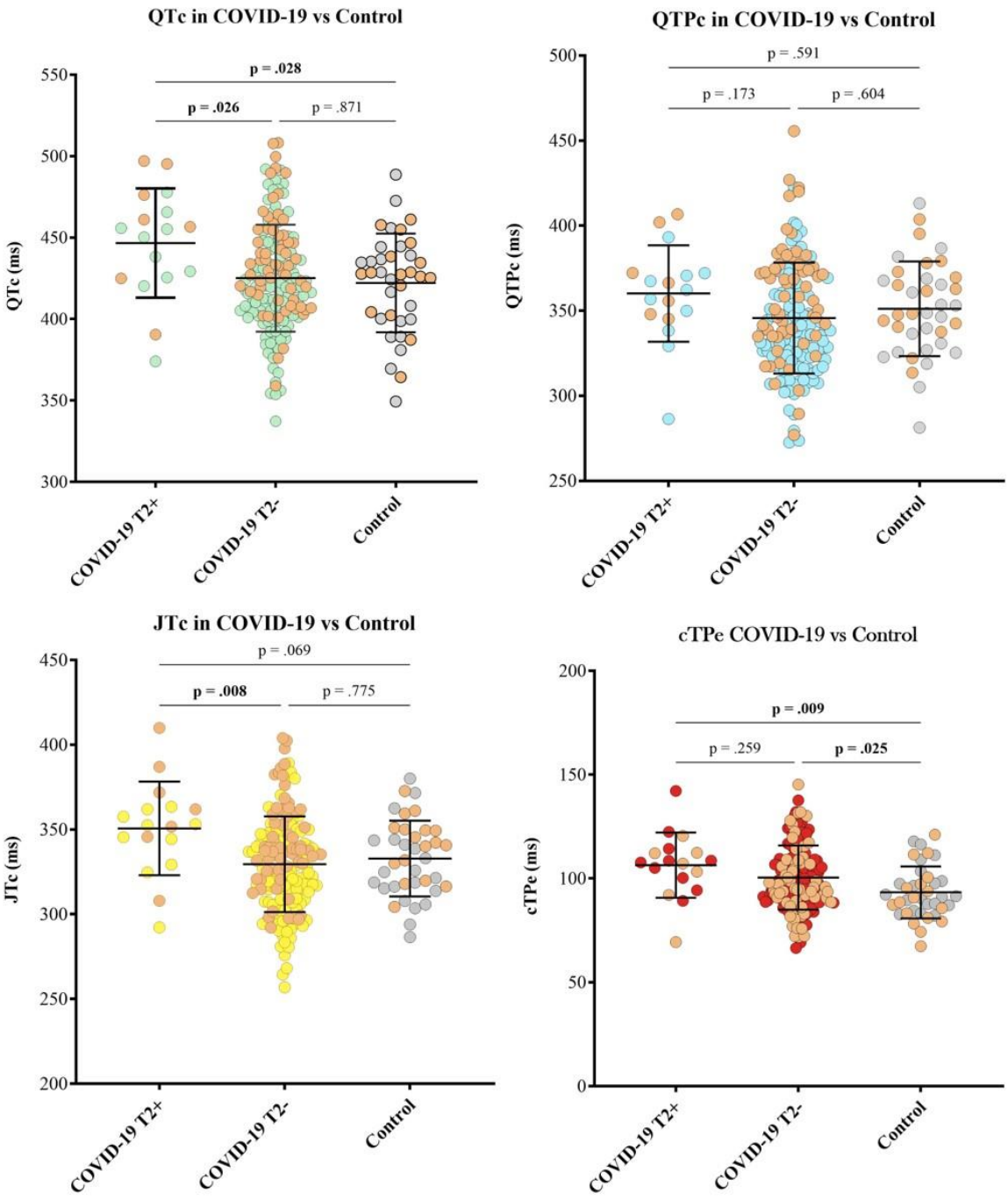


**Figure 3.4** Repolarisation parameters in COVID-19 patients with/out high T2 and controls.

Plots depicting mean values and variabilities for different repolarisation intervals between COVID-19 patients with high T2 (COVID-19 T2+), patients without high T2 (COVID-19 T2-) and control. P values based on Tukey's HSD post-hoc mean difference comparison or Bonferroni correction. Intervals are coded by colour ( green= QTc, blue = QTPc, yellow = JTc and red = cTPe). grey represents all controls, and brown represents female participants in the respective group. COVID-19 T2+ demonstrate significantly longer repolarisation intervals for QTc, JTc and cTPe, than COVID-19 T2- and/or controls.

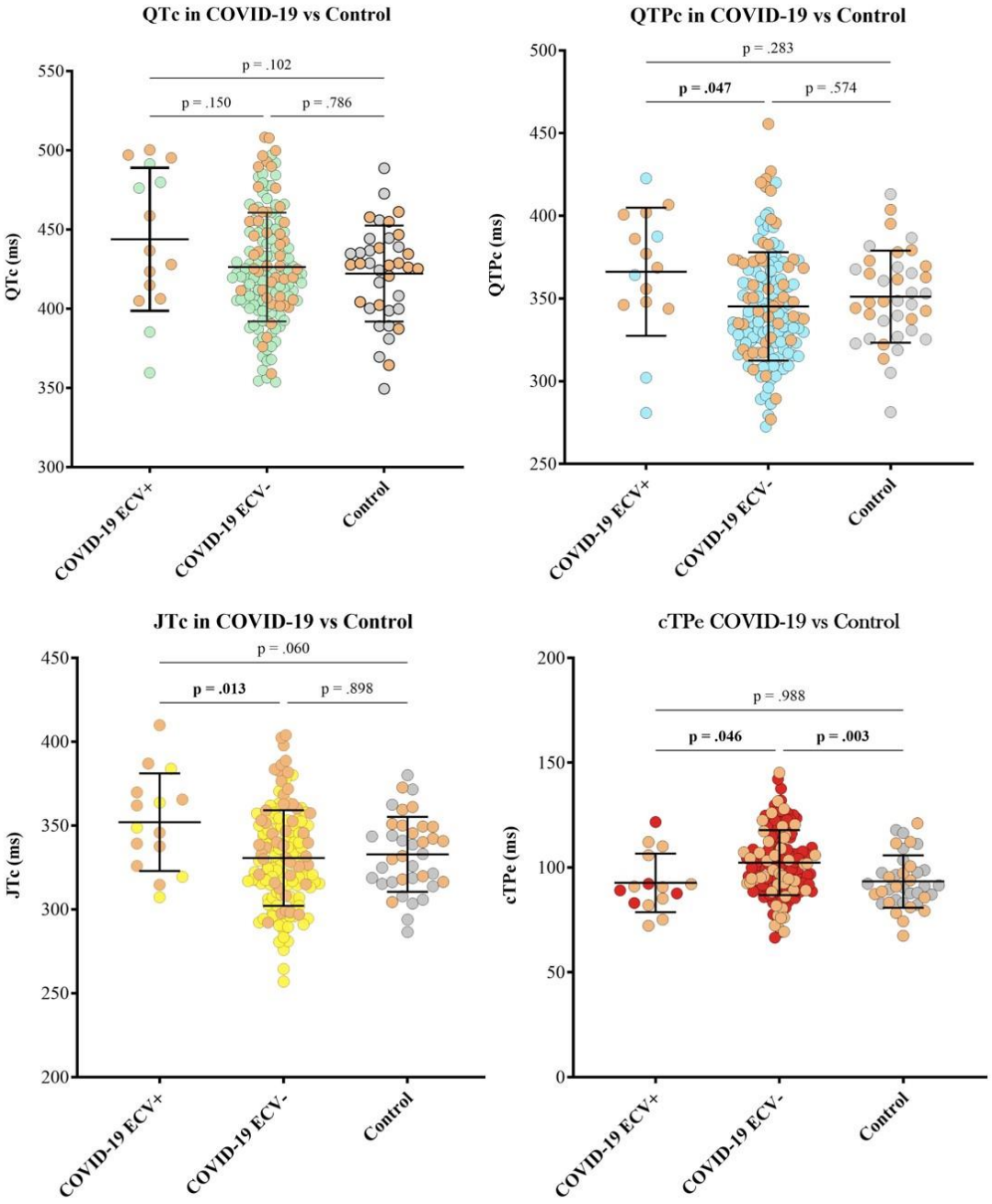


**Figure 3.5** Repolarisation parameters in COVID-19 with/out high ECV and controls.

Plots depicting mean values and variabilities for different repolarisation intervals between COVID-19 patients with high ECV (COVID-19 ECV+), patients without high ECV (COVID-19 ECV-) and controls. P values based on Tukey's HSD post-hoc mean difference comparison or Bonferroni correction. Intervals are coded by colour ( green= QTc, blue = QTPc, yellow = JTc and red = cTPe). grey represents all controls, and brown represents female participants in the respective group. COVID-19 ECV+ demonstrate significantly longer QTPc and JTc than COVID-19 ECV-.

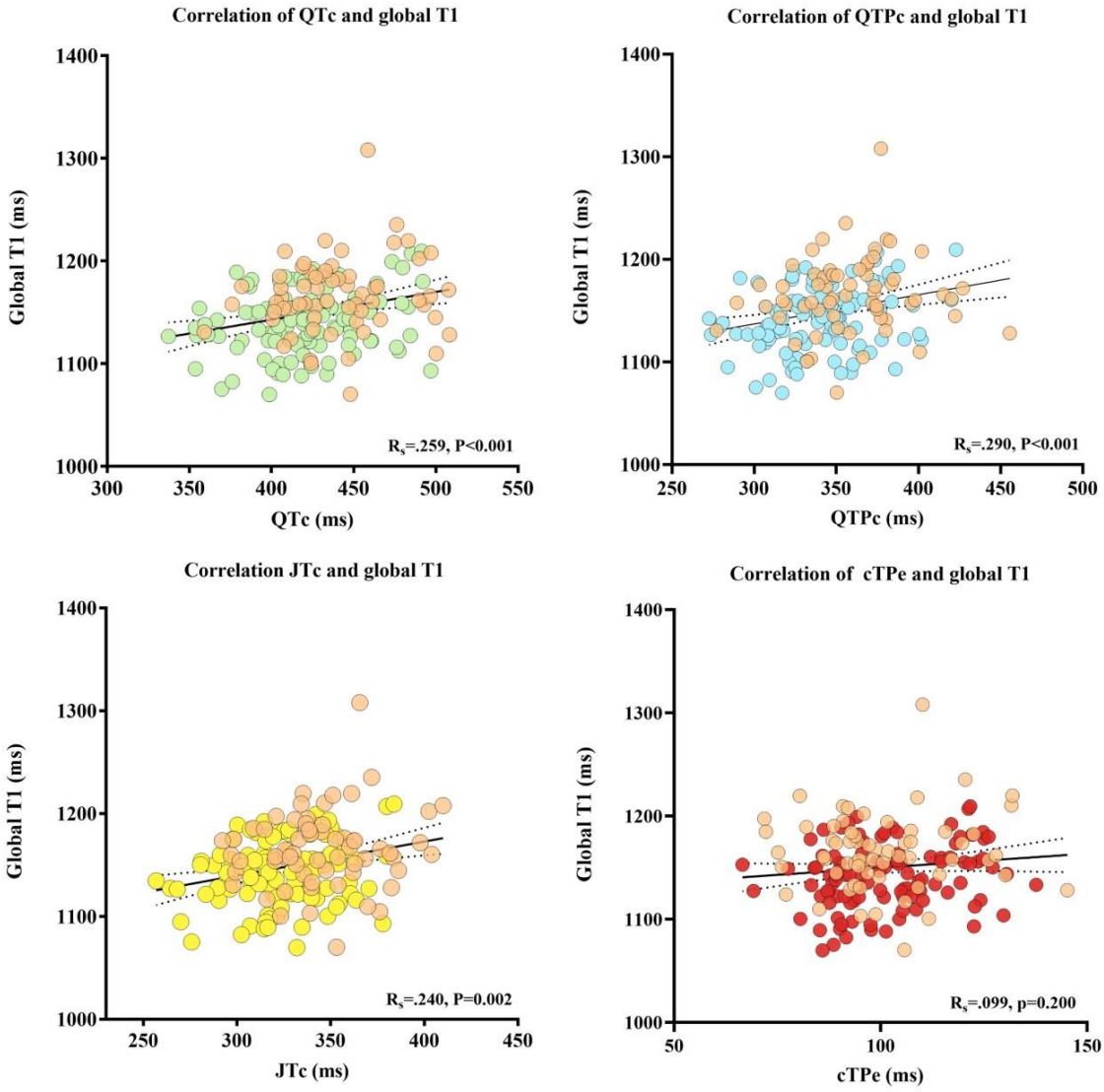


**Figure 3.6** Correlation of repolarisation parameters with global T1.

Scatter plot depicting correlations between repolarisation parameters and global T1 values. Positive correlations between global T1 values and QTc , QTPc and JTc intervals were observed. represents female participants. P values are based on Spearman's correlation analysis ($R_s$).

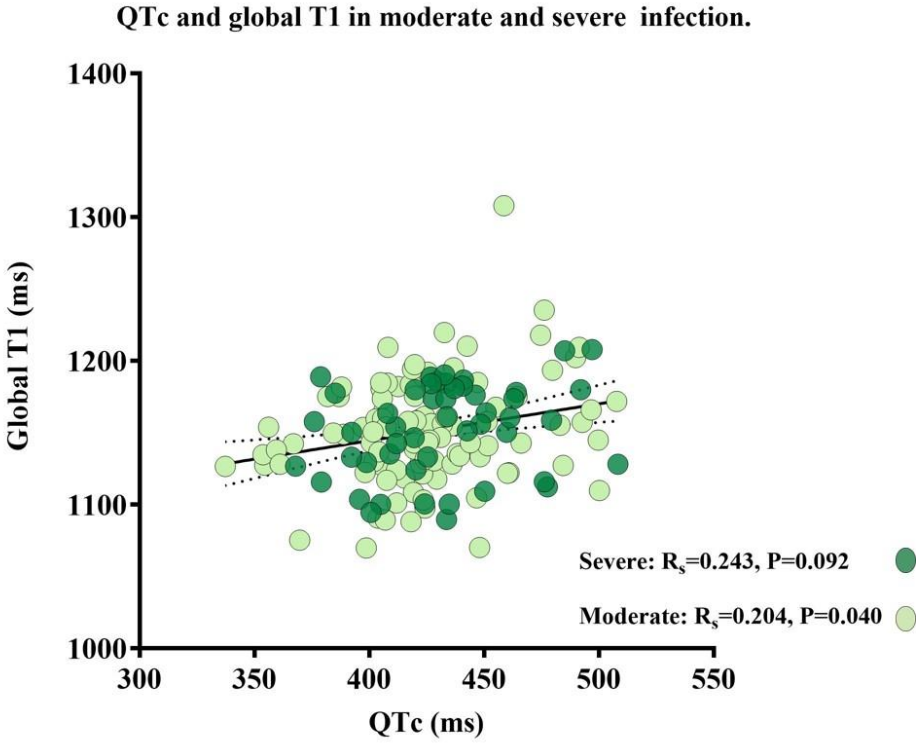


**Figure 3.7** Correlation of QTc and global T1 in moderate and severe infection.

Scatter plot depicting correlations between QTc and global T1 values among moderate COVID-19 infection (WHO score 3-5, n=133) and severe COVID-19 infection (WHO score 6-9, n=56). Note that the correlation is $R_s$=0.243, p=0.092 and $R_s$=0.204, p=0.040 among moderate and severe infection respectively. P values are based on Spearman's correlation analysis ($R_s$).

## CMR ABNORMALITIES IN PATIENTS WITH PROLONGED QT INTERVAL.

To further elucidate the association between established ECG marker of ventricular arrhythmia (QTc > 480 ms) with CMR abnormalities, I compared post-hospitalised COVID-19 patients with and without QTc > 480 ms with composite and individual CMR abnormalities (**Table 6).** Overall, 18 (8.5%) patients had QTc > 480 ms, 61% of whom were females. Their age, BMI and severity of the initial infection based on WHO scores were comparable. Patients with prolonged QTc > 480 ms showed a significant association with high T1 and high ECV (sensitive CMR marker of diffuse fibrosis) relative to patients without high T1 and ECV (**Table 6**). Composite and individual CMR abnormalities such as LVEF. RVEF, high T2 and pathological LGE were comparable.

**Table 6** Characteristics and CMR abnormalities among patients with and without QTc > 480 ms.

| **Prolonged QT and CMR abnormalities** | | | |
|---|---|---|---|
| | **COVID-19 with QTc > 480 ms (n=18)** | **COVID-19 with QTc ≤ 480 ms (n=194)** | **P values** |
| Age, years | 57.0 (48.8-62.3) | 57.0 (49.0-66.0) | 0.679[b] |
| Sex: female n (%) | 11 (61.1) | 66 (34.0) | **0.022[c]** |
| BMI, kg/m$^2$ | 30.9 (24.4-41.7) | 30.0 (27.0-33.7) | 0.435[b] |
| WHO criteria (hospitalised severe score 6-9) | 5/15 (33.3) | 51/174 (29.3) | 0.771[d] |
| CMR abnormal, n (%) | 7 (38.9) | 42 (21.6) | 0.097[c] |
| LVEF < 52%, n (%) | 2 (11.1) | 10 (5.2) | 0.270[d] |
| RVEF < 48%, n (%) | 1 (5.6) | 9 (4.6) | 0.597[d] |
| High T1, n (%) | 6/17 (35.3) | 10/192 (5.2) | **<0.001[c]** |
| High T2, n (%) | 2/14 (14.3) | 15/175 (8.6) | 0.365[d] |
| High ECV, n (%) | 4/17 (23.5) | 11/169 (6.5) | **0.014[d]** |
| Pathological LGE, n (%) | 2 (11.1) | 25 (12.9) | 1.000[d] |

[a]Independent T-Test, [b]Mann-Whitney Test,[c]Chi-Square Test, [d]Fisher's Exact Test.

## DIAGNOSTIC PERFORMANCE OF ECG PARAMETERS FOR COMPOSITE CMR ABNORMALITIES

### GROUP A ECG PARAMETER FOR COMPOSITE CMR ABNORMALITIES

The diagnostic performance of individual group A ECG parameters for CMR abnormalities is generally poor as summarised in **Appendix 2 Table 2**. The composite group A ECG parameters had a weak diagnostic performance for CMR abnormalities with an AUROC of 0.56 (95% CI 0.47-0.65, p=0.185). The SN was 82%, the SP was 31%, the NPV was 85%, and the negative likelihood ratio (-LR) was 0.60 (**Table 7**).

### GROUP B ECG PARAMETER FOR COMPOSITE CMR ABNORMALITIES

Individual repolarisation interval showed a poor-to-moderate discriminative index for composite CMR abnormalities (AUROC ranged from 0.48 to 0.61) (**Table 7**).

For each repolarisation interval, the optimal cut-off value was determined using Youden's index (described in **Appendix 1)** and generated into a categorical variable (e.g. QTc ≥ 450, JTc ≥ 340 ms, cTPe ≥ 100 ms). These cut-off values subsequently formed the basis for the analysis of the diagnostic performance (SN, SP, NPV, PPV, and LR). Overall, the diagnostic ability of individual ECG as categorical variables to discriminate patients with CMR abnormalities was poor, with SN of 45-59%, SP 51-76%, PPV 22-33%, NPV 76-84%, and poor likelihood ratio (**Table 7**).

## GROUP A ECG PARAMETERS WITH THE ADDITION OF REPOLARISATION INTERVALS FOR COMPOSITE CMR ABNORMALITIES

QTc disp, JTc and JTPc intervals (*intervals with significant individual c-index p<0.05 in* **Table 7**) were subsequently permutated in combination with the group A ECG (repolarisation intervals) to determine the best yield in the diagnostic performance. Adding the JTc or JTPc intervals with/out QTc disp to the abnormal ECG features, marginally increased the diagnostic strength from AUROC of 0.56 to 0.62-0.65, p<0.05 (**Table 7**).

Furthermore, the SN increased from 82% to 96-99.9%, NPV from 85% to 95-99.9% and -LR improved by nearly 60 folds from 0.60 to 0.01-0.19, when the repolarisation intervals (JTc ≥ 340 ms or JTPc ≥ 240 ms, with/out QTc disp ≥ 55 ms) were added (**Figure 3.8**). No significant improvement was observed in SP and PPV.

This suggests, if a post-hospitalised COVID-19 patient presented with a normal ECG (which included JTPc interval < 240 ms or JTc interval < 340 ms and/or QTc disp < 55 ms), one may potentially exclude CMR abnormalities in 99.9% of cases with an extremely low post-test probability of abnormal CMR.

**Table 7** Diagnostic performance of ECG for CMR abnormalities.

| CMR abnormalities | | | | | | | | | | |
|---|---|---|---|---|---|---|---|---|---|---|
| | **C-statistic** | **95% CI** | **P value** | **ECG parameters** | **SN (%)** | **SP (%)** | **PPV (%)** | **NPV (%)** | **+LR** | **-LR** |
| ECG abnormalities (Composite Group A) | 0.56 | 0.47-0.65 | 0.185 | ECG abnormalities | 81.6 | 30.7 | 26.1 | 84.7 | 1.18 | 0.60 |
| **Individual repolarisation parameters** | | | | | | | | | | |
| QTc | 0.56 | 0.46-0.65 | 0.240 | QTc ≥ 450 | 32.7 | 76.1 | 29.1 | 79.0 | 1.37 | 0.88 |
| QTc disp | 0.61 | 0.51-0.71 | **0.019** | QTc disp ≥ 55 | 55.1 | 52.1 | 25.7 | 79.4 | 1.15 | 0.86 |
| QTPc | 0.58 | 0.48-0.67 | 0.105 | QTPc ≥ 366 | 34.7 | 70.6 | 26.2 | 78.2 | 1.18 | 0.92 |
| JTc | 0.59 | 0.50-0.69 | **0.048** | JTc ≥ 340 | 49.0 | 66.9 | 30.8 | 81.3 | 1.48 | 0.76 |
| JTPc | 0.61 | 0.52-0.71 | **0.017** | JTPc ≥ 240 | 59.2 | 64.4 | 33.3 | 84.0 | 1.66 | 0.63 |
| cTPe | 0.48 | 0.38-0.57 | 0.590 | cTPe ≥ 100 | 44.9 | 50.9 | 21.6 | 75.5 | 0.91 | 1.08 |
| **ECG + repolarisation parameters** | | | | | | | | | | |
| ECG abnorm + QTc disp | 0.59 | 0.49-0.69 | 0.095 | ECG abnorm + QTc disp ≥ 55 | 91.8 | 17.8 | 25.1 | 87.9 | 1.12 | 0.46 |
| ECG abnorm + JTc | 0.62 | 0.53-0.71 | **0.011** | ECG abnorm + JTc ≥ 340 | 95.6 | 23.3 | 27.3 | 95.0 | 1.25 | 0.19 |
| ECG abnorm+ JTc + QTc disp | 0.64 | 0.55-0.74 | **0.002** | ECG abnorm + QTc disp ≥ 55 + JTc ≥ 340 | 98.0 | 16.0 | 25.9 | 96.3 | 1.17 | 0.13 |
| ECG abnorm + JTPc | 0.63 | 0.55-0.72 | **0.005** | ECG abnorm + JTPc ≥ 240 | 98.0 | 21.5 | 27.3 | 97.2 | 1.25 | 0.09 |
| ECG abnorm + QTc disp + JTPc | 0.65 | 0.56-0.74 | **0.001** | ECG abnorm + QTc disp ≥ 55 + JTPc ≥ 240 | 99.9 | 14.1 | 25.9 | 99.9 | 1.15 | 0.01 |

P values are based on concordance statistics and receiver operating characteristics curve analysis. Abnorm, Abnormalities; BBB, bundle branch block; CMR, cardiac magnetic resonance; C-statistics, concordance statistics; Disp, dispersion; ECG, electrocardiography; LR, likelihood ratio; NPV, negative predictive value; PPV, positive predictive value; QTc, corrected QT; QTPc, corrected QT peak; SN, sensitivity; SP, specificity; cTPe, corrected T-peak- to-T-end.

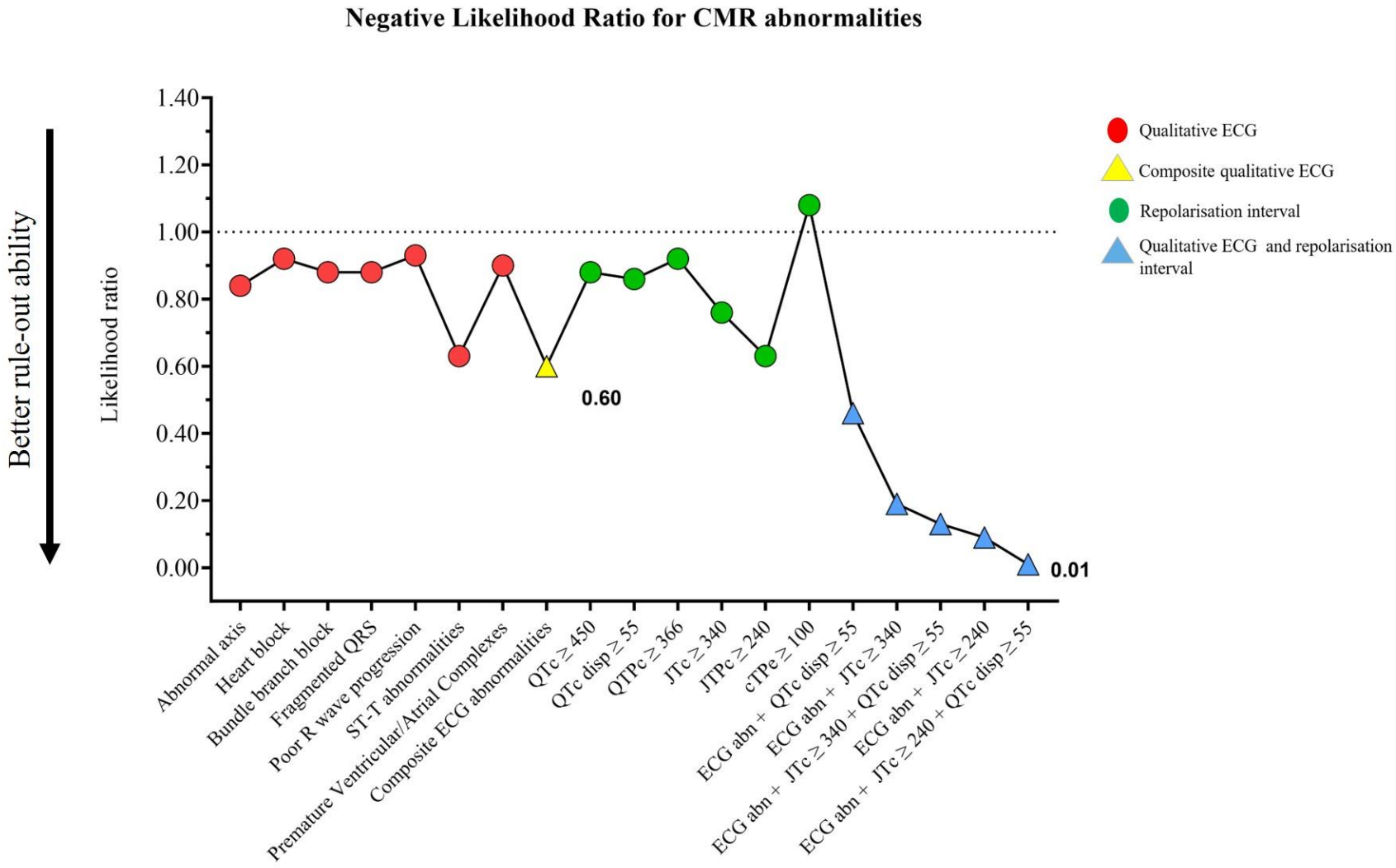
Negative Likelihood Ratio for CMR abnormalities
Better rule-out ability
Likelihood ratio
1.40
1.20
1.00
0.80
0.60
0.40
0.20
0.00
0.60
0.01
Qualitative ECG
Composite qualitative ECG
Repolarisation interval
Qualitative ECG and repolarisation interval
Abnormal axis
Heart block
Bundle branch block
Fragmented QRS
Poor R wave progression
ST-T abnormalities
Premature Ventricular/Atrial Complexes
Composite ECG abnormalities
QTc ≥ 450
QTc disp ≥ 55
QTPc ≥ 366
JTc ≥ 340
JTPc ≥ 240
cTPe ≥ 100
ECG abn + QTc disp ≥ 55
ECG abn + JTc ≥ 340
ECG abn + JTc ≥ 340 + QTc disp ≥ 55
ECG abn + JTc ≥ 240
ECG abn + JTc ≥ 240 + QTc disp ≥ 55

**Figure 3.8** Likelihood ratios of ECG parameters for CMR abnormalities.

Individual ● or composite ▲ group A ECG parameters were poor in ruling out CMR abnormalities (negative likelihood ratio (-LR) ranged between 0.63-0.96). Likewise, the -LR of individual group B repolarisation interval ● was equally poor (-LR ranged between 0.63 to 1.08). Combining the composite group A ECG abnormalities with the repolarisation interval ▲ substantially enhanced the overall -LR values of ECG to exclude CMR abnormalities. Notably, the addition of repolarisation intervals QTc disp ≥ 55ms and JTc ≥ 240 ms to the routine group A ECG features improved the -LR from 0.60 to 0.01. (ECG abn, composite group A ECG features; JTc, corrected JT interval; JTPc, corrected JT peak; QTc disp, QTc dispersion; QTc, corrected QT interval; cTPe, corrected T peak T end interval).
LR of **1.0** indicates no difference in the probability of positive or negative test between those with and without CMR abnormalities.
-LR approaching **0** indicates higher probability of a negative test in those without CMR abnormalities.

## DIAGNOSTIC PERFORMANCE OF REPOLARISATION INTERVALS FOR LV DYSFUNCTION AND INDIVIDUAL MYOCARDIAL TISSUE ABNORMALITIES

All findings are summarised in (**Appendix 2, Table 3**).

### LV DYSFUNCTION

The AUROC of the composite group A ECG abnormalities for patients with LV dysfunction was 0.60. Individually, QTc disp showed the best diagnostic performance for LVEF < 52%, with AUROC of 0.69. The AUROC of ECG improved from 0.60 to 0.72 when QTc disp was included to the diagnostic criteria. Notably, a combination of the composite group A ECG and QTc disp ≥ 55 ms improved the SN from 91% to 99.9%, but SP reduced from 29% to 16%. The -LR, improved from 0.31 to 0.01.

### MYOCARDIAL TISSUE ABNORMALITIES

#### COMPOSITE GROUP A ECG PARAMETER

The AUROC of composite group A ECG parameters was poor, ranging from 0.51 to 0.60, to detect individuals with myocardial tissue abnormalities (high T1/high T2/high ECV/pathological LGE) (**Appendix 2, Table 3**).

#### INDIVIDUAL REPOLARISATION ECG PARAMETER

The JTc interval displayed good discriminative potentials for high T1 or high T2 with AUROC of 0.82 (95% CI 0.71-0.93, p<0.001) and 0.72 (95% CI 0.60-0.85, p=0.002) respectively. For high ECV, the JTPc interval demonstrated a good discriminative potential with AUROC of 0.82 (95% CI 0.73-0.91, p<0.001). None of the repolarisation intervals

were discriminative of pathological LGE (AUROC ranged from 0.43-0.53) (**Appendix 2, Table 3**).

### COMPOSITE GROUP A ECG IN COMBINATION WITH REPOLARISATION PARAMETER FOR MYOCARDIAL TISSUE ABNORMALITIES

Findings are summarised in (**Appendix 2, Table 3**).

To detect for high T1, combination of group A ECG with JTc ≥ 340 ms, augmented the overall SN of ECG from 69% to 94%, NPV from 92% to 98% and the -LR improved by 8 folds from 1.10 to 0.30, denoting a substantial reduction in the probability of detecting high T1 when the ECG was normal.

For high myocardial T2, adding JTc interval to the composite group A ECG abnormalities improved the AUROC from 0.60 to 0.73. In particular, by adding JTc ≥ 340 ms to diagnostic criteria, the SN and NPV of ECG improved from 53% to 94% and 85% to 97%, respectively. Likewise, the -LR improved from 1.76 to 0.29.

For high ECV, combining the composite group A ECG features with the JTPc ≥ 240 ms augmented the SN from 77% to 99.9%, NPV from 94% to 99.9%, and -LR from 0.76 to 0.01.

For pathological LGE, group A ECG in combination with QTc disp, marginally improved the AUROC of ECG from 0.59 to 0.64. Adding QTc disp ≥ 55 ms improved the SN from 89% to 96%, NPV from 94% to 97% and -LR from 0.37 to 0.21. No substantial improvement was observed in SP and PPV values to detect all the individual CMR abnormalities.

The findings suggest that the robustness of this diagnostic capability is more prominent when the group B repolarisation parameters are added to the routinely reported group A ECG features.

## DIAGNOSTIC PERFORMANCE OF REPOLARISATION INTERVALS FOR MYOCARDIAL INFLAMMATION OR FIBROSIS (HIGH T1 OR LGE).

The diagnostic performance for ECG to detect high T1 or pathological LGE (a sensitive marker of myocardial inflammation or fibrosis) on CMR was conducted, and the results are summarised in (**Appendix 2, Table 4**).

### COMPOSITE GROUP A ECG PARAMETER

The discriminative ability of the composite group A ECG parameters to detect patients with myocardial inflammation or fibrosis (high T1 or pathological LGE) among patients was poor (AUROC 0.57, 95% CI 0.48-0.66, p=0.169) (**Appendix 2 Table 4**).

### INDIVIDUAL REPOLARISATION ECG PARAMETER

Individually, the QTc disp, QTPc, JTc and JTPc intervals displayed modest but significant discriminative potentials for high T1 and pathological LGE with AUROC ranging from 0.60-0.62 ($p<0.05$). The AUROC for QTc and cTPe were not significant at 0.58 and 0.48, respectively ($p>0.05$) (**Appendix 2 Table 4**).

## COMPOSITE GROUP A ECG IN COMBINATION WITH REPOLARISATION PARAMETER.

Combining group A ECG with QTc, QTc disp, JTc or JTPc interval increased the AUROC from 0.57 to 0.63-0.66, $p<0.05$. The overall rule-out capability of ECG in combination with these repolarisation intervals for myocardial tissue inflammation or fibrosis in COVID-19

was good, evidenced by the SN, which ranged from 93-95%, NPV 93-94% and -LR between 0.33 to 0.24 (**Appendix 2, Table 4**).

## DIAGNOSTIC PERFORMANCE OF NEWLY PROPOSED ECG CRITERIA FOR CMR ABNORMALITIES

The additive value of JT parameters (JTc or JTPc), with QTc disp over routinely reported composite group A ECG criteria to exclude CMR abnormalities in COVID-19 patients, demonstrated promising findings. Notably, adding either JTc ≥ 340 or JTPc ≥ 240 ms, with or without QTc disp ≥ 55 ms, yielded moderate discriminative potential with c-index between 0.62-0.65, coupled with excellent rule-out capabilities of SN (96%-99.9%), NPV (95-99.9%) and -LR (0.01-0.19) (**Table 7**).

## 3.6 DISCUSSION

To my knowledge, this is the first study to comprehensively examine the diagnostic utility of ECG as a screening tool for cardiac abnormalities on CMR in post-hospitalised COVID-19 patients. The main findings from this study are as follows: First, post-hospitalised COVID-19 patients have a high burden of ECG abnormalities relative to comorbidity-matched uninfected non-COVID-19 controls. Second, at a median of 5.6 months post-hospitalisation, COVID-19 patients had lower left ventricular systolic function relative to matched controls and higher LGE mass, but all other CMR abnormalities were comparable. Third, significant associations were observed between some ECG parameters (such as JTc and QTc disp) and CMR measures, including T1, T2, ECV and LGE, signifying a relationship between markers of oedema or fibrosis and repolarisation abnormalities. Fourth, a normal 12-lead ECG with normal repolarisation intervals was highly effective in ruling out significant CMR abnormalities.

### ECG ABNORMALITIES WERE COMMON IN POST-HOSPITALISED COVID-19 PATIENTS

Numerous studies have examined the prevalence of ECG abnormalities in the acute COVID-19 period, but only a few have systematically described this in the post-acute phase, and none as yet have evaluated its diagnostic accuracy for CMR abnormalities in a multicentre setting[20,90,155,156]. In the present study, we observed a high prevalence of ECG abnormalities among patients, which were more frequent in those with abnormal CMR findings. ECG abnormalities included, amongst others, ST-T abnormalities, abnormal R wave progression, fragmented QRS, bundle branch block, and premature atrial or ventricular and atrial complexes. Interestingly, even patients with a normal CMR or no known cardiac

comorbidities had abnormalities on ECG at 5.6 months post-hospitalisation for COVID-19. Whilst the findings suggest a possible link between hospitalisation with severe COVID-19 and prolonged repolarisation in patients, it remains difficult to confirm a causal association in the absence of preinfectional ECG. This corresponds with previous research that also noted a high frequency of ECG abnormalities (50-61%) at 3-12 months in a large prospective study of 594 patients in Wuhan[78]; however, they did not undertake CMR in their study and the performance of ECG as a screening tool for underlying cardiac abnormalities was not evaluated.

### CMR ABNORMALITIES BETWEEN POST-HOSPITALISED COVID-19 PATIENTS AND CONTROLS

At a median of 5.6 months after infection, post-hospitalised patients had lower LV systolic function and higher LGE burden. Whilst this was unexpected, our findings mirror observations from other single-centre follow-up studies that compared patients presenting months after infection and risk-factor matched controls[146,150]. Our study reinforces the message that ECG and CMR provide complementary information, and the presence of a normal CMR may not adequately exclude cardiac electrical abnormalities (e.g., arrhythmias), and highlight the need to continue monitoring patients with ECG in post-COVID clinics.

## MYOCARDIAL TISSUE ABNORMALITIES AND CARDIAC DYSFUNCTION ON CMR ASSOCIATED WITH REPOLARISATION PARAMETERS.

Advanced tissue characterisations on CMR using techniques such as native T1 and T2 mapping coupled with the more established LGE imaging, has improved the diagnostic accuracy of CMR for acute and chronic cardiac complications of infections[157,158]. Based on such imaging techniques, the reported burden of myocardial oedema in the early post-acute phase (up to three months post-COVID-19) has ranged from 3 to 70%[47,159], with selection bias (of symptomatic individuals) suggested to explain higher estimates[32].

In the present study, nearly a quarter of patients had pathological LGE patterns, or high myocardial T1/T2, at a median of 5.6 months from infection. Individuals with high myocardial T1 or T2 (markers sensitive to myocardial fibrosis and oedema[160,161]), were noted to have longer repolarisation intervals (including QTc, QTPc, JTc and cTPe) than those with normal tissue characteristics and controls. Positive correlations between repolarisation interval such as the QTc with global myocardial T1 among patients were also observed. Additionally, when compared between patients with and without elevated risk of arrhythmia defined by the prolonged QTc > 480 ms, the burden of high T1 and high ECV (CMR markers for diffuse fibrosis) were significantly higher among those with prolonged QTc.

Taken together, our findings suggest that prolonged repolarisation intervals and interval dispersion on ECG may be indicative of residual fibrosis or oedema in some patients[95], which may, in turn, reflect subtle inflammatory changes. An alternate explanation for this association is that the increased expression of cytokines that contributes to CMR abnormalities in the post-acute phase may also contribute to ionic remodeling[93]. For

instance, inflammatory cytokines such as tumour necrosis factor (TNF), IL-1 and IL-6 have been suggested to alter action potential durations by decreasing specific cardiac $K^+$ currents or/and increasing L-type $Ca^{2+}$ currents[93]. Specifically, TNFα causes inhibition of the transient outward rapidly activating repolarising $K^+$ currents and slowly activating repolarising $K^+$ currents, which in turn leads to prolongation of action potential duration (APD)[93]. The reduction in transient outward $K^+$, resulting from the downregulation of channel expression (mediated by the inflammatory cytokines) prolongs phases two and three of myocardial APD, which corresponds to the QT interval and TPe segment of the ECG[62,95].

Mechanistically, this is an important finding, as heterogeneity in ventricular repolarisation is a well-known risk factor for increased arrhythmogenicity, and is independently associated with the risk of sudden cardiac death in other diseases[162]. Indeed, this may also explain the high risk of cardiovascular mortality and arrhythmias observed in some retrospective cohort studies of post-COVID patients one year after hospitalisation[57,163].

## 3.7 CLINICAL APPLICATION

The 12-lead ECG provides a pragmatic screening solution for clinicians, especially in centres with limited CMR services. Our study has, for the first time, comprehensively evaluated the diagnostic utility of ECG as a screening tool for cardiac abnormalities defined by a reference non-invasive standard measure of cardiac pathology, namely CMR. We demonstrated that the strength of the ECG lies in its high NPV, reinforcing its role as a screening test that can be used to rule out significant cardiac disease in the follow-up of patients post-COVID-19.

In particular, the inclusion of the repolarisation parameter, JTc ≥ 340 ms (with or without QTc disp ≥ 55 ms), to the lists of other known ECG abnormalities, augmented the SN and NPV of the revised ECG criteria for CMR abnormalities. Thus, the probability of potentially missing an individual with ongoing cardiac damage using our revised criteria, is low. These findings would also allow clinicians to reassure certain patients (such as those with normal ECG), enabling early discharge and freeing up resources for others in need of such services.

From the practical standpoint, measurement of the JT interval is relatively easier, compared to the JT peak, as it does not require identifying the peak of the T wave, but rather, derived only from the deduction of QRS duration from the QT interval. I hence proposed combining QTc disp and JTc interval along with the composite group A ECG features for future use to reduce the rate of incorrect diagnosis (false negative) and to augment the SN and NPV to exclude CMR abnormalities (**Figure 3.9**).

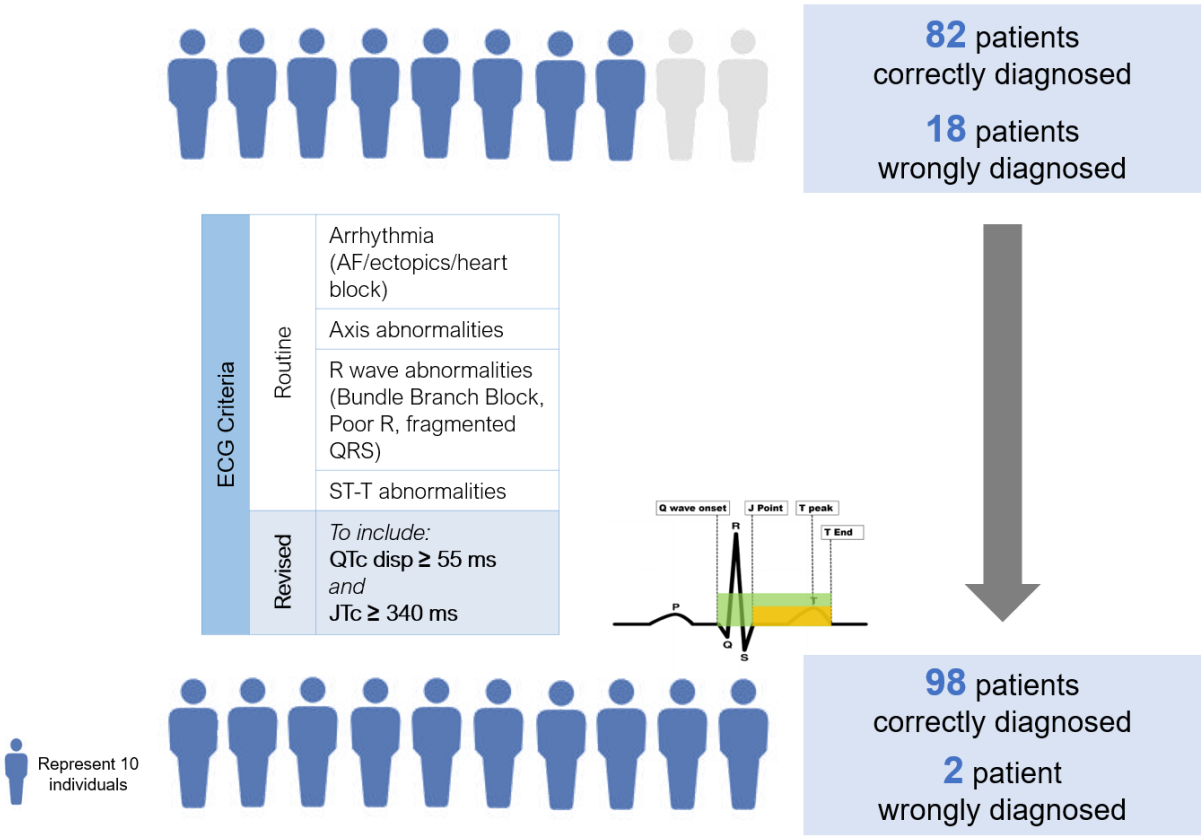


**Figure 3.9** Diagnostic performance of ECG with the addition of repolarisation intervals.

The illustration depicts the improvement in the diagnostic performance of ECG to detect post-hospitalised COVID-19 patients with CMR abnormalities when repolarisation intervals (QTc disp ≥ 55ms and JTc ≥ 340 ms) are included in the routinely reported group A ECG features.

## 3.8 LIMITATIONS

Overall, as the sample of the study is small, the findings are hypothesis-generating and should be considered exploratory in nature for a specific cohort of post-hospitalised moderate-to-severe COVID-19 patients. The lack of pre-COVID CMR or ECG among study patients prior to hospitalisation limits our ability to establish a clear causal relationship between SARS-CoV-2 infection and cardiac abnormalities. Furthermore, there may be systemic differences (non-cardiovascular and pulmonary conditions such as chronic obstructive pulmonary disease (COPD) or pulmonary hypertension) between the groups that may also affect the ECG and the CMR findings, which were not specifically explored in this study. Additionally, although some patients (6%) required oxygen supplementation due to low oxygen saturation during admission, it was unknown whether these patients had low oxygen saturation due to COVID-19-related lung pathology or another underlying chronic lung disease. Nonetheless, among those with low oxygen saturation, only one participant had underlying heart disease, hypertension, or left ventricular dysfunction (LVEF < 52%). None had abnormal right ventricular function (RVEF < 48%) or ECG abnormalities related to chronic lung disease, such as atrial fibrillation, abnormal P waves (pulmonale or mitrale) or prolonged P wave duration (> 200 ms), making chronic lung disease less likely among these patients. Additionally, the association of the ECG and CMR parameters of health with inflammatory blood markers was not explored, limiting insights into systemic inflammatory channelopathy. As patients were recruited from multiple sites across the UK with only a few centres utilising electronic ECG, artificial intelligence (AI) assisted analysis was not possible, limiting further AI-driven insights. Ideally, age, risk factors and comorbidities-matched non-COVID-19 post-hospitalised patients should be recruited as controls for a more effective comparison between COVID-19 and non-COVID-19 infection. However,

due to the COVID-19 restrictions, post-hospitalised non-COVID-19 control recruitment was not technically feasible during the period.

Nonetheless, our pragmatic approach can be viewed as a strength of this study, as the measured parameters were manually ascertained and can be inferred from computer-assisted ECG measurements (QRS and the QT intervals). With external validations, this approach may allow more widespread adoption of our study findings globally, which are relevant for an infection not contained by geographical or economic borders. Furthermore, external validation of the proposed cut-offs for ECG intervals is also absent, although the multicentre study design has potential advantages for our findings. Based on the established cut-off for QTc > 480 ms, about 10% of patients showed an elevated burden of myocardial fibrosis, which can be substrates to arrhythmogenesis. However, there was no Holter monitoring to confirm the incidence or development of any arrhythmic episode.

Finally, the prevalence of high T1 and T2 in this cohort is low, which may have exaggerated the NPV and reduced the PPV of the screening tests[164]. Therefore, more extensive studies on different cohorts are recommended to validate this relationship.

## 3.9 CONCLUSION

In post-hospitalised COVID-19 patients, a normal 12-lead ECG may rule out significant cardiac damage on CMR and offer biological insights into potential mechanisms for arrhythmias in post-hospitalised COVID-19 patients. Nonetheless, the relationship between specific ECG measures and tissue properties on CMR requires further evaluation as the present study is statistically underpowered due to small sample size.

(Key findings are summarised in the central illustration (**Figure 3.10**).

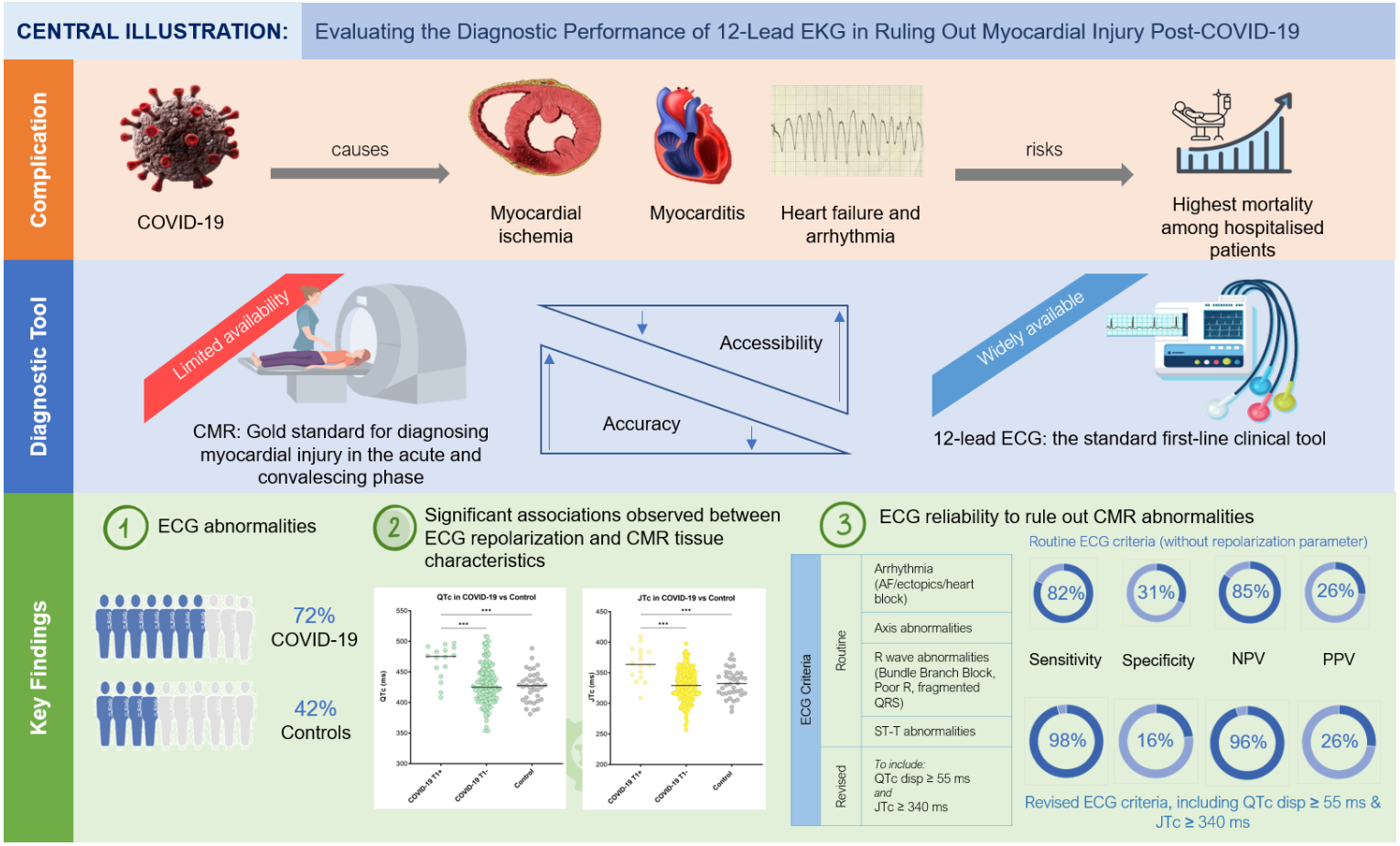


**Figure 3.10** Illustration of the key findings.

1) significantly higher burden of ECG abnormalities among post-hospitalised COVID-19 patients, 2) significant associations of repolarisation parameters with CMR myocardial tissue characteristics, iii) The diagnostic performance to exclude CMR abnormalities is better when QTc ≥ 55 ms and JTc ≥ 340 ms are added to the routinely-reported ECG abnormalities.

# CHAPTER 4: ROLE OF COVARIATES IN THE DIAGNOSTIC AND PREDICTIVE ABILITY OF ECG IN DETECTING MYOCARDIAL ABNORMALITIES IN COVID-19 PATIENTS

## 4.1 ABSTRACT

***Background***

Sex-based differences may impact the discriminative performance of a 12-lead ECG for CMR abnormalities. The study aimed to determine the impact of sex in the diagnostic utility of ECG in detecting composite and individual CMR abnormalities and examine the associations of ECG-CMR when adjusted for the clinical covariates, among post-hospitalised COVID-19 patients.

***Methods***

In this multicentre follow-up study, 212 patients, 135 (64%) male and 77 (36%) female, underwent CMR and 12-lead ECG. ECG and CMR analysis (as described in Chapter 3) was conducted, and comparisons were made between sexes. Sex-based diagnostic performance and the impact of covariates on the ECG-CMR association were determined.

***Results***

Women were more likely to have an incorrect ECG diagnosis based on the routinely reported ECG features (group A)[1] relative to men (women: Sensitivity (SN) 67%, Specificity (SP) 32% vs men: SN 90%, SP 30%). The addition of repolarisation intervals (Group B), such as the QTc disp and JTc interval, provided the most optimal sex-stratified diagnostic performance of ECG for CMR abnormalities, with a substantial increase in SN and negative predictive value (NPV) of ECG for CMR abnormalities in women (SN 67% to 94%), (NPV 76% to 91%) and in men (SN 90% to 100%), (NPV 91% to 100%). QTc disp remained a

[1] Presence of any arrhythmia (i.e. atrial fibrillation, atrial flutter, premature ventricular complexes (PVC) and premature atrial complexes (PAC)) or abnormal axis or heart block or poor QRS progression or fragmented QRS (fQRS) or bundle branch block (including left bundle branch block, right bundle branch block, incomplete bundle branch block and non-specific intraventricular conduction delay) or ST-T changes.

significant predictor for CMR abnormalities even after adjusting for the clinical covariates (age, sex, body mass index, hypertension and diabetes).

***Conclusion***

In this study, sex-based variations are present in the diagnostic performance of ECG to detect CMR abnormalities. The overall diagnostic and predictive performance of ECG for CMR abnormalities across sexes may potentially be optimised by adding the repolarisation intervals (group B ECG)[1]. Larger studies are required to validate these findings.

[1] Repolarisation parameters e.g. QTc interval, QTc disp and JTc interval. (Please refer Table 1 page 16).

## 4.2 INTRODUCTION

Sex-based differences in ECG are well-known, and the earliest evidence can be traced back to the early 1940-60s[165,166]. In the last decade, there has been an increased interest to further explore the sex-based differences in ECG based on animal and human studies, to explain the mechanisms and the impact of sex-based differences on diagnostic approach[167-169]. Reports on sex-based diagnostic performance of ECG for cardiac abnormalities based on CMR is unknown.

In pre-clinical studies, female canine ventricles demonstrated a greater L-type Ca2+ current measurement than male canines[170]. In female murine hearts, the density of transient outward K+ and slow delayed-rectifier K+ current are lower in the presence of high oestrogen levels, causing longer repolarisation intervals[171]. Likewise, there is an increased heterogeneity in ventricular repolarisation attributed to the sex-based differences in transmural distribution of the K+ channels[170], in female canine hearts. These findings support the sex-hormones impact on ionic channels modulation, which increases the risk of ventricular arrhythmia via perturbation of ventricular repolarisation[170].

In human hearts, physiological variations on a genetic or cellular level have been widely reported, with differences in expression linked to X- and Y-linked genes[172]. In healthy transplant donor hearts, women exhibit lower density and slower repolarising outward K+ currents due to reduced gene expression, such as HERG and minK, which encode for K+ channel subunits[168]. It is now established that sex hormones can affect the cellular electrophysiology of the cardiac myocytes, appreciable on the 12-lead ECG complexes and intervals[173], as summarised in **Appendix 3, Table 1**. Compared to males, females generally show longer action potential (AP) duration, slower AP recovery, shorter PR interval,

narrower QRS duration, and longer QT intervals[173]. The 12-lead ECG features between sexes are so distinctive that the patient's sex can be identified with over 90% accuracy using AI-assisted algorithms in a recent study[174]. The findings further support the need to explore the sex-based diagnostic performance of ECG for cardiac abnormalities in the setting of diseases of public health emergencies.

In the setting of COVID-19, sex-based differences in immune response[175] and outcomes such as hospitalisation, ICU admission, long COVID-19 syndrome and mortality, have been reported[176-178]. Men have higher odds of experiencing mortality or critical illness than women, based on a large meta-analysis involving more than 11 000 COVID-19 patients[176]. Women on the other hand, are more likely to be associated with long-COVID-19 syndrome[179]. Nonetheless, only a few of the sex-based COVID-19 studies reported on ECG findings for meaningful comparison. Omar et al. demonstrated greater proportion of QTc prolongation and ST-T changes among female COVID-19 patients[180], but the study was limited by lack of report on the diagnostic performance of ECG for cardiac abnormalities. Recently, studies exploring ECG-based prediction models using machine learning method showed that ECG was useful for early stratification of hospitalised COVID-19 patients with AUROC of 0.77 (95% CI 0.76-0.78), to detect SARS-CoV-2 infection[181,182]. Nonetheless, specific discussion on the sex-based differences are lacking in these studies, and the associations of ECG with CMR abnormalities or myocardial injury was not explored.

Taken together, there are specific unmet needs in clinical diagnostic areas especially related to ECG and CMR associations in COVID-19. Hence, in this chapter, I comprehensively explored the sex-based differences in the burden of ECG and CMR abnormalities. The diagnostic performance and predictive ability of ECG for CMR abnormalities was subsequently determined with adjustment of covariates such as age and sex.

## 4.3 METHODS

All participants underwent CMR and a 12-lead ECG on the same day between March 2020 and November 2021 based on the protocol previously described. Data were interpreted and analysed as described in **Chapter 2**.

## 4.4 STATISTICAL ANALYSIS

Variables were summarised and analysis of data were conducted as previously described in **Chapter 2**. One-way analysis of covariance (ANCOVA) with Bonferroni post-hoc test was conducted to detect a difference in means of ECG intervals between sexes, controlling for BMI as covariate. Univariable and multivariable binary logistic regression models were conducted**.** In the multivariable model, to predict for CMR myocardial abnormalities, we tested each ECG parameter and adjusted for a clinical model which included age and sex[183]. Evaluation of model performance based on its calibrative and discriminative ability are further described in **Appendix 1**. All p-values reported are from two-tailed tests. Data are presented with 95% Confidence Intervals (CI). All statistical analysis was performed with SPSS version 27.0 (IBM, Armonk, NY, USA).

## 4.5 RESULTS

### BASELINE CHARACTERISTICS OF MALE AND FEMALE COVID-19 PATIENTS

The baseline characteristics and the clinical data of male and female COVID-19 patients, are summarised in

**Table .** Out of the total 212, there were 135 (64%) male patients with a median age of 59 years (IQR 51-66) and 77 (36%) female patients with a median age of 55 years (IQR 48-63). There was no significant difference in the baseline characteristics apart from BMI which was higher among the female patients (32.0 ± 7.1 kg/$m^2$ vs 30.0 ± 4.9 kg/$m^2$, p=0.031), and the proportion of patients requiring oxygen supplementation which was more frequent among the male patients (83% vs 70%, p=0.032). For the laboratory results, the NT Pro-BNP and CRP levels were significantly higher in female than the male patients albeit within the normal range, with a median of 50.0 (IQR 35.0-101.0) pg/mL vs 35.0 (IQR 21.0-64.5) pg/mL, p=0.004 and CRP levels with a median of 5.0 (IQR 0.0-6.0) mg/L, vs 1.6 (IQR 0.0-5.0) mg/L, p=0.030.

**Table 1** Clinical parameters of male and female COVID-19 patients.

| | **Male COVID-19 (n=135)** | **Female COVID-19 (n=77)** | **P values** |
|---|---|---|---|
| Age (years) | 59 (51-66) | 55 (48-63) | 0.116[b] |
| Non-white ethnicity, n (%) | 38/124 (30.6) | 21/72 (29.2) | 0.828[c] |
| BMI kg/m$^2$ | 30.0 ± 4.9 | 32.0 ± 7.1 | **0.031[a]** |
| Systolic pressure mmHg | 129 (118-141) | 133 (117-147) | 0.291[b] |
| Diastolic pressure mmHg | 79 ± 13 | 75 ± 13 | 0.062[a] |
| Duration of admission days | 7 (3-10) | 5 (2-10) | 0.159[b] |
| Smoker and Ex-smoker, n (%) | 39/122 (32.0) | 18 /72 (25.0) | 0.303[c] |
| Hypertension, n (%) | 34/108 (31.5) | 16/68 (23.5) | 0.255[c] |
| Diabetes Mellitus, n (%) | 15/111 (13.5) | 7/68 (10.3) | 0.524[c] |
| History of ischemic heart disease, n (%) | 4/110 (3.6) | 2/68 (2.9) | 0.803[d] |
| Congestive heart failure, n (%) | 1/107 (0.9) | 1/68 (1.5) | 0.999[d] |
| Oxygen supplementation, n (%) | 102/123 (82.9) | 48 /69 (69.6) | **0.032[c]** |
| Invasive mechanical ventilation, n (%) | 11/123 (8.9) | 6/69 (8.7) | 0.954[c] |
| **Laboratory Results** | | | |
| White cell count x $10^9$/L | 6.6 (5.5-8.4) | 6.6 (5.7-8.4) | 0.802[b] |
| NT Pro-BNP, pg/mL | 35.0 (21.0-64.5) | 50.0 (35.0-101.0) | **0.004[b]** |
| Troponin, ng/L | 6.3 (5.0-16.4) | 7.0 (3.3-16.0) | 0.997[b] |
| C-Reactive Protein, mg/L | 1.6 (0.0-5.0) | 5.0 (0.0-6.0) | **0.030[b]** |

[a]Independent T-Test [b]Mann-Whitney Test, [c]Chi-Square Test, [d]Fisher-Freeman-Halton Exact Test.

Values are mean ± SD, median (IQR) or percentages. BBB, indicates bundle branch block; ECG, electrocardiography; PAC, premature atrial complex; PVC, premature ventricular complex; QTc, corrected QT; QTPc, corrected QT peak; cTPe, corrected T-peak- to-T-end; Disp, dispersion.

## ECG AND CMR FEATURES IN MALE AND FEMALE POST-COVID-19 PATIENTS

**Tables 2** and **3** summarise sex-based differences in the ECG and CMR parameters of post-hospitalised COVID-19 patients. Overall, the proportion of abnormal ECG (*composite group A features*) did not differ significantly between male and female patients. ST-T changes were the most commonly reported group A ECG abnormalities and were comparable in both sexes (**Figure 4.1**).

For group B ECG parameters, female patients had a higher average heart rate than the male patients. Females displayed longer repolarisation intervals, including the QTc, QTPc, JTc, and JTPc intervals. On the other hand, PR interval and QRS duration were significantly longer in male than female patients, whereas cTPe interval and QTc disp did not differ significantly between sexes (**Figure 4.2**). Analysis of the covariance adjusted for BMI was also conducted and revealed similar outcomes (**Appendix 3, Table 2**).

The overall burden of CMR abnormalities at 5.6 months post-hospitalisation was comparable between the sexes. All CMR functional parameters were normal among the males except for LVEF, and RVEF which were significantly lower among the male patients (**Table 3**). Around 7% of male patients had LVEF < 52% or RVEF < 48%, whereas only 3% of female patients had either low LV or RVEF. For myocardial tissue characteristics, female patients displayed a significantly higher burden of myocardial fibrosis or oedema evidenced by the higher proportion of high T1, and high ECV. Likewise, native global T1, global T2 and ECV (%) values were also greater among the female patients. The burden of pathological LGE was higher in male than female patients but was not statistically significant (**Figure 4.3**).

**Table 2** ECG characteristics of male and female COVID-19 patients.

| ECG | | | |
|---|---|---|---|
| | **Male COVID-19 (n=135)** | **Female COVID-19 (n=77)** | **P values** |
| Abnormal ECG (Composite Group A), n (%) | 101 (74.8) | 52 (67.5) | 0.255[c] |
| Atrial Fibrillation/Flutter, n (%) | 1 (0.7) | 0 (0) | 0.999[d] |
| Bundle Branch Block, n (%) | 17 (12.6) | 4 (5.2) | 0.083[c] |
| LBBB, n (%) | 2/131 (1.5) | 0 (0) | 0.536[d] |
| RBBB, n (%) | 7 (5.3) | 1 (1.4) | 0.263[d] |
| ILBBB/IRBBB/IVCD, n (%) | 8 (5.9) | 3 (3.9) | 0.750[d] |
| Abnormal axis, n (%) * | 31/118 (26.3) | 11/73 (15.1) | 0.069[c] |
| ST-T changes, n (%) * | 42/118 (35.6) | 24/73 (32.9) | 0.701[c] |
| Abnormal R prog, n (%) | 19 (14.1) | 19 (24.7) | 0.053[c] |
| Fragmented QRS n (%) * | 36/118 (30.5) | 15/73 (20.5) | 0.131[c] |
| Heart block n (%) | 11 (8.1) | 3 (3.9) | 0.231[d] |
| PVC/PAC n (%) | 8 (5.9) | 2 (2.6) | 0.336[d] |
| Heart rate (bpm) | 69 (61-81) | 75 (66-86) | **0.032[b]** |
| PR interval ms | 162.0 (146.0-178.0) | 155.0 (140.5-166.0) | **0.032[b]** |
| QRS ms | 94.0 (88.0-102.0) | 86.0 (81.0-94.0) | **<0.001[b]** |
| QTc ms | 421.1 ± 33.9 | 440.1 ± 32.6 | **<0.001[a]** |
| QTc disp ms | 55.7 (41.6-71.5) | 50.9 (39.4-64.9) | 0.251[b] |
| QTPc ms | 339.9 ± 30.3 | 360.6 ± 32.5 | **<0.001[a]** |
| JTc ms | 324.2 ± 26.76 | 345.0 ± 27.1 | **<0.001[a]** |
| JTPc ms | 220.9 (203.1-241.2) | 246.4 (232.8-256.8) | **<0.001[b]** |
| cTPe ms | 100.3 (90.2-112.1) | 95.9 (88.9-107.3) | 0.151[b] |

[a]Independent T-Test [b]Mann-Whitney Test, [c]Chi-Square Test, [d]Fisher-Freeman-Halton Exact Test.

Values are mean ± SD, median (IQR) or percentages. Abnormal R prog, abnormal R wave progression; BBB, bundle branch block; ECG, electrocardiography; ECV, extracellular volume; ILBBB, incomplete left bundle branch block; IRBBB, incomplete right bundle branch block; IVCD,

intraventricular conduction delay; PAC, premature atrial complex; PVC, premature ventricular complex; JTc, corrected JT; JTPc, corrected JT peak; QTc, corrected QT; QTPc, corrected QT peak; cTPe, corrected T-peak- to-T-end; disp, dispersion. *Bundle branch block cases were excluded in the analysis.

**Table 3** CMR characteristics of male and female COVID-19 patients.

| CMR | | | |
|---|---|---|---|
| | **Male COVID-19 (n=135)** | **Female COVID-19 (n=77)** | **P values** |
| CMR abnormal, n (%) | 31 (23.0) | 18 (23.4) | 0.945[c] |
| LVEDV ml | 157 (139-179) | 135 (104-155) | **<0.001[b]** |
| LVESV ml | 65 (54-76) | 50 (37-59) | **<0.001[b]** |
| LVSV ml | 92(82-103) | 84(68-97) | **0.002[b]** |
| LV mass g | 121 ± 23 | 92 ± 21 | **<0.001[a]** |
| LV mass index g/m$^2$ | 57 ± 10 | 47 ± 7 | **<0.001[a]** |
| LVEF (%) | 59 ± 6 | 63 ± 5 | **<0.001[a]** |
| LVEF < 52%, n (%) | 9 (6.7) | 2 (2.6) | 0.335[d] |
| RVEDV ml | 159 (138-176) | 128 (105-155) | **<0.001[b]** |
| RVESV ml | 69 (55-80) | 45 (36-59) | **<0.001[b]** |
| RVSV ml | 90 (82-102) | 79 (68-95) | **<0.001[b]** |
| RVEF (%) | 57 ± 6 | 63 ± 6 | **<0.001[a]** |
| RVEF < 48%, n (%) | 10 (7.4) | 0 (0) | **0.015[d]** |
| **Myocardial Tissue Characterisations** | | | |
| T1 normalised Z score | -0.33 ± 1.5 | 0.80 ± 1.9 | **<0.001[a]** |
| T2 normalised Z score | 0.63 (-0.07-1.32) | 0.82 (0.17-1.61) | **0.042[b]** |
| Global T1 ms ** | 1141 ± 31 | 1167 ± 37 | **<0.001[a]** |
| Global T2 ms ** | 41 ± 2 | 42 ± 2 | **0.027[a]** |
| ECV (%) | 0.27 ± 0.03 | 0.29 ± 0.03 | **<0.001[a]** |
| High T1, n (%) | 4 (3) | 12 (16) | **<0.001[c]** |
| High T2, n (%) | 10 (8) | 7 (10) | 0.711[c] |
| High ECV (>32), n (%) | 3/109 (2.8) | 10/56 (17.9) | **0.001[d]** |
| Pathological LGE, n (%) | 21/124 (16.9) | 6/71 (8.5) | 0.099[c] |
| LGE mass (g) | 3.7 (2.1 – 5.9) | 3.6 (1.7-4.6) | 0.422[b] |

| | | | |
|---|---|---|---|
| Non-pathological LGE, n (%) | 13/124 (10.5) | 3/71 (4.2) | 0.125[c] |
| RV insertion LGE, n (%) | 3/124 (2.4) | 2/71 (2.8) | 0.999[d] |
| Basal sub valvular LGE, n (%) | 3/124 (2.4) | 5/71 (7.0) | 0.143[d] |
| Ischemic LGE, n (%) | 10/124 (8.1) | 2/71 (2.8) | 0.217[d] |
| Myocarditis LGE, n (%) | 13/124 (10.5) | 4/71 (5.6) | 0.248[d] |
| Mixed LGE, n (%) | 2/124 (1.6) | 0 (0) | 0.535[d] |
| Cardiomyopathy LGE, n (%) | 3/124 (2.4) | 0 (0) | 0.555[d] |
| Pleural effusion, n (%) | 1/124 (0.8) | 1/71 (1.4) | 0.999[d] |

[a]Independent T-Test [b]Mann-Whitney Test, [c]Chi-Square Test, [d]Fisher's Exact Test.

Values are mean ± SD, median (IQR) or percentages. CMR, cardiac magnetic resonance; ECV, Extracellular volume; LGE, late gadolinium enhancement; LV, left ventricular; LVEDV, left ventricular end- diastolic volume; LVESV, left ventricular end-systolic volume; LVSV, left ventricular systolic volume; LVEF, left ventricular ejection fraction; LVCO, left ventricular cardiac output; RVEDV, right ventricular end-diastolic volume; RVESV, right ventricular end-systolic volume; RVSV, right ventricular systolic volume; RVEF, right ventricular ejection fraction; RVCO, right ventricular cardiac output. **SHMOLLI sequence only.

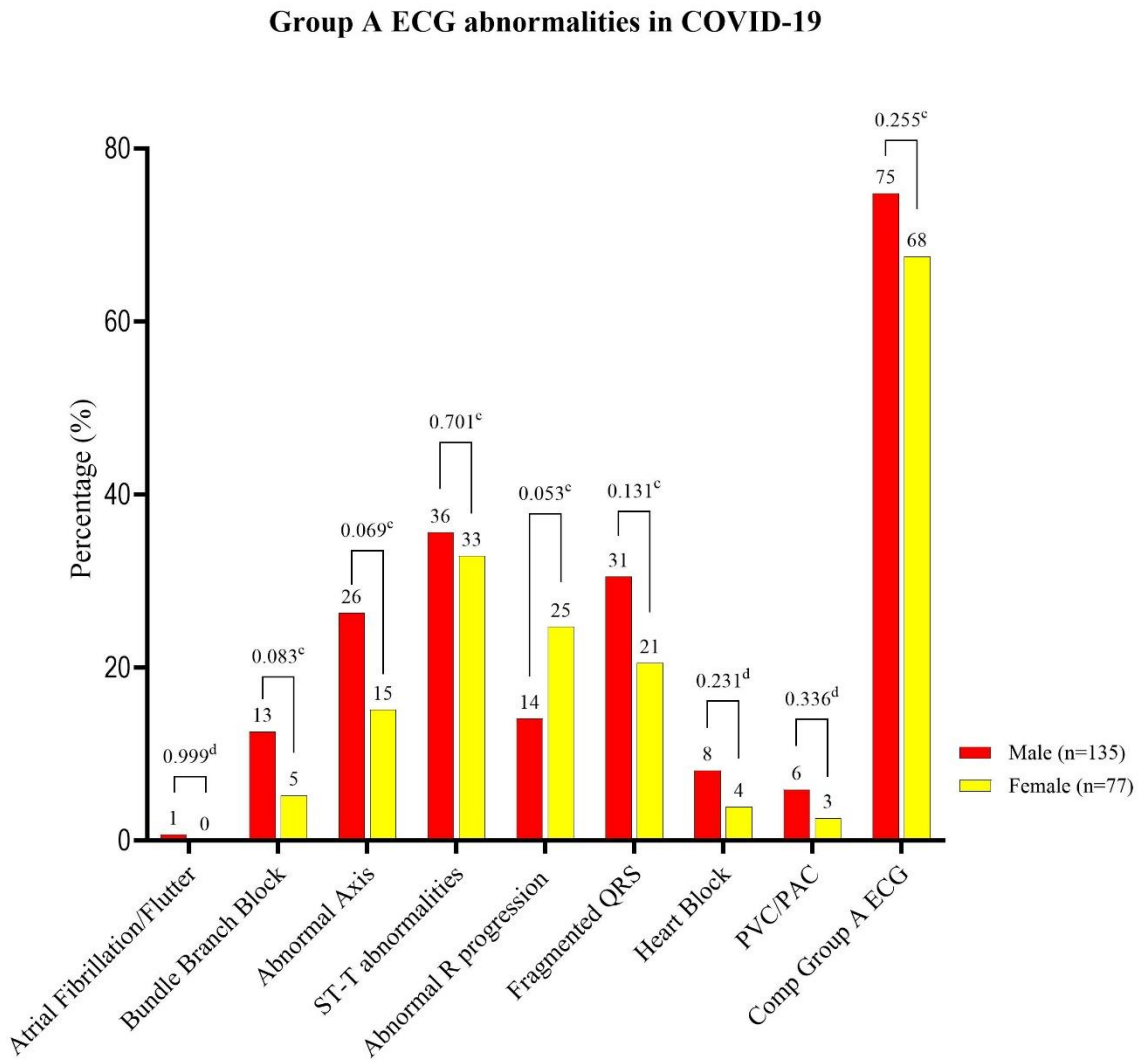


**Figure 7.1** Group A ECG abnormalities in COVID-19 based on sex.

[c]Chi Square Test, [d]Fisher Exact Test.
Comp, Composite; PAC, Premature atrial complex; PVC, Premature ventricular complex.
Male COVID-19 patients demonstrate a higher burden of abnormal group A ECG features than female patients, but the difference did not reach statistical significance.

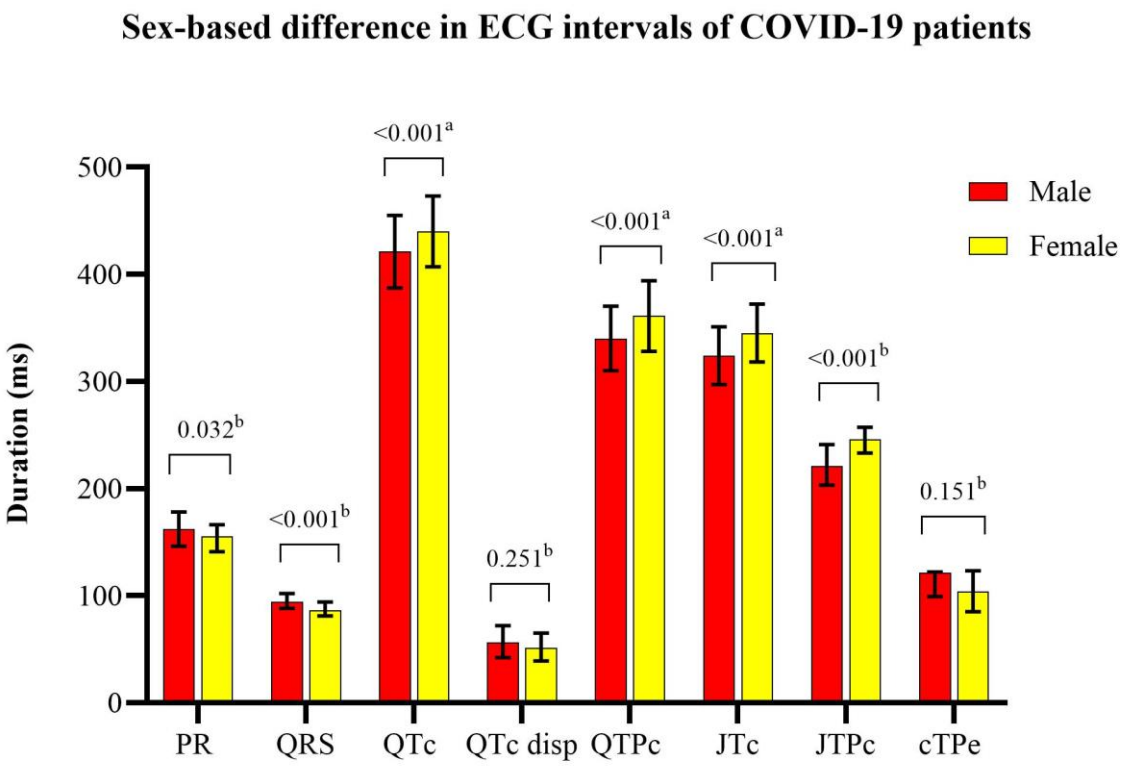


**Figure 4.2** Sex-based differences in ECG intervals of COVID-19 patients.

[a]Unpaired T test, [b]Mann Whitney U test.
JTc, corrected JT interval; JTPc, corrected JT peak interval; QTc, corrected QT interval; QTPc, corrected QT peak interval; cTPe, corrected T peak to T end interval.

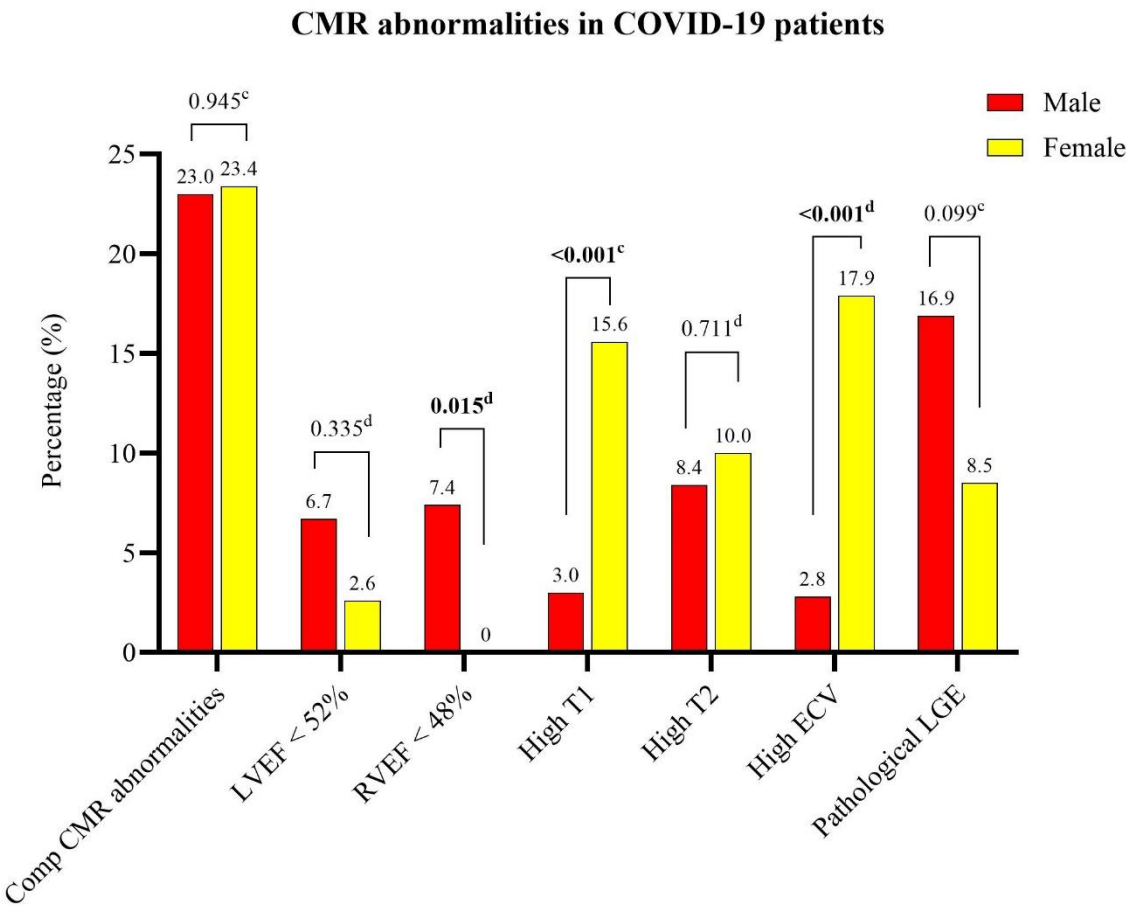


**Figure 4.3** Burden of CMR abnormalities (composite and individual) based on sex.

[c]Chi Square Test, [d]Fisher Exact Test.
Comp CMR, composite cardiac magnetic resonance imaging; ECV, extracellular volume; LGE, late gadolinium enhancement; LVEF, left ventricular ejection fraction; RVEF, right ventricular ejection fraction.

## SEX-SPECIFIC DISCRIMINATIVE ABILITY OF ECG FOR COMPOSITE CMR ABNORMALITIES

The findings are summarised in **Table 4** and **Figures 4.4-4.6**.

Overall, the discriminative ability of ECG for CMR abnormalities between sexes was significantly variable. The c-index for group A ECG features was 0.60 (p=0.389) in male and 0.49 (p=0.942) in female patients (**Table 4**). The discriminative power of individual repolarisation intervals for CMR abnormalities also showed sex-based variabilities, which were minimised when the repolarisation intervals were analysed along with the group A ECG features (**Table 4** and **Figure 4.4**).

Based on the group A ECG features, male patients demonstrated a SN of 90% vs 67% in female patients (**Figure 4.5A**). Therefore, there was an increased risk of misdiagnosis or false negative detection, especially among female patients. Adding the Group B ECG (such as the QTc ≥ 450 ms, JTc ≥ 340 ms, JTPc ≥ 240 ms QTc disp ≥ 55 ms) improved the sex-stratified diagnostic performance for CMR abnormalities. The SN improved from 90% to 99.9% among male patients and substantially from 67% to 94% among female patients (**Table 5** and **Figure 4.5A**). This also led to an increase in the NPV and -LR in both sexes (**Table 5** and **Figure 4.6A**). SP (**Figure 4.5B**) and PPV (**Figure 4.6B**) remained poor.
Adding the repolarisation intervals (Group B ECG) not only improved the overall diagnostic performance of ECG for CMR abnormalities but also minimised the sex-based variabilities. Importantly, the rates of misdiagnosis (false negative detection) in female patients, which otherwise would have been around 33%, were substantially reduced to 6% with the addition of QTc disp and the JTc parameters (**Figure 4.7**).

**Table 4** Discriminative potential of ECG for CMR abnormalities after adjusting for sex.

| **Composite CMR abnormalities** | | | |
|---|---|---|---|
| **ECG parameter** | **C- statistic 95% CI (P value)** | | |
| | **All patients** | **Male patients (n=135)** | **Female patients (n=77)** |
| ECG abnormalities (Composite Group A) | 0.56 [0.47-0.65] (p=0.185) | 0.60 [0.50-0.71] (p=0.090) | 0.49 [0.34-0.65] (p=0.942) |
| **Individual Repolarisation Parameters to detect CMR abnormalities** | | | |
| QTc | 0.56 [0.46-0.65] (p=0.240) | 0.50 [0.37-0.62] (p=0.967) | 0.65 [0.50-0.79] (p=0.064) |
| QTc disp | 0.57 [0.46-0.68] (p=0.208) | 0.59 [0.46-0.72] (p=0.124) | 0.62 [0.46-0.77] (p=0.161) |
| QTPc | 0.58 [0.48-0.67] (p=0.105) | 0.55 [0.43-0.66] (p=0.436) | 0.65 [0.49-0.80] (p=0.076) |
| JTc | 0.59 [0.50-0.69] **(p=0.048)** | 0.51 [0.39-0.64] (p=0.822) | 0.72 [0.59-0.86] **(p=0.007)** |
| JTPc | 0.61 [0.52-0.71] **(p=0.017)** | 0.57 [0.45-0.69] (p=0.239) | 0.72 [0.59-0.86] **(p=0.005)** |
| cTPe | 0.48 [0.38-0.57] (p=0.590) | 0.45 [0.33-0.57] (p=0.378) | 0.51 [0.36-0.66] (p=0.876) |
| **Group A ECG + individual repolarisation interval** | | | |
| ECG abnormalities + QTc | 0.58 [0.50-0.67] (p=0.080) | 0.59 [0.48-0.69] (p=0.149) | 0.54 [0.38-0.71] (p=0.594) |
| ECG abnormalities + QTc disp | 0.59 [0.49-0.69] (p=0.095) | 0.60 [0.46-0.73] (p=0.151) | 0.59 [0.43-0.75] (p=0.257) |
| ECG abnormalities + JTc | 0.62 [0.53-0.71] (**p=0.011**) | 0.59 [0.48-0.70] (p=0.140) | 0.65 [0.50-0.80] (p=0.072) |
| ECG abnormalities + JTPc | 0.63 [0.55-0.72] **(p=0.005)** | 0.63 [0.53-0.74] **(p=0.025)** | 0.67 [0.52-0.82] **(p=0.031)** |
| ECG abnormalities + QTc disp + JTc | 0.64 [0.55-0.74] (**p=0.002**) | 0.62 [0.50-0.73] (**p=0.047**) | 0.66 [0.50-0.82] (p=0.057) |
| ECG abnormalities + QTc disp + JTPc | 0.65 [0.56-0.74] **(p=0.001)** | 0.63 [0.52-0.75] **(p=0.024)** | 0.69 [0.54-0.84] **(p=0.016)** |

P values are based on concordance statistics and receiver operating characteristics curve analysis.

CMR, cardiac magnetic resonance; C-statistics, concordance statistics; Disp, dispersion; ECG, electrocardiography; JTc, corrected JT interval; JTPc, corrected JT peak interval QTc, corrected QT; QTPc, corrected QT peak; SN, sensitivity; SP, specificity; cTPe, corrected T-peak- to-T-end interval.

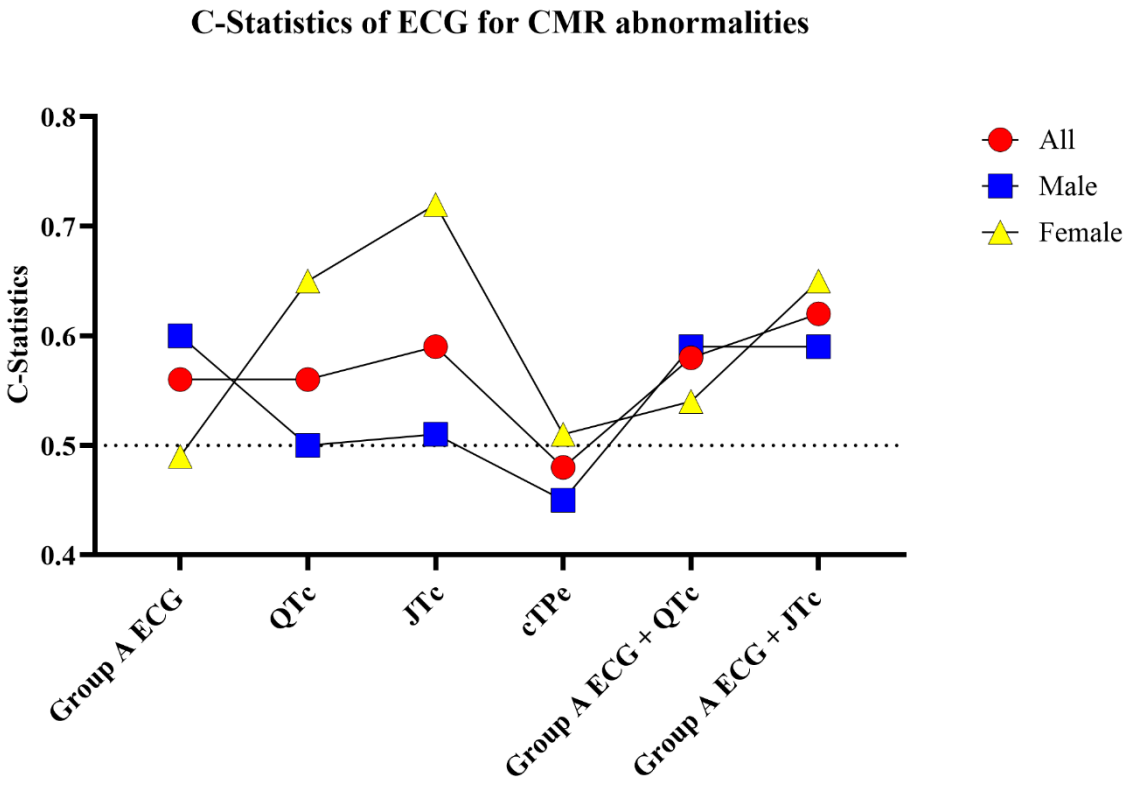


**Figure 4.4** C-Statistics of ECG for composite CMR abnormalities.

Group A ECG intervals showed substantial sex-based variabilities of c-statistics values between male (blue square) and female (yellow triangle) patients. Combining group A ECG features with group B repolarisation interval (e.g. Group A + QTc) improved the discriminative potential and reduced the sex-based variabilities.
(Group A ECG: ECG features without repolarisation intervals; JTc, corrected JT interval; QTc, corrected QT interval; cTPe, corrected T peak T end interval.)

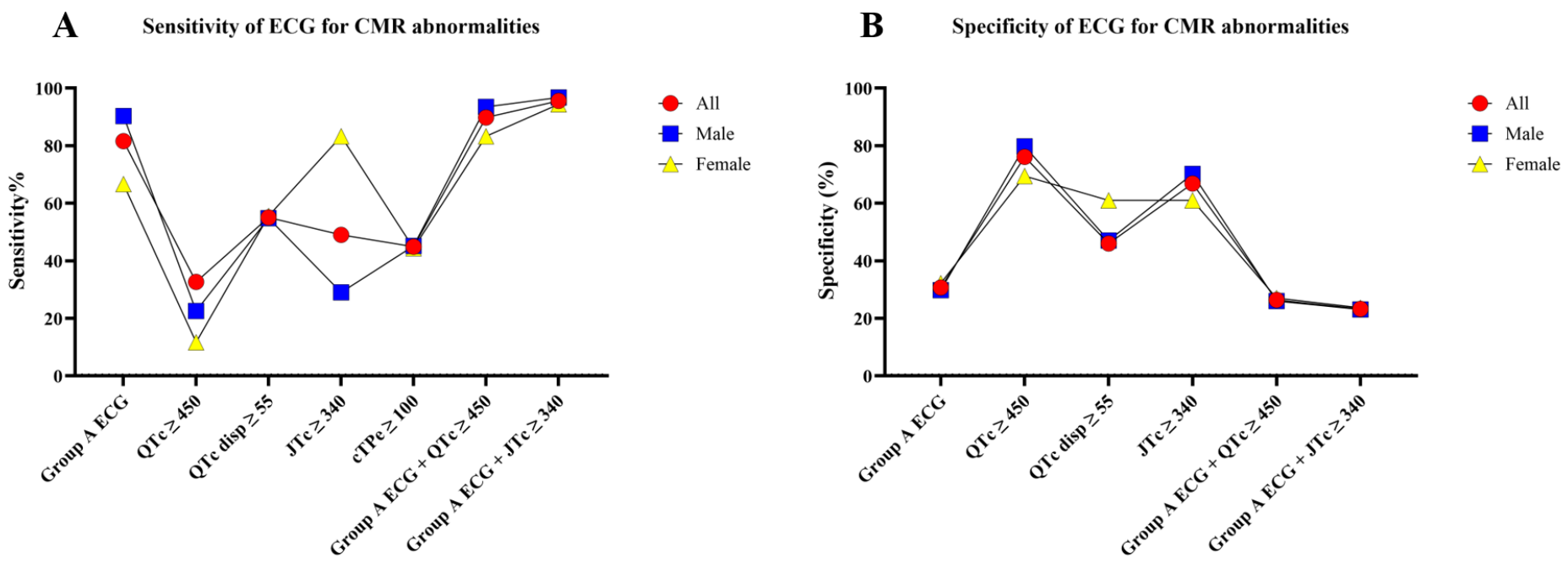


**Figure 4.5** Sex-based sensitivity and specificity analysis for CMR abnormalities.

**A**: The sensitivity of ECG and the sex-based variabilities for CMR abnormalities minimised when repolarisation intervals were added to the ECG criteria.
**B**: Specificity was generally poor and further reduced as sensitivity improved.

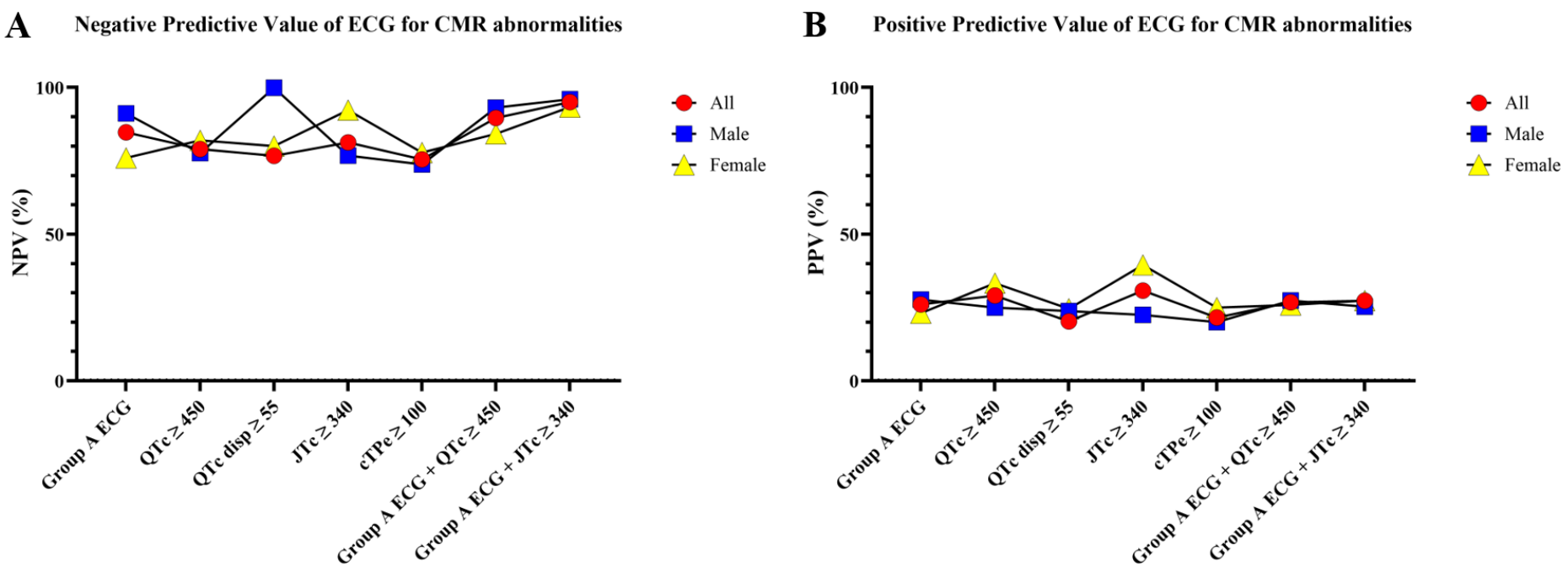


**Figure 4.6** Sex-based variabilities in likelihood ratios for CMR abnormalities.

**A**: Positive predictive values were generally low for ECG to detect CMR abnormalities.
**B:** Negative predictive values displayed sex-based variabilities. The NPV to rule out CMR abnormalities improved, and the sex-based variabilities were minimised with the addition of repolarisation intervals, particularly the QTc disp and JTc interval

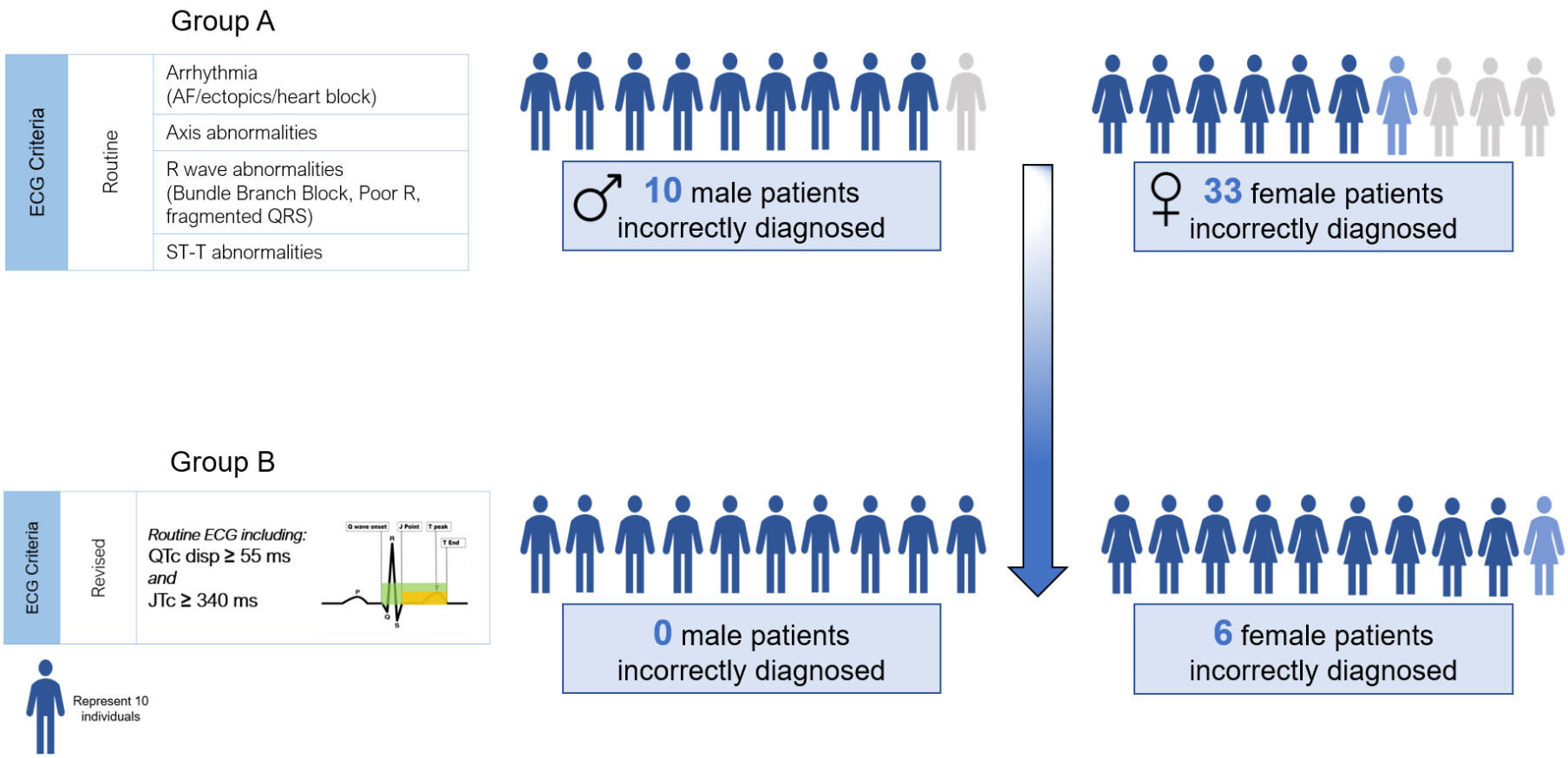


**Figure 4.7** Sex-based improvement in the rate of false negatives of ECG for CMR abnormalities.

This figure illustrates the magnitude of change in the diagnostic performance of ECG to rule out CMR abnormalities among post-hospitalised COVID-19 male and female patients. **Adding JTc ≥ 340 ms and QTc disp ≥ 55 ms** (Group B ECG features) to the Group A ECG criteria substantially reduced the rate of misdiagnosis (false negative) in both sexes particularly females.

## SEX-SPECIFIC DISCRIMINATIVE ABILITY OF ECG FOR LV DYSFUNCTION AND MYOCARDIAL TISSUE CHARACTERISTICS

Sex-based differences in the discriminatory potentials of various ECG parameters were tested to detect individual CMR abnormalities (LVEF <52% / high T1 / high T2 / high ECV or pathological LGE). Findings are summarised in **Figure 4.8** and **Appendix 3, Table 3**.

The heatmap in **Figure 4.8** demonstrates that the discriminative power of group A ECG for individual CMR abnormalities was poor-to-moderate, with c-statistics ranging between 0.37-0.67 (darker cells). Combining the composite group A and repolarisation parameters improved the discriminative power of ECG in both sexes in detecting high T1 or high T2 and was notably robust in discriminating female patients with poor LV function (LVEF < 52%) but not in male patients. For example, adding QTc improved the c-statistics for the detection of high T1 in both male and female patients from 0.37 to 0.83 and from 0.55 to 0.78, respectively. To discriminate patients with LVEF < 52%, the c-statistics among female patients improved from 0.67 to 0.91 but marginally increased from 0.58 to 0.62 in male patients. Most notably in female patients, adding QTc disp into the diagnostic ECG criteria displayed a robust discriminative power and a higher number of true positives than false negatives with c-statistics of 0.99 for poor LV function (**Figure 4.8** and **Appendix 3, Table 3).**

For detection of high ECV or poor LV function, although adding the repolarisation intervals generally improved the discriminative potentials, the sex-based differences persisted. None of the ECG parameters showed any significant discriminatory potentials for detection of pathological LGE (**Figure 4.8**).

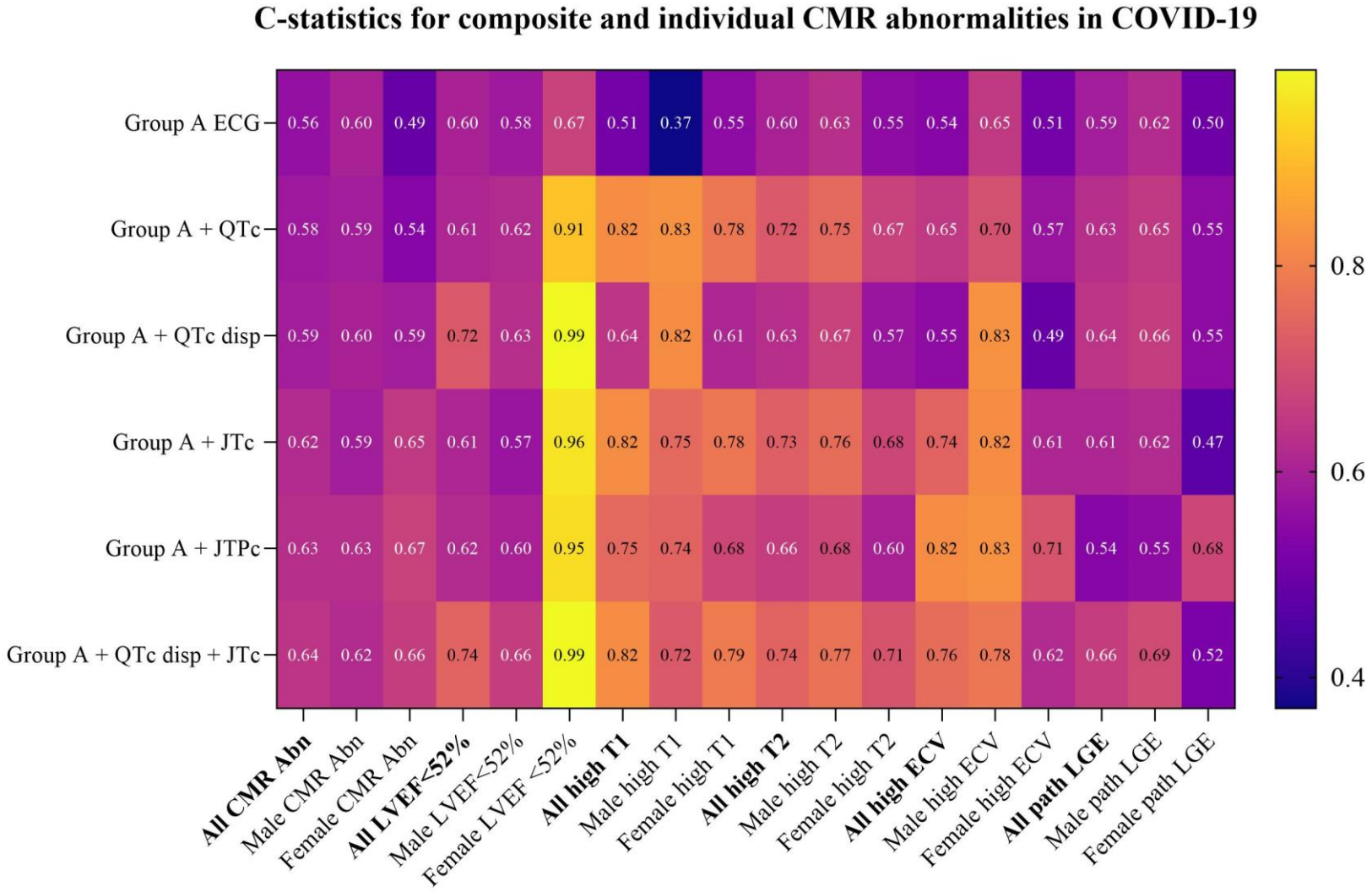
C-statistics for composite and individual CMR abnormalities in COVID-19
Group A ECG
Group A + QTc
Group A + QTc disp
Group A + JTc
Group A + JTPc
Group A + QTc disp + JTc
0.56 0.60 0.49 0.60 0.58 0.67 0.51 0.37 0.55 0.60 0.63 0.55 0.54 0.65 0.51 0.59 0.62 0.50
0.58 0.59 0.54 0.61 0.62 0.91 0.82 0.83 0.78 0.72 0.75 0.67 0.65 0.70 0.57 0.63 0.65 0.55
0.59 0.60 0.59 0.72 0.63 0.99 0.64 0.82 0.61 0.63 0.67 0.57 0.55 0.83 0.49 0.64 0.66 0.55
0.62 0.59 0.65 0.61 0.57 0.96 0.82 0.75 0.78 0.73 0.76 0.68 0.74 0.82 0.61 0.61 0.62 0.47
0.63 0.63 0.67 0.62 0.60 0.95 0.75 0.74 0.68 0.66 0.68 0.60 0.82 0.83 0.71 0.54 0.55 0.68
0.64 0.62 0.66 0.74 0.66 0.99 0.82 0.72 0.79 0.74 0.77 0.71 0.76 0.78 0.62 0.66 0.69 0.52
All CMR Abn
Male CMR Abn
Female CMR Abn
All LVEF<52%
Male LVEF<52%
Female LVEF <52%
All high T1
Male high T1
Female high T1
All high T2
Male high T2
Female high T2
All high ECV
Male high ECV
Female high ECV
All path LGE
Male path LGE
Female path LGE
0.8
0.6
0.4

**Figure 4.8** is a matrix heatmap representing the c-statistic values. The rows represent different ECG variables, and the columns represent composite or individual CMR abnormalities. Each cell represents the discriminative potential, with a gradient coding and annotated c-index value.

A value approaching 0 (*dark cells*) indicates poor discriminative ability, a value of 0.5 indicates discriminative ability that is no better than classifying outcomes randomly by chance, and values approaching 1.0 (bright cells) indicate excellent discriminative ability.
(CMR Abn, composite cardiac magnetic resonance imaging abnormalities; disp, dispersion; ECV, extracellular volume; F, female; M, male; path LGE, pathological late gadolinium enhancement).

## SEX-SPECIFIC DIAGNOSTIC PERFORMANCE OF ECG PARAMETERS FOR INDIVIDUAL CMR ABNORMALITIES

In this section, I further tested the SN, SP, NPV, PPV, and LR of ECG for individual CMR abnormalities based on sex. The findings are summarised in **PREDICTIVE ABILITY OF ECG PARAMETERS FOR CMR ABNORMALITIES BASED ON LOGISTIC REGRESSION ANALYSIS.**

Logistic regression analysis was conducted to assess the association between ECG repolarisation parameters and CMR abnormalities.

**Table 6** summarises the univariable and multivariable analysis of individual ECG depolarisation and repolarisation for composite CMR abnormalities. In the univariable analyses, the QTc disp, JTc and JTPc intervals were significantly associated with composite CMR abnormalities. QTc disp displayed the strongest association with CMR abnormalities (OR 1.03 (95% CI 1.01-1.04), p=0.002).

In the multivariable analysis (adjusted for age, sex, body mass index, hypertension and diabetes as clinical covariates), only QTc disp remained a significant predictor for composite CMR abnormalities. The odds of abnormal CMR increased by 3% with prolongation of the QTc disp. The clinical model that included QTc disp also displayed the highest adjusted r squared ($R^2$) values, at 19.3%, which represents the percentage of variance in the outcome explained by the model.

.

As shown previously for composite of CMR abnormalities, the SN of group A ECG was also higher among male than female patients for detection of individual abnormal tissue

characteristics such as high T1, high T2, high ECV or pathological LGE. The rate of false negative was significant especially among women, where close to half of the female patients can be wrongly diagnosed (**Table 5**).

Importantly, when repolarisation intervals were added to the ECG criteria, the diagnostic performance substantially improved in both sexes, with the greatest margin of increment observed among the female patients. For example, to detect post-hospitalised COVID-19 patients with high T2, adding JTc ≥ 340 ms to the ECG criteria substantially improved the SN in both sexes from 50% to 90% in male patients, and 57% to 100% in female patients (**Table 5**). The NPV and -LR also improved signifying ECG's ability as a rule-out tool in the context of screening and risk stratification in both sexes. However, the SP, PPV, and +LR remained low, indicating ECG's poor role as a rule-in test in both sexes (**Table 5**).

**Table 5** Diagnostic performance of ECG for CMR abnormalities based on sex.

| **ECG parameters**<br>**CMR abnormalities (n=212)** | **SN (%)** | | **SP (%)** | | **PPV (%)** | | **NPV (%)** | | **+LR** | | **-LR** | |
|---|---|---|---|---|---|---|---|---|---|---|---|---|
| | **M** | **F** | **M** | **F** | **M** | **F** | **M** | **F** | **M** | **F** | **M** | **F** |
| ECG abnormalities (Composite Group A) | 90.3 | 66.7 | 29.8 | 32.2 | 27.7 | 23.1 | 91.2 | 76.0 | 1.29 | 0.98 | 0.33 | 1.03 |
| ECG abnorm + QTc disp ≥ 55 + JTPc ≥ 240 | 99.9 | 99.9 | 13.5 | 14.1 | 25.6 | 25.9 | 99.9 | 99.9 | 1.15 | 1.16 | 0.01 | 0.01 |
| ECG abnorm + QTc disp ≥ 55 + JTc ≥ 340 | 99.9 | 94.4 | 15.4 | 16.9 | 26.1 | 25.8 | 99.9 | 90.9 | 1.18 | 1.14 | 0.01 | 0.33 |
| **LVEF < 52% (n=212)** | | | | | | | | | | | | |
| ECG abnormalities | 88.9 | 99.9 | 26.2 | 33.3 | 7.9 | 3.8 | 97.1 | 99.9 | 1.20 | 1.50 | 0.42 | 0.00 |
| ECG abnorm + QTc disp ≥ 55 | 99.9 | 99.9 | 14.3 | 20.0 | 7.7 | 3.2 | 99.9 | 99.9 | 1.17 | 1.25 | 0.01 | 0.01 |
| **High T1 (n=209)** | | | | | | | | | | | | |
| ECG abnormalities | 99.9 | 58.3 | 26.8 | 31.7 | 4.1 | 14.0 | 99.9 | 80.0 | 1.36 | 0.85 | 0.00 | 1.32 |
| ECG abnorm + JTc ≥ 340 ms | 99.0 | 91.7 | 19.7 | 22.2 | 3.8 | 18.3 | 99.9 | 93.3 | 1.23 | 1.18 | 0.05 | 0.37 |
| **High T2 (n=185)** | | | | | | | | | | | | |
| ECG abnormalities | 50.0 | 57.1 | 23.4 | 32.8 | 5.7 | 8.9 | 83.3 | 87.0 | 0.65 | 0.85 | 2.14 | 1.31 |
| ECG abnorm + JTc ≥ 340 ms | 90.0 | 99.9 | 19.6 | 21.3 | 9.5 | 12.7 | 95.5 | 99.0 | 1.12 | 1.27 | 0.51 | 0.00 |
| **High ECV (n=186)** | | | | | | | | | | | | |
| ECG abnormalities | 99.9 | 70.0 | 27.7 | 28.8 | 5.5 | 15.9 | 99.9 | 83.3 | 1.38 | 0.98 | 0.00 | 1.04 |
| ECG abnorm + JTPc ≥ 240 ms | 99.9 | 99.9 | 21.0 | 11.5 | 5.1 | 17.9 | 99.9 | 99.9 | 1.26 | 1.13 | 0.01 | 0.01 |
| **Pathological LGE (n=212)** | | | | | | | | | | | | |
| ECG abnormalities | 95.2 | 66.7 | 28.9 | 32.4 | 19.8 | 7.7 | 97.1 | 92.0 | 1.34 | 0.99 | 0.17 | 1.03 |
| ECG abnorm + QTc disp ≥ 55 | 99.9 | 83.3 | 15.8 | 19.7 | 17.9 | 8.1 | 99.9 | 93.3 | 1.19 | 1.04 | 0.01 | 0.85 |

Abnorm, Abnormalities; BBB, bundle branch block; CMR, cardiac magnetic resonance; C-statistics, concordance statistics; Disp, dispersion; ECG, electrocardiography; LR, likelihood ratio; NPV, negative predictive value; PPV, positive predictive value; QTc, corrected QT; QTPc, corrected QT peak; SN, sensitivity; SP, specificity; cTPe, corrected T-peak- to-T-end.

## PREDICTIVE ABILITY OF ECG PARAMETERS FOR CMR ABNORMALITIES BASED ON LOGISTIC REGRESSION ANALYSIS.

Logistic regression analysis was conducted to assess the association between ECG repolarisation parameters and CMR abnormalities.

**Table 6** summarises the univariable and multivariable analysis of individual ECG depolarisation and repolarisation for composite CMR abnormalities. In the univariable analyses, the QTc disp, JTc and JTPc intervals were significantly associated with composite CMR abnormalities. QTc disp displayed the strongest association with CMR abnormalities (OR 1.03 (95% CI 1.01-1.04), p=0.002).

In the multivariable analysis (adjusted for age, sex, body mass index, hypertension and diabetes as clinical covariates), only QTc disp remained a significant predictor for composite CMR abnormalities. The odds of abnormal CMR increased by 3% with prolongation of the QTc disp. The clinical model that included QTc disp also displayed the highest adjusted r squared ($R^2$) values, at 19.3%, which represents the percentage of variance in the outcome explained by the model.

**Table 6** Univariable and multivariable logistic regression analyses of ECG for composite CMR abnormalities.

| ECG variable | Composite CMR abnormalities | | | | Adjusted R Squared (%)[2] |
|---|---|---|---|---|---|
| | Univariable analysis | | Multivariable analysis[1] | | |
| | OR (95% CI) | P value | OR (95% CI) | P value | |
| QRS | 1.02 (1.00-1.04) | 0.055 | 1.01 (0.99-1.04) | 0.333 | 13.4 |
| QTc | 1.01 (1.00-1.02) | 0.149 | 1.01 (1.00-1.02) | 0.211 | 13.9 |
| QTc disp | **1.03 (1.01-1.04)** | **0.002** | **1.03 (1.01-1.05)** | **0.006** | **19.3** |
| QTPc | 1.01 (1.00-1.02) | 0.060 | 1.01 (1.00-1.03) | 0.063 | 15.6 |
| JTc | **1.01 (1.00-1.03)** | **0.021** | 1.01 (0.99-1.03) | 0.087 | 15.1 |
| JTPc | **1.02 (1.00-1.03)** | **0.010** | 1.02 (1.01-1.03) | 0.064 | 15.6 |
| cTPe | 0.99 (0.97-1.02) | 0.578 | 0.99 (0.97-1.02) | 0.587 | 12.6 |

[1]Clinical model = age + sex + body mass index + hypertension + diabetes. Each ECG variable was added to the clinical model separately, one at a time. For example, OR (High T1) = age + sex + body mass index + hypertension + diabetes + each ECG parameter. Odds ratio and p values represent values of clinical model + individual ECG variable in logistic regression analysis.

[2] $R^2$ represent the proportion of the variance in the outcome measured explained by the predictive model.

JTc, corrected JT interval; JTPc, corrected JT peak interval; QTc disp, QTc dispersion; QTc, corrected QT interval; cTPe, corrected T peak T end interval.

## PREDICTIVE ABILITY OF CLINICAL MODELS FOR CMR ABNORMALITIES BASED ON LOGISTIC REGRESSION ANALYSIS.

Logistic regression analysis was subsequently conducted on the clinical model that included QTc disp to assess how the addition of predictor variables, such as age, sex, body mass index, hypertension and diabetes and composite group A ECG abnormalities, affect the association of QTc disp with CMR abnormalities. **Table 7** summarises the findings. Based on the $R^2$ values, the clinical model alone explained about 13% of the variance in predicting CMR abnormalities among the post-hospitalised COVID-19 patients. Composite group A ECG abnormalities were not a significant predictor for CMR abnormalities, and adding this feature to the clinical model only increased the $R^2$ to 15%.

When all predictor variables are considered together (age + sex + body mass index + hypertension + diabetes + group A ECG + QTc disp), they significantly predicted CMR abnormalities, $X^2 = 24.56$, df = 7, $p < 0.001$ (**Table 7**). The $R^2$ estimates indicated that approximately 21% of the variance in predicting CMR abnormalities can be predicted from the linear combination of the clinical model that included composite group A ECG abnormalities and QTc disp. The OR was significant for QTc disp and age in the model, at 1.03 (95% CI 1.01-1.05) p=0.008 and 1.05 (95% CI 1.02-1.09) p=0.002 respectively. These suggest that the odds of CMR abnormalities increased by 1.03 for each unit increase in QTc disp and by 1.05 for every one-year increase in age.

**Table 7** Logistic regression of different models in predicting CMR abnormalities.

| Variable | B | SE | Odds ratio (95%CI) | P value | Adjusted R Squared (%)[2] |
|---|---|---|---|---|---|
| **Clinical Model[1]** | | | | | |
| Age | 0.06 | 0.02 | 1.06 (1.02-1.10) | **0.001** | 12.6 |
| Sex | 0.02 | 0.41 | 1.02 (0.46-2.26) | 0.967 | |
| BMI | 0.03 | 0.04 | 1.03 (0.96-1.10) | 0.437 | |
| Hypertension | 0.36 | 0.44 | 1.43 (0.61-3.36) | 0.410 | |
| Diabetes | -0.21 | 0.61 | 0.81 (0.24-2.68) | 0.728 | |
| **Clinical Model + ECG abnormalities** | | | | | |
| Age | 0.06 | 0.02 | 1.06 (1.02-1.10) | **0.004** | 15.0 |
| Sex | 0.06 | 0.41 | 1.20 (0.60-2.41) | 0.601 | |
| BMI | 0.02 | 0.04 | 1.02 (0.95-1.09) | 0.591 | |
| Hypertension | 0.29 | 0.44 | 1.33 (0.56-3.16) | 0.512 | |
| Diabetes | -0.31 | 0.62 | 0.73 (0.22-2.46) | 0.617 | |
| Abnormal ECG (Comp Group A) | 0.87 | 0.54 | 1.65 (0.72-3.76) | 0.109 | |
| **Clinical Model + ECG abnormalities + QTc disp** | | | | | |
| Age | 0.50 | 0.02 | 1.05 (1.02-1.09) | **0.002** | 21.1 |
| Sex | 0.26 | 0.43 | 1.30 (0.56-3.02) | 0.544 | |
| BMI | -0.03 | 0.04 | 1.00 (0.93-1.07) | 0.940 | |
| Hypertension | 0.27 | 0.46 | 1.30 (0.53-3.18) | 0.561 | |
| Diabetes | -0.18 | 0.65 | 0.83 (0.23-3.00) | 0.778 | |
| Abnormal ECG | 0.79 | 0.55 | 2.20 (0.75-6.46) | 0.153 | |
| QTc disp | 0.03 | 0.01 | 1.03 (1.01-1.05) | **0.008** | |

[1]Clinical model = age + sex + body mass index + hypertension + diabetes.
[2] $R^2$ represent the proportion of the variance in the outcome measured explained by the predictive model.
Odds ratio and p values represent values of clinical model + individual ECG variable in logistic regression analysis. B, beta coefficient (the predicted change in Log Odds-for 1 unit change in the predictor); Comp, composite; QTc disp, QTc dispersion; SE, standard error.

## DISCRIMINATIVE ABILITY OF ECG FOR CMR ABNORMALITIES ADJUSTED FOR THE COVARIATES

Based on the regression model and $R^2$ values in **Table 7**, I conducted the AUROC analysis on the best clinical model (QTc disp + age + sex + body mass index + hypertension + diabetes) to determine their discriminative ability for composite CMR abnormalities compared to the model of QTc disp alone without the clinical covariates. As depicted in **Figure 4.9**, as a stand-alone parameter, the discriminative ability of QTc disp was 0.63 (95% CI 0.52-0.74), p=0.015. The discriminative power to detect COVID-19 patients with CMR abnormalities was augmented to 0.74 (95% CI 0.65-0.82) p<0.001, when adjusted for the clinical covariates (age + sex + BMI + hypertension + diabetes).

The impact of this finding is twofold. First, it shows that, individually, QTc disp albeit weak, potentially display a reasonable discriminative potential for CMR abnormalities, which warrants further exploration. Secondly, the findings further reiterate the influence of clinical covariates, particularly age, sex, BMI, hypertension and diabetes, in the associations of ventricular repolarisation with CMR parameters of health among post-hospitalised COVID-19 patients.

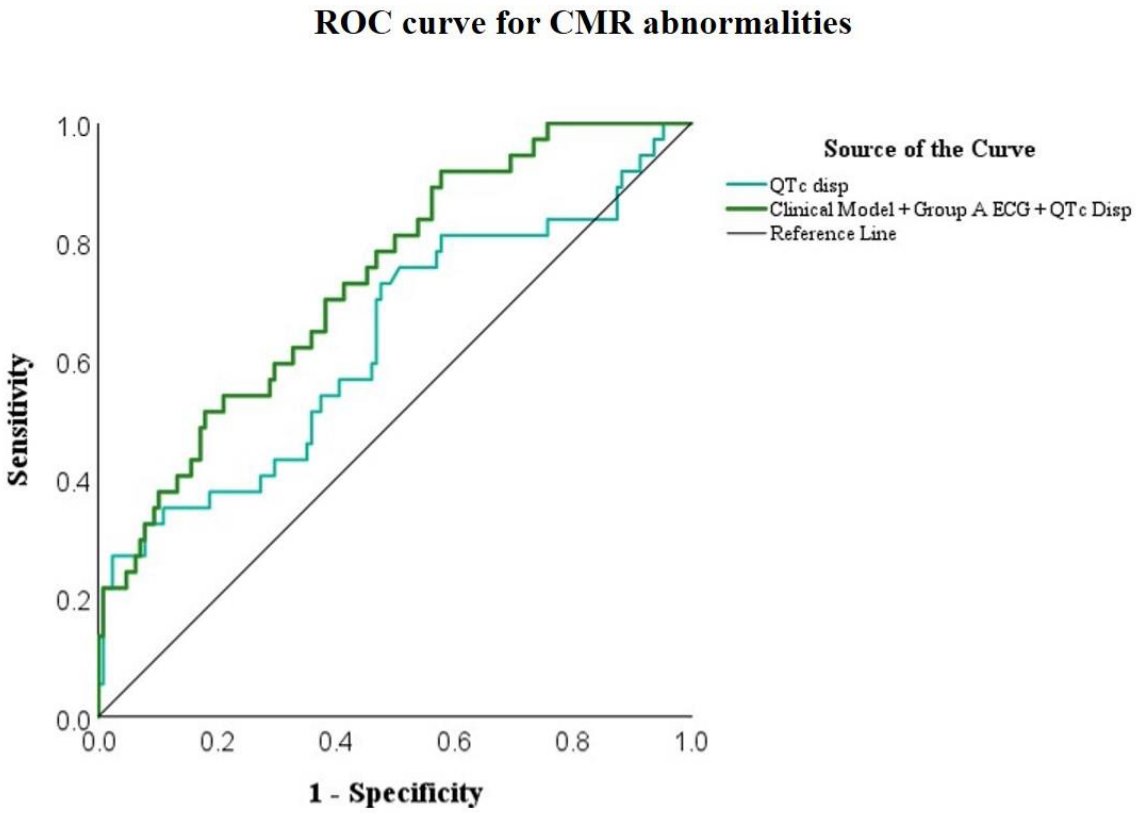


| Model | C-Statistics | 95% Confidence Interval | P value |
|---|---|---|---|
| QTc disp | 0.63 | 0.52-0.74 | 0.015 |
| Age, Sex, BMI, Hypertension, DM, QTc disp | 0.74 | 0.61-0.78 | <0.001 |

**Figure 4.9** ROC curve of QTc dispersion adjusted for the clinical covariates.

ROC curve of QTc disp and JTc interval to discriminate post-hospitalised COVID-19 patients with CMR abnormalities adjusted for age and sex. Predicting CMR abnormalities. The area under the receiver operating characteristics curve (AUROC) as a measure of model performance for the prediction of CMR abnormalities defined as the presence of i) abnormal left ventricular ejection fraction (LVEF) < 52% and right ventricular ejection fraction (RVEF) < 48% and/or ii) pathological pattern (basal sub valvular, ischemic, myocarditis, mixed pathology, cardiomyopathy, nonspecific) of late gadolinium enhancement (LGE) and/or iii) high T1 and high T2 and/or iv) high extracellular volume fraction (ECV) (>0.32 %).

## PREDICTIVE ABILITY OF ECG PARAMETERS FOR INDIVIDUAL CMR ABNORMALITIES BASED ON LOGISTIC REGRESSION ANALYSIS.

Error! Reference source not found. summarises the regression analysis of ECG intervals for individual CMR abnormalities.

Overall, QTc disp was the only ECG parameter significantly associated with LV dysfunction. For high T1, QTc, QTc disp, JTc, and JTPc intervals demonstrated significant associations in univariable and multivariable analysis. The clinical model with JTc indicated that close to 40% (*based on adjusted* $R^2$) of the variance to predict high T1 can be explained by the combination of the clinical model and JTc interval.

In multivariable analysis, JT parameters (either JTc or JTPc intervals) also significantly predicted high T2 and high ECV. None of the ECG parameters showed significant associations with pathological LGE (**Table 8**).

**Table 8** Univariable and multivariable associations of ECG parameters with individual CMR abnormalities.

| ECG variable | LVEF <52% | | | | Adjusted $R^2$ Squared (%) |
|---|---|---|---|---|---|
| | Univariable analysis | | Multivariable analysis[1] | | |
| | OR (95% CI) | P value | OR (95% CI) | P value | |
| QRS | 1.04 (1.01-1.07) | **0.010** | 1.02 (0.98-1.06) | 0.361 | 26.4 |
| QTc | 0.99 (0.98-1.02) | 0.877 | 1.01 (0.99-1.03) | 0.383 | 26.4 |
| QTc disp | **1.03 (1.01-1.06)** | **0.013** | **1.04 (1.01-1.07)** | **0.023** | **33.7** |
| QTPc | 1.00 (0.98-1.02) | 1.000 | 1.02 (0.99-1.04) | 0.155 | 28.4 |
| JTc | 1.00 (0.98-1.03) | 0.710 | 1.03 (1.00-1.05) | 0.071 | 30.7 |
| JTPc | 1.01 (0.99-1.02) | 0.441 | 1.02 (1.00-1.05) | 0.077 | 30.5 |
| cTPe | 0.98 (0.94-1.03) | 0.453 | 1.00 (0.95-1.05) | 0.966 | 25.2 |
| **ECG variable** | **High T1** | | | | **Adjusted $R^2$ Squared (%)** |
| | **Univariable analysis** | | **Multivariable analysis[1]** | | |
| | **OR (95% CI)** | **P value** | **OR (95% CI)** | **P value** | |
| QRS | 0.94 (0.89-0.99) | 0.024 | 0.93 (0.87-1.01) | 0.067 | 19.8 |
| QTc | **1.04 (1.02-1.06)** | **<0.001** | **1.04 (1.02-1.07)** | **<0.001** | **36.7** |
| QTc disp | **1.02 (1.00-1.05)** | **0.049** | **1.04 (1.01-1.07)** | **0.007** | **24.7** |
| QTPc | **1.03 (1.01-1.05)** | **<0.001** | **1.03 (1.01-1.05)** | **0.003** | **28.0** |
| JTc | **1.05 (1.03-1.08)** | **<0.001** | **1.06 (1.03-1.09)** | **<0.001** | **38.3** |
| JTPc | **1.04 (1.02-1.06)** | **<0.001** | **1.03 (1.01-1.06)** | **0.006** | **26.3** |
| cTPe | 1.03 (0.99-1.06) | 0.137 | **1.04 (1.00-1.08)** | **0.042** | **20.2** |
| **ECG variable** | **High T2** | | | | **Adjusted $R^2$ Squared (%)** |
| | **Univariable analysis** | | **Multivariable analysis[1]** | | |
| | **OR (95% CI)** | **P value** | **OR (95% CI)** | **P value** | |
| QRS | 0.97 (0.93-1.02) | 0.199 | 0.94 (0.86-1.02) | 0.143 | 15.7 |
| QTc | **1.02 (1.00-1.04)** | **0.12** | **1.04 (1.01-1.07)** | **0.011** | **26.4** |
| QTc disp | 1.01 (0.98-1.03) | 0.534 | 1.02 (0.99-1.06) | 0.238 | 13.3 |
| QTPc | 1.01 (1.00-1.03) | 0.081 | 1.03 (1.00-1.06) | 0.050 | 18.9 |

| | | | | | |
|---|---|---|---|---|---|
| JTc | **1.03 (1.01-1.05** | **0.005** | **1.05 (1.01-1.09)** | **0.008** | **29.8** |
| JTPc | **1.02 (1.00-1.04)** | **0.043** | **1.04 (1.02-1.07)** | **0.037** | **20.7** |
| cTPe | 1.03 (0.99-1.06) | 0.124 | 1.04 (0.99-1.09) | 0.115 | 15.6 |
| **ECG variable** | **High ECV** | | | | **Adjusted $R^2$ Squared (%)** |
| | **Univariable analysis** | | **Multivariable analysis[1]** | | |
| | **OR (95% CI)** | **P value** | **OR (95% CI)** | **P value** | |
| QRS | 0.97 (0.93-1.02) | 0.199 | 0.98 (0.94-1.04) | 0.588 | 21.7 |
| QTc | **1.02 (1.00-1.04)** | **0.12** | 1.02 (1.00-1.03) | 0.110 | 24.8 |
| QTc disp | 1.01 (0.98-1.03) | 0.534 | 1.02 (0.99-1.05) | 0.190 | 23.6 |
| QTPc | 1.01 (1.00-1.03) | 0.081 | 1.01 (1.00-1.03) | 0.146 | 24.1 |
| JTc | **1.03 (1.01-1.05** | **0.005** | **1.03 (1.00-1.05)** | **0.041** | **27.5** |
| JTPc | **1.02 (1.00-1.04)** | **0.043** | **1.04 (1.01-1.07)** | **0.004** | **34.6** |
| cTPe | 1.03 (0.99-1.06) | 0.124 | 0.96 (0.91-1.01) | 0.102 | 25.4 |
| **ECG variable** | **Pathological LGE** | | | | **Adjusted $R^2$ Squared (%)** |
| | **Univariable analysis** | | **Multivariable analysis[1]** | | |
| | **OR (95% CI)** | **P value** | **OR (95% CI)** | **P value** | |
| QRS | 1.02 (1.00-1.05) | 0.061 | 1.01 (0.99-1.04) | 0.338 | 26.3 |
| QTc | 1.00 (0.99-1.10) | 0.596 | 1.00 (0.98-1.01) | 0.573 | 25.8 |
| QTc disp | **1.02 (1.00-1.04)** | **0.039** | 1.02 (1.00-1.04) | 0.178 | 27.2 |
| QTPc | 1.00 (0.99-1.01) | 0.762 | 1.00 (0.99-1.02) | 0.969 | 25.5 |
| JTc | 1.00 (0.99-1.02) | 0.940 | 1.00 (0.98-1.02) | 0.898 | 25.5 |
| JTPc | 1.01 (0.99-1.02) | 0.501 | 1.00 (0.98-1.02) | 0.912 | 25.5 |
| cTPe | 0.98 (0.96-1.01) | 0.202 | 0.99 (0.96-1.03) | 0.601 | 25.8 |

[1]Clinical model = age + sex + BMI + hypertension + diabetes mellitus. Each ECG variable was added to the clinical model separately, one at a time. For example, OR (High T1) = Clinical model + each ECG parameter. Odds ratio and p values represent values clinical model + individual ECG variable. P values based on logistic regression analysis.

[2] $R^2$ represent the proportion of the variance in the outcome measured explained by the predictive model.

JTc, corrected JT interval; JTPc, corrected JT peak interval; QTc disp, QTc dispersion; QTc, corrected QT interval; cTPe, corrected T peak T end interval.

## 4.6 DISCUSSION

The main findings from this chapter are as follows: first, the overall burden of ECG and CMR abnormalities did not differ significantly between sexes among post-hospitalised COVID-19 patients. However, there were sex-based differences observed in the ECG repolarisation intervals and CMR parameters of health. Secondly, the ECG diagnostic performance to detect CMR abnormalities displayed significant sex-based variabilities. Importantly, we demonstrated that utilising group A ECG features alone increased the risks of misdiagnosis, especially among female patients. The diagnostic performance substantially improved, and the rate of false negative was minimised by adding the repolarisation intervals (Group B ECG) to the ECG diagnostic criteria. Thirdly, repolarisation parameters (particularly the QTc disp, JTc and JTPc) were significant predictors of abnormal CMR in univariable analysis. After adjusting for clinical covariates such as age, sex, BMI, hypertension and diabetes mellitus, only QTc disp remained a significant predictor. The present study also showed that the discriminative power of ECG to detect CMR abnormalities was relatively stronger when the clinical covariates were taken into consideration.

Sex-based changes prolongation of repolarisation intervals on surface ECG, have been well documented and linked to the risk of arrhythmia and sudden cardiac death[166,172,173,184,185]. However, the sex-based differences of ECG parameters in association with CMR abnormalities in COVID-19 patients have never been comprehensively explored. To my knowledge, this is the first study conducted to characterise the sex-based differences in ECG-CMR diagnostics and predictive performance among post-hospitalised moderate-to-severe COVID-19 patients.

## SEX-BASED DIFFERENCES IN ECG REPOLARISATION INTERVALS

In the present study, female patients displayed longer QTc and JTc interval whereas QRS duration was shorter in female than male patients. The QT interval encompasses combination of QRS and the JT interval. Hence, the prolongation of the QT interval among women is primarily contributed by the JT interval, which represents the ventricular repolarisation of part of the myocardium[173]. Similarly, previous studies, found sex- and age-related variation in QT interval that were explained by the differences in the early repolarisation phase (JT and JT peak intervals) on the surface ECG[167,186]. Sex-based differences in ECG also are partly explainable by the effects of inherent physiological variations on gene expression linked to ionic channel distribution on myocardium[172], electrochemical stability[187], body mass index[188], systemic inflammation[93] and sex hormones[167,189].

## SEX-BASED HORMONE EFFECT DUE TO COVID-19

Healthy adult men generally demonstrate shorter QT interval than women due to the effect of testosterone in men[189]. Shorter QTc in men is primarily due to the inhibition of L-type calcium current (ICaL: inward depolarising current) by testosterone[167], resulting in shorter early repolarisation. Although sex-based differences are expected, the influence of sex hormones on repolarisation in women is still a subject of debate[190], which suggests that other possible mechanistic explanations may also have taken place[52,93,188]. In the context of COVID-19 infection, a study in Germany found that high estrogen and low testosterone levels to be associated with critical illness in patients[191]. Lower testosterone concentration was also associated with increased inflammation in hospitalised COVID-19 patients in USA[192]. Notably, testosterone concentrations were inversely associated with IL-6 and CRP,

which have been implicated in myocardial channelopathies and prolonged QT interval secondary to systemic inflammation[93,192]. Nonetheless, the real impact of sex hormones and their influence on repolarisation intervals in these studies is unknown, as no ECG was reported. Previous studies have confirmed the hormonal influence, especially testosterone and oestrogen, on repolarisation intervals among healthy individuals[167,189]. In the present study, the recruited patients had moderate-to-severe COVID-19 infection, with a proportion requiring invasive mechanical ventilation during admission. Although lacking the admission of blood inflammatory parameters such as IL-1 and IL-6, the CRP level was higher among female patients hence it can be postulated that the myocardial channelopathies mediated by the inflammatory cytokines may exaggerate the inherent influence of sex hormones on the repolarisation phase in COVID-19 patients[59,93]. This hypothesis may form a basis to explain the long-term risk of arrhythmia and mortality reported in several post-hospitalised COVID-19 studies[75,193].

### AGE, BMI AND CRP ASSOCIATION WITH SEX-BASED DIFFERENCES IN ECG FEATURES

Sex-based differences in repolarisation intervals are non-existent during childhood, appear during puberty, and persist until around 60-65 years old[173]. With increasing age, the sex-based differences become less apparent as QTc prolongs in men, due to an increase in the duration of the early repolarisation phase[167] caused by the natural decline of testosterone levels. Therefore, age plays a significant role in the context of ECG interpretation.

In the present study, the sex-based variabilities in ECG repolarisation could also partly be explained by BMI, which was significantly greater in female patients. A meta-analysis of 22 studies concluded that high BMI was associated with significant QT prolongation[188]. Moreover, female patients in this study also had higher levels of CRP than their male

counterparts. Recent histopathological evidence showed that ACE2 receptors, (an essential SAR-CoV-2 cellular entry points), are found within the EAT layer of COVID-19 patients[96]. EAT is believed to be a potential reservoir for the immune response against SARS-CoV-2, as dense macrophage infiltrates and inflammatory cytokines were also observed in this layer[98,99]. The previous findings of direct anatomical and functional contiguity coupled with the evidence of SARS-CoV-2 infection of percolating adipocytes within the myocardium and visceral epicardium[52,96], may be extrapolated in the present study to provide explanations for the prolongation of repolarisation and the sex-based differences especially in female COVID-19 patients.

Taken together, our findings are consistent with previously reported studies on sex-based variation in ECG and highlight the imperative need to stratify and adjust these relevant covariates to reliably determine the diagnostic and predictive performance of ECG for CMR abnormalities. Furthermore, the findings also consolidate the recommendation for a sex-based reference cut-off for ECG intervals in clinical settings[131].

### SEX-BASED DIFFERENCES IN CMR PARAMETERS

In this study, we expectedly observed that male patients had greater values for left and right ventricular volume and mass than females. Conversely, females showed greater value for left and right ventricular function (LVEF and RVEF). Sex-specific reference ranges for cardiac structures and function based on CMR have been described before[148]. Females also demonstrated greater T1, T2 and ECV map values for myocardial tissue characteristics than males in our study.

The sex-and-age-specific range for myocardial tissue characteristics has been previously reported and consistently shows that females demonstrate significantly greater native T1

values than males[194-196]. However, the potential roles of myocardial injury or fibrosis in contributing to the prolongation of repolarisation intervals in female patients, cannot be excluded, as the burden of abnormal ECV, a sensitive CMR marker of interstitial fibrosis which is less sensitive to age and sex[194,195], were significantly higher among female than male patients in the present study. As prolonged repolarisation increases the risk of malignant arrhythmia in females in other conditions[197], long-term studies are imperative to evaluate the risk of arrhythmia in this cohort of COVID-19 patients with prolonged repolarisation and evidence of myocardial fibrosis.

## ECG DIAGNOSTIC AND PREDICTIVE PERFORMANCE FOR CMR ABNORMALITIES ADJUSTED FOR COVARIATES

In the present study, we described the diagnostic performance of group A ECG abnormalities as sex-dependent. A higher rate of misdiagnoses was observed among women compared to men, which was minimised when repolarisation parameters were included in the diagnostic ECG criteria.

Importantly, we showed that CMR abnormalities may reliably be excluded in male and female patients when other group A ECG features were interpreted along with group B repolarisation parameters such as the QTc disp and/or JT parameters. Potentially, JT intervals, which dominate the epicardial repolarisation, may be affected by sub-clinical myocarditis, which commonly showed mid-myocardial and subepicardial injury patterns in COVID-19 patients[26].

Association of QTc disp with myocardial abnormalities[198,199], and risk of sudden cardiac death has been previously reported[200,201]. Although the understanding of its relationship with cardiac abnormalities is unclear[202], QTc disp is considered a crude measure of repolarisation

abnormalities. Our data shows that QTc disp is a significant predictor for composite CMR abnormalities in multivariable analysis and demonstrated significant association with individual CMR tissue markers for fibrosis, such as raised native T1 and pathological LGE, consistent with previous CMR studies on QTc disp in cardiac disease[203,204].

## 4.7 CLINICAL APPLICATION

For the first time, this study has comprehensively evaluated the diagnostic utility of ECG as a screening tool for cardiac abnormalities in COVID-19 based on CMR, stratified based on sex. I demonstrated that routinely reported group A features on ECG have a poor sex-dependent diagnostic performance for CMR abnormalities.

Clinical practitioners must consider the inherent variabilities of ECG features between sexes. While important group A features such as the ST-T abnormalities, including the magnitude of depression or elevation, can be less obvious in females[173], predisposing them to false negatives, adding repolarisation intervals which tend to be longer in female patients[167], as we have shown, minimises this risk.

Thus, our findings may build on the growing evidence of sex-specific differences in COVID-19[177] and potentially complement the evidence for using ECG as a diagnostic tool in the acute and convalescence phase of COVID-19[182]. However, larger studies are needed to validate these findings.

## 4.8 LIMITATIONS

Essentially, the statistical output of these analyses needs to be interpreted cautiously as the study was statistically underpowered, and the sex-based comparison further reduced the number of samples with positive outcome measures in each group, which may influence the diagnostic performance defined by the c-statistics and the predictive values[205]. Although diagnostically, we have shown that ECG was a reliable rule-out test, with excellent SN, NPV and -LR, the clinical application is limited as the overall discriminative ability (AUROC) was moderate. Finally, while our findings suggest that repolarisation intervals were significant predictors for composite and individual CMR abnormalities even after adjusting for the clinical covariates, most of the predictive models only explained about one-third of the variance (*based on adjusted* $R^2$) observed in the outcome measured, hence the predictive application is still clinically limited, hence requires further exploration.

## 4.9 CONCLUSION

The findings in this study are hypothesis-generating. Among post-hospitalised COVID-19 patients, sex-dependent variation in ECG features may influence its diagnostic and predictive ability for CMR abnormalities. The sex-based diagnostic performance can be optimised by evaluating both ECG parameters: group A (routinely reported ECG features) and group B (repolarisation intervals). Repolarisation intervals, particularly the QTc disp and/or JT parameters, predict myocardial injury on CMR even after adjusting for the covariates.

# CHAPTER 5: NATURAL HISTORY OF ECG AND CMR ASSOCIATION AMONG MODERATE-TO-SEVERE POST-HOSPITALISED COVID-19 PATIENTS OVER TIME: A PROSPECTIVE, SINGLE-CENTRE FOLLOW UP STUDY

## 5.1 ABSTRACT

***Background***

The longitudinal trajectories of ECG abnormalities and their association with myocardial injury following COVID-19 infection are unclear. This study described the natural history of ECG and CMR associations and assessed the diagnostic ability of ECG to detect CMR abnormalities at three- and six-months post-hospitalisation.

***Methods***

In this single-centre follow-up study, post-hospitalised COVID-19 patients (n=50 at three months, n=38 at six months) and age-and-comorbidities-matched controls (n=43) underwent CMR and 12-lead ECG. ECG intervals (group A and group B features) were analysed. CMR abnormalities were defined as abnormal ventricular systolic function and/or high T1 and T2 and/or high ECV and/or pathological LGE.

***Results***

The burden of ECG abnormalities was 72% at three months and 74% by six months, compared to 51% of controls. All the repolarisation intervals were greater among patients at three-and-six months compared to controls ($p<0.001$). The burden of CMR abnormalities was 36% at three months and 29% by six months, comparable to 30% of controls. Ventricular function was comparable although RVEF was lower between patients at three than six months. Global T1 was increased in patients at three months, subsequently reduced and was comparable to controls by six months. The diagnostic ability of ECG for CMR abnormalities decreased over time.

***Conclusion***

The burden of ECG abnormalities and ventricular repolarisation, which is a marker of arrhythmia, remains high in the medium-to-long-term phase of post-COVID-19 infection. ECG-CMR parameters and diagnostic performance of ECG for CMR abnormalities were

significant at three months and reduced over time post-infection. Larger studies are required to validate the findings.

## 5.2 INTRODUCTION

The medium-to-long-term risks of arrhythmia and burden of ECG abnormalities following COVID-19 infection and its association with CMR parameters of health over time are unknown. Early report in Wuhan, showed that the total burden of ECG abnormalities was elevated in high-risk patients (51% at three months, and increased to 61% at six months)[78]. In this study in China, the burden of ST-T abnormalities increased from 20% at three months post-discharge, to 24% at six months[78]. A large follow up study in the US, involving more than 153 000 COVID-19 patients, demonstrated that the 12 months risks of dysrhythmia was 69% higher in patients than controls[57]. However, these studies were limited by the ECG definitions, which mainly included routine ECG parameters such as arrhythmia and ST-T changes. Moreover, these earlier studies did not explore the CMR parameters limiting insights on the association of ECG and CMR findings. Although, multitude of CMR studies among COVID-19 patients have been published[47,159,206,207], the association of the CMR findings with ECG parameters along with the repolarisation intervals over time were rarely explored. Previous studies have shown that systemic inflammation may contribute to a form of cardiac channelopathy[59] which may lead to prolonged repolarisation, commonly evident in acute and severe COVID-19 infection[84]. Studies exploring the association of myocardial injury including inflammation and ECG abnormalities among the post-hospitalised patients are lacking and how these associations change over time is unknown.

The present study explored whether the burden of ECG abnormalities is high in an independent validation cohort (C-MORE cohort) at two time points and whether the association of ECG and CMR remain significant. Second, to describe the natural history of changes in ECG and CMR parameters and third, to determine the diagnostic ability of ECG to screen for CMR abnormalities at three-and-six- months post-COVID-19 hospitalisation.

## 5.3 METHODS

### PARTICIPANTS

In this single-centre study, the eligibility criteria are similar to the description in **Chapter 2**. Participants were prospectively recruited and underwent cardiac MRI, ECG and blood sampling at three and six months, between March 2020 and November 2021, as part of a follow-up study in Oxford University Hospital called the Capturing MultiORgan Effects of COVID-19 (**Figure 5.1**). The study was supported by the NIHR Oxford Biomedical Research Centre, Oxford British Heart Foundation (BHF) Centre of Research Excellence (RE/18/3/34214) United Kingdom Research Innovation and Wellcome Trust and funded by the Medical Research Council and Department of Health and Social Care/National Institute for Health Research Grant (MR/V027859/1) ISRCTN number 10980107.

### ELECTROCARDIOGRAPHY AND CMR ANALYSIS

12-lead resting digital ECG was conducted on the same day as the CMR, using the CARDIOVIT FT-1 Schiller ECG, Baar, Switzerland), according to the 2007 AHA/ACC guidelines on ECG[208]. The CARDIOVIT FT-1 Schiller ECG has the highest acquisition signal quality with a sampling rate at 32000 Hz. Details in **Chapter 2**.

Participants underwent CMR carried out on a 3 Tesla scanner (Siemens Healthineers, Erlangen, Germany). Details on CMR acquisition and analysis are provided in **Chapter 2**. The definition of ECG and CMR abnormalities is as described in **Chapter 2**. Specific for this chapter, abnormal myocardial tissue characteristics were defined based on the threshold above the 90th percentile of the entire study population, i.e., high global T1 was defined as T1 > 1216.7 ms, high global T2 as T2 > 45 ms, and high ECV as ECV > 0.32 or 32%.

## 5.4 STATISTICAL ANALYSIS

Variables and data normality test were conducted and summarised as described in **Chapter 2**. Group differences were evaluated using Student's paired or unpaired t-tests, Mann Whitney U-tests, Wilcoxon signed-ranks test, one-way analysis of variance (ANOVA) with Post-hoc Tukey Honest Significant Difference (HSD) analysis or Kruskal-Wallis as appropriate. Chi-square test and the Fisher-Freeman-Halton exact tests were used for categorical variables. McNemar's test was conducted for paired categorical data. Pearson's or Spearman's test were used to describe the bivariate correlation analysis where appropriate. All p-values reported are from two-tailed tests. The discriminative ability of the repolarisation parameter model to differentiate between two outcome classes was evaluated using AUROC curve as previously described. Logistic regression analysis for CMR abnormalities was also conducted as previously described. Data are presented with 95% Confidence Intervals (CI). All statistical analysis was performed with SPSS version 27.0 (IBM, Armonk, NY, USA).

### SAMPLE SIZE

For the sample calculation in this chapter, I used alpha value of 0.05 and power (1-β) of 0.80. To determine the discriminative potential of ECG for CMR abnormalities i.e. high T1 based on AUROC, I used value from the previous chapter as reference i.e. 0.82, null hypothesis value 0.5, and ratio of 12 between sample sizes in negative: positive groups, prevalence (ratio of positive cases/total sample size) of 0.08. The total sample size required to determine the diagnostic performance was 56. (MedCalc Software Ltd version 22.009 – 32-bit).

## 5.5 RESULTS

### BASELINE CHARACTERISTICS

**Table 1** shows demographic, clinical, and biochemical data. **Figure 5.1** shows the recruitment of post-hospitalised COVID-19 patients**.**

Fifty post-hospitalised moderate-to-severe patients and 43 risk factor-matched controls were included. The mean age of patients was 55.6 ± 13.8 years. Twenty-one (42%) were women. Nine (18%) belonged to the minority ethnic group. Half of the patients (50%) had a severe infection based on the WHO score (6-9), and about a quarter (24%) of patients required invasive mechanical ventilation during hospitalisation. Eighteen (36%) patients were smokers and ex-smokers, had underlying asthma or hypertension, five (10%) had diabetes, and less than 5% had coronary artery disease. This was comparable to the burden of cardiac comorbidities among controls.

At three months, patients had a median CRP of 2.0 (IQR 0.9-4.8) mg/L which was within the normal range but statistically higher than controls 0.95 (IQR 0.5-2.1) mg/L. The median for CRP decreased at six months but remained higher than controls. Full blood count, renal profile including electrolytes and glomerular filtration rate (GFR) showed no significant difference between patients and controls.

Cardiac biomarkers such as high-sensitivity troponin levels showed no elevation at three and six months and were comparable to controls. On the other hand, N-Terminal Pro-B-Type Natriuretic Peptide (NT Pro-BNP) differed significantly at three months compared to controls, but the level was still within the normal range (58.2 (IQR 35.2-110.5) versus 41.4 (IQR 20.0-80.9) pg/ml, p=0.022). By six months, NT Pro-BNP slightly reduced but remained higher than controls.

**Table 4** Baseline characteristics of COVID-19 patients (at three- and six- months) and controls.

| | **Baseline characteristics** | | | **P values** | | |
|---|---|---|---|---|---|---|
| | **COVID-19, 3months (n= 50)** | **COVID-19, 6months (n= 38)** | **Control (n=43)** | **3months vs Controls** | **6 months vs controls** | **3 months vs 6 months** |
| Age (years) | 55.6 ± 13.8 | 56.1 ± 12.7 | 50.9 ± 12.0 | 0.087[a] | 0.063[a] | - |
| Sex: female n (%) | 21 (42) | 14 (36.8) | 17 (39.5) | 0.809[c] | 0.823[c] | - |
| Non-white ethnicity n (%) | 9 (18.0) | 6 (15.8) | 9 (20.9) | 0.809[c] | 0.582[c] | - |
| BMI kg/m$^2$ | 30.2 (26.3-35.3) | 30.6 (26.7-35.6) | 28.4 (23.8-32.1) | 0.130[b] | 0.110[b] | **0.001[e]** |
| Systolic pressure mmHg | 138 (127-152) | 141 (129-152) | 131 (120-153) | 0.434[b] | 0.283[b] | - |
| Diastolic pressure mmHg | 78 (69 -87) | 81 (73-89) | 75 (63-88) | 0.335[b] | 0.167[b] | - |
| WHO criteria (severe score 6-9) | 25 (50) | - | - | - | - | - |
| WHO criteria (moderate score 4-5) | 25 (50) | - | - | - | - | - |
| Low eGFR n (%) | 0 (0) | 0 (0) | 1 (2.3) | 0.278[d] | 1.000[c] | - |
| Active cancer n (%) | 0 (0) | 0 (0) | 1 (2.3) | 0.278[d] | 1.000[c] | - |
| Smoker and Ex-smoker n (%) | 18 (36.0) | 15 (39.5) | 8 (18.6) | 0.062[c] | **0.049[c]** | - |
| Asthma n (%) | 18 (36.0) | 14 (36.8) | 8 (18.6) | 0.062[c] | 0.082[c] | - |
| COPD n (%) | 2 (4.0) | 1 (2.6) | 0 (0) | 0.497[d] | 0.469[c] | - |
| TIA n (%) | 1 (2.0) | 0 (0) | 1 (2.3) | 1.000[d] | 1.000[c] | - |
| Atrial Fibrillation n (%) | 3 (6.0) | 3 (7.9) | 2 (4.7) | 1.000[d] | 0.661[c] | - |
| Hypertension n (%) | 18 (36.0) | 14 (36.8) | 13 (30.2) | 0.556[c] | 0.638[c] | - |
| Coronary artery disease n (%) | 2 (4.0) | 1 (2.6) | 1 (2.3) | 1.000[d] | 1.000[c] | - |
| Diabetes Mellitus n (%) | 5 (10.2) | 5 (13.5) | 7 (16.3) | 0.388[c] | 0.765[c] | - |
| Hypercholesterolemia n (%) | 12 (24.0) | 9 (23.7) | 5 (11.6) | 0.124[c] | 0.239[c] | - |
| Chronic kidney disease n (%) | 3 (6.0) | 3 (7.9) | 1 (2.3) | 0.621[d] | 0.337[c] | - |
| Oxygen supplementation n (%) | 46 (92.0) | 36 (94.7) | - | - | - | - |
| Invasive mechanical ventilation n (%) | 12 (24.0) | 11 (28.9) | - | - | - | - |
| ACE inhibitor, n (%) | 9 (18.0) | - | - | - | - | - |

| | | | | | | |
|---|---|---|---|---|---|---|
| Beta Blocker, n (%) | 8 (16.0) | - | - | - | - | - |
| Calcium Channel Blocker, n (%) | 10 (20.0) | - | - | - | - | - |
| NSAIDs, n (%) | 3 (6) | - | - | - | - | - |
| **Laboratory Results** | | | | | | |
| White cell count x $10^9$/L | 6.4 (5.3-8.0) | 6.1 (4.9-7.1) | 6.2 (5.0-7.2) | 0.471[b] | 0.673[b] | 0.054[e] |
| Neutrophil | 3.9 (2.9-4.6) | 3.5 (2.8-4.6) | 3.5 (2.7-4.3) | 0.843[b] | 0.821[b] | 0.556[e] |
| Neutrophil (%) | 56.0(51.0-61.5) | 60 .0 (53.0-64.0) | 57.0 (51.8-63.0) | 0.295[b] | 0.309[b] | **0.032[e]** |
| Lymphocyte | 1.8 (1.6-2.3) | 1.7 (1.4-2.1) | 1.80 (1.5-2.3) | 0.811[b] | 0.099[b] | **0.002[e]** |
| Lymphocyte (%) | 31.0 (24.0-36.0) | 28.0 (22.8-33.3) | 30.5 (25.0-35.3) | 0.849[b] | 0.164[b] | **0.027[e]** |
| Monocyte | 0.59 (0.44-0.67) | 0.51 (0.44-0.61) | 0.50 (0.36-0.65) | 0.146[b] | 0.750[b] | 0.019[e] |
| Monocyte (%) | 9.0 (7.0-10.0) | 9.0 (7.0-10.0) | 8.0 (7.0-9.0) | **0.030[b]** | 0.102[b] | 0.475[e] |
| Hb g/dL | 13.5 (12.6-14.2) | 14.2 (12.8-15.2) | 14.1 (12.8-15.3) | 0.056[b] | 0.981[b] | **0.004[e]** |
| Platelet x $10^9$/L | 263.0 (211.5-292.0) | 247.5 (213.0-272.3) | 257.5 (211.5-284.0) | 0.786[b] | 0.421[b] | **0.002[e]** |
| Hct (%) | 40.9 (38.8-43.5) | 42.2 (40.3-44.5) | 42.1 (38.1-45.5) | 0.337[b] | 0.599[b] | **0.039[e]** |
| Sodium mEq/L | 141.0 (139.0-141.3) | 141.0 (139.8-142.0) | 140.0 (139.0-141.0) | 0.072[b] | 0.005[b] | **0.010[e]** |
| Potassium mEq/L | 3.9 (3.7-4.1) | 3.9 (3.8-4.1) | 3.9 (3.6-4.1) | 0.867[b] | 0.230[b] | 0.799[e] |
| Urea mmol/L | 4.7 (3.8-6.0) | 5.3 (4.4-7.1) | 4.9 (4.2-5.8) | 0.285[b] | 0.183[b] | **<0.001[e]** |
| Creatinine µmol/L | 70.0 (62.3-80.3) | 75.5 (65.8-87.0) | 78.0 (64.8-86.3) | 0.096[b] | 0.885[b] | **0.005[e]** |
| GFR ml/min | 90.0 (81.8-90.0) | 88.5 (73.8-90.0) | 90.0 (83.8-90.0) | 0.880[b] | 0.210[b] | **0.009[e]** |
| Procalcitonin ng/ml | 0.02 (0.02-0.03) | 0.02 (0.02-0.03) | 0.02 (0.01-0.03) | 0.070[b] | 0.419[b] | 0.115[e] |
| NT Pro-BNP, pg/mL | 58.2 (35.2-110.5) | 57.0 (31.6-99.6) | 41.4 (20.0-80.9) | **0.026[b]** | 0.065[b] | 0.366[e] |
| Troponin, ng/L | 2.0 (2.0-3.0) | 2.0 (2.0-4.0) | 2.0 (2.0-2.0) | 0.094[b] | **0.028[b]** | 0.148[e] |
| C-Reactive Protein, mg/L | 2.0 (0.9-4.8) | 1.7 (0.9-5.8) | 0.95 (0.5-2.1) | **0.001[b]** | **0.009[b]** | 0.884[e] |

[a]Independent T-Test, [b]Mann-Whitney Test, [c]Chi-square Test, [d]Fisher-Freeman-Halton Exact Test, [e]Wilcoxon Signed Rank Test.

Values are mean ± SD, median (IQR) or percentages. BMI, body mass index; BSA, body surface area; COPD, chronic obstructive pulmonary disease; eGFR, estimated glomerular filtration rate; Hb, haemoglobin; Hct, Haematocrit; Inv, invasive; LDH, lactate dehydrogenase; NT Pro-BNP, N-terminal pro B-type natriuretic peptide, TIA, transient ischemic attack.

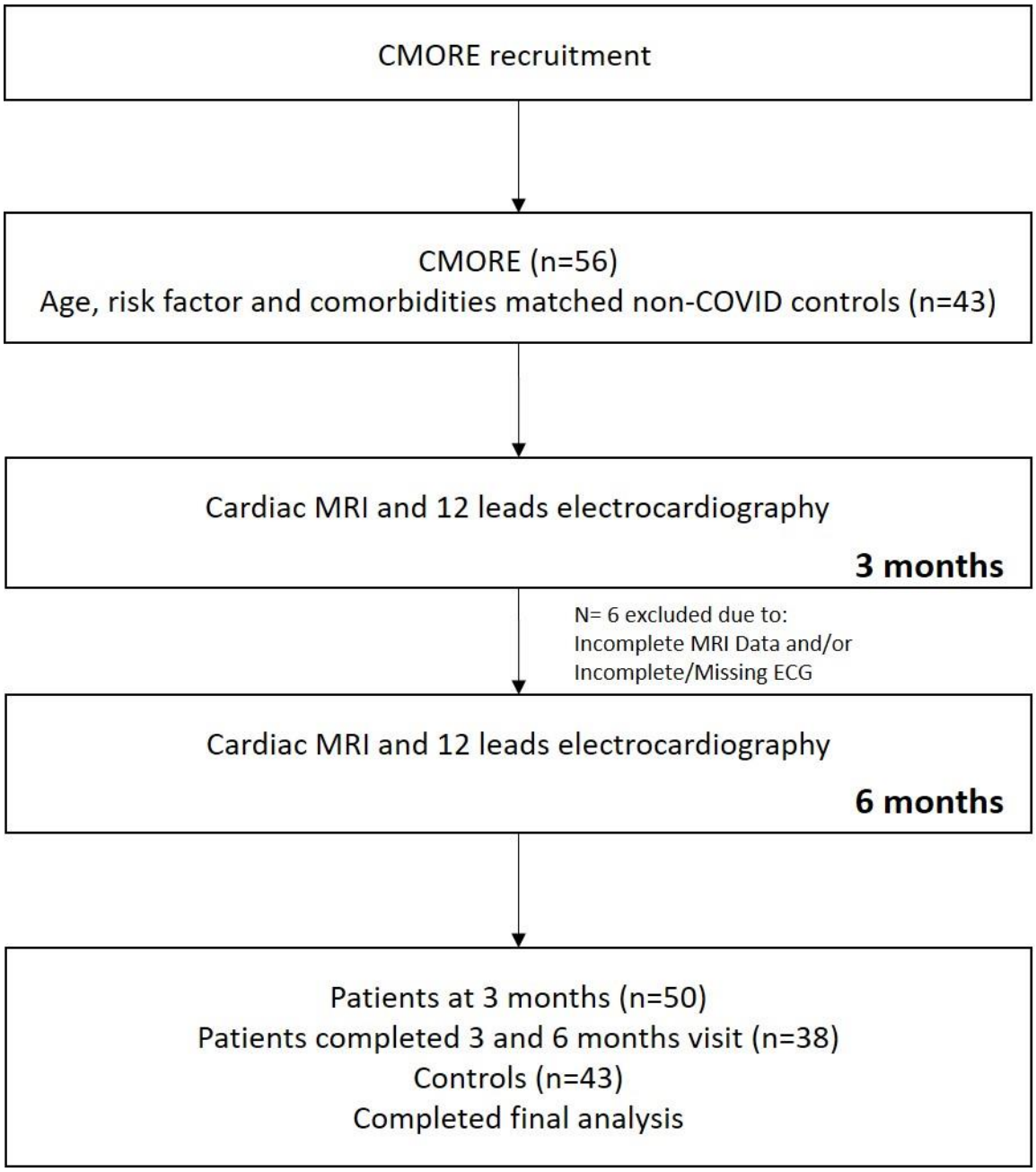


**Figure 5.1** Flow chart of Capturing Multiorgan Effects of COVID-19 (CMORE) study.

## ECG CHARACTERISTICS IN COVID-19 PATIENTS VS CONTROLS

**Table 2** summarises the ECG characteristics of COVID-19 patients at 3- and 6-months post-discharge relative to controls.

The burden of ECG abnormalities defined as composite of group A ECG parameters were greater among patients than controls at three months (72% vs 51%, p=0.039). Among the entire study population, ST-T changes were the most reported abnormalities, with comparable frequency between patients and controls (36% vs 37%, p=0.802) (**Table 2**). At three months, QRS abnormalities such as poor R progression and fragmented QRS tended to be more common among patients than controls (20% vs 14%, p=0.441) and (28% vs14%, p=0.137) respectively. Two (4%) patients had first degree heart block, one (2%) patient had right bundle branch block (RBBB) but no arrhythmias, such as atrial fibrillation or ventricular ectopic, were reported.

By six months, the burden of ECG abnormalities remained significantly higher among patients than controls (74% vs 51%, p=0.037). The prevalence of ST-T changes reduced to 32% (*24% dropped out in follow-up*), whilst the prevalence of heart block, all of which were first-degree, increased to four (11%) patients. The patient who had RBBB at three months, had missed the six-month follow-up. However, there was an incidence of two (5%) new BBB cases; intraventricular conduction delay (IVCD) and incomplete right bundle branch block (IRBBB) were reported at six months. PVCs were not reported at three months, but the cumulative incidence was five (13%) new patients at six months. No other types of arrhythmias were detected from the 12-lead ECG at 6 months.

Group B ECG analysis revealed that patients had higher ventricular rate than controls (74 ± 13 vs 68 ± 12 ms, p=0.019). At three and six months, PR interval and QRS duration, which

represent atrial and ventricular depolarisation did not differ between patients and controls. By contrast, all the ventricular repolarisation intervals i.e. QTc, QTc disp, QTPC, JTc, JTPc, and cTPe were significantly greater in patients than controls ($p<0.001$ for all variables) at both time points. Among COVID-19 patients, no significant difference in the intervals was observed at three-and-six months except for the JTc interval, which was relatively greater by six months (**Table 2**).

### ECG AND CMR RESULTS AMONG PATIENTS WHO COMPLETED BOTH VISITS

It is worth noting that, at six months, only 38/50 (76%) patients from the initial cohort attended the follow-up visit. Therefore, to address the potential outcome bias contributed by the missing patients, analysis was also conducted involving *only patients who completed both visits (n=38 at three-and-six months*). The findings are summarised in **Appendix 4 Table 1**. Overall, the findings are consistent and comparable to analyses in **Table 2** (n=50 at three months, n=38 at six months).

## CMR CHARACTERISTICS IN COVID-19 PATIENTS VS CONTROLS

At three- and six-months post-hospitalisation, more than a quarter of patients had cardiac abnormalities on CMR, which was comparable to the comorbidities-matched controls. LV volumes, mass, and function did not differ between patients (at three and six months) and controls (**Table 3**).

RV volumes (end diastolic and end systolic) did not differ with controls but were lower among patients at three months compared to six months. Similarly, the RV ejection fraction was lower at three months than six months post-hospitalisation (57.6 ± 7.7% vs 60.0 ± 6.3%, $p<0.001$), but was comparable to controls. At three months, five (10%) patients had RVEF below the cut-off of 48%. By six months only one of them had RVEF < 48%.

Global myocardial T1 (a biomarker sensitive to inflammation and fibrosis) was significantly higher in patients at three months than control (**Table 3**). By six months, the myocardial native T1 reduced and was comparable to controls. Global native T2 (a biomarker sensitive to oedema) was not significantly different between patients and controls. Extracellular volume fraction (ECV; a biomarker sensitive to diffuse fibrosis) was not statistically different but relatively higher in patients at three months than controls. By six months, the ECV decreased with values comparable to controls. The burden of LGE (a biomarker of focal fibrosis) did not differ between patients and controls (**Table 3**).

**Table 2** ECG parameters of all patients at three- and six- months relative to controls. **(*n=50 at 3 months*).**

| (All patients at 3 months) | ECG | | | P values | | |
|---|---|---|---|---|---|---|
| | **COVID-19, 3 months (n=50)** | **COVID-19, 6 months (n=38)** | **Control (n=43)** | **3months vs control** | **6months vs control** | **3months vs 6months** |
| Age (years) | 55.6 ± 13.8 | 55.6 ± 12.6 | 50.9 ± 12.0 | 0.087[a] | 0.091[a] | - |
| Sex: female n (%) | 21(42.0) | 14 (36.8) | 17(39.5) | 0.809[c] | 0.803[c] | - |
| Abnormal ECG n (%) | 36 (72.0) | 28 (73.7) | 22 (51.2) | **0.039[c]** | **0.037[c]** | 1.000[e] |
| Bundle Branch Block n (%) | 1(2.0) | 2 (5.3) | 0 (0) | 1.000[d] | 0.217[d] | 0.500[e] |
| Abnormal axis * n (%) | 15 (30.0) | 14 (36.8) | 8 (18.6) | 0.184[c] | 0.066[c] | 1.000[e] |
| ST-T changes * n (%) | 18 (36.0) | 12 (31.6) | 16 (37.2) | 0.802[c] | 0.595[c] | 0.727[e] |
| Poor QRS progression n (%) | 10 (20.0) | 6 (15.8) | 6(14.0) | 0.441[c] | 0.816[c] | 1.000[e] |
| Fragmented QRS * n (%) | 14 (28.0) | 9 (23.7) | 6 (14.0) | 0.137[c] | 0.261[c] | 1.000[e] |
| Heart block n (%) | 2 (4.0) | 4 (10.5) | 0 (0) | 0.497[d] | **0.044[d]** | 0.500[e] |
| PVC/PAC n (%) | 0 (0) | 5 (13.2) | 0 (0) | - | **0.020[d]** | 0.063[e] |
| | **Group B ECG** | | | **P values** | | |
| Heart rate (bpm) | 74 ± 13 | 70 ± 14 | 68 ± 12 | **0.019[a]** | 0.322[a] | 0.051[f] |
| PR interval (ms) | 160.0 (145.5-179.5) | 155.0 (143.8-184.3) | 154.0 (142.0-173.0) | 0.111[b] | 0.356[b] | 0.369[g] |
| QRS (ms) | 88.6 ± 8.3 | 90.9 ± 11.1 | 88.8 ± 8.8 | 0.873[a] | 0.355[a] | 0.127[b] |
| QTc (ms) | 456.8 ± 28.4 | 464.6 ± 32.5 | 419.8± 29.3 | **<0.001[a]** | **<0.001[a]** | 0.120[f] |
| QTc disp (ms) | 71.7 ± 21.7 | 81.8 ± 31.2 | 51.1 ± 18.0 | **<0.001[a]** | **<0.001[a]** | 0.088[f] |
| QTPc (ms) | 376.6 ± 32.7 | 379.0 ± 32.9 | 347.6 ± 28.8 | **<0.001[a]** | **<0.001[a]** | 0.594[f] |
| JTc (ms) | 358.6 ± 26.7 | 367.4 ± 28.5 | 330.3 ± 22.8 | **<0.001[a]** | **<0.001[a]** | **0.041[f]** |
| JTPc (ms) | 253 ± 4 | 258.5 ± 31.5 | 235.3 ± 25.9 | **0.004[a]** | **<0.001[a]** | 0.129[f] |
| cTPe (ms) | 107.0 ± 16.2 | 108.4 ± 17.6 | 94.9 ± 12.8 | **<0.001[a]** | **<0.001[a]** | 0.875[f] |

[a]Independent T-Test, [b]Mann-Whitney Test, [c]Chi-square Test, [d]Fisher-Freeman-Halton Exact Test, [e]McNemar Test, [f] Paired T-Test, [g]Wilcoxon Signed Rank Test

Values are mean ± SD, median (IQR) or percentages. BBB indicates bundle branch block; ECG, electrocardiography; JTc, corrected JT; JTPc, corrected JT peak; PAC, premature atrial complex; PVC, premature ventricular complex; QTc, corrected QT; QTPc, corrected QT peak; cTPe, corrected T-peak- to-T-end; Disp dispersion. * Bundle branch block cases excluded.

**Table 3** CMR parameters of all patients at three- and six- months relative to controls.

| | CMR | | | P values | | |
|---|---|---|---|---|---|---|
| | **COVID-19, 3months (n=50)** | **COVID-19, 6months (n=38)** | **Control (n=43)** | **3months vs control** | **6months vs control** | **3months vs 6months** |
| CMR abnormal n (%) | 18 (36.0) | 11(28.9) | 13 (30.2) | 0.556[c] | 0.181[c] | 0.063[e] |
| LVEDV ml | 144.8 (127.8-168.3) | 151.9 (126.9-183.4) | 148.4(129.5-171.3) | 0.811[b] | 0.524[b] | 0.202[g] |
| LVESV ml | 53.8 (42.3-72.0) | 54.9 (45.5-71.0) | 53.7 (48.9-65.6) | 0.890[b] | 0.841[b] | 0.259[g] |
| LVSV ml | 93.9 ± 19.6 | 97.7 ± 22.4 | 93.9 ± 21.0 | 0.998[a] | 0.423[a] | 0.052[f] |
| LV mass g | 116.2 (100.9-135.5) | 119.5 (99.3-130.6) | 110.5 (87.8-132.9) | 0.261[b] | 0.262[b] | 0.206[g] |
| LV mass index g/m$^2$ | 58.9 (49.7-66.2) | 57.0 (50.4-64.8) | 53.7 (49.5-62.1) | 0.178[b] | 0.158[b] | 0.104[g] |
| LVEF (%) | 62.8 ± 7.7 | 62.8 ± 6.7 | 63.0 ± 5.8 | 0.882[a] | 0.922[a] | 0.206[f] |
| LVEF < 52% n (%) | 5 (2.3) | 1 (2.5) | 1(2.3) | 0.212[d] | 1.000[c] | 1.000[e] |
| LVCO L/min | 7.1 (5.7-7.8) | 6.2 (5.4-7.9) | 6.1 (5.3-7.1) | 0.056[b] | 0.432[b] | 0.388[g] |
| RVEDV ml | 165.5 ± 36.9 | 161.8 ± 40.6 | 160.6 ± 41.9 | 0.553[a] | 0.835[a] | **0.038[f]** |
| RVESV ml | 71.3 ± 23.5 | 66.1 ± 23.2 | 68.6 ± 26.5 | 0.597[a] | 0.637[a] | **<0.001[f]** |
| RVSV ml | 92.7 (79.6-108.8) | 92.3 (82.1-111.2) | 89.2 (81.0-102.2) | 0.706[b] | 0.643[b] | 0.510[g] |
| RVEF (%) | 57.6 ± 7.7 | 60.0 ± 6.3 | 59.1 ± 6.4 | 0.317[a] | 0.450[a] | **<0.001[f]** |
| RVEF < 48% n (%) | 5 (10.0) | 1 (2.6) | 1 (2.3) | 0.369[d] | 1.000[c] | 0.250[e] |
| RVCO L/min | 6.9 ± 1.6 | 6.6 ± 1.8 | 6.2 ± 1.6 | **0.046[a]** | 0.726[b] | 0.416[f] |
| **Myocardial Tissue Characterisations** | | | | | | |
| Global T1 ms | 1177.2 ± 32.9 | 1150.4 ± 35.9 | 1152.7 ± 39.5 | **0.002[a]** | 0.778[a] | **<0.001[f]** |
| High T1 n (%) ** | 6 /49 (12.2) | 1 (2.5) | 3/42 (7.1) | 0.498[d] | 0.616[d] | 0.625[e] |
| Global T2 ms | 42.4 ± 2.1 | 42.0 ± 1.6 | 42.3 ± 2.5 | 0.768[a] | 0.505[a] | 0.175[f] |
| High T2 n (%) ** | 5/49 (10.2) | 1 (2.5) | 5/42 (11.9) | 1.000[d] | 0.203[f] | 1.000[e] |
| ECV n (%) | 29.8 (27.5-31.1) | 28.0 (26.2-30.2) | 28.6 (26.1-30.6) | 0.198[b] | 0.566[b] | **0.006[g]** |
| High ECV (>32) (%) | 3/40 (7.5) | 3 (7.9) | 4/31 (12.9) | 0.691[d] | 0.692[b] | 1.000[e] |
| Pathological LGE n (%) | 11/49 (22.5) | 9 (23.7) | 8 /42 (19.0) | 0.691[c] | 0.656[c] | 1.000[e] |

[a]Independent T-Test, [b]Mann-Whitney Test, [c]Chi-square Test, [d]Fisher-Freeman-Halton Exact Test, [e]McNemar Test, [f] Paired T-Test, [g]Wilcoxon Signed Rank Test

Values are mean ± SD, median (IQR) or percentages. CMR, cardiac magnetic resonance; ECV, Extracellular volume; LGE, late gadolinium enhancement; LV, left ventricular; LVEDV, left ventricular end-diastolic volume; LVESV, left ventricular end-systolic volume; LVSV, left ventricular systolic volume; LVEF, left ventricular ejection fraction; LVCO, left ventricular cardiac output; RVEDV, right ventricular end-diastolic volume; RVESV, right ventricular end-systolic volume; RVSV, right ventricular systolic volume; RVEF, right ventricular ejection fraction; RVCO, right ventricular cardiac output. ** (>90$^{th}$ centile T1>1216.7 ms, T2 >45 ms).

## COMPARISON OF ECG PARAMETERS IN PATIENTS WITH COMPOSITE CMR ABNORMALITIES VERSUS CONTROLS

To delineate the temporal relationship of electrical conduction and myocardial abnormalities, I compared ECG parameters of patients with and without CMR abnormalities (*composite*) versus controls, at three- and six- months post-hospitalisation. Findings are summarised in **Table 4**.

At three months, 36% of patients had CMR abnormalities and reduced to 29% by six months. The average age and BMI were comparable across the groups at both time points. The median of the PR interval and QRS duration was comparable, whereas ECG markers of ventricular repolarisation i.e. QTc, JTc, and cTPe intervals demonstrated significant mean difference across the three groups (**Table 4**). Post-hoc analysis revealed longer repolarisation intervals among patients with CMR abnormalities versus controls ($p<0.001$ for most variables), whilst no significant mean difference was observed between patients with and without CMR abnormalities (**Table 4**). By six months, comparable to the trends at three months post hospitalisation, the ventricular repolarisation parameters remained significantly higher among patients with and without CMR abnormalities, relative to controls (**Table 4**).

**Table 4** ECG findings of patients with/without CMR abnormalities compared to controls at three- and six-months post-hospitalisation.

| **3 months** | **COVID-19 with CMR abn (n=18)** | **COVID-19 without CMR abn (n=32)** | **Control (n=43)** | **P values** |
|---|---|---|---|---|
| Age years | 58 ± 13 | 54 ± 14 | 51 ± 12 | 0.147[a] |
| Sex: Female n (%) | 4 (22.2) | 17 (53.1) | 17 (39.5) | 0.100[c] |
| BMI kg/m$^2$ | 29.9 (25.5-34.3) | 30.8 (26.5-36.5) | 28.4 (23.8-32.1) | 0.268[b] |
| PR interval ms | 170.0 (145.5-193.0) | 158.0 (145.0-171.0) | 155.0 (142.5-173.3) | 0.152[b] |
| QRS ms | 89.0 (85.8-93.5) | 87.5 (81.3-94.5) | 89.0 (82.8-94.0) | 0.619[b] |
| QTc ms | 454.8 ± 28.4 | 460.0 ± 30.5 | 420.3 ± 29.5* | **<0.001[a]** |
| QTc disp ms | 69.2 ± 21.9 | 73.8 ± 20.3 | 51.2 ± 18.4* | **<0.001[a]** |
| QTPc ms | 364.2 ± 23.5 | 381.6 ± 37.4 | 347.3 ± 19.0** | **<0.001[a]** |
| JTc ms | 354.2 ± 21.6 | 362.2 ± 30.6 | 330.1 ± 23.0* | **<0.001[a]** |
| JTPc ms | 241.0 ± 25.6 | 260.4 ± 32.9 | 235.3 ± 25.9** | **0.001[a]** |
| cTPe ms | 109.9 (97.9-126.7) | 99.4 (91.5-111.8) | 91.9 (85.4-101.3) *** | **<0.001[b]** |
| **6 months** | **COVID-19 with CMR abn (n=11)** | **COVID-19 without CMR abn (n=27)** | **Control (n=43)** | **P values** |
| Age years | 58 ± 10 | 54 ± 14 | 51 ± 12 | 0.222[a] |
| Sex: Female n (%) | 2 (18.2) | 12 (44.4) | 17 (39.5) | 0.100[c] |
| BMI kg/m$^2$ | 30.6 ± 4.8 | 31.0 ± 6.0 | 29.2 ± 6.4 | 0.439[a] |
| PR interval ms | 163.0 (142.0-200.0) | 152.0 (144.0-179.0) | 155.0 (142.5-173.3) | 0.152[b] |
| QRS ms | 90.0 ±10.9 | 91.3 ± 11.3 | 88.8 ± 8.8 | 0.614[a] |
| QTc ms | 467.5 ± 31.8 | 462.5 ± 31.9 | 420.3 ± 29.5* | **<0.001[a]** |
| QTc disp ms | 80.9 ± 23.7 | 79.3 ± 32.3 | 51.2 ± 18.4* | **<0.001[a]** |
| QTPc ms | 384.0 ± 35.4 | 373.9 ± 32.7 | 347.3 ± 19.0* | **<0.001[a]** |
| JTc ms | 372.0 ± 31.7 | 364.7 ± 29.0 | 330.1 ± 23.0* | **<0.001[a]** |
| JTPc ms | 260.9 ± 39.4 | 257.6 ± 28.4 | 235.3 ± 25.9* | **0.002[a]** |
| cTPe ms | 111.1 ± 20.4 | 107.1 ± 17.3 | 94.8 ±12.9* | **<0.001[a]** |

[a]One-way ANOVA; [b]Kruskal Wallis; [c]Chi-square Test.
* P values (p<0.05) with post-hoc Tukey HSD test *vs* patients **with and without** CMR abnormalities.
** P values (p<0.05) with post-hoc Tukey HSD test *vs* patients **without** CMR abnormalities.
*** P values (p<0.05) with Bonferroni correction *vs* patients **with** CMR abnormalities.
Values are mean ± SD, median (IQR) or percentages. BBB, bundle branch block; BMI, body mass index; CMR abn, composite of CMR abnormalities; ECG, electrocardiography; JTc, corrected JT; JTPc, corrected JT peak; PAC, premature atrial complex; PVC, premature ventricular complex; QTc, corrected QT; QTPc, corrected QT peak; cTPe, corrected T-peak- to-T-end; disp, dispersion.

## ASSOCIATION OF ECG REPOLARISATION PARAMETER AND MYOCARDIAL TISSUE CHARACTERISTICS AT THREE- AND SIX-MONTH POST-HOSPITALISATION.

**Figure 5.2** shows bivariate correlations to further elucidate the relationship between ECG repolarisation and global native T1, a sensitive biomarker for inflammation or fibrosis. Overall, the higher the global T1 values, the longer the corresponding repolarisation intervals. The QTc and QTPc intervals demonstrated significant correlations at R=.38, p=0.007 and R=0.30, p=0.035, respectively. Likewise, the JTc interval demonstrated a positive correlation but was not statistically significant at R=0.28, p=0.052.

The relationship was subsequently re-explored at 6 months post-hospitalisation. Although the global T1 values have generally reduced in most patients, evidenced by the downward shifts of the scatter plots, the correlations remained observable but not statistically significant for QTc, JTc and cTPe interval with Rs=0.26., p=0.118, R=.30, p=0.066, and R=0.24, p=0.149 respectively (**Figure 5.3**).

Likewise, when categorised based on QTc > 450 ms (mild prolongation), versus QTc ≤ 450 ms (normal), global T1 was statistically higher among patients with prolonged QTc at three months (p=0.013) (**Figure 5.4)**. At six months, global native T1 remained higher among patients with prolonged QTc (p=0.328) (**Figure 5.4).** The association was more evident when patients were categorised based on QTc > 480 ms versus QTc ≤ 480 ms (an established ECG marker of ventricular arrhythmia) (**Figure 5.5**). Moreover, correlation analysis revealed a more robust association between the QTc interval and global T1 values when stratified according to the WHO severity scale (**Figure 5.6**). COVID-19 patients with severe infection (WHO score 6-9) demonstrated R=.52, p=0.008 compared to R=.26, p=0.230

among patients with moderate infection (WHO score 4-5). Among the severe patients (WHO score 6-9), the correlation subsequently decreased to R=.23, p=0.305 at 6 months. No significant correlations were observed with other parameters of myocardial tissue health, i.e. global native T2 and global ECV.

Thus, there is a plausible association between ECG repolarisation intervals and CMR markers of inflammation or fibrosis, especially among those with severe COVID-19 infection, which subsequently decreased from three months to six months post-hospitalisation.

**3 months**

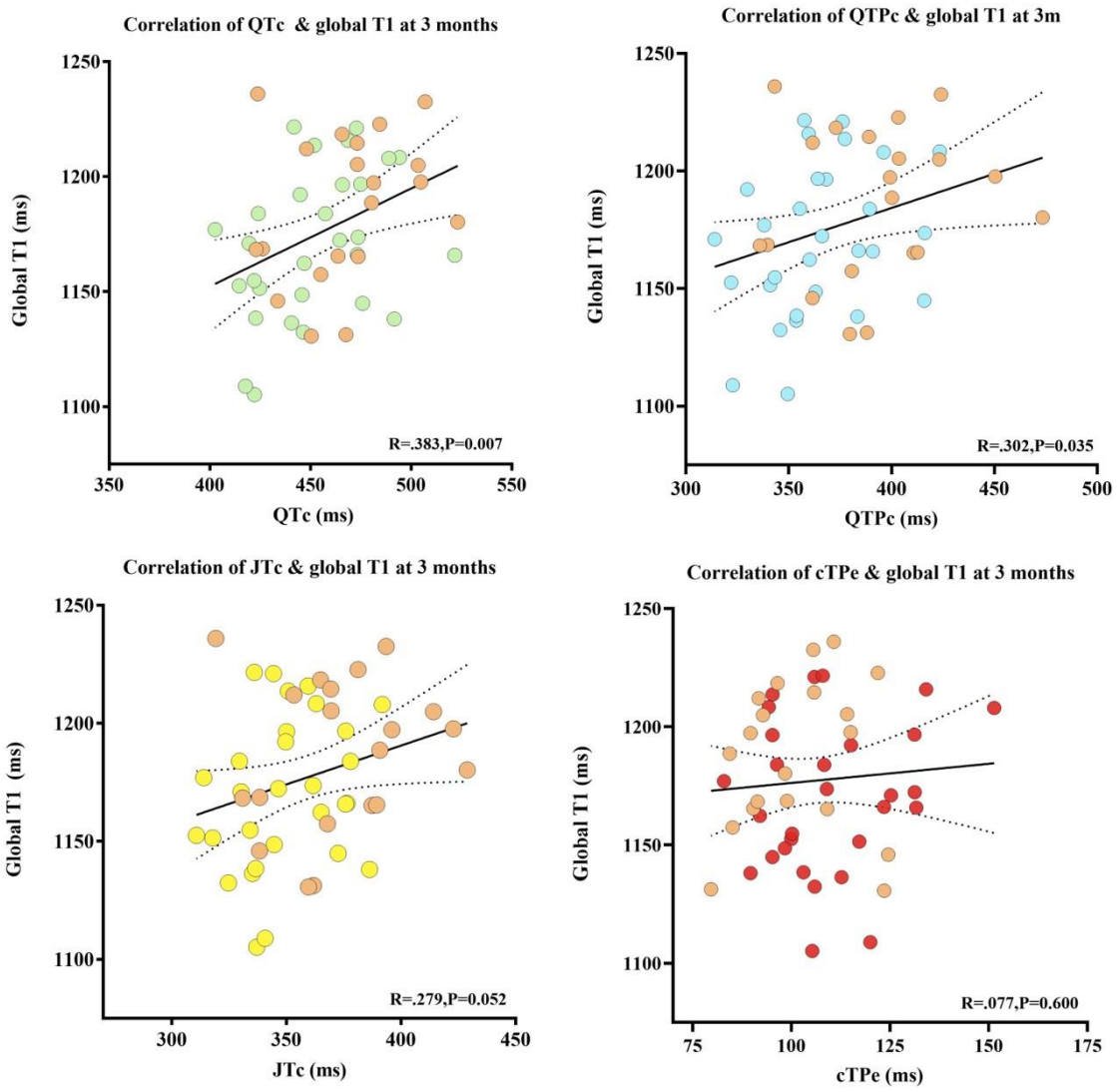


**Figure 5.2** Correlation between the repolarisation intervals and global T1 at three months. P values are based on Pearson's correlation analysis (R). Positive correlations between global T1 values and QTc, QTPc and JTc intervals were observed. represents female participants.

**6 months**

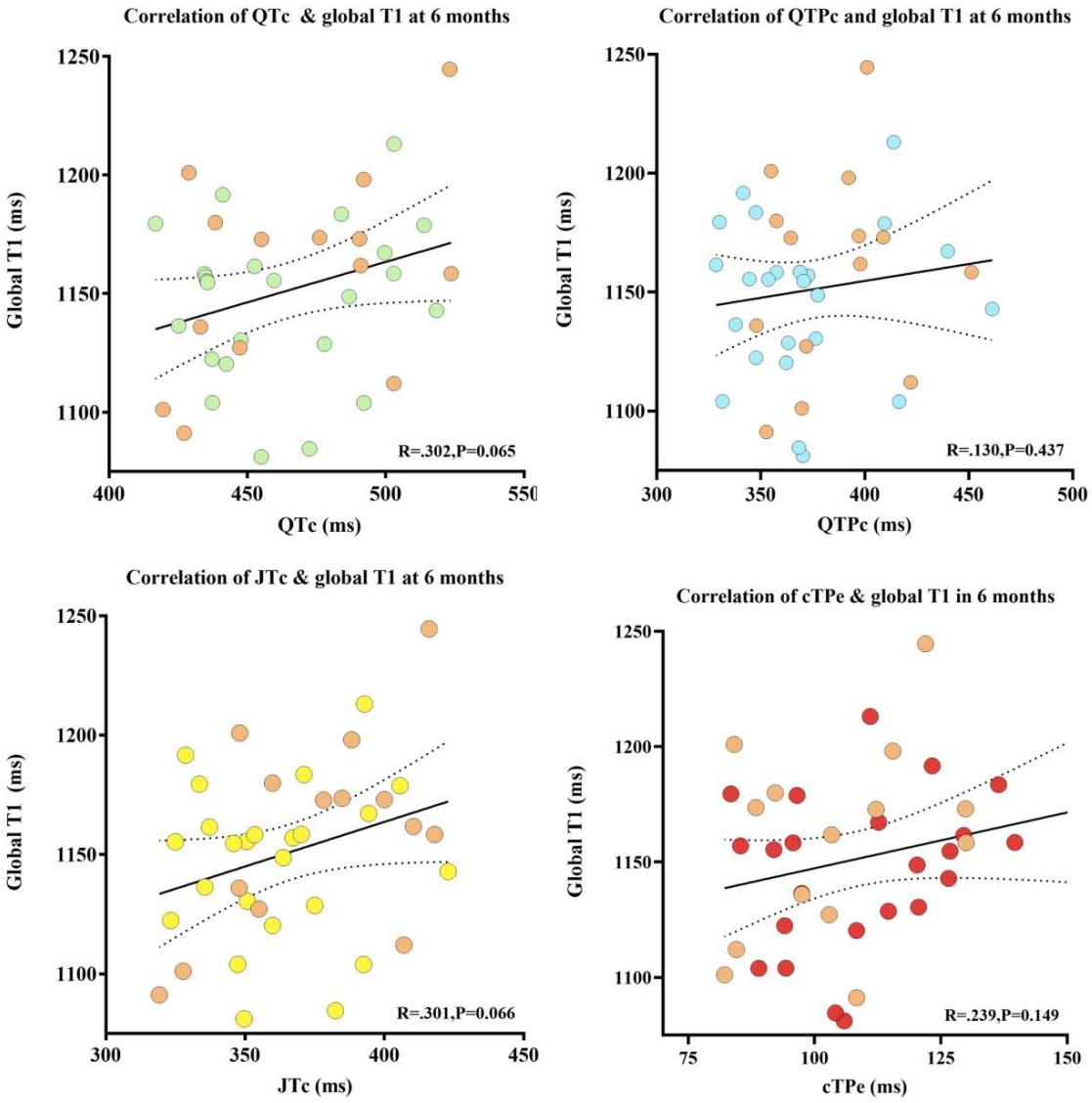


**Figure 5.3** Positive correlations observed between the repolarisation intervals and global T1 at six months. P values are based on Pearson's correlation analysis (R). Intervals are colour-coded ( = QTc, = QTPc, = JT, = cTPe and represents female participants).

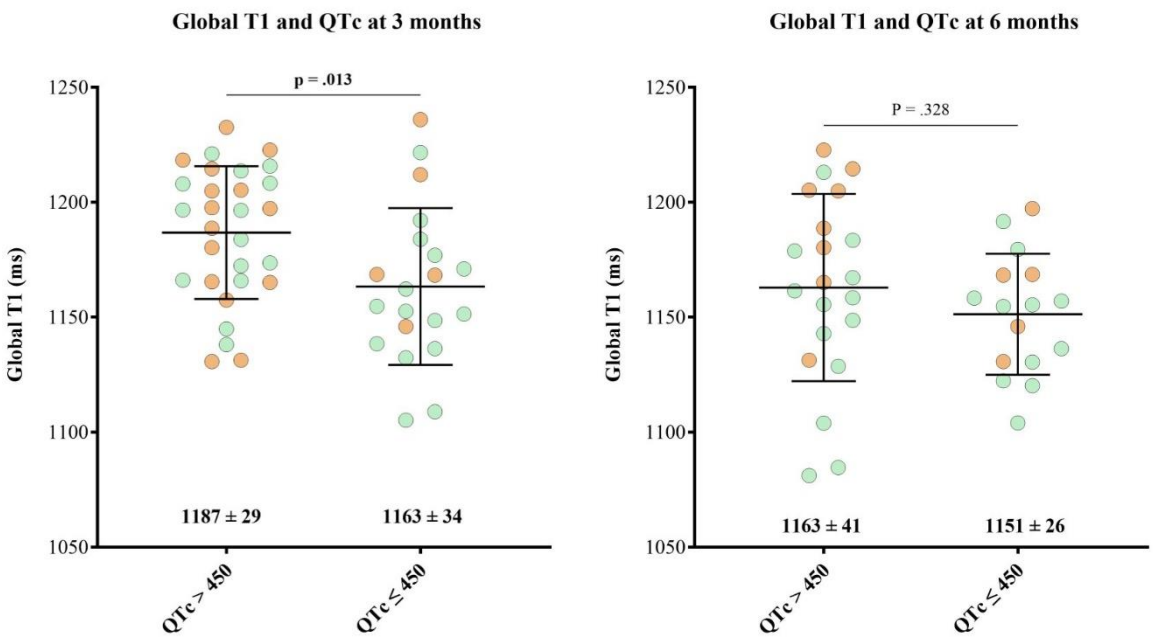


**Figure 5.4**. Global T1 in patients with and without QTc prolongation at three months (left) (n=50) and six months (right) (n=38) post-hospitalisation. Values are mean ± SD. P values are based on unpaired student's T test. ○ represents female participants.

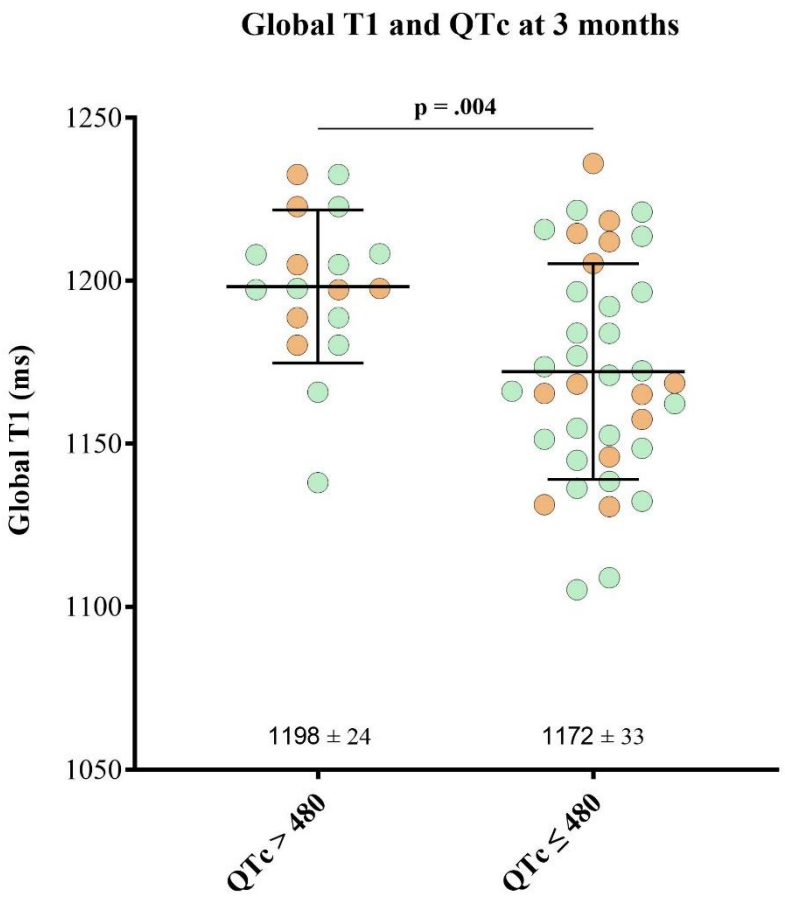


**Figure 5.5**. Global T1 values are significantly higher in patients with QTc prolongation > 480 ms than QTc ≤ 480 ms. Note that the average global T1 values for patients with QTc > 480 ms are also higher than those patients with QTc > 450 ms (Figure 5.4), indicating a possible association between myocardial injury (inflammation or fibrosis) and ventricular repolarisation. Values are mean ± SD. P values are based on unpaired student's T-test. ○ represents female participants.

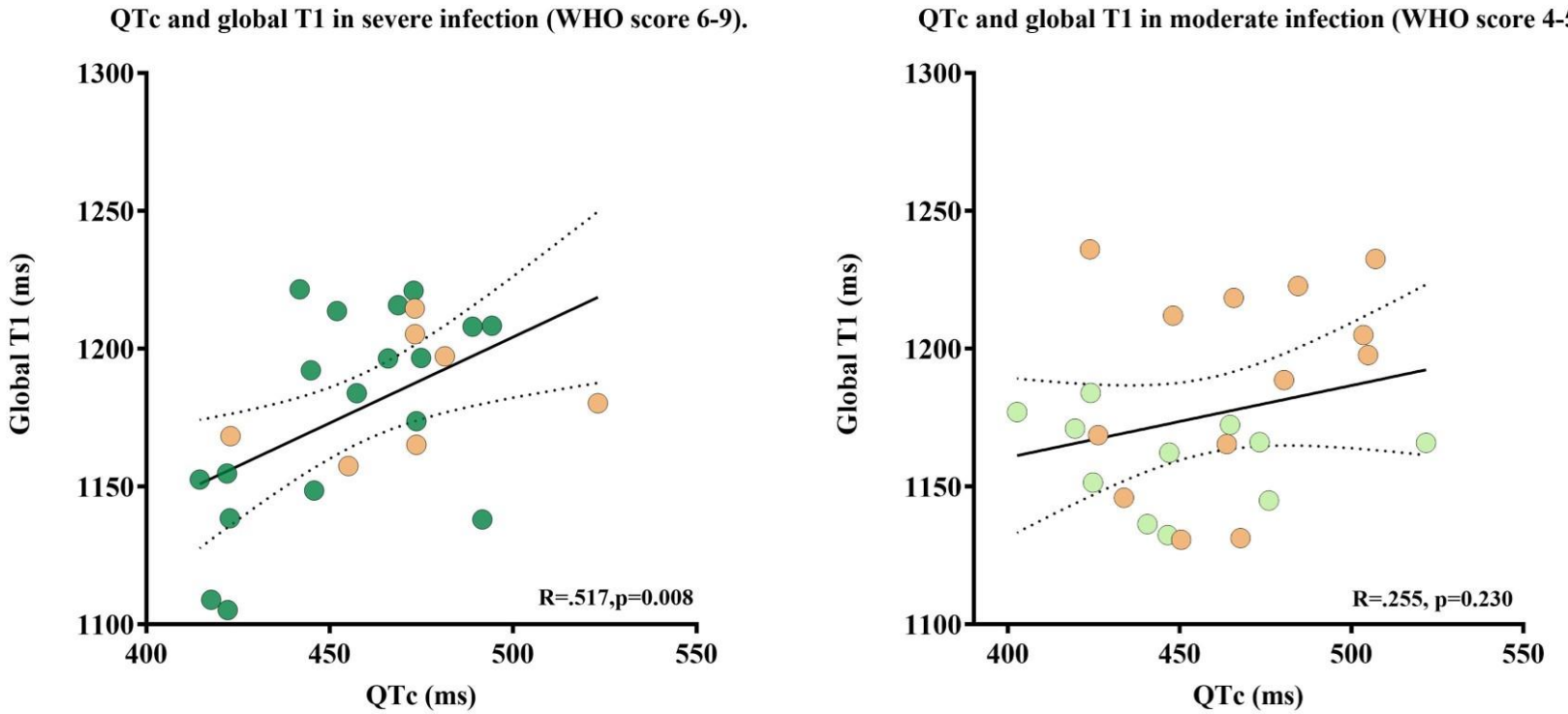


**Figure 5.6** Scatter plot depicting correlations between QTc and global T1 values among moderate COVID-19 infection (WHO score 4-5, n=25) and severe COVID-19 infection (WHO score 6-9, n=25). Note that the correlation is R=0.517, p=0.008 among severe infection, whereas R=0.255, p=0.230 among patients with moderate infection. P values are based on Pearson's correlation analysis (R). represents female participants.

## DIAGNOSTIC PERFORMANCE OF ECG PARAMETERS FOR CMR ABNORMALITIES

Clinical utility of ECG for detecting myocardial injury relies on the strength of its diagnostic performance. **Table 5** summarises the discriminative ability of ECG parameters for composite CMR abnormalities among patients at three months post-hospitalisation. Composite of group A ECG abnormalities showed poor discriminative power with c-statistics at 0.50 (95% 0.31-0.69, p=1.000). Combining the repolarisation intervals with the group A ECG abnormalities improved the discriminative power of ECG (**Table 5**).

**Figure 5.5A**, showed an augmentation of AUROC curve from 0.50 to 0.73 with the addition of the cTPe interval to the diagnostic ECG criteria (95% CI 0.57-0.90 p=0.015). Other combinations were not statistically significant. In addition, the discriminative power of ECG for composite CMR abnormalities, reduced over time, to AUROC of 0.69 at six months (**Figure 5.5B**).

**Table 5** Discriminative ability of ECG for CMR abnormalities in COVID-19 patients

| Composite CMR abnormalities | | |
|---|---|---|
| **ECG parameter** | **C- statistic 95% CI** | **P value** |
| ECG abnormalities (Composite group A) | 0.50 [0.31-0.69] | 1.000 |
| ECG abnormalities + QTc | 0.61 [0.44-0.79] | 0.240 |
| ECG abnormalities + QTc disp | 0.54 [0.35-0.73] | 0.650 |
| ECG abnormalities + JTc | 0.56 [0.37-0.74] | 0.557 |
| ECG abnormalities + JTPc | 0.67 [0.49-0.84] | 0.083 |
| ECG abnormalities + cTPe | 0.73 [0.58-0.87] | **0.009** |

P values are based on concordance statistics and receiver operating characteristics curve analysis.
ECG abnormalities = group A ECG features presence of arrhythmia/premature ventricular or atrial complex/abnormal axis deviation/heart block/bundle branch block/fragmented QRS complex/poor R wave progression/ST-T change.

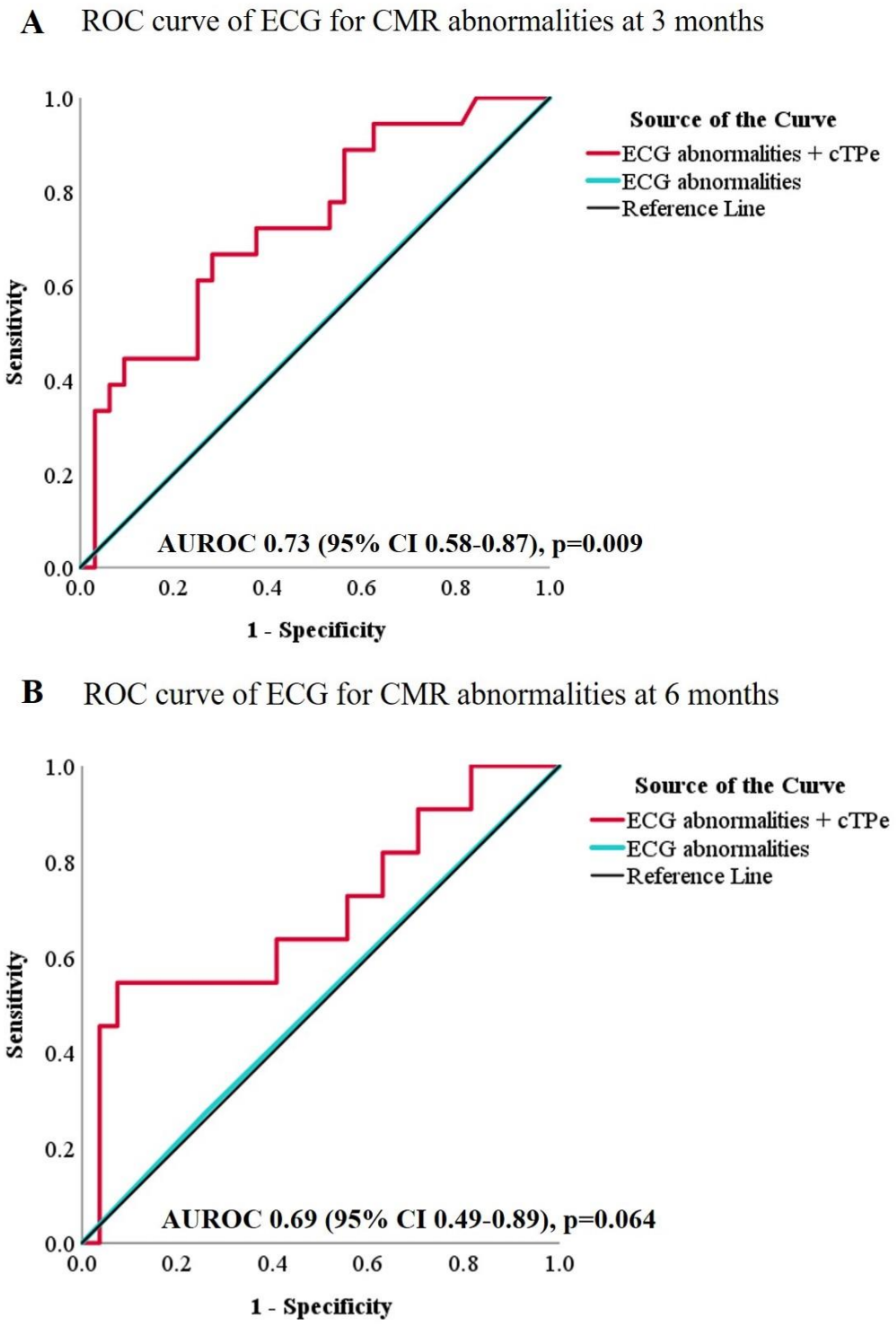


**Figure 5.5** ROC curve for composite group A ECG (blue line) overlaps with the reference line (black line), indicating poor discriminative potential. The ROC curve improved when the cTPe interval was added to the group A ECG features (red line). The discriminative ability is more robust at A) three months than B) six months post hospitalisation. P values are based on concordance statistics and receiver operating characteristics curve analysis.

**Table 6** demonstrates the diagnostic performance of ECG for composite CMR abnormalities at three-and-six months, based on the cut-off values established in **Chapter 3**. Abnormal group A ECG features displayed modest SN (72%) with poor overall rule-out abilities (-LR). Inclusion of group B repolarisation intervals, improved the SN but the overall diagnostic performance remains mediocre, evidenced by the poor NPV and -LR values at three months. By six months, the diagnostic performance of group A ECG abnormalities was comparable to that of three months. However, adding QTc ≥ 450 ms into the diagnostic ECG features significantly improved the rule-out ability as the -LR reduced from 1.05 to 0.01 indicating a significant decrease in the odds of having CMR abnormalities in patients with negative ECG test (**Table 6**).

**Table 7** summarises the sub-analysis of the diagnostic performance of ECG to detect COVID-19 patients with high T1/LGE (CMR marker for myocardial inflammation or fibrosis). At three months, group A ECG abnormalities displayed reasonable diagnostic ability to rule out high T1/LGE with SN of 88% and -LR of 0.35. The SN was augmented with the inclusion of the group B repolarisation interval, particularly the cTPe interval which indicated a 16-fold decrease in the odds of having a high T1/LGE in patients with a negative result (-LR decreased from 0.35 to 0.19, **Table 7**). By six months, the diagnostic utility of group A ECG with or without the group B repolarisation intervals was reduced, with the exception of adding QTc. The combination of group A abnormal ECG and QTc ≥ 450 ms maintained a reasonable diagnostic ability for high T1/LGE at both three-and-six months, evidenced by the excellent SN, NPV and -LR values (**Table 7)**.

**Table 6** Diagnostic performance of ECG for CMR abnormalities at 3- and 6-months post hospitalisation.

| **3 months (n=50)** | | | | | | |
|---|---|---|---|---|---|---|
| **ECG parameters** | **SN (%)** | **SP (%)** | **PPV (%)** | **NPV (%)** | **+LR** | **-LR** |
| ECG abnormalities (Composite group A) | 72.2 | 28.1 | 36.1 | 64.3 | 1.00 | 0.99 |
| ECG abnorm + QTc ≥ 450 | 83.3 | 15.6 | 35.7 | 62.5 | 0.99 | 1.07 |
| ECG abnorm + QTc disp ≥ 55 | 83.3 | 3.1 | 32.6 | 25.0 | 0.86 | 5.39 |
| ECG abnorm + JTc ≥ 340 | 83.3 | 6.3 | 33.3 | 40.0 | 0.89 | 2.65 |
| ECG abnorm + JTPc ≥ 240 | 83.3 | 9.4 | 34.1 | 50.0 | 0.92 | 1.78 |
| ECG abnorm + cTPe ≥ 100 | 88.9 | 9.4 | 35.6 | 60.0 | 0.98 | 1.18 |
| **6 months (n=38)** | | | | | | |
| **ECG parameters** | **SN (%)** | **SP (%)** | **PPV (%)** | **NPV (%)** | **+LR** | **-LR** |
| ECG abnormalities | 72.7 | 40.7 | 28.6 | 70.0 | 0.98 | 1.05 |
| ECG abnorm + QTc ≥ 450 | 99.9 | 11.1 | 31.4 | 99.9 | 1.12 | 0.01 |
| ECG abnorm + QTc disp ≥ 55 | 90.9 | 3.7 | 26.3 | 50.0 | 0.94 | 2.46 |
| ECG abnorm + JTc ≥ 340 | NA | NA | NA | NA | NA | NA |
| ECG abnorm + JTPc ≥ 240 | NA | NA | NA | NA | NA | NA |
| ECG abnorm + cTPe ≥ 100 | 81.8 | 7.4 | 26.5 | 50.0 | 0.88 | 2.46 |

ECG abnorm = group A ECG features presence of arrhythmia/premature ventricular or atrial complex/abnormal axis deviation/heart block/bundle branch block/fragmented QRS complex/poor R wave progression/ST-T changes. JTc, corrected JT interval; JTPc, corrected JT peak interval; QTc disp, QTc dispersion; QTc, corrected QT interval; cTPe, corrected T peak T end interval.

**Table 7** Diagnostic performance of ECG for high T1/LGE at three- and six-months post hospitalisation.

| **3 months (n=50)** | | | | | | |
|---|---|---|---|---|---|---|
| **ECG parameters** | **SN (%)** | **SP (%)** | **PPV (%)** | **NPV (%)** | **+LR** | **-LR** |
| ECG abnormalities (Composite group A) | 87.5 | 35.3 | 38.9 | 85.7 | 1.35 | 0.35 |
| ECG abnorm + QTc ≥ 450 | 93.8 | 20.6 | 35.7 | 87.5 | 1.18 | 0.30 |
| ECG abnorm + QTc disp ≥ 55 | 93.8 | 8.8 | 32.6 | 75.0 | 1.03 | 0.70 |
| ECG abnorm + JTc ≥ 340 | 93.8 | 11.8 | 33.3 | 80.0 | 1.06 | 0.53 |
| ECG abnorm + JTPc ≥ 240 | 93.8 | 14.7 | 34.1 | 83.3 | 1.10 | 0.42 |
| ECG abnorm + cTPe ≥ 100 | 93.8 | 33.3 | 33.3 | 80.0 | 1.41 | 0.19 |
| **6 months (n=38)** | | | | | | |
| **ECG parameters** | **SN (%)** | **SP (%)** | **PPV (%)** | **NPV (%)** | **+LR** | **-LR** |
| ECG abnormalities | 70 | 25.9 | 25.9 | 70 | 0.94 | 1.16 |
| ECG abnorm + QTc ≥ 450 | 99.9 | 11.1 | 29.4 | 99.9 | 1.12 | 0.01 |
| ECG abnorm + QTc disp ≥ 55 | 90 | 3.7 | 25.7 | 50.0 | 0.93 | 2.70 |
| ECG abnorm + JTc ≥ 340 | NA | NA | NA | NA | NA | NA |
| ECG abnorm + JTPc ≥ 240 | NA | NA | NA | NA | NA | NA |
| ECG abnorm + cTPe ≥ 100 | 80 | 7.4 | 24.2 | 50.0 | 0.86 | 2.70 |

ECG abnorm = group A ECG features presence of arrhythmia/premature ventricular or atrial complex/abnormal axis deviation/heart block/bundle branch block/fragmented QRS complex/poor R wave progression/ST-T changes. JTc, corrected JT interval; JTPc, corrected JT peak interval; QTc disp, QTc dispersion; QTc, corrected QT interval; cTPe, corrected T peak T end interval.

## 5.6 DISCUSSION

In this single centre follow-up study of moderate-to-severe of COVID-19 patients, the key findings are as follows: First, serial measures revealed that burden of ECG abnormalities and repolarisation intervals were greater in patients compared to controls over time. Secondly, there was significant associations observed between repolarisation intervals on the 12-lead ECG with CMR parameters of myocardial health especially among patients with severe infection. Thirdly, the diagnostic performance of ECG as a screening tool for myocardial injury on CMR decreased over time, but may potentially be optimised with the analysis of both group A and group B ECG repolarisation parameters.

### ECG ABNORMALITIES IN COVID-19 PATIENTS AT THREE- AND SIX-MONTHS POST HOSPITALISATION

COVID-19 patients showed a high burden of ECG abnormalities at three-and-six months post-hospitalisation as more than two third of patients had ECG abnormalities. I have demonstrated that, longitudinally the repolarisation parameters were greater among patients than controls at three and six months post-COVID-19 infection. Some had very prolonged repolarisation (QTc > 480 ms) which may suggest elevated risks of arrhythmia among patients in the post-hospitalisation phase.

In acute setting, the incidence of arrhythmia was reported around 17% based on a large meta-analysis involving more than 17000 COVID-19 patients[193]. Although the true incidence of arrhythmia in post-hospitalised COVID-19 is unclear, its occurrence has been reported at around 12% at three months, 8% at six months and remained high at 16% at 12 months among moderate-to-severe COVID-19 patients[78]. Likewise, the largest longitudinal follow-up study to date, which involved more than 150 000 COVID-19 patients and more than 10

million controls, found that the excess burden of ventricular arrhythmia was 84% higher in patients than in control, a year after infection[57]. Based on the current study, the true incidence of arrhythmia is unknown as there was lack of any long-term arrhythmic monitoring. Nonetheless, serial 12-lead ECGs at three-and-six months post-hospitalisation showed cumulative incidence of BBB and PVCs to be 5% and 13% respectively, with 60% of those with PVCs demonstrating prolonged QT intervals. These findings support the previous reports on high burden of ECG abnormalities among the post-hospitalised COVID-19 patients[47,78] and emphasise the need for continued monitoring in selected high-risk patients, as prolonged repolarisation is a known risk factor for arrhythmia and a novel predictor of one-year mortality in patients with COVID-19[75].

### CMR ABNORMALITIES BETWEEN POST-HOSPITALISED COVID-19 PATIENTS AT THREE- AND SIX- MONTHS AND CONTROLS

Early studies have raised concerns of high burden of myocardial injury among post-hospitalised COVID-19 patients[47,146]. Consistent with previous studies, the burden of CMR abnormalities was 36% among post-hospitalised patients at three months, but reduced to 29% at six months, which was not different to that seen in controls. At three months, patients exhibited higher global native T1 values relative to controls. Increased native T1 measures has been strongly related to poor outcome in patients with nonischemic cardiomyopathies[209], and represent diffuse myocardial fibrosis and/or oedema, whereas native T2 values specifically represents oedema[210]. At six months, among patients, myocardial native T1 decreased and was no longer significantly different from the control group. This finding could be explainable by the inflammatory process which partly contributes to the pathophysiology of myocardial injury in COVID-19, that subsequently recovers over time [20,47].

In the present study, RV systolic function albeit normal, was lower at three months, and subsequently improved by six months. Although, right ventricular dysfunction in COVID-19 has been associated with myocardial injury[211], and mortality among severe patients[212], long term outcome studies are lacking and most patients as we demonstrated, improved over time[213], further implicating the transient nature of myocardial injury in COVID-19[213].

## DIAGNOSTIC PERFORMANCE OF ECG FOR CMR ABNORMALITIES OVER TIME

The present study demonstrates that relying solely on the group A ECG parameters is insufficient and clinically futile as the AUROC was only 0.5; a decision akin to tossing a coin. By contrast, simply adding the group B repolarisation parameters significantly enhanced the diagnostic power of ECG. However, the diagnostic potential decreased at six months given the resolution of inflammation on CMR and blood tests CRP. Thus, it can be hypothesized that the diagnostic performance of ECG for CMR abnormalities among the post-hospitalised COVID-19 patients is time-sensitive and corresponds potentially to the burden of cardiac injuries particularly the myocardial inflammation, which improves over time and does not appear to be common in the long-term phase of infection[150,214]. Alternatively, the diagnostic performance metrics should be interpreted cautiously due to the small sample size and drop-out of study population as they may be prone to inaccuracies. Therefore, further studies are needed to test this hypothesis.

Importantly, the present study also showed that the electrical abnormalities such as the prolonged repolarisation persist despite the recovery of tissue and structural changes post infection. It can be speculated that, there are permanent ion channelopathies which develop with myocardial inflammation, that remain irreversible with structural improvement.

## 5.7 CLINICAL APPLICATION

This study contributes to the growing body of evidence indicating that patients previously hospitalised due to COVID-19 may carry an elevated risk of arrhythmia evidenced by the prolonged repolarisation intervals during the post-acute phase of infection. The diagnostic ability of ECG parameters for ruling out structural abnormalities on CMR (as described in **Chapter 3**) has now been validated in a distinct cohort, although, it must be noted that the greatest benefit of ECG screening tends to be in the early post-acute phase (3-5 months from infection) in view of the natural resolution of CMR abnormalities among these patients with time. The presence of prolonged abnormalities in repolarisation despite an improvement in markers of inflammation are also of potential interest and suggests two possible scenarios. The first is that such abnormalities may have been present even prior to infection. The second is that these abnormalities may have developed after the infection, due to persistent inflammatory signaling which has induced more long-term ionic remodeling. While further studies may be required to definitively parse the precise underlying mechanisms, our findings are intriguing and suggest a potential explanation for persistent arrhythmic risk following COVID-19.

## 5.8 LIMITATIONS

Although data homogeneity and acquisition consistencies from a single centre may serve as a strength, the sample size of participants in this chapter are relatively small, limiting the generalisability. Furthermore, the missing participants at the follow-up visit reduced the statistical strength. Therefore, the findings must be interpreted cautiously and be regarded as exploratory in nature. Although the prospective nature of the study permits the ECG-CMR associations to be explored over time, there were no pre-COVID-19 ECG and CMR studies as a baseline comparison; hence, it is unknown if the ECG and CMR findings may have been pre-existing. Additionally, laboratory investigation at baseline, three months and six months should include blood markers such as IL-6, IL-1, and TNF-alpha so the association between repolarisation intervals, myocardial fibrosis and systemic inflammation can be further comprehensively explored. Ideally, Holter monitoring also should be conducted among this cohort upon discharge to explore the true incidence of arrhythmia in the post-hospitalisation phase which is unknown in this study.

## 5.9 CONCLUSION

The burden of ECG abnormalities is high in the medium-to-long-term phase of post-COVID-19 infection. The repolarisation intervals were significantly longer among patients relative to matched controls, with observable relationship between markers of myocardial injury on CMR and ventricular repolarisation particularly in severe infection. Prolongation of repolarisation may be explained partly by myocardial fibrosis or inflammation, particularly in the early post-acute phase (three-to-five months) of COVID-19 infection. ECG's diagnostic performance to detect CMR abnormalities reduced over time but the overall applicability requires larger studies for validation.

# CHAPTER 6: CONCLUSION AND FUTURE DIRECTIONS

## 6.1 CONCLUSION

The overarching aim of this work was to assess the burden of ECG abnormalities, explore the association of ECG and CMR parameters and determine the diagnostic and predictive role of ECG in detecting myocardial abnormalities on CMR among moderate-to-severe post-hospitalised COVID-19 patients. This thesis is the first effort to comprehensively explore the association of 12-lead ECG and myocardial abnormalities based on CMR in this cohort. Overall, at least 350 post-hospitalised ECGs, including 4200 leads and a minimum of 25 000 ECG intervals, have been analysed in detail, including the QT, QT disp, QT peak, JT, JT peak and T peak to T end intervals along with hundreds of CMR image analyses for volume, function and myocardial tissue characteristics.

As a whole, the studies are statistically underpowered to sufficiently address the research hypotheses increasing the risks of type I error (false positive), hence should be considered exploratory in nature with hypothesis generating findings. I have demonstrated several key findings. First, the ECG burden is high months after infection, and the risk of arrhythmia may be elevated, due to prolonged repolarisation intervals, notably among patients with CMR abnormalities. Secondly, ECG is potentially a reliable diagnostic tool with significant sex-based differences in the diagnostic performance to screen for patients with CMR abnormalities. Notably, the ECG criteria based only on the group A parameters which are the commonly reported features, may miss up to a third of patients with CMR abnormalities, especially among women. Evaluating the repolarisation parameters, particularly the QTc disp and JT intervals, substantially improved the diagnostic performance in both sexes. When both the group A ECG and the group B repolarisation abnormalities are absent, CMR abnormalities can be ruled out with a high degree of certainty. Thus, the findings provide proof of the concept of ECG as a reliable and pragmatic screening tool for CMR abnormalities. The method offers a potentially beneficial strategy, especially in a limited-

resource setting, and may serve as an impetus for future prospective studies to determine the diagnostic and predictive ability of 12-lead ECG for CMR abnormalities including for other clinical conditions.

Finally, exploring the ECG-CMR association over three-and-six months in a single-centre follow-up study of a separate cohort of moderate-to-severe COVID-19 infection allows us to understand the natural history of COVID-19 particularly from the stand point of ECG-CMR association, and partly to validate the findings in the earlier chapters. I have shown that the burden of ECG abnormalities and the risk of arrhythmia remained elevated at three- and six-months post-hospitalisation, with significant associations observed between ECG parameters and CMR markers of myocardial tissue health. Notably, although the discriminative potential of ECG for CMR abnormalities was optimised when both the group A and group B repolarisation intervals were analysed, the diagnostic capability decreased at six months post-infection and likely due to resolution of myocardial inflammation on CMR. Together, these findings highlight the complex relationship between electrical and structural remodeling induced by moderate-to-severe COVID-19 infections which may vary with time.

Some limitations of this work include the relatively small sample size to represent the post-hospitalised COVID-19 population. The lacks of pre-COVID CMR or ECG also limits our ability to establish a clear causal relationship between SARS-CoV-2 infection and cardiac abnormalities. Additionally, although some patients had prolonged markers of repolarisation, the true incidence of arrhythmia is unknown in this study due to lack of objective measure based on Holter post-discharge. Our findings, however, provide novel insights into the risk of arrhythmia among post-hospitalised COVID-19 patients and the clinically important association between ECG parameters and CMR markers of myocardial health, particularly in the early post-acute phase.

In summary, the burden of ECG abnormalities and the risk of arrhythmia may be elevated among post-hospitalised patients, with significant associations observed between ECG and CMR parameters. ECG may be reliable to rule out myocardial abnormalities on CMR with specific sex-based consideration. Analysing large-scale data sets using an AI-driven approach may provide further insight and perhaps is the best way forward to validate these findings.

## 6.2 FUTURE DIRECTIONS

As part of the efforts to validate these associations in a disease cohort other than the inflammatory conditions such as COVID-19, I have also conducted a pilot analysis of ECG-CMR association among the variant carriers pre-hypertrophic and overt HCM patients, a known cardiac genetic disorder associated with abnormal heart muscle thickening and elevated risks of lethal arrhythmia due to myocardial fibrosis[215]. The benefits of establishing the ECG-CMR associations, particularly in the diagnostic and predictive performance index, are multifold. First, it may hypothetically improve the prediction of patients with elevated risks of sudden cardiac death based on the association of repolarisation parameters with CMR markers of myocardial fibrosis such as T1, ECV and LGE. Secondly, ECG-CMR associations, especially if repolarisation intervals can be mapped out to correspond with the area of maximal wall thickness or highest burden of scarring, may facilitate clinicians in monitoring the risk of ventricular arrhythmia or SCD over time. The research question to be addressed stemmed from the observation that a significant association between repolarisation intervals and CMR markers of myocardial tissue abnormalities were found among the COVID-19 populations despite having a much lower burden of myocardial fibrosis. I hypothesised that ECG, notably the repolarisation intervals, would strongly associate with CMR parameters of myocardial health and function, and ECG may have a robust diagnostic performance to detect CMR abnormalities in this HCM cohort. Further exploration was also conducted using a more sophisticated CMR method called diffusion tensor imaging, which objectively measured the degree of cellular disarray in the myocardium[216].

The early findings indicated an exciting and promising outlook on the role of ECG as a diagnostic tool for myocardial abnormalities in HCM disease. Repolarisation abnormalities

and significant associations with CMR abnormalities are not merely observed among the overt HCM population but also among the variant gene carriers who have yet to develop muscular thickening and are associated with myocardial disarray, an important arrhythmic substrate[216]. Importantly, the preliminary findings demonstrated an effective discriminative power of repolarisation interval such as the JTc interval to detect the prehypertrophic sarcomeric variant carriers from controls AUROC (0.88, CI 0.76-1.00, $p<0.001$). Although the HCM research is still well underway, the potential clinical implications may include better surveillance of the prehypertrophic HCM patients and improved risk stratification of overt HCM patients. Above all, the early findings are still hypothesis-generating but concurred with the outcome of the present study which indicated potential associations between ECG parameters and CMR abnormalities among the HCM cohort. Ideally, a larger scale of ECG and CMR correlations based on the HCM registry or using the UK biobank, assisted with AI input needs to be conducted, to validate the association of ECG-CMR parameters in a more diverse population. A novel cardiac electrical biomarker (CEB) generated with AI algorithms from 12-lead ECG have recently shown promising outlook in ruling in and ruling out patients with myocardial injuries, including acute chest pain in the emergency settings[217], as well as among those with coronary artery occlusion not severe enough to cause myonecrosis[218]. An early study have shown that CEB also improved the diagnostic accuracy for prediction of left ventricular scar in unselected patients undergoing CMR[219].

Taken together, the growing evidence although limited, are excitingly promising that highlights the potential role ECG in detecting CMR abnormalities. Additionally, although my research is inherently limited by the small sample size, the findings were hypothesis generating which suggests that 12-lead ECG potentially offers a pragmatic solution to reliably screen and exclude those with low risk of detectable myocardial abnormalities based

on a sophisticated, precise and highly reliable tool such as CMR. Moreover, the prospect of utilising AI-assisted algorithm such as CEB on top of the conventional ECG criteria as a diagnostic tool for myocardial injuries should be further explored in larger cohorts and synergized with advanced CMR techniques such as the myocardial tissue mapping, LGE, diffusion tensor imaging as well as magnetic resonance spectroscopy, to unlock and optimise the diagnostic utility of ECG in the clinical settings.

# REFERENCES


1. Morris F, Brady WJ, Camm AJ. *Abc of clinical electrocardiography*. John Wiley & Sons; 2009.
2. Antzelevitch C, Yan GX, Ackerman MJ, et al. J-wave syndromes expert consensus conference report: Emerging concepts and gaps in knowledge. *J Arrhythm*. 2016;32:315-339
3. Take Y, Morita H. Fragmented qrs: What is the meaning? *Indian Pacing Electrophysiol J*. 2012;12:213-225
4. riskElliott PM, Anastasakis A, Borger MA, et al. 2014 esc guidelines on diagnosis and management of hypertrophic cardiomyopathy: The task force for the diagnosis and management of hypertrophic cardiomyopathy of the european society of cardiology (esc). *Eur Heart J*. 2014;35:2733-2779
5. Burch GE. Development in clinical electrocardiography since einthoven. *American Heart Journal*. 1961;61:324-346
6. Zhang T, Miao W, Wang S, Wei M, Su G, Li Z. Acute myocarditis mimicking st-elevation myocardial infarction: A case report and review of the literature. *Experimental and therapeutic medicine*. 2015;10:459-464
7. Sheldon SH, Crandall MA, Jaffe AS. Myocarditis with st elevation and elevated cardiac enzymes misdiagnosed as an st-elevation myocardial infarction. *The Journal of Emergency Medicine*. 2012;43:996-999
8. Larson DM, Menssen KM, Sharkey SW, et al. "False-positive" cardiac catheterization laboratory activation among patients with suspected st-segment elevation myocardial infarction. *Jama*. 2007;298:2754-2760
9. Orchard JJ, Neubeck L, Orchard JW, et al. Ecg-based cardiac screening programs: Legal, ethical, and logistical considerations. *Heart Rhythm*. 2019;16:1584-1591
10. Jacobus WE, Taylor IV GJ, Hollis DP, Nunnally RL. Phosphorus nuclear magnetic resonance of perfused working rat hearts. *Nature*. 1977;265:756-758
11. Pohost GM. The history of cardiovascular magnetic resonance. *JACC: Cardiovascular Imaging*. 2008;1:672-678
12. Valkovič L, Clarke WT, Schmid AI, et al. Measuring inorganic phosphate and intracellular ph in the healthy and hypertrophic cardiomyopathy hearts by in vivo 7t 31 p-cardiovascular magnetic resonance spectroscopy. *Journal of Cardiovascular Magnetic Resonance*. 2019;21:1-11
13. Kwong RY, Ge Y, Steel K, et al. Cardiac magnetic resonance stress perfusion imaging for evaluation of patients with chest pain. *J Am Coll Cardiol*. 2019;74:1741-1755
14. Manka R, Paetsch I, Schnackenburg B, Gebker R, Fleck E, Jahnke C. Bold cardiovascular magnetic resonance at 3.0 tesla in myocardial ischemia. *Journal of Cardiovascular Magnetic Resonance*. 2010;12:54
15. Mahmod M, Raman B, Chan K, et al. Right ventricular function declines prior to left ventricular ejection fraction in hypertrophic cardiomyopathy. *J Cardiovasc Magn Reson*. 2022;24:36
16. Qin L, Zhu S, Liu P, et al. Additional prognostic values of strain and strain rate over late gadolinium enhancement in hypertrophic cardiomyopathy patients. *Int J Cardiol*. 2023;370:427-434
17. Tschöpe C, Ammirati E, Bozkurt B, et al. Myocarditis and inflammatory cardiomyopathy: Current evidence and future directions. *Nature Reviews Cardiology*. 2021;18:169-193
18. Disertori M, Rigoni M, Pace N, et al. Myocardial fibrosis assessment by lge is a powerful predictor of ventricular tachyarrhythmias in ischemic and nonischemic lv dysfunction a meta-analysis. *JACC Cardiovasc Imaging*. 2016;9:1046-1055

19. Ferreira VM, Piechnik SK, Dall'Armellina E, et al. Non-contrast t1-mapping detects acute myocardial edema with high diagnostic accuracy: A comparison to t2-weighted cardiovascular magnetic resonance. *J Cardiovasc Magn Reson*. 2012;14:1-12
20. Petersen SE, Friedrich MG, Leiner T, et al. Cardiovascular magnetic resonance for patients with covid-19. *JACC Cardiovasc Imaging*. 2022;15:685-699
21. Thongsongsang R, Songsangjinda T, Tanapibunpon P, Krittayaphong R. Native t1 mapping and extracellular volume fraction for differentiation of myocardial diseases from normal cmr controls in routine clinical practice. *BMC Cardiovascular Disorders*. 2021;21:270
22. Popescu IA, Werys K, Zhang Q, et al. Standardization of t1-mapping in cardiovascular magnetic resonance using clustered structuring for benchmarking normal ranges. *Int J Cardiol*. 2021;326:220-225
23. Ogbole GI, Adeyomoye AO, Badu-Peprah A, Mensah Y, Nzeh DA. Survey of magnetic resonance imaging availability in west africa. *Pan Afr Med J*. 2018;30:240-240
24. Giustino G, Croft LB, Stefanini GG, et al. Characterization of myocardial injury in patients with covid-19. *J Am Coll Cardiol*. 2020;76:2043-2055
25. Jagia P, Ojha V, Naik N, Sharma S. Myocardial fibrosis detected by cardiovascular magnetic resonance in absence of myocardial oedema in a patient recovered from covid-19. *BMJ case reports*. 2020;13
26. Vidula MK, Rajewska-Tabor J, Cao JJ, et al. Myocardial injury on cmr in patients with covid-19 and suspected cardiac involvement. *JACC Cardiovasc Imaging*. 2023;16:609-624
27. Huang C, Wang Y, Li X, et al. Clinical features of patients infected with 2019 novel coronavirus in wuhan, china. *Lancet*. 2020;395:497-506
28. Hessami A, Shamshirian A, Heydari K, et al. Cardiovascular diseases burden in covid-19: Systematic review and meta-analysis. *The American journal of emergency medicine*. 2020:S0735-6757(0720)30908-30906
29. Wiersinga WJ, Rhodes A, Cheng AC, Peacock SJ, Prescott HC. Pathophysiology, transmission, diagnosis, and treatment of coronavirus disease 2019 (covid-19): A review. *Jama*. 2020;324:782-793
30. Worldometers. Number of coronavirus (covid-19) cases worldwide as of may 2, 2023, by country or territory. *Number of coronavirus (COVID-19) cases worldwide*. 2023;2023
31. Hamming I, Timens W, Bulthuis M, Lely A, Navis Gv, van Goor H. Tissue distribution of ace2 protein, the functional receptor for sars coronavirus. A first step in understanding sars pathogenesis. *The Journal of Pathology: A Journal of the Pathological Society of Great Britain and Ireland*. 2004;203:631-637
32. Raman B, Bluemke DA, Lüscher TF, Neubauer S. Long covid: Post-acute sequelae of covid-19 with a cardiovascular focus. *Eur Heart J*. 2022;43:1157-1172
33. Wu T, Zuo Z, Kang S, et al. Multi-organ dysfunction in patients with covid-19: A systematic review and meta-analysis. 2020;11:874
34. Loganathan S, Kuppusamy M, Wankhar W, et al. Angiotensin-converting enzyme 2 (ace2): Covid 19 gate way to multiple organ failure syndromes. *Respiratory physiology & neurobiology*. 2021;283:103548-103548
35. Lucke B, Wight T, Kime E. Pathologic anatomy and bacteriology of influenza: Epidemic of autumn, 1918. *Archives of Internal Medicine*. 1919;24:154-237
36. Yu C, Wong RS, Wu E, et al. Cardiovascular complications of severe acute respiratory syndrome. *Postgraduate medical journal*. 2006;82:140-144
37. Bennett JE, Dolin R, Blaser MJ. *Mandell, douglas, and bennett's principles and practice of infectious diseases e-book: 2-volume set*. Elsevier health sciences; 2019.
38. Shi S, Qin M, Shen B, et al. Association of cardiac injury with mortality in hospitalized patients with covid-19 in wuhan, china. *JAMA Cardiol*. 2020;5:802-810
39. Ho JS, Sia C-H, Chan MY, Lin W, Wong RC. Coronavirus-induced myocarditis: A meta-summary of cases. *Heart Lung*. 2020;49:681-685
40. Shi S, Qin M, Cai Y, et al. Characteristics and clinical significance of myocardial injury in patients with severe coronavirus disease 2019. *Eur Heart J*. 2020;41:2070-2079

41. Bertini M, Ferrari R, Guardigli G, Malagu M, Vitali F, Zucchetti O. Electrocardiographic 636 features of 431 consecutive, critically ill covid-19 patients: An insight into the mechanisms of cardiac 637 involvement. *EP Europace*. 2020;22:1848-1854
42. Pelà G, Goldoni M, Cavalli C, et al. Long-term cardiac sequelae in patients referred into a diagnostic post-covid-19 pathway: The different impacts on the right and left ventricles. *Diagnostics (Basel)*. 2021;11
43. Tavazzi G, Pellegrini C, Maurelli M, et al. Myocardial localization of coronavirus in covid-19 cardiogenic shock. *European journal of heart failure*. 2020;22:911-915
44. Sivalokanathan S, Foley M, Cole G, Youngstein T. Gastroenteritis and cardiogenic shock in a healthcare worker: A case report of covid-19 myocarditis confirmed with serology. *European Heart Journal - Case Reports*. 2021;5(2) (no pagination)
45. Thomas MR, Scully M. Clinical features of thrombosis and bleeding in covid-19. *Blood, The Journal of the American Society of Hematology*. 2022;140:184-195
46. Dherange P, Lang J, Qian P, et al. Arrhythmias and covid-19. *JACC Clin Electrophysiol*. 2020;6:1193-1204
47. Puntmann VO, Carerj ML, Wieters I, et al. Outcomes of cardiovascular magnetic resonance imaging in patients recently recovered from coronavirus disease 2019 (covid-19). *JAMA Cardiol*. 2020;5:1265-1273
48. Guzik TJ, Mohiddin SA, Dimarco A, et al. Covid-19 and the cardiovascular system: Implications for risk assessment, diagnosis, and treatment options. *Cardiovascular research*. 2020;116:1666-1687
49. Driggin E, Madhavan Mahesh V, Bikdeli B, et al. Cardiovascular considerations for patients, health care workers, and health systems during the covid-19 pandemic. *J Am Coll Cardiol*. 2020;75:2352-2371
50. Giustino G, Pinney SP, Lala A, et al. Coronavirus and cardiovascular disease, myocardial injury, and arrhythmia: Jacc focus seminar. *J Am Coll Cardiol*. 2020;76:2011-2023
51. Chen C, Zhang X, Ju Z, He W. Advances in the research of cytokine storm mechanism induced by corona virus disease 2019 and the corresponding immunotherapies. *Chinese journal of burns*. 2020:E005-E005
52. Hanson PJ, Liu-Fei F, Ng C, et al. Characterization of covid-19-associated cardiac injury: Evidence for a multifactorial disease in an autopsy cohort. *Laboratory Investigation*. 2022;102:814-825
53. Cinti S, Graciotti L, Giordano A, Valerio A, Nisoli E. Covid-19 and fat embolism: A hypothesis to explain the severe clinical outcome in people with obesity. *International Journal of Obesity*. 2020;44:1800-1802
54. Gupte M, Boustany-Kari CM, Bharadwaj K, et al. Ace2 is expressed in mouse adipocytes and regulated by a high-fat diet. *American Journal of Physiology-Regulatory, Integrative and Comparative Physiology*. 2008;295:R781-R788
55. Sun Z, Hou Y, Zhang Z, Cai B, Li J. Electrocardiogram abnormalities and higher body mass index as clinically applicable factors for predicting poor outcome in patients with coronavirus disease 2019. *Frigid Zone Medicine*. 2022;2:251-256
56. Zou F, Qian Z, Wang Y, Zhao Y, Bai J. Cardiac injury and covid-19: A systematic review and meta-analysis. *CJC Open*. 2020;2:386-394
57. Xie Y, Xu E, Bowe B, Al-Aly Z. Long-term cardiovascular outcomes of covid-19. *Nat Med*. 2022;28:583-590
58. Kaye AD, Okeagu CN, Pham AD, et al. Economic impact of covid-19 pandemic on healthcare facilities and systems: International perspectives. *Best Practice & Research Clinical Anaesthesiology*. 2021;35:293-306
59. Lazzerini PE, Boutjdir M, Capecchi PL. Covid-19, arrhythmic risk, and inflammation: Mind the gap! *Circulation*. 2020;142:7-9
60. Saffitz JE, Hoyt RH, Luke RA, Lee Kanter H, Beyer EC. Cardiac myocyte interconnections at gap junctions: Role in normal and abnormal electrical conduction. *Trends in Cardiovascular Medicine*. 1992;2:56-60
61. Wei X, Yohannan S, Richards JR. Physiology, cardiac repolarization dispersion and reserve. 2019

62. Antzelevitch C, Fish J. Electrical heterogeneity within the ventricular wall. *Basic Research in Cardiology*. 2001;96:517-527
63. Drouin E, Charpentier F, Gauthier C, Laurent K, Le Marec H. Electrophysiologic characteristics of cells spanning the left ventricular wall of human heart: Evidence for presence of m cells. *J Am Coll Cardiol*. 1995;26:185-192
64. Antzelevitch C. M cells in the human heart. *Circ Res*. 2010;106:815-817
65. Sicouri S, Antzelevitch C. Drug-induced early and delayed afterdepolarizations and triggered activity in deep subepicardial cells (m cells) of the canine ventricle. *Circulation*. 1990;82:645-645
66. Sicouri S, Antzelevitch C. A subpopulation of cells with unique electrophysiological properties in the deep subepicardium of the canine ventricle. The m cell. *Circulation research*. 1991;68:1729-1741
67. Liu DW, Antzelevitch C. Characteristics of the delayed rectifier current (ikr and iks) in canine ventricular epicardial, midmyocardial, and endocardial myocytes. A weaker iks contributes to the longer action potential of the m cell. *Circ Res*. 1995;76:351-365
68. Zygmunt AC, Eddlestone GT, Thomas GP, Nesterenko VV, Antzelevitch C. Larger late sodium conductance in m cells contributes to electrical heterogeneity in canine ventricle. *American Journal of Physiology-Heart and Circulatory Physiology*. 2001;281:H689-H697
69. Alsagaff MY, Oktaviono YH, Dharmadjati BB, et al. Electrocardiography on admission is associated with poor outcomes in coronavirus disease 2019 (covid-19) patients: A systematic review and meta-analysis. *J Arrhythm*. 2021;37:877-885
70. Mehraeen E, Seyed Alinaghi SA, Nowroozi A, et al. A systematic review of ecg findings in patients with covid-19. *Indian Heart J*. 2020;72:500-507
71. Deng Q, Hu B, Zhang Y, et al. Suspected myocardial injury in patients with covid-19: Evidence from front-line clinical observation in wuhan, china. *Int J Cardiol*. 2020
72. Mahmoudi E, Mollazadeh R, Mansouri P, et al. Ventricular repolarization heterogeneity in patients with covid-19: Original data, systematic review, and meta-analysis. *Clinical cardiology*. 2022;45:110-118
73. Romero J, Gabr M, Diaz JC, et al. Electrocardiographic features of patients with covid-19: An updated review. *Cardiac Electrophysiology Clinics*. 2022;14:63-70
74. Fishbein J, Coleman KM, Bhullar A, et al. Delayed cardiac repolarisation as a predictor of in-hospital mortality in patients with covid-19. *Heart*. 2022
75. Banai A, Szekely Y, Lupu L, et al. Qt interval prolongation is a novel predictor of 1-year mortality in patients with covid-19 infection. *Frontiers in cardiovascular medicine*. 2022;9:869089
76. Priori SG, Wilde AA, Horie M, et al. Hrs/ehra/aphrs expert consensus statement on the diagnosis and management of patients with inherited primary arrhythmia syndromes: Document endorsed by hrs, ehra, and aphrs in may 2013 and by accf, aha, paces, and aepc in june 2013. *Heart rhythm*. 2013;10:1932-1963
77. Saririan M, Armstrong R, George JC, et al. St-segment elevation in patients presenting with covid-19: Case series. *European Heart Journal - Case Reports*. 2021;5
78. Liu T, Wu D, Yan W, et al. Twelve-month systemic consequences of coronavirus disease 2019 (covid-19) in patients discharged from hospital: A prospective cohort study in wuhan, china. *Clin Infect Dis*. 2021;74:1953-1965
79. Romero J, Alviz I, Parides M, et al. T-wave inversion as a manifestation of covid-19 infection: A case series. *Journal of Interventional Cardiac Electrophysiology*. 2020;59:485-493
80. Regan W, O'Byrne L, Stewart K, et al. Electrocardiographic changes in children with multisystem inflammation associated with covid-19: Associated with coronavirus disease 2019. *The Journal of Pediatrics*. 2021
81. Nemati R, Ganjoo M, Jadidi F, Tanha A, Baghbani R. Electrocardiography in early diagnosis of cardiovascular complications of covid-19; a systematic literature review. *Arch Acad Emerg Med*. 2021;9:e10

82. McCullough SA, Goyal P, Krishnan U, Choi JJ, Safford MM, Okin PM. Electrocardiographic findings in coronavirus disease-19: Insights on mortality and underlying myocardial processes. *Journal of Cardiac Failure*. 2020;26:626-632
83. Schiavone M, Gasperetti A, Gherbesi E, et al. Arrhythmogenic risk and mechanisms of qt-prolonging drugs to treat covid-19. *Cardiac Electrophysiology Clinics*. 2022;14:95-104
84. Yenerçağ M, Arslan U, Doğduş M, et al. Evaluation of electrocardiographic ventricular repolarization variables in patients with newly diagnosed covid-19. *J Electrocardiol*. 2020;62:5-9
85. Loghin C, Chauhan S, Lawless SM. Pseudo-acute myocardial infarction in a young covid-19 patient. *JACC: Case Reports*. 2020;2:1284-1288
86. Yang D, Li J, Gao P, et al. The prognostic significance of electrocardiography findings in patients with coronavirus disease 2019: A retrospective study. *Clinical cardiology*. 2021;44:963-970
87. Pavri BB, Kloo J, Farzad D, Riley JM. Behavior of the pr interval with increasing heart rate in patients with covid-19. *Heart Rhythm*. 2020;17:1434-1438
88. He J, Wu B, Chen Y, et al. Characteristic electrocardiographic manifestations in patients with covid-19. *Canadian Journal of Cardiology*. 2020;36:966.e961-966.e964
89. Vidovich MI. Transient brugada-like ecg pattern in a patient with coronavirus disease 2019 (covid-19). *JACC. Case reports*. 2020
90. Reynbakh O, Braunstein ED, Hsu M, et al. Arrhythmia patterns during and after hospitalization for covid-19 infection detected via patch-based mobile cardiac telemetry. *Am Heart J Plus*. 2022;13:100084
91. Liu Q, Chen H, Zeng Q. Clinical characteristics of covid-19 patients with complication of cardiac arrhythmia. *Journal of Infection*. 2020;81:e6-e8
92. Solaimanzadeh J, Freilich A, Sood MR. Ventricular tachycardia with epicardial and pericardial fibrosis 6 months after resolution of subclinical covid-19: A case report. *Journal of Medical Case Reports*. 2021;15:1-6
93. Lazzerini PE, Laghi-Pasini F, Boutjdir M, Capecchi PL. Cardioimmunology of arrhythmias: The role of autoimmune and inflammatory cardiac channelopathies. *Nat Rev Immunol*. 2019;19:63-64
94. Lazzerini PE, Capecchi PL, El-Sherif N, Laghi-Pasini F, Boutjdir M. Emerging arrhythmic risk of autoimmune and inflammatory cardiac channelopathies. *Journal of the American Heart Association*. 2018;7:e010595
95. Lazzerini PE, Laghi-Pasini F, Bertolozzi I, et al. Systemic inflammation as a novel qt-prolonging risk factor in patients with torsades de pointes. *Heart*. 2017;103:1821-1829
96. Malavazos AE, Goldberger JJ, Iacobellis G. Does epicardial fat contribute to covid-19 myocardial inflammation? *Eur Heart J*. 2020;41:2333-2333
97. Katwa LC, Mendoza C, Clements M. Cvd and covid-19: Emerging roles of cardiac fibroblasts and myofibroblasts. *Cells*. 2022;11:1316
98. Couselo-Seijas M, Almengló C, M Agra-Bermejo R, et al. Higher ace2 expression levels in epicardial cells than subcutaneous stromal cells from patients with cardiovascular disease: Diabetes and obesity as possible enhancer. *European Journal of Clinical Investigation*. 2021;51:e13463
99. Iacobellis G, Corradi D, Sharma A. Epicardial adipose tissue. *anatomic, biomolecular and clinical relationships with the heart*. 2020;2005:2
100. Barker-Davies RM, O'Sullivan O, Senaratne KPP, et al. The stanford hall consensus statement for post-covid-19 rehabilitation. *Br J Sports Med*. 2020;54:949-959
101. Lakkireddy DR, Chung MK, Deering TF, et al. Guidance for rebooting electrophysiology through the covid-19 pandemic from the heart rhythm society and the american heart association electrocardiography and arrhythmias committee of the council on clinical cardiology. *Circ Arrhythm Electrophysiol*. 2020;13:e008999
102. Geethanath S, Vaughan Jr. JT. Accessible magnetic resonance imaging: A review. *J Magn Reson Imaging*. 2019;49:e65-e77
103. Rider OJ, Ntusi N, Bull SC, et al. Improvements in ecg accuracy for diagnosis of left ventricular hypertrophy in obesity. *Heart*. 2016;102:1566-1572

104. de Luna AB, Cino JM, Pujadas S, et al. Concordance of electrocardiographic patterns and healed myocardial infarction. Location detected by cardiovascular magnetic resonance. *American Journal of Cardiology*. 2006;97:443-451
105. Strauss DG, Selvester RH, Lima JA, et al. Ecg quantification of myocardial scar in cardiomyopathy patients with or without conduction defects: Correlation with cardiac magnetic resonance and arrhythmogenesis. *Circ Arrhythm Electrophysiol*. 2008;1:327-336
106. Wieslander B, Xia X, Jablonowski R, et al. The ability of the electrocardiogram in left bundle branch block to detect myocardial scar determined by cardiovascular magnetic resonance. *J Electrocardiol*. 2018;51:779-786
107. Selvanayagam JB, Kardos A, Nicolson D, et al. Anteroseptal or apical myocardial infarction: A controversy addressed using delayed enhancement cardiovascular magnetic resonance imaging. *J Cardiovasc Magn Reson*. 2004;6:653-661
108. Lyon A, Ariga R, Mincholé A, et al. Distinct ecg phenotypes identified in hypertrophic cardiomyopathy using machine learning associate with arrhythmic risk markers. *Frontiers in Physiology*. 2018;9
109. Raman SV, Sparks EA, Baker PM, McCarthy B, Wooley CF. Mid-myocardial fibrosis by cardiac magnetic resonance in patients with lamin a/c cardiomyopathy: Possible substrate for diastolic dysfunction. *Journal of Cardiovascular Magnetic Resonance*. 2007;9:907-913
110. Cheema O, Qamar MU, Xu J, Quinones M, Zoghbi WA, Shah DJ. Patterns of myocardial fibrosis by cmr in patients with conduction abnormalities. *Journal of Cardiovascular Magnetic Resonance*. 2012;14:P213
111. Inoue YY, Ambale-Venkatesh B, Mewton N, et al. Electrocardiographic impact of myocardial diffuse fibrosis and scar: Mesa (multi-ethnic study of atherosclerosis). *Radiology*. 2017;282:690
112. Rodrigues JC, Amadu AM, Ghosh Dastidar A, et al. Ecg strain pattern in hypertension is associated with myocardial cellular expansion and diffuse interstitial fibrosis: A multi-parametric cardiac magnetic resonance study. *European Heart Journal–Cardiovascular Imaging*. 2017;18:441-450
113. Zareba KM, Truong VT, Mazur W, et al. T-wave and its association with myocardial fibrosis on cardiovascular magnetic resonance examination. *Ann Noninvasive Electrocardiol*. 2020:e12819
114. Hart WS, Miller E, Andrews NJ, et al. Generation time of the alpha and delta sars-cov-2 variants: An epidemiological analysis. *The Lancet Infectious Diseases*. 2022;22:603-610
115. A minimal common outcome measure set for covid-19 clinical research. *Lancet Infect Dis*. 2020;20:e192-e197
116. World Health Organisation. Clinical management of covid-19 interim guidance. Accessed on Aug 2, 2020
117. Moody GB, Koch H, Steinhoff U. The physionet/computers in cardiology challenge 2006: Qt interval measurement. *2006 Computers in Cardiology*. 2006:313-316
118. Malik M. Errors and misconceptions in ecg measurement used for the detection of drug induced qt interval prolongation. *J Electrocardiol*. 2004;37:25-33
119. Davies JE, Sen S, Dehbi HM, et al. Use of the instantaneous wave-free ratio or fractional flow reserve in pci. *N Engl J Med*. 2017;376:1824-1834
120. Waddell-Smith K, Gow RM, Skinner JR. How to measure a qt interval. *Medical Journal of Australia*. 2017;207:107-110
121. Moss AJ. Measurement of the qt interval and the risk associated with qtc interval prolongation: A review. *Am J Cardiol*. 1993;72:23b-25b
122. Davey PP. Which lead for q-t interval measurements? *Cardiology*. 2001;94:159-164
123. Scott PA, Rosengarten JA, Shahed A, et al. The relationship between left ventricular scar and ventricular repolarization in patients with coronary artery disease: Insights from late gadolinium enhancement magnetic resonance imaging. *EP Europace*. 2012;15:899-906
124. Woosley RL, Sale M. Qt interval: A measure of drug action. *The American Journal of Cardiology*. 1993;72:B36-B43
125. Prineas RJ, Crow RS, Zhang Z-M. *The minnesota code manual of electrocardiographic findings*. Springer Science & Business Media; 2009.

126. Long B, Brady WJ, Bridwell RE, et al. Electrocardiographic manifestations of covid-19. *Am J Emerg Med*. 2021;41:96-103
127. Kautzner J, Gang Y, Kishore R, et al. Interobserver reproducibility of qt interval measurement and qt dispersion in patients after acute myocardial infarction. *Annals of Noninvasive Electrocardiology*. 1996;1:363-374
128. Lepeschkin E, Surawicz B. The measurement of the qt interval of the electrocardiogram. *Circulation*. 1952;6:378-388
129. Kasamaki Y, Ozawa Y, Ohta M, et al. Automated versus manual measurement of the qt interval and corrected qt interval. *Annals of Noninvasive Electrocardiology*. 2011;16:156-164
130. Rosenthal TM, Masvidal D, Abi Samra FM, et al. Optimal method of measuring the t-peak to t-end interval for risk stratification in primary prevention. *Ep Europace*. 2018;20:698-705
131. Rautaharju PM, Surawicz B, Gettes LS, et al. Aha/accf/hrs recommendations for the standardization and interpretation of the electrocardiogram: Part iv: The st segment, t and u waves, and the qt interval: A scientific statement from the american heart association electrocardiography and arrhythmias committee, council on clinical cardiology; the american college of cardiology foundation; and the heart rhythm society. Endorsed by the international society for computerized electrocardiology. *J Am Coll Cardiol*. 2009;53:982-991
132. Goldenberg I, Moss AJ, Zareba W. Qt interval: How to measure it and what is "normal". *Journal of cardiovascular electrophysiology*. 2006;17:333-336
133. Bogossian H, Linz D, Heijman J, et al. Qtc evaluation in patients with bundle branch block. *International journal of cardiology. Heart & vasculature*. 2020;30:100636
134. Hall JE, Hall ME. Electrocardiographic interpretation of cardiac muscle and coronary blood flow abnormalities : Vectorial analysis. *Guyton and hall textbook of medical physiology, fourteenth edition*. Elsevier Health Sciences; 2020:143-156.
135. Steger A, Sinnecker D, Berkefeld A, et al. Fragmented qrs. Relevance in clinical practice. *Herzschrittmachertherapie & Elektrophysiologie*. 2015;26:235-241
136. Smith SW, Dodd KW, Henry TD, Dvorak DM, Pearce LA. Diagnosis of st-elevation myocardial infarction in the presence of left bundle branch block with the st-elevation to s-wave ratio in a modified sgarbossa rule. *Ann Emerg Med*. 2012;60:766-776
137. Bazett H. An analysis of the time-relations of. *Heart*. 1920;7:353
138. Karamitsos TD, Dass S, Suttie J, et al. Blunted myocardial oxygenation response during vasodilator stress in patients with hypertrophic cardiomyopathy. *J Am Coll Cardiol*. 2013;61:1169-1176
139. Dass S, Cochlin LE, Suttie JJ, et al. Exacerbation of cardiac energetic impairment during exercise in hypertrophic cardiomyopathy: A potential mechanism for diastolic dysfunction. *Eur Heart J*. 2015;36:1547-1554
140. Schulz-Menger J, Bluemke DA, Bremerich J, et al. Standardized image interpretation and post-processing in cardiovascular magnetic resonance-2020 update. *Journal of Cardiovascular Magnetic Resonance*. 2020;22:1-22
141. Dass S, Cochlin LE, Suttie JJ, et al. Exacerbation of cardiac energetic impairment during exercise in hypertrophic cardiomyopathy: A potential mechanism for diastolic dysfunction. *Eur Heart J*. 2015;36:1547-1554
142. Cassar MP, Tunnicliffe EM, Petousi N, et al. Symptom persistence despite improvement in cardiopulmonary health–insights from longitudinal cmr, cpet and lung function testing post-covid-19. *EClinicalMedicine*. 2021;41:101159
143. Piechnik SK, Ferreira VM, Dall'Armellina E, et al. Shortened modified look-locker inversion recovery (shmolli) for clinical myocardial t1-mapping at 1.5 and 3 t within a 9 heartbeat breathhold. *J Cardiovasc Magn Reson*. 2010;12
144. Huang L, Zhao P, Tang D, et al. Cardiac involvement in patients recovered from covid-2019 identified using magnetic resonance imaging. *JACC: Cardiovascular Imaging*. 2020
145. Piechnik SK, Jerosch-Herold M. Myocardial t1 mapping and extracellular volume quantification: An overview of technical and biological confounders. *Int J Cardiovasc Imaging*. 2018;34:3-14

146. Artico J, Shiwani H, Moon JC, et al. Myocardial involvement after hospitalization for covid-19 complicated by troponin elevation: A prospective, multicenter, observational study. *Circulation*. 2023;147:364-374
147. Hudsmith LE, Petersen SE, Francis JM, Robson MD, Neubauer S. Normal human left and right ventricular and left atrial dimensions using steady state free precession magnetic resonance imaging. *Journal of Cardiovascular Magnetic Resonance*. 2005;7:775-782
148. Petersen SE, Aung N, Sanghvi MM, et al. Reference ranges for cardiac structure and function using cardiovascular magnetic resonance (cmr) in caucasians from the uk biobank population cohort. *J Cardiovasc Magn Reson*. 2017;19:18
149. Kramer CM. Role of cardiac mr imaging in cardiomyopathies. *Journal of nuclear medicine*. 2015;56:39S-45S
150. Cassar MP, Tunnicliffe EM, Petousi N, et al. Symptom persistence despite improvement in cardiopulmonary health – insights from longitudinal cmr, cpet and lung function testing post-covid-19. *EClinicalMedicine*. 2021;41:101159
151. Li X, Wang H, Zhao R, et al. Elevated extracellular volume fraction and reduced global longitudinal strains in participants recovered from covid-19 without clinical cardiac findings. *Radiology*. 2021;299:E230-e240
152. Wang H, Li R, Zhou Z, et al. Cardiac involvement in covid-19 patients: Mid-term follow up by cardiovascular magnetic resonance. *Journal of Cardiovascular Magnetic Resonance*. 2021;23:1-12
153. Yıldırım A, Karaca İO, Yılmaz FK, Güneş HM, Çakal B. Fragmented qrs on surface electrocardiography as a predictor of cardiac mortality in patients with sars-cov-2 infection. *J Electrocardiol*. 2021;66:108-112
154. Raman B, Cassar MP, Tunnicliffe EM, et al. Medium-term effects of sars-cov-2 infection on multiple vital organs, exercise capacity, cognition, quality of life and mental health, post-hospital discharge. *EClinicalMedicine*. 2021;31:100683
155. Starekova J, Bluemke DA, Bradham WS, et al. Evaluation for myocarditis in competitive student athletes recovering from coronavirus disease 2019 with cardiac magnetic resonance imaging. *JAMA Cardiol*. 2021
156. Eiros R, Barreiro-Pérez M, Martín-García A, et al. Pericardial and myocardial involvement after sars-cov-2 infection: A cross-sectional descriptive study in healthcare workers. *Rev Esp Cardiol (Engl Ed)*. 2022;75:734-746
157. Ferreira VM, Schulz-Menger J, Holmvang G, et al. Cardiovascular magnetic resonance in nonischemic myocardial inflammation: Expert recommendations. *J Am Coll Cardiol*. 2018;72:3158-3176
158. Sanghvi SK, Schwarzman LS, Nazir NT. Cardiac mri and myocardial injury in covid-19: Diagnosis, risk stratification and prognosis. *Diagnostics*. 2021;11
159. Raman B, Cassar MP, Tunnicliffe EM, et al. Medium-term effects of sars-cov-2 infection on multiple vital organs, exercise capacity, cognition, quality of life and mental health, post-hospital discharge. *EClinicalMedicine*. 2021;31:100683
160. Mewton N, Liu CY, Croisille P, Bluemke D, Lima JA. Assessment of myocardial fibrosis with cardiovascular magnetic resonance. *J Am Coll Cardiol*. 2011;57:891-903
161. White SK, Sado DM, Flett AS, Moon JC. Characterising the myocardial interstitial space: The clinical relevance of non-invasive imaging. *Heart*. 2012;98:773-779
162. Riza Demir A, Celik Ö, Sevinç S, et al. The relationship between myocardial fibrosis detected by cardiac magnetic resonance and tp-e interval, 5-year sudden cardiac death risk score in hypertrophic cardiomyopathy patients. *Ann Noninvasive Electrocardiol*. 2019;24:e12672
163. Raisi-Estabragh Z, Cooper J, Salih A, et al. Cardiovascular disease and mortality sequelae of covid-19 in the uk biobank. *Heart*. 2023;109:119-126
164. Trevethan R. Sensitivity, specificity, and predictive values: Foundations, pliabilities, and pitfalls in research and practice. *Front Public Health*. 2017;5:307
165. Deeds D, Barnes AR. The characteristics of the chest lead electrocardiograms of 100 normal adults. *American Heart Journal*. 1940;20:261-294

166. Simonson E, Blackburn Jr H, Puchner TC, Eisenberg P, Ribeiro F, Meja M. Sex differences in the electrocardiogram. *Circulation*. 1960;22:598-601
167. Vicente J, Johannesen L, Galeotti L, Strauss DG. Mechanisms of sex and age differences in ventricular repolarization in humans. *American heart journal*. 2014;168:749-756. e743
168. Gaborit N, Varro A, Le Bouter S, et al. Gender-related differences in ion-channel and transporter subunit expression in non-diseased human hearts. *Journal of Molecular and Cellular Cardiology*. 2010;49:639-646
169. Hnatkova K, Smetana P, Toman O, Schmidt G, Malik M. Sex and race differences in qrs duration. *Ep Europace*. 2016;18:1842-1849
170. Xiao L, Zhang L, Han W, Wang Z, Nattel S. Sex-based transmural differences in cardiac repolarization and ionic-current properties in canine left ventricles. *American Journal of Physiology-Heart and Circulatory Physiology*. 2006;291:H570-H580
171. Saito T, Ciobotaru A, Bopassa JC, Toro L, Stefani E, Eghbali M. Estrogen contributes to gender differences in mouse ventricular repolarization. *Circulation research*. 2009;105:343-352
172. Krisai P, Cheniti G, Takagi T, et al. Sex differences in ventricular arrhythmia: Epidemiology, pathophysiology and catheter ablation. *Reviews in Cardiovascular Medicine*. 2022;23:14
173. Carbone V, Guarnaccia F, Carbone G, et al. Gender differences in the 12-lead electrocardiogram: Clinical implications and prospects. *Journal of Sex-and Gender-Specific Medicine*. 2020;6:126-141
174. Attia ZI, Friedman PA, Noseworthy PA, et al. Age and sex estimation using artificial intelligence from standard 12-lead ecgs. *Circ Arrhythm Electrophysiol*. 2019;12:e007284
175. Takahashi T, Ellingson MK, Wong P, et al. Sex differences in immune responses that underlie covid-19 disease outcomes. *Nature*. 2020;588:315-320
176. Saville O, Elbatarny M, Tera Y, Deng Y, Othman M. Sex differences in d-dimer and critical illness in patients with covid-19: A systematic review and meta-analysis. *Research and Practice in Thrombosis and Haemostasis*. 2023;7:100042
177. Hockham C, Linschoten M, Asselbergs FW, Ghossein C, Woodward M, Peters SAE. Sex differences in cardiovascular complications and mortality in hospital patients with covid-19: Registry based observational study. *BMJ Med*. 2023;2:e000245
178. Wray S, Arrowsmith S. The physiological mechanisms of the sex-based difference in outcomes of covid19 infection. *Frontiers in Physiology*. 2021;12:627260
179. Sylvester SV, Rusu R, Chan B, Bellows M, O'Keefe C, Nicholson S. Sex differences in sequelae from covid-19 infection and in long covid syndrome: A review. *Current Medical Research and Opinion*. 2022;38:1391-1399
180. Omar T, Karayakalı M, Perincek G. Do cardiological characteristics explain the mortality rate disparity between genders in covid-19? *E Journal of Cardiovascular Medicine*. 2021;9
181. Attia ZI, Kapa S, Dugan J, et al. Rapid exclusion of covid infection with the artificial intelligence electrocardiogram. *Mayo Clin Proc*. 2021;96:2081-2094
182. van de Leur RR, Bleijendaal H, Taha K, et al. Electrocardiogram-based mortality prediction in patients with covid-19 using machine learning. *Netherlands Heart Journal*. 2022;30:312-318
183. Piechnik SK, Ferreira VM, Lewandowski AJ, et al. Normal variation of magnetic resonance t1 relaxation times in the human population at 1.5 t using shmolli. *J Cardiovasc Magn Reson*. 2013;15:1-11
184. Al-Zaiti SS, Fallavollita JA, Wu Y-WB, Tomita MR, Carey MG. Electrocardiogram-based predictors of clinical outcomes: A meta-analysis of the prognostic value of ventricular repolarization. *Heart & Lung*. 2014;43:516-526
185. Nielsen JB, Graff C, Rasmussen PV, et al. Risk prediction of cardiovascular death based on the qtc interval: Evaluating age and gender differences in a large primary care population. *Eur Heart J*. 2014;35:1335-1344
186. Nakagawa M, Takahashi N, Watanabe M, et al. Gender differences in ventricular repolarization: Terminal t wave interval was shorter in women than in men. *Pacing and clinical electrophysiology*. 2003;26:59-64

187. Noordam R, Young WJ, Salman R, et al. Effects of calcium, magnesium, and potassium concentrations on ventricular repolarization in unselected individuals. *J Am Coll Cardiol*. 2019;73:3118-3131
188. Omran J, Firwana B, Koerber S, Bostick B, Alpert M. Effect of obesity and weight loss on ventricular repolarization: A systematic review and meta-analysis. *obesity reviews*. 2016;17:520-530
189. Bidoggia H, Maciel JP, Capalozza N, et al. Sex differences on the electrocardiographic pattern of cardiac repolarization: Possible role of testosterone. *Am Heart J*. 2000;140:678-683
190. Vink AS, Clur S-AB, Wilde AAM, Blom NA. Effect of age and gender on the qtc-interval in healthy individuals and patients with long-qt syndrome. *Trends in Cardiovascular Medicine*. 2018;28:64-75
191. Schroeder M, Schaumburg B, Mueller Z, et al. High estradiol and low testosterone levels are associated with critical illness in male but not in female covid-19 patients: A retrospective cohort study. *Emerging microbes & infections*. 2021;10:1807-1818
192. Dhindsa S, Zhang N, McPhaul MJ, et al. Association of circulating sex hormones with inflammation and disease severity in patients with covid-19. *JAMA network open*. 2021;4:e2111398-e2111398
193. Liao S-C, Shao S-C, Cheng C-W, Chen Y-C, Hung M-J. Incidence rate and clinical impacts of arrhythmia following covid-19: A systematic review and meta-analysis of 17,435 patients. *Critical care*. 2020;24:1-7
194. Roy C, Slimani A, de Meester C, et al. Age and sex corrected normal reference values of t1, t2 t2* and ecv in healthy subjects at 3t cmr. *Journal of Cardiovascular Magnetic Resonance*. 2017;19:1-12
195. Dabir D, Child N, Kalra A, et al. Reference values for healthy human myocardium using a t1 mapping methodology: Results from the international t1 multicenter cardiovascular magnetic resonance study. *Journal of Cardiovascular Magnetic Resonance*. 2014;16:1-12
196. Bulluck H, Bryant JA, Tan JZ, et al. Gender differences in native myocardial t1 in a healthy chinese volunteer cohort. *Cardiovasc Imaging Asia*. 2017;1:110-115
197. Zareba W, Moss AJ, Locati EH, et al. Modulating effects of age and gender on the clinical course of long qt syndrome by genotype. *J Am Coll Cardiol*. 2003;42:103-109
198. Sgreccia A, Morelli S, Ferrante L, et al. Qt interval and qt dispersion in systemic sclerosis (scleroderma). *Journal of internal medicine*. 1998;243:127-132
199. Ichkhan K, Molnar J, Somberg J. Relation of left ventricular mass and qt dispersion in patients with systematic hypertension. *American Journal of Cardiology*. 1997;79:508-511
200. Magrì D, Santolamazza C, Limite L, et al. Qt spatial dispersion and sudden cardiac death in hypertrophic cardiomyopathy: Time for reappraisal. *Journal of Cardiology*. 2017;70:310-315
201. Magrì D, Piccirillo G, Ricotta A, et al. Spatial qt dispersion predicts nonsustained ventricular tachycardia and correlates with confined systodiastolic dysfunction in hypertrophic cardiomyopathy. *Cardiology*. 2015;131:122-129
202. Malik M, Batchvarov VN. Measurement, interpretation and clinical potential of qt dispersion. *J Am Coll Cardiol*. 2000;36:1749-1766
203. Hurtado-de-Mendoza D, Corona-Villalobos CP, Pozios I, et al. Diffuse interstitial fibrosis assessed by cardiac magnetic resonance is associated with dispersion of ventricular repolarization in patients with hypertrophic cardiomyopathy. *J Arrhythm*. 2017;33:201-207
204. De Mendoza DH, Corona-Villalobos CP, Vakrou S, et al. Qtc dispersion on 12-lead electrocardiogram is inversely correlated with t1 relaxation times in patients with hypertrophic cardiomyopathy. *J Am Coll Cardiol*. 2014;1):A1197
205. Hanczar B, Hua J, Sima C, Weinstein J, Bittner M, Dougherty ER. Small-sample precision of roc-related estimates. *Bioinformatics*. 2010;26:822-830
206. Ojha V, Verma M, Pandey NN, et al. Cardiac magnetic resonance imaging in coronavirus disease 2019 (covid-19): A systematic review of cardiac magnetic resonance imaging findings in 199 patients. *Journal of Thoracic Imaging*. 2021;36

207. Breitbart P, Koch A, Schmidt M, et al. Clinical and cardiac magnetic resonance findings in post-covid patients referred for suspected myocarditis. *Clinical Research in Cardiology*. 2021;110:1832-1840
208. Kligfield P, Gettes LS, Bailey JJ, et al. Recommendations for the standardization and interpretation of the electrocardiogram. *Circulation*. 2007;115:1306-1324
209. Puntmann VO, Carr-White G, Jabbour A, et al. T1-mapping and outcome in nonischemic cardiomyopathy: All-cause mortality and heart failure. *JACC: Cardiovascular Imaging*. 2016;9:40-50
210. Puntmann VO, Valbuena S, Hinojar R, et al. Society for cardiovascular magnetic resonance (scmr) expert consensus for cmr imaging endpoints in clinical research: Part i-analytical validation and clinical qualification. *Journal of Cardiovascular Magnetic Resonance*. 2018;20:67
211. Lan Y, Liu W, Zhou Y. Right ventricular damage in covid-19: Association between myocardial injury and covid-19. *Frontiers in cardiovascular medicine*. 2021;8:606318
212. Paternoster G, Bertini P, Innelli P, et al. Right ventricular dysfunction in patients with covid-19: A systematic review and meta-analysis. *Journal of cardiothoracic and vascular anesthesia*. 2021;35:3319-3324
213. Bieber S, Kraechan A, Hellmuth JC, et al. Left and right ventricular dysfunction in patients with covid-19-associated myocardial injury. *Infection*. 2021;49:491-500
214. Raman B, McCracken C, Cassar MP, et al. Multiorgan mri findings after hospitalisation with covid-19 in the uk (c-more): A prospective, multicentre, observational cohort study. *The Lancet Respiratory Medicine*. 2023
215. Raman B, Ariga R, Spartera M, et al. Progression of myocardial fibrosis in hypertrophic cardiomyopathy: Mechanisms and clinical implications. *European heart journal. Cardiovascular Imaging*. 2019;20:157-167
216. Ariga R, Tunnicliffe EM, Manohar SG, et al. Identification of myocardial disarray in patients with hypertrophic cardiomyopathy and ventricular arrhythmias. *J Am Coll Cardiol*. 2019;73:2493-2502
217. Strebel I, Twerenbold R, Boeddinghaus J, et al. Diagnostic value of the cardiac electrical biomarker, a novel ecg marker indicating myocardial injury, in patients with symptoms suggestive of non-st-elevation myocardial infarction. *Annals of noninvasive electrocardiology*. 2018;23:e12538
218. Chattopadhyay S, Adjei F, Kardos A. Changes in cardiac electrical biomarker in response to coronary arterial occlusion: An experimental observation. *J Cardiovasc Transl Res*. 2024
219. Ricci F, Mantini C, Melissa De Maio M, et al. Cardiac electrical biomarker improves ecg prediction of left ventricular scar. *European Heart Journal Supplements*. 2019;21:J180-J180
220. Deeks JJ, Altman DG. Diagnostic tests 4: Likelihood ratios. *Bmj*. 2004;329:168-169
221. Guyatt G, Haynes B, Jaeschke R. Introduction: The philosophy of evidence-based medicine. Chapter 1a in: Guyatt g, rennie d, eds. User's guide to the medical literature: A manual for evidence-based practice. 2002
222. Metz CE. Basic principles of roc analysis. *Seminars in Nuclear Medicine*. 1978;8:283-298
223. Hajian-Tilaki K. Receiver operating characteristic (roc) curve analysis for medical diagnostic test evaluation. *Caspian journal of internal medicine*. 2013;4:627
224. Messroghli DR, Moon JC, Ferreira VM, et al. Clinical recommendations for cardiovascular magnetic resonance mapping of t1, t2, t2* and extracellular volume: A consensus statement by the society for cardiovascular magnetic resonance (scmr) endorsed by the european association for cardiovascular imaging (eacvi). *J Cardiovasc Magn Reson*. 2017;19:75
225. Popescu IA, Werys K, Zhang Q, et al. Standardization of t1-mapping in cardiovascular magnetic resonance using clustered structuring for benchmarking normal ranges. *Int J Cardiol*. 2021;326:220-225

# APPENDIX 1: SUPPLEMENTARY MATERIAL FOR CHAPTER 2, 3 AND 4

---

## EVALUATION OF MODEL PERFORMANCE

### Calibration

Calibration is related to goodness-of-fit of the model, which represents the agreement between the predicted and the observed outcomes. Hosmer-Lemeshow test was used to assess the model for binary outcomes. A p value of $< 0.05$ would indicate poor calibration of the model. The Hosmer-Lemeshow test on our clinical models indicated good logistic regression model fit with $p > 0.05$ (e.g. $p=0.793$ for a model with QTc and $p=0.218$ for the model with JTc interval to predict high T1).

### Discrimination

Discriminative ability of the repolarisation parameter model to differentiate between two outcome classes was evaluated using area under the AUROC curve and concordance statistics (C-index). Diagnostic performance and optimal cut-off point of ECG repolarisation intervals were also determined and different intervals were compared by their sensitivities, specificities, and predictive values.

## DIAGNOSTIC PERFORMANCE ANALYSIS

### Sensitivity

Sensitivity (SN) is defined as the probability of a screening test to detect patients who have the disease of interest, solely among all the patients who truly have the disease. Based on **Figure 1**, the formula for SN is **[ A / (A + C) ] x 100**[164]. (**A**) refers to the true positive rate, and (**C**) refers to false negative rate. The higher the proportion of true positive cases correctly being identified by the test, the higher the SN.

### Specificity

Specificity (SP) is defined as the probability of the screening test to correctly detect patients who do not have the disease of interest solely among patients who truly do not have the disease. It is the ability of the test to detect true negative cases. Based on **Figure 1**, it is the proportion of true negative cases (**D**) over the combination of true negative and false positive cases (**B**); **[ D/ (B + D ) ] x 100**[164]. The higher the proportion of true negative cases correctly being identified, the higher the SP.

It is important to note that, interpretation of SN is not a stand-alone concept. The SP and predictive values (PV) must be considered as well. The SN and SP, alongside the negative or positive predictive values that provide clinicians the overall picture of the clinical applicability and reliability of the test.

| | **Has the condition** | **Does not have the condition** | |
|---|---|---|---|
| **Positive Test** | **A (True Positive)** | **B (False Positive)** | **A + B** |
| **Negative Test** | **C (False Negative)** | **D (True Negative)** | **C + D** |
| | **A + C** | **B + D** | **A + B + C + D (Total cases)** |

**Figure 1** Contingency 2 x 2 table.

**Predictive Values**

Positive predictive value (PPV) of a test represent the probability of detecting the truly positive cases when the test is positive. Whereas negative predictive value (NPV) represent the probability of detecting the truly negative cases when the test is negative. Based on the **Figure 1**, PPV and NPV are measured based on the following formula:

**Positive Predictive Value**

Probability that when the test is positive, the subjects indeed have the condition/ disease of interest **[A/(A+B)] x 100**.[164] True positive cases **(A)** / True positive + False Positive **(A+B).**

**Negative Predictive Value**

Probability that when the test is negative, the subjects indeed do not have the condition/disease of interest. **[D/(C+D)] x 100**.[164] True negative cases (**D**) / True negative + False negative cases **(C + D).**

**Likelihood ratio**

Positive likelihood ratio (+LR) is the probability of positive cases in patients with the condition (true positive) over positive cases in patients without the condition (false positive). Negative likelihood ratio (-LR) is the probability of negative cases in patients with the condition (false negative), over negative cases in patients without the condition (true negative).

The formula to generate likelihood ratio is as follows:

- **+LR = Sensitivity / (1 - Specificity)**
- **-LR = (1 – Sensitivity) / Specificity**

A likelihood ratio value of 1 means there is no difference in the probability of detecting the presence of absence of the disease, hence the diagnostic test is considered not clinically useful. The further the LR values are from 1, the more robust the evidence is for the presence or absence of disease. Generally, +LR above 10 or -LR below 0.1 have been considered strong evidence to rule in or rule out a disease condition, respectively[220,221].

**Area under the curve for Receiver Operator Characteristic (AUROC)**

Description of disease detectability based on the various thresholds corresponding to a true positive fraction (SN) on the Y-Axis and a false positive fraction (1- specificity) on the X axis[222]. Receiver operating characteristics (ROC) and area under the curve (AUC) have been widely used to quantify the accuracies of diagnostic tests to discriminate between two cardiac disease states[223]. The ROC curve, which is mainly a tradeoff between the true positive fraction (TPF) and false positive fraction (FPF), is an excellent method to discriminate between two patient states, i.e. COVID-19 with and without myocardial injury, depending on the cut-off values.

The cut-off values on ROC curve is determined using the Youden's index. It is the maximum vertical distance between the ROC curve and the diagonal line, as depicted below.

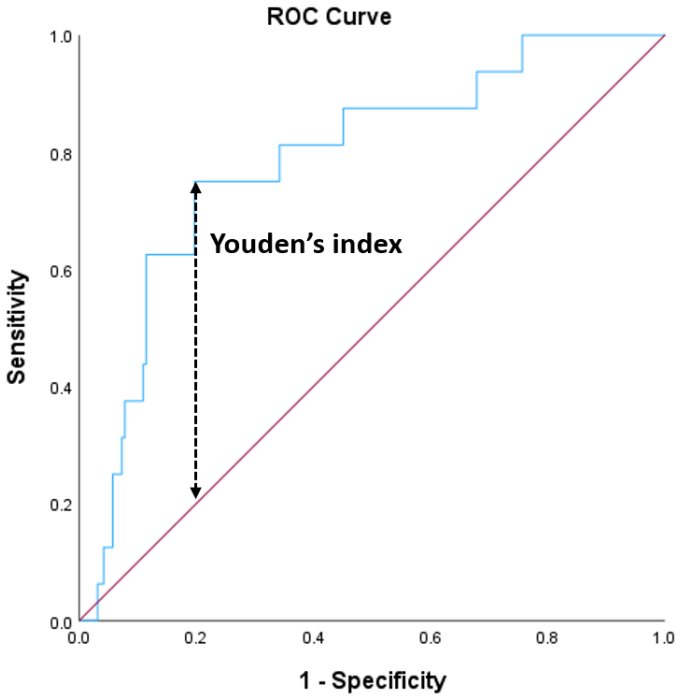


**Figure 2** Youden's index

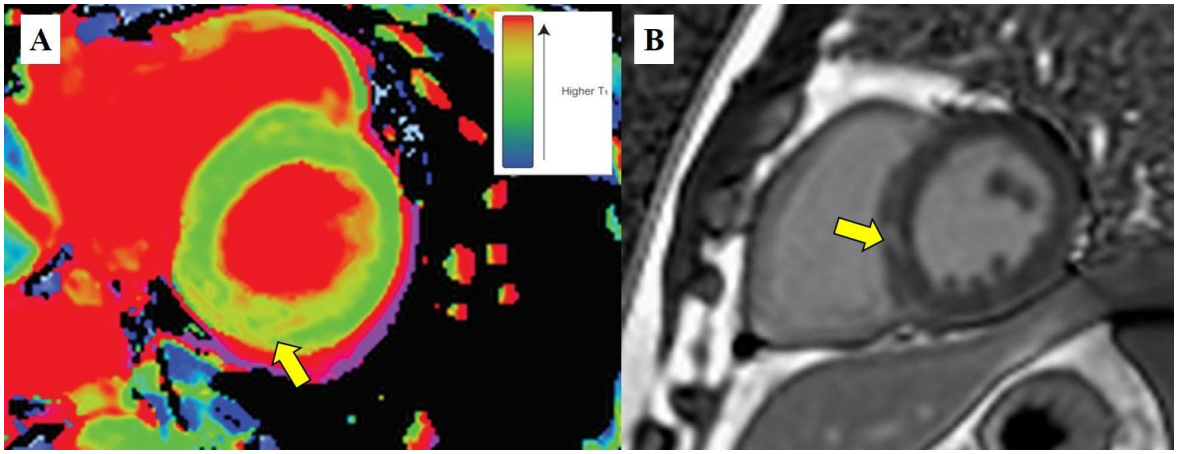


**Figure 3** Representative cases of a post-hospitalised COVID-19 patient with elevated T1 (A) and late gadolinium enhancement (LGE) (B). Note the areas of red (yellow arrow, A) within the patient's myocardium, indicative of high native T1 values (reflective of inflammation). Bright area at the septal region of the myocardium (yellow arrow, B) indicative of LGE (reflective of fibrosis).

# APPENDIX 2: SUPPLEMENTARY MATERIAL FOR CHAPTER 3

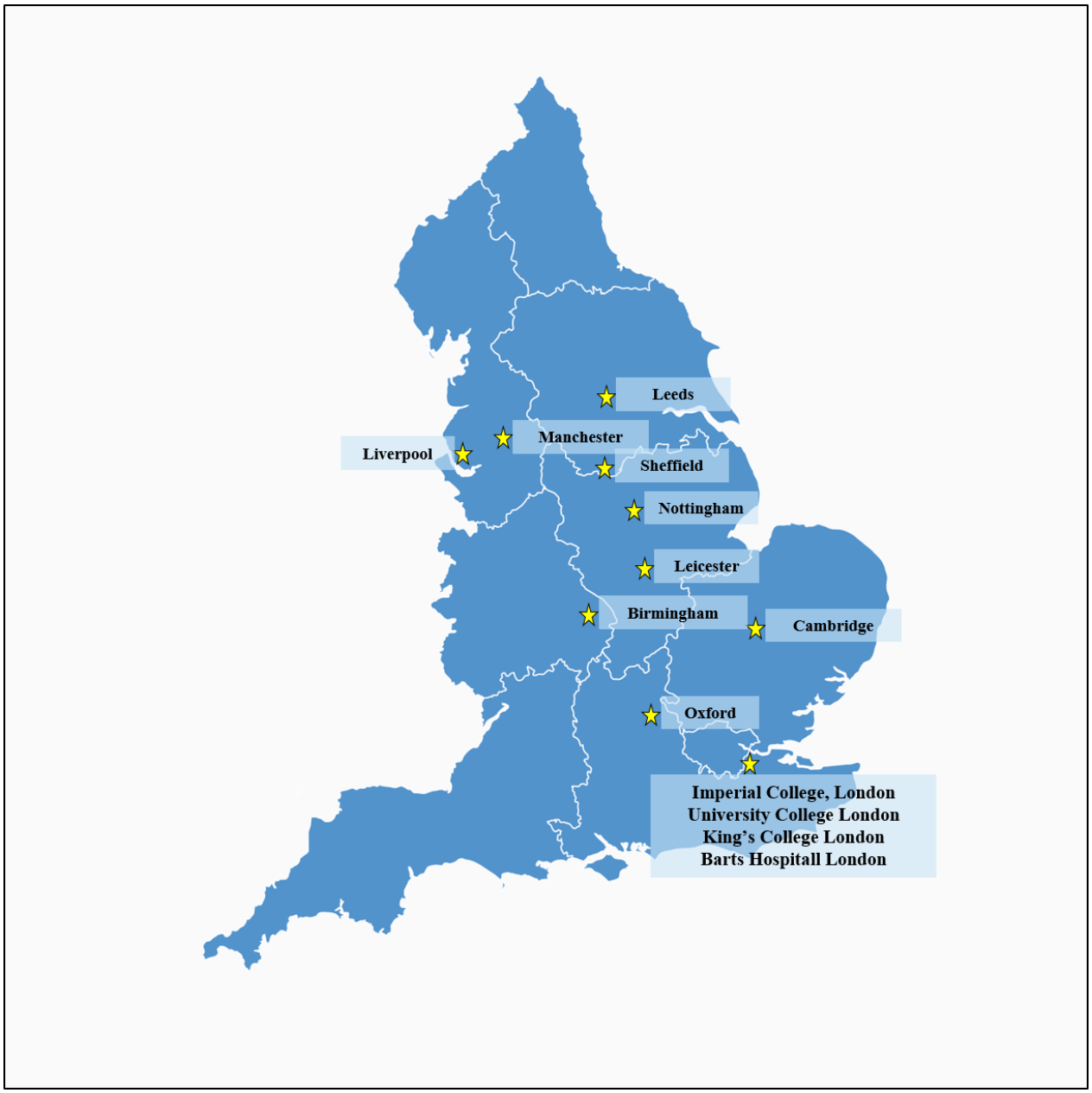


**Figure 1.** Participating sites involved in the PHOSP-COVID study in England which provided data for the analysis and results in chapter 3 and 4. In Chapter 5, Oxford was the only centre for data recruitment for the CMORE study.

## HARMONISATION OF T1 AND T2 MAPPING

Specific for **Chapters 3** and **4**, we conducted harmonization of T1 and T2 mapping to mitigate the variations in values of myocardial T1 and T2 between scanners, as previously reported[146 224]. In line with prior observation[225], the observed variation in the reported normal SDs between sites precluded the meaningful application of z-scores; instead, the normalised z scores nT1 and nT2 were reported, obtained by dividing the individual T1 and T2 measurements by the corresponding normal mean value for the appropriate site/scanner/sequence combination. There was no significant inter-scanner variability in ECV, and ECV was thus used directly, in line with the SCMR consensus[145].


**Figure 2** Age distribution among COVID-19 patients and controls.

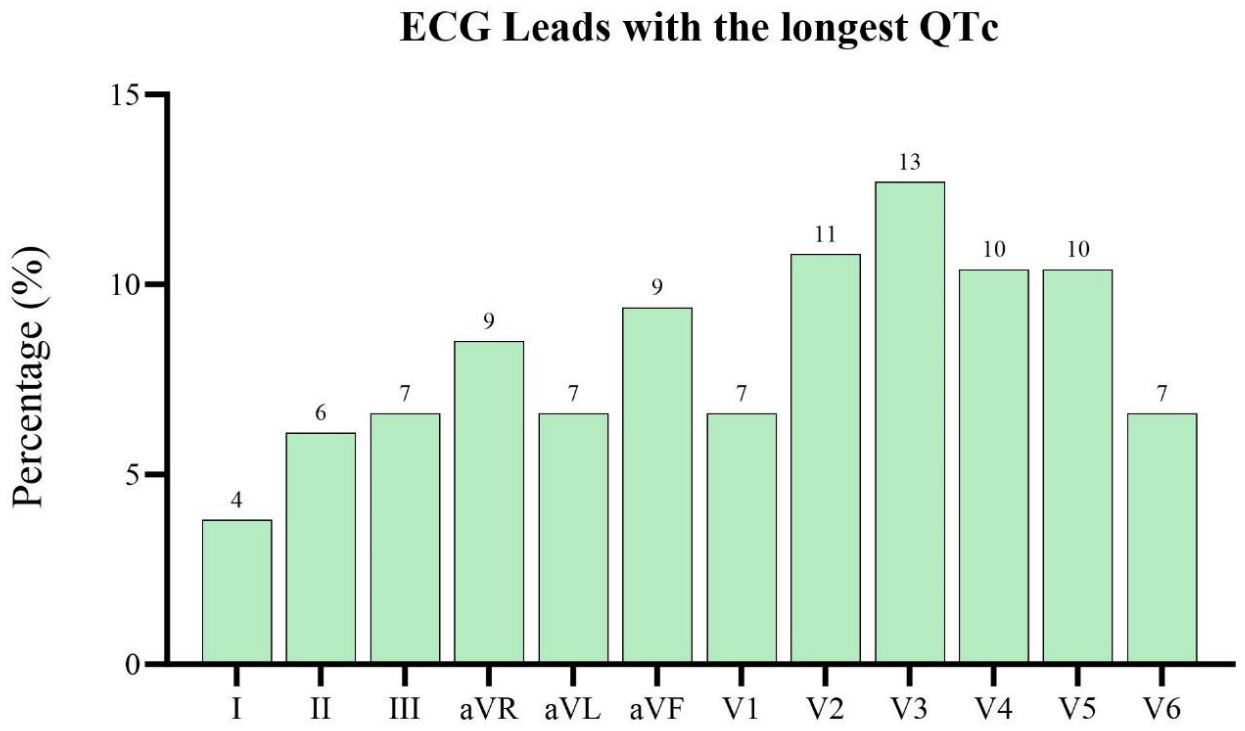


**Figure 3** shows the 12 leads ECG and the burden of the longest QT interval observed in each lead. Note that in 58% of cases, the longest QT intervals were observed among the pre-cordial leads (V1-V6) and the highest burden of the longest QT interval was observed in lead V3 (13%).

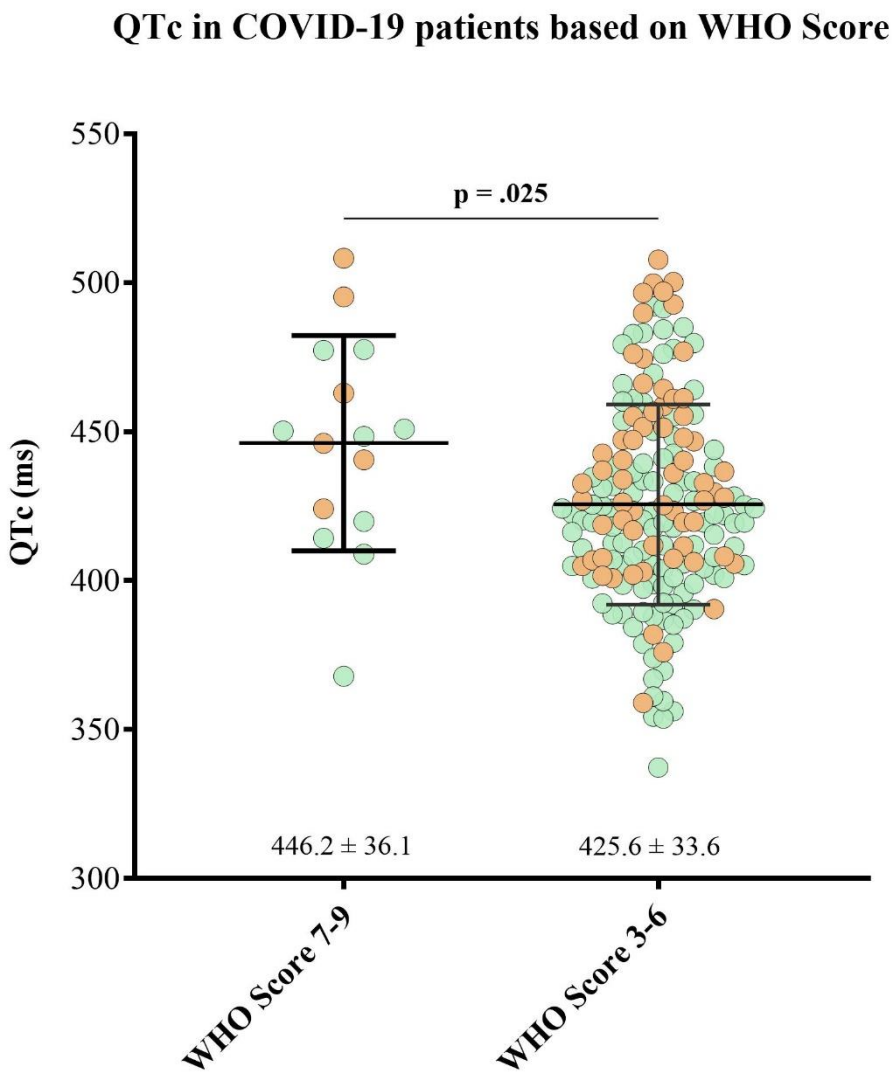


**Figure 4** QTc interval among post-hospitalised COVID-19 patients based on WHO Score 7-9 versus WHO Score 3-6. A score of 7-9 is indicative of severe infection requiring invasive mechanical ventilation. QTc interval is significantly longer among patients with a WHO score of 7-9 compared to a WHO score of 3-6. (green= QTc, and brown represents female participants in the respective group). P values are based on independent students' T-tests.

**Table 1** ECG and CMR characteristics based on severity of infection among post-hospitalised COVID-19 patients.

| **ECG** | | | |
|---|---|---|---|
| | **Moderate infection WHO score 4-5 (n=133)** | **Severe infection WHO score 6-9 (n=56)** | **P values** |
| Age, years | 57.0 (47.0-66.0) | 56.0 (49.3-62.8) | 0.442[b] |
| Sex: female n (%) | 51 (38.3) | 18 (32.1) | 0.419[c] |
| BMI, kg/m$^2$ | 30.1 (26.7-34.7) | 31.1 (26.6-35.2) | 0.703[b] |
| Smoker and ex-smoker n (%) | 36/130 (27.7) | 16/47 (34.0) | 0.413[c] |
| Hypertension, n (%) | 31/118 (26.3) | 19/54 (35.2) | 0.232[c] |
| Diabetes mellitus, n (%) | 17/117 (14.5) | 5/54 (9.3) | 0.339[c] |
| History of IHD, n (%) | 6/118 (5.1) | 0 (0) | 0.178[d] |
| Congestive heart failure, n (%) | 0 (0) | 2 (3.7) | 0.098[d] |
| ACE inhibitor, n (%) | 13/114 (11.4) | 6/49 (12.2) | 0.878[c] |
| Antibiotics, n (%) | 7/115 (6.1) | 5/50 (10.0) | 0.514[d] |
| NSAIDs, n (%) | 4/113 (3.5) | 1/50 (2.0) | 1.000[d] |
| **Group A ECG** | **ECG** | | |
| Abnormal ECG, n (%) | 96 (72.2) | 39 (69.6) | 0.724[c] |
| Bundle Branch Block, n (%) | 11 (8.3) | 6 (10.7) | 0.592[c] |
| -LBBB, n (%) | 0 (0) | 1 (1.8) | 0.296[d] |
| -RBBB, n (%) | 5 (3.8) | 2 (3.6) | 1.000[d] |
| -ILBBB/IRBBB/IVCD, n (%) | 6 (4.5) | 3 (5.4) | 0.803[d] |
| Abnormal axis, n (%) * | 29 (21.8) | 14 (25.0) | 0.632[c] |
| ST-T changes, n (%) * | 50 (37.6) | 20 (35.7) | 0.807[c] |
| Abnormal R prog, n (%) | 23 (17.3) | 9 (16.1) | 0.838[c] |
| Fragmented QRS, n (%) * | 38 (28.6) | 19 (33.9) | 0.464[c] |
| Heart block, n (%) | 7 (5.3) | 4(7.1) | 0.735[d] |
| PVC/PAC, n (%) | 6 (4.5) | 4 (7.1) | 0.488[d] |
| **Group B ECG** | **Moderate (n=133)** | **Severe (n=56)** | **P values** |

| | | | |
|---|---|---|---|
| Heart rate (bpm) | 73.7 ± 13.3 | 72.5 ± 15.9 | 0.571[b] |
| PR interval, ms | 160.0 (146.3-173.5) | 160.0 (1421.3-175.8) | 0.987[b] |
| QRS ms | 92.5 (86.0-100.8) | 92.0 (84.0-98.0) | 0.281[b] |
| QTc ms | 425.5 ± 34.2 | 431.4 ± 34.0 | 0.275[a] |
| QTc disp ms | 51.3 (40.3-65.9) | 58.2 (46.0-73.5) | **0.043[b]** |
| JTc ms | 329.0 ± 28.4 | 336.2 ± 29.0 | 0.119[a] |
| JTPc ms | 229.2 (209.3-247.2) | 227.0 (210.7-249.1) | 0.694[b] |
| cTPe ms | 99.5 ± 14.7 | 103.9 ± 15.6 | 0.071[a] |
| **CMR – Myocardial Function and tissue characteristics** | | | |
| CMR abnormal, n (%) | 49 (23.1) | 7 (18.4) | 0.592[b] |
| LVEF < 52%, n (%) | 11 (5.2) | 1 (2.6) | 0.699[d] |
| RVEF < 48%, n (%) | 10 (4.7) | 1 (2.6) | 0.999[d] |
| T1 normalised Z score | 0.08 (-1.05 – 1.27) | 0.02 (-1.30 – 2.3) | 0.637[b] |
| T2 normalised Z score | 0.63 (-0.07-1.32) | 0.82 (0.17-1.61) | 0.219[b] |
| ECV (%) | 0.28 ± 0.03 | 0.29 ± 0.03 | 0.096[a] |
| High ECV (>0.32), n (%) | 15/186 (8.1) | 1 (14.8) | 0.274[d] |
| Pathological LGE, n (%) | 27/195 (13.8) | 4 (10.5) | 0.581[d] |

[a]Independent T-Test, [b]Mann-Whitney Test, [c]Chi-Square Test, [d]Fisher's Exact Test.

Values are mean ± SD, median (IQR) or percentages. Abnormal R prog, abnormal R wave progression; BBB, bundle branch block; BMI, body mass index; CMR, cardiac magnetic resonance; ECG, electrocardiography; Disp, dispersion; IVCD, intraventricular conduction delay; ILBBB, incomplete left bundle branch block; IRBBB, incomplete right bundle branch block; LBBB, left bundle branch block; PAC, premature atrial complex; PVC, premature ventricular complex; QTc, corrected QT; QTPc, corrected QT peak; RBBB, right bundle branch block; cTPe, corrected T-peak- to-T-end; *cases with BBB excluded.

**Table 2** Diagnostic performance of individual group A ECG parameters for CMR abnormalities.

| **CMR abnormalities** | **ECG parameters** | **SN (%)** | **SP (%)** | **PPV (%)** | **NPV (%)** | **+LR** | **-LR** |
|---|---|---|---|---|---|---|---|
| | Abnormal axis | 32.7 | 79.8 | 32.7 | 79.8 | 1.62 | 0.84 |
| | Heart block | 12.2 | 95.1 | 42.9 | 78.3 | 2.49 | 0.92 |
| | Bundle branch block* | 18.4 | 92.6 | 42.9 | 79.1 | 2.49 | 0.88 |
| | LBBB | 4.3 | 99.4 | 66.7 | 77.7 | 7.17 | 0.96 |
| | fQRS | 36.7 | 71.8 | 28.1 | 79.1 | 1.30 | 0.88 |
| | Poor R wave progression | 22.4 | 83.4 | 28.9 | 78.2 | 1.35 | 0.93 |
| | ST abnormal | 28.6 | 81.6 | 31.8 | 79.2 | 1.55 | 0.88 |
| | T wave abnormal | 44.9 | 74.2 | 34.4 | 81.8 | 1.74 | 0.74 |
| | ST-T abnormal | 57.1 | 68.1 | 35.0 | 84.1 | 1.79 | 0.63 |
| | PVC/PAC | 12.2 | 97.5 | 60.0 | 78.6 | 4.88 | 0.90 |
| **LVEF < 52%** | | **SN (%)** | **SP (%)** | **PPV (%)** | **NPV (%)** | **+LR** | **-LR** |
| | Abnormal axis | 63.6 | 79.1 | 14.3 | 97.5 | 3.04 | 0.46 |
| | Heart block | 18.2 | 94.0 | 14.3 | 95.5 | 3.03 | 0.87 |
| | Bundle branch block* | 36.4 | 91.5 | 19.0 | 96.3 | 4.28 | 0.70 |
| | LBBB | 9.1 | 99.0 | 33.3 | 95.0 | 9.10 | 0.92 |
| | fQRS | 36.4 | 70.1 | 6.3 | 95.3 | 1.22 | 0.91 |
| | Poor R wave progression | 18.2 | 82.1 | 5.3 | 94.8 | 1.02 | 1.00 |
| | ST abnormal | 45.5 | 80.6 | 11.4 | 96.4 | 2.35 | 0.68 |
| | T wave abnormal | 45.5 | 70.6 | 7.8 | 95.9 | 1.55 | 0.77 |
| | ST-T abnormal | 81.8 | 64.7 | 11.3 | 98.5 | 2.32 | 0.28 |
| | PVC/PAC | 36.4 | 97.0 | 40.0 | 96.5 | 12.13 | 0.66 |
| **High T1** | | **SN (%)** | **SP (%)** | **PPV (%)** | **NPV (%)** | **+LR** | **-LR** |
| | Abnormal axis | 6.3 | 75.8 | 2.1 | 90.6 | 0.26 | 1.24 |
| | Heart block | 6.3 | 93.2 | 7.1 | 92.2 | 0.93 | 1.01 |
| | Bundle branch block* | 0 | 88.9 | 0 | 91.4 | 0.00 | 1.12 |
| | LBBB | 0 | 98.4 | 0 | 92.0 | 0.00 | 1.02 |
| | fQRS | 25.0 | 70.0 | 6.6 | 91.7 | 0.83 | 1.07 |
| | Poor R wave progression | 25.0 | 82.6 | 10.8 | 92.9 | 1.44 | 0.91 |
| | ST abnormal | 18.8 | 78.9 | 7.0 | 92.0 | 0.89 | 1.03 |
| | T wave abnormal | 43.8 | 70.0 | 10.9 | 93.7 | 1.46 | 0.80 |
| | ST-T abnormal | 31.3 | 61.1 | 6.3 | 91.3 | 0.80 | 1.12 |
| | PVC/PAC | 6.3 | 95.8 | 11.1 | 92.3 | 1.50 | 0.98 |
| **High T2** | | **SN (%)** | **SP (%)** | **PPV (%)** | **NPV (%)** | **+LR** | **-LR** |
| | Abnormal axis | 17.6 | 78.7 | 7.5 | 90.3 | 0.83 | 1.05 |
| | Heart block | 5.9 | 93.5 | 8.3 | 90.8 | 0.91 | 1.01 |
| | Bundle branch block* | 5.9 | 89.3 | 5.3 | 90.4 | 0.55 | 1.05 |
| | LBBB | 0 | 98.2 | 0 | 90.5 | 0.00 | 1.02 |
| | fQRS | 29.4 | 71.4 | 9.4 | 90.9 | 1.03 | 0.99 |
| | Poor R wave progression | 11.8 | 82.7 | 6.5 | 90.3 | 0.68 | 1.07 |
| | ST abnormal | 0 | 75.0 | 0 | 88.1 | 0.00 | 1.33 |

| | | | | | | | |
|---|---|---|---|---|---|---|---|
| | T wave abnormal | 35.3 | 70.2 | 10.7 | 91.5 | 1.18 | 0.92 |
| | ST-T abnormal | 35.3 | 60.1 | 8.2 | 90.2 | 0.88 | 1.08 |
| | PVC/PAC | 5.9 | 95.8 | 12.5 | 91.0 | 1.40 | 0.98 |
| **High ECV** | | **SN (%)** | **SP (%)** | **PPV (%)** | **NPV (%)** | **+LR** | **-LR** |
| | Abnormal axis | 26.7 | 75.4 | 8.7 | 92.1 | 1.09 | 0.97 |
| | Heart block | 6.7 | 92.4 | 7.1 | 91.9 | 0.88 | 1.01 |
| | Bundle branch block* | 6.7 | 88.9 | 5.0 | 91.6 | 0.60 | 1.05 |
| | LBBB | 0 | 98.2 | 0 | 91.7 | 0.00 | 1.02 |
| | fQRS | 40.0 | 70.8 | 10.7 | 93.1 | 1.37 | 0.85 |
| | Poor R wave progression | 20.0 | 83.0 | 9.4 | 92.2 | 1.18 | 0.96 |
| | ST abnormal | 13.3 | 78.9 | 5.3 | 91.2 | 0.63 | 1.10 |
| | T wave abnormal | 33.3 | 69.0 | 8.6 | 92.2 | 1.07 | 0.97 |
| | ST-T abnormal | 33.3 | 61.4 | 7.0 | 91.3 | 0.86 | 1.09 |
| | PVC/PAC | 6.7 | 95.3 | 11.1 | 92.1 | 1.43 | 0.98 |
| **Pathological LGE** | | **SN (%)** | **SP (%)** | **PPV (%)** | **NPV (%)** | **+LR** | **-LR** |
| | Abnormal axis | 40.7 | 79.8 | 25.4 | 89.3 | 2.01 | 0.74 |
| | Heart block | 11.1 | 94.6 | 25.0 | 86.9 | 2.06 | 0.94 |
| | Bundle branch block* | 22.2 | 91.7 | 30.0 | 88.0 | 2.67 | 0.85 |
| | LBBB | 3.8 | 98.8 | 33.3 | 86.5 | 3.17 | 0.97 |
| | fQRS | 40.7 | 72.0 | 19.0 | 88.3 | 1.45 | 0.82 |
| | Poor R wave progression | 29.6 | 83.9 | 22.9 | 88.1 | 1.84 | 0.84 |
| | ST abnormal | 33.3 | 81.5 | 22.5 | 88.4 | 1.80 | 0.82 |
| | T wave abnormal | 37.0 | 70.8 | 16.9 | 87.5 | 1.27 | 0.89 |
| | ST-T abnormal | 59.3 | 66.1 | 21.9 | 91.0 | 1.75 | 0.62 |
| | PVC/PAC | 18.5 | 97.6 | 55.6 | 88.1 | 7.71 | 0.84 |

* Left bundle branch block, right bundle branch block, incomplete bundle branch block and non-specific intraventricular conduction delay

**Table 3** Diagnostic performance of ECG for individual CMR abnormalities.

| **LVEF < 52%** | | | | | | | | | | |
|---|---|---|---|---|---|---|---|---|---|---|
| | **C-statistic** | **95% CI** | **P value** | **ECG parameters** | **SN (%)** | **SP (%)** | **PPV (%)** | **NPV (%)** | **+LR** | **-LR** |
| ECG abnormalities | 0.60 | 0.45-0.75 | 0.270 | ECG abnormalities | 90.9 | 28.9 | 6.5 | 98.3 | 1.28 | 0.31 |
| ***Individual repolarisation parameters*** | | | | | | | | | | |
| QTc | 0.49 | 0.31-0.67 | 0.918 | QTc ≥ 450 ms | 18.2 | 73.6 | 3.6 | 94.3 | 0.69 | 1.11 |
| QTc disp | 0.69 | 0.50-0.88 | **0.035** | QTc disp ≥ 55 ms | 72.7 | 51.7 | 7.6 | 97.2 | 1.51 | 0.53 |
| QTPc | 0.49 | 0.29-0.69 | 0.942 | QTPc ≥ 366 ms | 36.4 | 69.7 | 6.2 | 95.2 | 1.20 | 0.91 |
| JTc | 0.51 | 0.32-0.70 | 0.914 | JTc ≥ 340 ms | 36.4 | 63.2 | 5.1 | 94.8 | 0.99 | 1.01 |
| JTPc | 0.52 | 0.44-0.60 | 0.671 | JTPc ≥ 240 | 36.4 | 58.7 | 4.6 | 94.4 | 0.86 | 1.08 |
| cTPe | 0.43 | 0.27-0.60 | 0.446 | cTPe ≥ 100 ms | 45.5 | 51.7 | 4.9 | 94.5 | 0.94 | 1.05 |
| ***ECG + repolarisation parameters*** | | | | | | | | | | |
| ECG abnorm + QTc disp | 0.72 | 0.54-0.89 | **0.016** | ECG abnorm + QTc disp ≥ 55 | 99.9 | 16.4 | 6.1 | 99.9 | 1.19 | 0.01 |
| **High T1** | | | | | | | | | | |
| | **C-statistic** | **95% CI** | **P value** | | **SN (%)** | **SP (%)** | **PPV (%)** | **NPV (%)** | **+LR** | **-LR** |
| ECG abnorm | 0.51 | 0.37-0.66 | 0.851 | ECG abnorm | 68.8 | 28.4 | 7.5 | 91.5 | 0.96 | 1.10 |
| ***Individual repolarisation parameters*** | | | | | | | | | | |
| QTc | 0.81 | 0.70-0.92 | **<0.001** | QTc ≥ 456 ms | 75.0 | 84.2 | 28.6 | 97.6 | 4.75 | 0.30 |
| QTc disp | 0.66 | 0.53-0.80 | **0.030** | QTc disp ≥ 55 ms | 93.8 | 16.6 | 8.5 | 97.0 | 1.12 | 0.37 |
| QTPc | 0.77 | 0.66-0.87 | **<0.001** | QTPc ≥ 366 ms | 75.0 | 73.7 | 19.4 | 97.2 | 2.85 | 0.34 |
| JTc | 0.82 | 0.71-0.93 | **<0.001** | JTc ≥ 340 ms | 81.3 | 67.4 | 17.3 | 97.7 | 2.49 | 0.28 |
| JTPc | 0.76 | 0.62-0.89 | **0.001** | JTPc ≥ 240 | 81.3 | 62.2 | 15.1 | 97.6 | 2.15 | 0.30 |
| cTPe | 0.61 | 0.46-0.76 | 0.145 | cTPe ≥ 100 ms | 62.5 | 52.6 | 10.0 | 94.3 | 1.32 | 0.71 |
| ***ECG + repolarisation parameter*** | | | | | | | | | | |
| ECG abnorm + JTc | 0.82 | 0.72-0.93 | **<0.001** | ECG abnorm + JTc ≥ 340 ms | 93.8 | 20.5 | 9.0 | 97.5 | 1.18 | 0.30 |
| **High T2** | | | | | | | | | | |

| | C-statistic | 95% CI | P value | | SN (%) | SP (%) | PPV (%) | NPV (%) | +LR | -LR |
|---|---|---|---|---|---|---|---|---|---|---|
| ECG abnorm | 0.60 | 0.45-0.75 | 0.169 | ECG abnorm | 52.9 | 26.8 | 6.8 | 84.9 | 0.72 | 1.76 |
| ***Individual repolarisation parameter*** | | | | | | | | | | |
| QTc | 0.70 | 0.57-0.83 | **0.007** | QTc ≥ 450 ms | 62.5 | 76.7 | 22.2 | 95.0 | 2.68 | 0.49 |
| QTc disp | 0.57 | 0.44-0.70 | 0.347 | QTc disp ≥ 55 ms | 58.8 | 52.3 | 10.9 | 92.8 | 1.23 | 0.79 |
| QTPc | 0.66 | 0.56-0.77 | **0.033** | QTPc ≥ 356 ms | 62.5 | 60.7 | 14.5 | 93.8 | 1.59 | 0.62 |
| JTc | 0.72 | 0.60-0.85 | **0.002** | JTc ≥ 340 ms | 76.5 | 68.5 | 19.7 | 96.6 | 2.43 | 0.34 |
| JTPc | 0.65 | 0.52-0.77 | **0.046** | JTPc ≥ 240 | 64.7 | 60.5 | 13.9 | 94.5 | 1.64 | 0.58 |
| cTPe | 0.65 | 0.52-0.78 | 0.05 | cTPe ≥ 100 ms | 76.5 | 55.4 | 14.8 | 95.9 | 1.72 | 0.42 |
| ***ECG + repolarisation parameters*** | | | | | | | | | | |
| ECG abnorm + JTc | 0.73 | 0.59-0.87 | **0.002** | ECG abnorm + JTc ≥ 340 ms | 94.1 | 20.2 | 10.7 | 97.1 | 1.18 | 0.29 |
| **High ECV** | | | | | | | | | | |
| | **C-statistic** | **95% CI** | **P value** | | **SN (%)** | **SP (%)** | **PPV (%)** | **NPV (%)** | **+LR** | **-LR** |
| ECG abnorm | 0.54 | 0.39-0.69 | 0.605 | ECG abnorm | 76.9 | 30.3 | 8.6 | 93.9 | 1.10 | 0.76 |
| ***Individual repolarisation parameters*** | | | | | | | | | | |
| QTc | 0.62 | 0.45-0.80 | 0.111 | QTc ≥ 456 ms | 46.7 | 81.3 | 17.9 | 94.6 | 2.50 | 0.66 |
| QTc disp | 0.56 | 0.39-0.72 | 0.482 | QTc disp ≥ 55 ms | 60.0 | 49.7 | 9.5 | 93.4 | 1.19 | 0.80 |
| QTPc | 0.69 | 0.54-0.85 | **0.014** | QTPc ≥ 366 ms | 53.3 | 73.1 | 14.8 | 94.7 | 1.98 | 0.64 |
| JTc | 0.71 | 0.57-0.84 | **0.008** | JTc ≥ 340 ms | 60.0 | 64.9 | 13.0 | 94.9 | 1.71 | 0.62 |
| JTPc | 0.82 | 0.73-0.91 | **<0.001** | JTPc ≥ 240 | 86.7 | 63.2 | 17.1 | 98.2 | 2.29 | 0.21 |
| cTPe | 0.32 | 0.17-0.47 | **0.022** | cTPe ≥ 100 ms | 26.7 | 49.7 | 4.4 | 88.5 | 0.53 | 1.47 |
| ***ECG + repolarisation parameters*** | | | | | | | | | | |
| ECG abnorm + JTPc | 0.82 | 0.74-0.91 | **<0.001** | ECG abnorm + JTPc ≥ 240 | 99.9 | 18.1 | 9.7 | 99.9 | 1.37 | 0.01 |
| **Pathological LGE** | | | | | | | | | | |
| | **C-statistic** | **95% CI** | **P value** | | **SN (%)** | **SP (%)** | **PPV (%)** | **NPV (%)** | **+LR** | **-LR** |
| ECG abnorm | 0.59 | 0.49-0.69 | 0.097 | ECG abnorm | 88.9 | 29.8 | 16.9 | 94.3 | 1.27 | 0.37 |
| ***Individual repolarisation parameters*** | | | | | | | | | | |
| QTc | 0.46 | 0.34-0.58 | 0.483 | QTc ≥ 456 ms | 22.2 | 81.0 | 15.8 | 86.6 | 1.17 | 0.96 |

| | | | | | | | | | | |
|---|---|---|---|---|---|---|---|---|---|---|
| QTc disp | 0.53 | 0.34-0.69 | 0.627 | QTc disp ≥ 55 ms | 55.6 | 51.4 | 14.3 | 88.8 | 1.12 | 0.86 |
| QTPc | 0.52 | 0.40-0.63 | 0.766 | QTPc ≥ 366 ms | 29.6 | 69.0 | 13.3 | 85.9 | 0.95 | 1.02 |
| JTc | 0.50 | 0.38-0.62 | 0.944 | JTc ≥ 340 ms | 37.0 | 66.7 | 15.2 | 86.8 | 1.11 | 0.94 |
| JTPc | 0.54 | 0.42-0.67 | 0.487 | JTPc ≥ 240 | 51.9 | 60.5 | 16.1 | 89.9 | 1.31 | 0.80 |
| cTPe | 0.43 | 0.31-0.54 | 0.231 | cTPe ≥ 100 ms | 37.0 | 51.8 | 11.0 | 83.7 | 0.77 | 1.22 |
| ***ECG + repolarisation parameters*** | | | | | | | | | | |
| ECG abnorm + QTc disp | 0.64 | 0.53-0.75 | **0.019** | ECG abnorm + QTc disp ≥ 55 | 96.3 | 17.3 | 14.5 | 97.0 | 1.15 | 0.21 |

P values are based on concordance statistics and receiver operating characteristics curve analysis. ECG abnorm; Group A ECG abnormalities; QTc, corrected QT; QTPc, corrected QT peak; cTPe, corrected T-peak- to-T-end; disp, dispersion, JTc, corrected JT; JTPc, corrected JT peak.

**Table 4** Diagnostic performance of ECG for myocardial inflammation or fibrosis (high T1/pathological LGE)

| | High T1/Pathological LGE | | | | | | | | | |
|---|---|---|---|---|---|---|---|---|---|---|
| | **C-statistic** | **95% CI** | **P value** | | **SN (%)** | **SP (%)** | **PPV (%)** | **NPV (%)** | **+LR** | **-LR** |
| ECG abnorm | 0.57 | 0.48-0.66 | 0.169 | ECG abnorm | 82.9 | 31.0 | 22.7 | 88.1 | 1.20 | 0.55 |
| ***Individual repolarisation parameters*** | | | | | | | | | | |
| QTc | 0.58 | 0.48-0.69 | 0.109 | QTc ≥ 456 ms | 39.0 | 84.5 | 38.1 | 85.0 | 2.52 | 0.72 |
| QTc disp | 0.60 | 0.50-0.71 | **0.038** | QTc disp ≥ 55 ms | 61.0 | 54.2 | 24.5 | 85.0 | 1.33 | 0.72 |
| QTPc | 0.61 | 0.51-0.70 | **0.034** | QTPc ≥ 366 ms | 43.9 | 72.6 | 28.1 | 84.1 | 1.60 | 0.77 |
| JTc | 0.60 | 0.50-0.70 | **0.042** | JTc ≥ 340 ms | 51.2 | 66.7 | 27.3 | 84.8 | 1.54 | 0.73 |
| JTPc | 0.62 | 0.51-0.72 | **0.020** | JTPc ≥ 240 ms | 61.0 | 63.7 | 29.1 | 87.0 | 1.68 | 0.61 |
| cTPe | 0.48 | 0.38-0.59 | 0.587 | cTPe ≥ 100 ms | 46.3 | 50.6 | 18.6 | 79.4 | 0.94 | 1.06 |
| ***ECG + repolarisation parameters*** | | | | | | | | | | |
| ECG abnorm + QTc | 0.65 | 0.56-0.74 | **0.003** | ECG abnorm + QTc ≥ 456 ms | 92.7 | 28.0 | 23.9 | 94.0 | 1.29 | 0.26 |
| ECG abnorm + QTc disp | 0.63 | 0.53-0.72 | **0.012** | ECG abnorm + QTc disp ≥ 55 ms | 95.1 | 18.5 | 22.2 | 93.9 | 1.17 | 0.26 |
| ECG abnorm + JTc | 0.65 | 0.56-0.74 | **0.004** | ECG abnorm + JTc ≥ 340 ms | 92.7 | 22 | 22.5 | 92.5 | 1.19 | 0.33 |
| ECG abnorm + JTPc | 0.66 | 0.56-0.75 | **0.002** | ECG abnorm + JTPc ≥ 240 ms | 95.1 | 20.2 | 22.5 | 94.4 | 1.19 | 0.24 |
| ECG abnorm + cTPe | 0.58 | 0.49-0.68 | 0.097 | ECG abnorm + cTPe ≥ 100 ms | 90.2 | 13.7 | 20.3 | 85.2 | 1.05 | 0.72 |

P values are based on concordance statistics and receiver operating characteristics curve analysis. ECG abnorm; Group A ECG abnormalities; QTc, corrected QT; QTPc, corrected QT peak; cTPe, corrected T-peak- to-T-end; disp, dispersion, JTc, corrected JT; JTPc, corrected JT peak.

# APPENDIX 3: SUPPLEMENTARY TABLES FOR CHAPTER 4

**Table 1** Sex-based differences in standard 12-lead ECG parameters.

| Features | Male | Female |
|---|---|---|
| | | |
| APD duration | Shorter ↓ | Longer ↑ |
| Recovery | Faster ↑ | Slower ↓ |
| Transmural heterogeneity | Lesser ↓ | Greater ↑ |
| Phase 1 | Prominent with a notch | Less / No notching |
| **ECG** | | |
| Heart rate | Slower ↓ | Faster ↑ |
| Heart rate variability | Higher ↑ | Lower ↓ |
| P wave amplitude | Shorter ↓ | Taller ↑ |
| P wave duration | Longer ↑ | Shorter ↓ |
| PR interval | Longer ↑ | Shorter ↓ |
| QRS complex amplitude | Higher ↑ | Lower ↓ |
| QRS complex duration | Longer ↑ | Shorter ↓ |
| QT interval | Shorter ↓ | Longer ↑ |
| JT interval | Shorter ↓ | Longer ↑ |
| QT dispersion | Higher ↑ | Lower ↓ |
| J point | Higher ↑ | Lower ↓ |
| ST segment amplitude | Higher ↑ | Lower ↓ |
| T wave amplitude | Higher ↑ | Lower ↓ |
| T wave duration | Shorter ↓ | Longer ↑ |

**Table 2** ECG intervals adjusted means based on ANCOVA adjusted for BMI.

| | **Male COVID-19 (n=127)** | **Female COVID-19 (n=73)** | **P values** |
|---|---|---|---|
| Heart rate (bpm) | 69 (61-81) | 75 (66-86) | **0.032**[f] |
| PR interval ms | 165.4 ± 28.5 | 155.3 ± 20.7 | **0.012**[g] |
| QRS ms | 97.0 ± 16.3 | 88.4 ± 11.1 | **<0.001**[g] |
| QTc ms | 420.1 ± 34.4 | 441.3 ± 31.9 | **<0.001**[g] |
| QTc disp ms | 57.8 ± 22.1 | 54.4 ± 19.6 | 0.132[g] |
| QTPc ms | 339.2 ± 30.8 | 362.2 ± 31.8 | **<0.001**[g] |
| JTc ms | 323.1 ± 26.8 | 345.2 ± 27.1 | **<0.001**[g] |
| JTPc ms | 221.6 ± 25.2 | 247.1 ± 27.9 | **<0.001**[g] |
| cTPe ms | 101.5 ± 14.9 | 98.2 ± 16.1 | 0.134[g] |

[f]Mann-Whitney Test [g]Analysis of covariance (ANCOVA) with Benferroni post-hoc test.
Values are mean ± SD, median (IQR) or percentages.
QTc, corrected QT; QTPc, corrected QT peak; cTPe, corrected T-peak- to-T-end; disp, dispersion, JTc, corrected JT; JTPc, corrected JT peak.

**Table 3** Discriminative potential of ECG for LVEF dysfunction and individual myocardial tissue abnormalities (adjusted for sex).

| **LVEF < 52%** | | | |
|---|---|---|---|
| | **C- statistic 95% CI (P value)** | | |
| **ECG parameter** | **All patients** | **Male patients (n=135)** | **Female patients (n=77)** |
| ECG abnormalities | 0.60 [0.45-0.75] (p=0.270) | 0.58 [0.40-0.75] (p=0.451) | 0.67 [0.39-0.95] (p=0.423) |
| **Individual Repolarisation Parameter to detect LVEF < 52%** | | | |
| QTc | 0.49 [0.31-0.67] (p=0.918) | 0.46 [0.27-0.64] (p=0.659) | 0.86 [0.74-0.98] (p=0.084) |
| QTc disp | 0.69 [0.50-0.88] **(p=0.035)** | 0.60 [0.39-0.81] (p=0.319) | 1.00 [1.00-1.00] **(p<0.001)** |
| QTPc | 0.49 [0.29-0.69] (p=0.942) | 0.45 [0.25-0.66] (p=0.646) | 0.91 [0.85-0.98] **(p=0.047)** |
| JTc | 0.51 [0.32-0.70] (p=0.914) | 0.48 [0.30-0.67] (p=0.867) | 0.93 [0.84-1.00] **(p=0.037)** |
| JTPc | 0.52 [0.35-0.70] (p=0.799) | 0.53 [0.37-0.69] (p=0.778) | 0.93 [0.84-0.99] **(p=0.037)** |
| cTPe | 0.43 [0.27-0.60] (p=0.446) | 0.41 [0.22-0.61] (p=0.390) | 0.41 [0.10-0.72] (p=0.677) |
| **ECG group A + individual repolarisation interval** | | | |
| ECG abnormalities + QTc | 0.61 [0.45-0.77] (p=0.212) | 0.62 [0.44-0.80] (p=0.241) | 0.91 [0.82-0.99] (p=0.051) |
| ECG abnormalities + QTc disp | 0.72 [0.54-0.89] **(p=0.016)** | 0.63 [0.44-0.83] (p=0.183) | 1.00 [1.00-1.00] **(p=0.016)** |
| ECG abnormalities + JTc | 0.61[0.45-0.78] (p=0.217) | 0.57 [0.40-0.74] (p=0.497) | 0.96 [0.89-1.00] **(p=0.027)** |
| ECG abnormalities + JTPc | 0.62 [0.46-0.78] (p=0.183) | 0.60 [0.44-0.76] (p=0.319) | 0.95 [0.88-0.99] **(p=0.029)** |
| ECG abnormalities + QTc disp + JTc | 0.74 [0.57-0.92] **(p=0.006)** | 0.66 [0.45-0.87] (p=0.116) | 0.99 [0.98-1.00] (p=0.018) |
| **High T1** | | | |
| | **C- statistic 95% CI (P value)** | | |
| **ECG parameter** | **All patients** | **Male patients (n=132)** | **Female patients (n=77)** |
| ECG abnormalities | 0.51 [0.37-0.66] (p=0.851) | 0.37 [0.15-0.58] (p=0.363) | 0.55 [0.37-0.73] (p=0.588) |
| **Individual Repolarisation Parameter to detect High T1** | | | |
| QTc | 0.81 [0.70-0.92] **(p<0.001)** | 0.84 [0.63-1.00] **(p=0.021)** | 0.78 [0.64-0.91] **(p=0.003)** |
| QTc disp | 0.66 [0.53-0.80] **(p=0.030)** | 0.84 [0.66-1.00] **(p=0.019)** | 0.62 [0.46-0.78] (p=0.193) |
| QTPc | 0.77 [0.66-0.87] **(p<0.001)** | 0.82 [0.64-1.00] **(p=0.029)** | 0.69 [0.54-0.84] **(p=0.037)** |
| JTc | 0.82 [0.71-0.93] **(p<0.001)** | 0.76 [0.47-1.00] (p=0.082) | 0.78 [0.64-0.91] **(p=0.003)** |
| JTPc | 0.76 [0.62-0.89] **(p=0.001)** | 0.76[0.48-0.99] (p=0.075) | 0.67 [0.49-0.86] (p=0.061) |

| | | | |
|---|---|---|---|
| cTPe | 0.61 [0.46-0.76] (p=0.145) | 0.65 [0.42-0.87] (p=0.322) | 0.63 [0.45-0.82] (p=0.144) |
| **ECG group A + individual repolarisation interval** | | | |
| ECG abnormalities + QTc | 0.82 [0.72-0.93] **(p<0.001)** | 0.83 [0.61-1.00] **(p=0.025)** | 0.78 [0.64-0.92] **(p=0.002)** |
| ECG abnormalities + QTc disp | 0.64 [0.51-0.78] (p=0.055) | 0.82 [0.62-1.00] (**p=0.030**) | 0.61 [0.45-0.77] (p=0.230) |
| ECG abnormalities + JTc | 0.82 [0.72-0.93] **(p<0.001)** | 0.75 [0.46-1.00] (p=0.089) | 0.78 [0.66-0.91] **(p=0.002)** |
| ECG abnormalities + JTPc | 0.75 [0.62-0.89] **(p=0.001)** | 0.74 [0.46-0.99] (p=0.105) | 0.68 [0.49-0.86] (p=0.051) |
| ECG abnormalities + QTc disp + JTc | 0.82 [0.71-0.93] **(p<0.001)** | 0.72 [0.41-1.00] (p=0.141) | 0.79 [0.66-0.91] **(p=0.002)** |
| **High T2** | | | |
| **ECG parameter** | **C- statistic 95% CI (P value)** **All patients** | **Male patients (n=119)** | **Female patients (n=70)** |
| ECG abnormalities | 0.60 [0.45-0.75] (p=0.169) | 0.63 [0.44-0.83] (p=0.165) | 0.55 [0.32-0.78] (p=0.664) |
| **Individual Repolarisation Parameter to detect High T2** | | | |
| QTc | 0.70 [0.57-0.83] **(p=0.007)** | 0.71 [0.55-0.87] **(p=0.026)** | 0.69 [0.44-0.93] (p=0.109) |
| QTc disp | 0.57 [0.44-0.70] (p=0.347) | 0.58 [0.43-0.74] (p=0.386) | 0.56 [0.37-0.76] (p=0.579 |
| QTPc | 0.66 [0.56-0.77] **(p=0.033)** | 0.67 [0.50-0.85] (p=0.070) | 0.61 [0.42-0.79] (p=0.358) |
| JTc | 0.72 [0.60-0.85] **(p=0.002)** | 0.75 [0.60-0.91] **(p=0.008)** | 0.71 [0.49-0.92] (p=0.077) |
| JTPc | 0.65 [0.52-0.77] **(p=0.046)** | 0.66 [0.49-0.83] (p=0.094) | 0.62 [0.41-0.82] (p=0.313) |
| cTPe | 0.65 [0.52-0.78] **(p=0.05)** | 0.65 [0.50-0.80] (p=0.118) | 0.61 [0.38-0.85] (p=0.328) |
| **ECG group A + individual repolarisation interval** | | | |
| ECG abnormalities + QTc | 0.72 [0.58-0.86] (p=0.003) | 0.75 [0.57-0.93] (p=0.009) | 0.67 [0.43-0.91] (p=0.134) |
| ECG abnormalities + QTc disp | 0.63 [0.48-0.77] (p=0.087) | 0.67 [0.48-0.86] (p=0.079) | 0.57 [0.36-0.79] (p=0.525) |
| ECG abnormalities + JTc | 0.73 [0.59-0.87] **(p=0.002)** | 0.76 [0.59-0.94] **(p=0.006)** | 0.68 [0.44-0.92] (p=0.109) |
| ECG abnormalities + JTPc | 0.66 [0.51-0.81] **(p=0.028)** | 0.68 [0.47-0.88] (p=0.066) | 0.60 [0.37-0.83], (p=0.384) |
| ECG abnormalities + QTc disp + JTc | 0.74 [0.59-0.88] **(p=0.001)** | 0.77 [0.58-0.96] **(p=0.005)** | 0.71 [0.46-0.95] (p=0.077) |
| **High ECV** | | | |
| **ECG parameter** | **C- statistic 95% CI (P value)** **All patients** | **Male patients (n=124)** | **Female patients (n=62)** |
| ECG abnormalities | 0.54 [0.38-0.70] (p=0.668) | 0.65 [0.41-0.89] (p=0.389) | 0.51 [0.32-0.71] (p=0.898) |
| **Individual Repolarisation Parameter to detect High ECV** | | | |

| | | | |
|---|---|---|---|
| QTc | 0.65 [0.48-0.81] (p=0.082) | 0.68 [0.23-1.00] (p=0.300) | 0.56 [0.36-0.76] (p=0.578) |
| QTc disp | 0.58 [0.40-0.75] (p=0.374) | 0.78 [0.49-1.00] (p=0.103) | 0.50 [0.31-0.69] (p=0.983) |
| QTPc | 0.73 [0.59-0.87] **(p=0.006)** | 0.62 [0.17-1.00] (p=0.482) | 0.66 [0.51-0.82] (p=0.109) |
| JTc | 0.73 [0.60-0.87] **(p=0.005)** | 0.80 [0.50-1.00] (p=0.078) | 0.60 [0.42-0.79] (p=0.304) |
| JTPc | 0.82 [0.73-0.91] **(p<0.001)** | 0.81 [0.62-0.99] **(p=0.020)** | 0.73 [0.59-0.97] **(p=0.022)** |
| cTPe | 0.32 [0.20-0.48] **(p=0.031)** | 0.34 [0.00-0.75] (p=0.354) | 0.62 [0.45-0.80] (p=0.231) |
| **ECG group A + individual repolarisation interval** | | | |
| ECG abnormalities + QTc | 0.65 [0.49-0.81] (p=0.072) | 0.70 [0.29-1.00] (p=0.236) | 0.57 [0.38-0.76] (p=0.507) |
| ECG abnormalities + QTc disp | 0.55 [0.40-0.71] (p=0.518) | 0.83 [0.61-1.00] (p=0.054) | 0.49 [0.31-0.67] (p=0.915) |
| ECG abnormalities + JTc | **0.74 [0.61-0.87] (p=0.004)** | 0.82 [0.55-1.00] (p=0.061) | 0.61 [0.43-0.79] (p=0.304) |
| ECG abnormalities + JTPc | 0.82 [0.74-0.91] **(p<0.001)** | 0.83 [0.66-0.99] **(p=0.013)** | 0.71 [0.57-0.85] **(p=0.037)** |
| ECG abnormalities + QTc disp + JTc | 0.76 [0.66-0.87] **(p=0.002)** | 0.78 [0.56-0.99] (p=0.103) | 0.62 [0.45-0.80] (p=0.231) |
| **Pathological LGE** | | | |
| **ECG parameter** | **C- statistic 95% CI (P value)** **All patients** | **Male patients (n=135)** | **Female patients (n=77)** |
| ECG abnormalities | 0.59 [0.49-0.69] (p=0.097) | 0.62 [0.51-0.74] (p=0.079) | 0.50 [0.25-0.74] (p=0.970) |
| **Individual Repolarisation Parameters to detect pathological LGE** | | | |
| QTc | 0.46 [0.33-0.57] (p=0.412) | 0.47 [0.33-0.62] (p=0.680) | 0.44 [0.21-0.66] (p=0.608) |
| QTc disp | 0.58 [0.45-0.71] (p=0.190) | 0.57 [0.41-0.73] (p=0.325) | 0.61 [0.38-0.83] (p=0.392) |
| QTPc | 0.51 [0.40-0.63] (p=0.839) | 0.57 [0.43-0.70] (p=0.322) | 0.46 [0.23-0.68] 9p=0.718) |
| JTc | 0.48 [0.36-0.60] (p=0.782) | 0.50 [0.36-0.64] (p=0.952) | 0.58 [0.36-0.80] (p=0.518) |
| JTPc | 0.54 [0.42-0.67] (p=0.49) | 0.55 [0.41-0.70] (p=0.455) | 0.68 [0.48-0.88] (p=0.146) |
| cTPe | 0.42 [0.30-0.54] (p=0.178) | 0.43 [0.29-0.58] (p=0.337) | 0.32 [0.15-0.48] (p=0.138) |
| **ECG group A + individual repolarisation interval** | | | |
| ECG abnormalities + QTc | 0.63 [0.52-0.74] (p=0.023) | 0.65 [0.53-0.77] (p=0.032) | 0.55 [0.29-0.82] (p=0.662) |
| ECG abnormalities + QTc disp | 0.64 [0.53-0.75] **(p=0.019)** | 0.66 [0.54-0.79] **(p=0.019)** | 0.55 [0.31-0.79] (p=0.704) |
| ECG abnormalities + JTc | 0.61 [0.50-0.71] (p=0.054) | 0.62 [0.50-0.74] (p=0.078) | 0.47 [0.23-0.72] (p=0.834) |
| ECG abnormalities + JTPc | 0.61 [0.51-0.72] (p=0.059) | 0.66 [0.54-0.78] **(p=0.020)** | 0.57 [0.35-0.80] (p=0.556) |

| | | | |
|---|---|---|---|
| ECG abnormalities + QTc disp + JTc | 0.66 [0.55-0.78] **(p=0.007)** | 0.69 [0.56-0.81] **(p=0.007)** | 0.52 [0.27-0.78] (p=0.849) |

P values are based on concordance statistics and receiver operating characteristics curve analysis JTc, corrected JT interval; JTPc, corrected JT peak interval; QTc, corrected QT; QTPc, corrected QT peak; cTPe, corrected T-peak- to-T-end; disp, dispersion.

# APPENDIX 4: SUPPLEMENTARY TABLES FOR CHAPTER 5

**Table 1** ECG and CMR parameters of patients at three- and six- months relative to controls (***only those completed both visits n=38 at three months***).

| | ECG | | | P values | | |
|---|---|---|---|---|---|---|
| | **COVID-19, 3months (n=38) β** | **COVID-19, 6months (n=38)** | **Control (n=43)** | **3months vs control** | **6months vs control** | **3months vs 6months** |
| Abnormal ECG n (%) | 29 (76.3) | 28 (73.7) | 22 (51.2) | **0.019[c]** | **0.037c** | 1.000[e] |
| Bundle Branch Block n (%) | 0(0) | 2 (5.3) | 0 (0) | - | 0.217[d] | 0.500[e] |
| Abnormal axis ** n (%) | 13 (34.2) | 14 (36.8) | 8 (18.6) | 0.110[c] | 0.066[c] | 1.000[e] |
| ST-T changes ** n (%) | 14 (36.8) | 6 (15.8) | 16 (37.2) | 0.973[c] | **0.031[c]** | **0.008[e]** |
| Poor R progression n (%) | 7 (18.4) | 6 (15.8) | 6(14.0) | 0.585[c] | 0.816[c] | 1.000[e] |
| Fragmented QRS ** n (%) | 10 (26.3) | 9 (23.7) | 6 (14.0) | 0.163[c] | 0.261[c] | 1.000[e] |
| Heart block n (%) | 2 (5.3) | 4 (10.5) | 0 (0) | 0.217[d] | **0.044[d]** | 0.500[e] |
| PVC/PAC n (%) | 0 (0) | 5 (13.2) | 0 (0) | - | **0.020[d]** | 0.063[e] |
| | **Group B ECG** | | | | | |
| Heart rate (bpm) | 74.9 ± 13.6 | 70.4 ± 14.3 | 67.5 ± 11.9 | **0.010[a]** | 0.322[a] | 0.052[f] |
| PR interval (ms) | 159.5 (144.8-177.3) | 155.0 (143.8-184.3) | 154.0 (142.0-173.0) | 0.366[b] | 0.356[b] | 0.369[g] |
| QRS (ms) | 89.2 ± 8.8 | 90.9 ± 11.1 | 88.8 ± 8.8 | 0.879[a] | 0.355[a] | 0.127[b] |
| QTc (ms) | 457.2 ± 27.7 | 464.6 ± 32.5 | 419.8± 29.3 | **<0.001[a]** | **<0.001[a]** | 0.175[f] |
| QTc disp (ms) | 72.0 ± 20.6 | 81.8 ± 31.2 | 51.1 ± 18.0 | **<0.001[a]** | **<0.001[a]** | 0.107[f] |
| QTPc (ms) | 373.6 ± 32.6 | 379.0 ± 32.9 | 346.9 ± 28.8 | **<0.001[a]** | **<0.001[a]** | 0.714[f] |
| JTc (ms) | 357.9 ± 27.2 | 367.4 ± 28.5 | 330.1 ± 23.0 | **<0.001[a]** | **<0.001[a]** | 0.053[f] |
| JTPc (ms) | 251.2 ± 31.6 | 258.5 ± 31.5 | 235.3 ± 25.9 | **0.016[a]** | **<0.001[a]** | 0.128[f] |
| cTPe (ms) | 106.8 ± 16.2 | 108.4 ± 17.6 | 94.9 ± 12.8 | **<0.001[a]** | **<0.001[a]** | 0.626[f] |
| | **CMR** | | | **P values** | | |
| | **COVID-19, 3months (n=38) β** | **COVID-19, 6months (n=38)** | **Control (n=43)** | **3months vs control** | **6months vs control** | **3months vs 6months** |
| CMR abnormal n (%) | 13 (34.2) | 11(28.9) | 13 (30.2) | 0.702[c] | 0.136[c] | 0.625[e] |

| | | | | | | |
|---|---|---|---|---|---|---|
| LVEDV ml | 146.3 (127.6-173.6) | 151.1 (124.7-183.1) | 148.4(129.5-171.3) | 0.940[b] | 0.656[b] | 0.255[g] |
| LVESV ml | 59.9 ± 22.7 | 58.6 ± 20.8 | 56.2 ± 17.0 | 0.407[a] | 0.569[b] | 0.485[g] |
| LVSV ml | 91.0 (75.8-101.8) | 94.2 (80.7-108.8) | 91.8 (80.0-103.6) | 0.677[b] | 0.484[b] | 0.109[g] |
| LV mass g | 117.7 (101.2-136.4) | 119.5 (99.3-130.6) | 110.5 (87.8-132.9) | 0.185[b] | 0.298[b] | 0.157[g] |
| LV mass index g/m$^2$ | 59.4 (49.5-66.9) | 57.0 (50.1-64.3) | 53.7 (49.5-62.1) | 0.118[b] | 0.212[b] | 0.086[g] |
| LVEF (%) | 61.6 ± 7.6 | 62.8 ± 6.6 | 63.0 ± 5.9 | 0.364[a] | 0.918[a] | 0.225[f] |
| LVEF < 52% n (%) | 5 (13.2) | 1 (2.6) | 1(2.3) | 0.094[d] | 1.000[c] | 0.125[e] |
| LVCO L/min | 6.8 ± 1.4 | 6.7 ± 1.9 | 6.3 ± 1.5 | 0.090[b] | 0.239[b] | 0.678[g] |
| RVEDV ml | 167.4 ± 39.5 | 159.7 ± 40.4 | 160.6 ± 41.9 | 0.460[a] | 0.905[a] | **0.028[f]** |
| RVESV ml | 74.0 ± 24.2 | 65.1 ± 23.2 | 66.6 ± 23.4 | 0.346[a] | 0.529[a] | **<0.001[f]** |
| RVSV ml | 92.7 (77.3-104.0) | 93.1 (81.3-108.2) | 88.5 (80.6-102.2) | 0.992[b] | 0.490[b] | 0.510[g] |
| RVEF (%) | 56.5 ± 7.1 | 60.1 ± 6.5 | 59.3 ± 6.4 | 0.317[a] | 0.488[a] | **<0.001[f]** |
| RVEF < 48% n (%) | 3 (7.9) | 1 (2.6) | 1 (2.3) | 0.337[d] | 1.000[c] | 0.500[e] |
| RVCO L/min | 7.0 ± 1.5 | 6.6 ± 1.8 | 6.3 ± 1.5 | **0.048[a]** | 0.395[b] | 0.416[f] |
| **Myocardial Tissue Characterisations** | | | | | | |
| Global T1 ms | 1175.9 ± 31.2 | 1151.3 ± 36.7 | 1152.9 ± 39.1 | **0.005[a]** | 0.866[a] | **<0.001[f]** |
| High T1 n (%) * | 3/37 (8.1) | 1 (2.5) | 3 (7.0) | 1.000[d] | 0.616[d] | 0.625[e] |
| Global T2 ms | 42.3 ± 2.0 | 41.9 ± 1.6 | 42.3 ± 2.5 | 0.913[a] | 0.415[a] | 0.131[f] |
| High T2 n (%) * | 2/37 (5.4) | 1 (2.5) | 5 (11.6) | 0.442[d] | 0.203[f] | 1.000[e] |
| ECV n (%) | 30.0 (27.3-31.1) | 28.0 (26.2-30.2) | 28.6 (26.1-30.6) | 0.198[b] | 0.566[b] | **0.010[g]** |
| High ECV (>0.32) (%) | 2/32 (6.3) | 3/39 (7.7) | 4/31 (12.9) | 0.691[d] | 0.692[b] | 1.000[e] |
| Pathological LGE n (%) | 9/37 (24.3) | 9/39 (23.1) | 8 /42 (47.1) | 0.569[c] | 0.656[c] | 1.000[e] |

[a]Independent T-Test, [b]Mann-Whitney Test, [c]Chi-square Test, [d]Fisher-Freeman-Halton Exact Test, [e]McNemar Test, [f] Paired T-Test, [g]Wilcoxon Signed Rank Test

Values are mean ± SD, median (IQR) or percentages. CMR, cardiac magnetic resonance; ECV, Extracellular volume; LGE, late gadolinium enhancement; LV, left ventricular; LVEDV, left ventricular end-diastolic volume; LVESV, left ventricular end-systolic volume; LVSV, left ventricular systolic volume; LVEF, left ventricular ejection fraction; LVCO, left ventricular cardiac output; RVEDV, right ventricular end-diastolic volume; RVESV, right ventricular end-systolic volume; RVSV, right ventricular systolic volume; RVEF, right ventricular ejection fraction; RVCO, right ventricular cardiac output.

* (>90$^{th}$ centile T1>1216.7 ms, T2 >45 ms), ** BBB excluded, **β** analysis conducted involving only participants who completed both visits n=38.

# APPENDIX 5: MANUSCRIPTS / ABSTRACT ARISING FROM DPHIL WORK

---

1. Cassar, Mark Philip, Elizabeth M. Tunnicliffe, Nayia Petousi, Adam J. Lewandowski, Cheng Xie, Masliza Mahmod, **Azlan Helmy Abd Samat**, Rachael A. Evans, Christopher E. Brightling, Ling-Pei Ho, Stefan K. Piechnik, Nick P. Talbot, David Holdsworth, Vanessa M. Ferreira, Stefan Neubauer, and Betty Raman. **2021**. 'Symptom Persistence Despite Improvement in Cardiopulmonary Health – Insights from longitudinal CMR, CPET and lung function testing post-COVID-19', *EClinicalMedicine*, 41: 101159. **(Manuscript Published)**

2. Mahmod, M., B. Raman, K. Chan, S. Sivalokanathan, R. W. Smillie, **A. H. A. Samat**, R. Ariga, S. Dass, E. Ormondroyd, H. Watkins, and S. Neubauer. **2022**. 'Right ventricular function declines prior to left ventricular ejection fraction in hypertrophic cardiomyopathy', *J Cardiovasc Magn Reson*, 24: 36. **(Manuscript Published)**

3. Betty Raman, Celeste McCracken, Mark P Cassar, Alastair J Moss, Lucy Finnigan, **Azlan Helmy A Samat**, Prof Godwin Ogbole, Elizabeth M Tunnicliffe, Fidel Alfaro-Almagro, Ricarda Menke, Cheng Xie, Prof Fergus Gleeson, Elena Lukaschuk, Hanan Lamlum, Kevin McGlynn, Iulia Propescu, Zeena-Britt Sanders, Laura Saunders, Prof Stefan K Piechnik, Prof Vanessa M Ferreira, Chrysovalantou Nikolaidou, Prof Najib M Rahman, Prof Ling-Pei Ho, Victoria C Harris, Aarti Shikotra, Amisha Singapuri, Paul Pfeffer, Prof Charlotte Manisty, Prof Onn Min Kon, Mark Beggs, Prof Declan P O'Regan, Jonathan Fuld, Jonathan R Weir-McCall, Dhruv Parekh, Prof Rick Steeds, Krisnah Poinasamy, Prof Dan J Cuthbertson, Prof Graham J Kemp, Prof Malcolm G Semple, Prof Alexander Horsley, Prof Christopher A Miller, Caitlin O'Brien, Prof Ajay M Shah, Prof Amedeo Chiribiri, Olivia C Leavy, Matthew Richardson, Omer Elneima, Hamish J C McAuley, Marco Sereno, Ruth M Saunders, Linzy Houchen-Wolloff, Neil J Greening, Prof Charlotte E Bolton, Prof Jeremy S Brown, Gourab Choudhury, Prof Nawar Diar Bakerly, Nicholas Easom, Carlos Echevarria, Michael Marks, Prof John R Hurst, Mark G Jones, Daniel G Wootton, Prof Trudie Chalder, Prof Melanie J Davies, Prof Anthony De Soyza, Prof John R Geddes, Prof William Greenhalf, Prof Luke S Howard, Joseph Jacob, William D-C Man, Prof Peter J M Openshaw, Joanna C Porter, Matthew J Rowland, Prof Janet T Scott, Prof Sally J Singh, David C Thomas, Mark Toshner, Prof Keir Lewis, Prof Liam G Heaney, Prof Ewen M Harrison, Steven Kerr, Annemarie B Docherty, Nazir I Lone, Prof Jennifer K Quint, Prof Aziz Sheikh, Bang Zheng, Prof Gisli Jenkins, Eleanor F Cox, Prof Susan Francis, Prof Mark Halling-Brown, Prof James D Chalmers, Prof John P Greenwood, Prof Sven Plein, Paul J C Hughes, A A Roger Thompson, Prof Sarah Rowland-Jones, Prof James M Wild, Matthew Kelly, Thomas A Treibel, Steven Bandula, Raminder Aul, Prof Karla Miller, Prof Peter Jezzard, Prof Stephen Smith, Prof Thomas E Nichols, Prof Gerry P McCann, Rachael A Evans, Prof Louise V Wain, Prof Christopher E Brightling, Prof Stefan Neubauer.**2023.**'Multiorgan MRI findings after hospitalisation with COVID-19 in the UK

(C-MORE): a prospective, multicentre, observational cohort study', *The Lancet Respiratory Medicine,* (**Manuscript Published**)

4. **Azlan Helmy Abd Samat**, Mark P Cassar, Abid Akhtar, ZakariyeAshkir, Celeste McCracken, Rebecca Mills, Lucy Finnigan, Adam J Lewandowski, Masliza Mahmod, Godwin Ogbole, Elizabeth M Tunnicliffe, Elena Lukaschuk, Stefan Piechnik, Vanessa M Ferreira, Chrysovalantou Nikolaidou, Najib M Rahman, Ling Pei Ho, Stefan Neubauer, Betty Raman on behalf of the PHOSP-COVID collaborative group., 'Electrocardiography rules out Myocardial Abnormalities in Cardiac Magnetic Resonance Imaging: COVID-19 Follow-up Study', *RDM Annual Symposium*, Said Business School, University of Oxford, 14th March **2023** (**Poster presentation**)

5. **Azlan Helmy A Samat**, Masliza Mahmod, Adam J Lewandowski, Mark P Cassar Abid M Akhtar, Alastair J Moss, Charlotte Manisty, Thomas A Treibel, Zakariye M Ashkir, Celeste McCracken, Elena Lukaschuk, Stefan K Piechnik, Vanessa M Ferreira, Cheng Xie, Dan J Cuthbertson PhD, Graham J Kemp, Chrysovalantou Nikolaidou, Christopher A Miller, Amedeo Chiribiri, Declan P O'Regan , Susan T Francis, Richard P Steeds, Jonathan R Weir-McCall, James M Wild, Sven Plein, Gerry P McCann, Rachael A Evans, Christopher E. Brightling, Stefan Neubauer and Betty Raman on behalf of the PHOSP-COVID collaborative group. **'**EKG rules out myocardial abnormalities on cardiac magnetic resonance imaging in post-hospitalised COVID-19 patients: a multicenter observational study', *American Heart Association Conference*, Philadelphia, USA, 10-13th Nov **2023** (**Poster presentation and abstract published in Circulation** https://doi.org/10.1161/circ.148.suppl_1.14282).

**6.** *Ashkir Z, ***Abd Samat A**, Finnigan, Jermy S, Sarto G, Murthy P, Wong B, E. Wicks, Thomson K, Mahmod M, Tunnicliffe L, Ariga R, Watkins H, Neubauer S, Raman B, Bridging the gap between ECG indicators of arrhythmic risk and the continuum of myocardial disarray and fibrosis across hypertrophic cardiomyopathy stages, *Association of inherited cardiac conditions Conference, London, **2023***
* Joint first author (**Poster presentation**)

7. **Azlan Helmy A Samat** DrEmMed, Mark P Cassar MD , Abid M Akhtar MBBS,Celeste McCracken MSc, Zakariye M Ashkir MBChB, Rebecca Mills MSc, Alastair J Moss PhD, Lucy E M Finnigan PhD, Adam J Lewandowski DPhil, Masliza Mahmod DPhil, Godwin I Ogbole MD, Elizabeth M Tunnicliffe PhD, Elena Lukaschuk MSc, Stefan K Piechnik DSc, Vanessa M Ferreira DPhil, Chrysovalantou Nikolaidou PhD, Najib M Rahman DPhil, Ling-Pei Ho DPhil, Victoria C Harris MSc, Amisha Singapuri BSc, Charlotte Manisty PhD, Declan P O'Regan PhD, Jonathan R Weir-McCall PhD, Richard P Steeds MD, Krisnah Poinasamy LLM, Dan J Cuthbertson PhD, Graham J Kemp DSc, Alexander Horsley PhD, Christopher A Miller PhD, Caitlin O'Brien DPhil, Amedeo Chiribiri PhD, Susan T Francis PhD, James D Chalmers PhD, Sven Plein PhD ,Ana-Maria Poener MD, James M Wild PhD, Thomas A Treibel PhD, Michael Marks PhD, Mark Toshner MD, Louise V Wain PhD, Rachael A Evans PhD, Christopher E Brightling MD, Stefan Neubauer MD, Gerry P McCann MD, Betty Raman DPhil on behalf of PHOSP-COVID Collaborative group, 'Diagnostic utility of electrocardiogram in screening for cardiac injury on cardiac magnetic

resonance in post-hospitalised COVID-19 patients: a prospective multicenter study', *International Journal of Cardiology* **2024 (Manuscript submitted and under review)**

8. **Azlan Helmy A Samat**, Masliza Mahmod, Adam J Lewandowski, Celeste McCracken, Mark P Cassar, Abid M Akhtar, Zakariye M Ashkir, Alastair J Moss, Charlotte Manisty, Thomas A Treibel, Elena Lukaschuk, Stefan K Piechnik, Vanessa M Ferreira, Chrysovalantou Nikolaidou, Christopher A Miller, Amedeo Chiribiri, Declan P O'Regan, Richard P Steeds, Jonathan R Weir-McCall, Sven Plein, Gerry P McCann, Rachael A Evans, Christopher E. Brightling, Stefan Neubauer and Betty Raman on behalf of the PHOSP-COVID collaborative group, 'Improving sex-based differences in ECG diagnostic performance for CMR abnormalities post-severe COVID-19 infections', *Society of Cardiac Magnetic Resonance Imaging (CMR) Conference*, London, 25-27th January **2024 (Oral 3 minutes Fire Abstract Presentation, and abstract published in Journal of Cardiovascular Magnetic Resonance)**

9. *Ashkir Z, ***Abd Samat A**, Finnigan, Jermy S, Sarto G, Murthy P, Wong B, E. Wicks, Thomson K, Mahmod M, Tunnicliffe L, Ariga R, Watkins H, Neubauer S, Raman B, Bridging the gap between ECG indicators of arrhythmic risk and the continuum of myocardial disarray and fibrosis across hypertrophic cardiomyopathy stages. **2024**
   * Joint first author (**Manuscript in preparation**)

10. Ashkir Z, ***Abd Samat A**, Finnigan, Jermy S, Sarto G, Murthy P, Wong B, E. Wicks, Thomson K, Mahmod M, Tunnicliffe L, Ariga R, Watkins H, Neubauer S, Raman B, Bridging the gap between ECG indicators of arrhythmic risk and the continuum of myocardial disarray and fibrosis across hypertrophic cardiomyopathy stages. *Society of Cardiac Magnetic Resonance Imaging (CMR) Conference*, London, 25-27th January **2024 (Award winner for Early Career Award for Translational Research,** presented by Ashkir Z**, and abstract published in Journal of Cardiovascular Magnetic Resonance)**

11. Maron, M. S., Mahmod, M., **Abd Samat, A. H**., Choudhury, L., Massera, D., Phelan, D. M., ... & Watkins, H. (**2024**). Safety and Efficacy of Metabolic Modulation With Ninerafaxstat in Patients With Nonobstructive Hypertrophic Cardiomyopathy. *Journal of the American College of Cardiology*. (**Manuscript Published, and presented during a Late Breaking Clinical Trial Session at ACC 24**)

12. **Azlan Helmy A Samat**, Masliza Mahmod, Adam J Lewandowski, Mark P Cassar Abid M Akhtar, Alastair J Moss, Charlotte Manisty, Thomas A Treibel, Zakariye M Ashkir, Celeste McCracken, Elena Lukaschuk, Stefan K Piechnik, Vanessa M Ferreira, Cheng Xie, Dan J Cuthbertson PhD, Graham J Kemp, Chrysovalantou Nikolaidou, Christopher A Miller, Amedeo Chiribiri, Declan P O'Regan , Susan T Francis, Richard P Steeds, Jonathan R Weir-McCall, James M Wild, Sven Plein, Gerry P McCann, Rachael A Evans, Christopher E. Brightling, Stefan Neubauer and Betty Raman on behalf of the PHOSP-COVID collaborative group. **'**Electrocardiography rules out myocardial abnormalities on cardiac magnetic resonance imaging in post-hospitalised COVID-19 patients: a multicenter observational study', 26th March **2024** Oxford School of Emergency Medicine (OSEM Conference), Oxford, United Kingdom (**Poster presentation**)